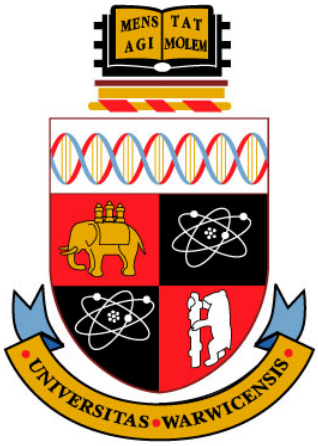

The Effect of Solvent, Ligand and Initiator upon Aqueous Cu(0)-mediated Reversible Deactivation Radical Polymerisation

Danielle Lloyd

A thesis submitted in partial fulfilment of the requirements for the degree of

Doctor of Philosophy in Chemistry

Department of Chemistry

University of Warwick

August 2017

“Two plus two equals four; I put sugar in my coffee and it tastes sweet; the sun comes up because the world turns; these things are beautiful to me. Although there are mysteries that I will never understand, everywhere I look I see proof that for every effect there is a corresponding cause. Even if I can’t see it, I find that reassuring.”

Table of Contents

List of Abbreviations

AA	Acrylic acid
AgOAc	Silver acetate
AIBN	2,2'-Azobis(2-methylproprionitrile)
ARGET	Activators regenerated by electron transfer
AsI	4-(*N*-(2-Bromoisobutyryl)amino)phenylarsonic acid
ATRP	Atom transfer radical polymerisation
BDE	Bond dissociation energy
BPE	Bis(2-bromopropionyl)ethane
BPED	*N*,*N*′-Di(3-hexoxo-3-oxopropyl)-*N*,*N*′-bis(2-pyridylmethyl)ethane-1,2-diamine
BPO	Dibenzoyl peroxide
BrPPA	2-Bromo-*N*-phenyl-propionamide
Bpy	Bipyridine
C	Concentration of solute in solution
CCTP	Catalytic chain transfer polymerisation
C_s	Chain transfer constant
CTA	Chain transfer agent
C-X	Carbon-halide bond
Cyclam	1,4,8,11-Tetraazacyclotetradecane
d	Doublet
DCM	Dichloromethane
DHPBMP	2,3-Dihydroxypropyl-2-bromo-2-methylpropanoate
$Đ_m$	Dispersity
DMAm	*N,N*-Dimethylacrylamide

DMAPAA	*N*-[3-(Dimethylamino)propyl]acrylamide
DMSO	Dimethyl sulfoxide
DP	Degree of polymerisation
DT	Degenerative chain transfer
EBiB	Ethyl 2-bromoisobutyrate
EBP	Ethyl 2-bromopropionate
EDA	Ethylenediamine
EOR	Enhanced oil recovery
EPR	Electron paramagnetic resonance
EtOH	Ethanol
f	Initiator efficiency
FID	Flame ionisation detector
FRP	Free radical polymerisation
FT	Fourier transform
GC	Gas chromatography
G_p	Gibbs free energy
h	Hour
HBr	Hydrobromic acid
HCl	Hydrochloric acid
HEA	2-Hydroxyethyl acrylate
HEAm	*N*-Hydroxyethyl acrylamide
HEBiB	2-Hydroxyethyl 2-bromoisobutyrate
HMTETA	1,1,4,7,10,10-Hexamethyltriethylenetetramine
H_p	Enthalpy

HPLC	High performance liquid chromatography
I	Initiator
ICAR	Initiators for continuous activator regeneration
I_{eff}	Initiator efficiency
$IM^{\bullet}$	Initiating radical
IPA	Isopropanol
IR	Infrared
ISET	Inner sphere electron transfer
K_{act}	Rate of activation
k_{act}	Activation rate constant
k_{add}	Addition rate constant
k_{β}	β-Scission rate constant
K_{com}	Rate of comproportionation
k_d	Decomposition rate constant
K_{dis}	Rate of disproportionation
K_{deact}	Rate of deactivation
k_{deact}	Deactivation rate constant
K_H	Henry's constant
k_i	Initiation rate constant
k_p	Propagation rate constant
k_{dp}	Depropagation rate constant
k_t	Termination rate constant
k_{tc}	Termination by combination rate constant
k_{td}	Termination by disproportionation rate constant

k_{tr}	Chain transfer rate constant
L	Ligand
LAM	Less activated monomer
LCST	Lower critical solution temperature
LRP	Living radical polymerisation
m	Multiplet
M	Monomer
MAA	Methacrylic acid
MALDI	Matrix-assisted laser desorption/ionisation
MAM	More activated monomer
MBrPA	Methyl-2-bromo-2-phenylacetate
MBP	Methyl bromopropionate
Me_4Cyclam	1,4,8,11-Tetramethyl-1,4,8,11-tetraazacyclotetradecane
Me_6Cyclam	5,5,7,12,12,14-Hexamethyl-1,4,8,11-tetraazacyclotetradecane
Me_6TREN	Tris[2-(dimethylamino)ethyl]amine
MMA	Methyl methacrylate
M_n	Number average molecular weight
MS	Mass spectrometry
Mt	Metal centre
MW	Molecular weight
M_w	Weight average molecular weight
MWD	Molecular weight distribution

NaAMPS	(2-Acrylamido-2-methylpropane sulfonic acid) sodium salt
NAM	*N*-Acryloylmorpholine
n-BuLi	n-Butyllithium
NIPAm	*N*-Isopropyl acrylamide
NMP	Nitroxide mediated polymerisation
NMR	Nuclear magnetic resonance
OEOMEBr	Oligo(ethylene glycol)methyl ether 2-bromoisobutyrate
OSET	Outer sphere electron transfer
p	Partial pressure
P	Poly
PBI	Phosphonic ester bearing initiators
PBS	Phosphate buffered saline
PEO	Polyethylene oxide
PHC	Principle of halogen conservation
PLP	Pulsed laser photoloysis
PMDETA	*N,N,N′,N′,N″*-Pentamethyldiethylenetriamine
PMR	Principle of microscopic reversibility
$P_n^{\bullet}$	Polymeric radicals
ppm	Parts per million
PRE	Persistent radical effect
PS	Polystyrene
PTFE	Polytetrafluoroethylene
PTH	10-Phenylphenothiazine

q	Quartet
qn	Quintet
R	Alkyl group
RAFT	Reversible addition – fragmentation chain transfer
RDRP	Reversible deactivation radical polymerisation
R_i	Rate of initiation
RI	Refractive index
R_p	Rate of propagation
R_{polym}	Rate of polymerisation
R_r	Rate of re-initiation
R_{tc}	Rate of termination by combination
R_{td}	Rate of termination by disproportionation
s	Singlet
S	Solvent
SARA	Supplemental activator reducing agent
SEC	Size exclusion chromatography
SET	Single electron transfer
sc	Supercritical
SIP	Self immolative polymer
S_p	Entropy
t	Time
t	Triplet
T_c	Ceiling temperature
TEA	Triethylamine

TEABr	Tetraethylammonium bromide
TEMPO	2,2,6,6-Tetramethylpiperidinyl-1-oxy
th	Theoretical
THF	Tetrahydrofuran
TM	Transition metal
TMEDA	*N,N,N′,N′*-Tetramethylethylenediamine
TMM	Transition metal mediated
ToF	Time of flight
TPMA	Tris(2-pyridylmethyl)amine
TREN	Tris(2-aminoethyl)amine
UV	Ultraviolet
VC	Vinyl chloride
V_h	Hydrodynamic volume
Vis	Visible
X	Halogen

List of Equations

List of Figures

List of Schemes

List of Tables

Acknowledgements

First and foremost, I would like to thank Professor David Haddleton for not only giving me the opportunity to pursue a PhD., but to be part of his research group. Without you, none of this would have been possible and I would not be where I am today. I am incredibly grateful to you for your support, particularly over the last few months when I've come to you in a panic and you've calmed me down.

Secondly, I would like to thank BASF for my funding and more importantly, my industrial supervisor Dr. Adam Blanazs. Thank you for the constant support and guidance during my PhD. Your advice has been invaluable, and I cannot possibly thank you enough for the countless emails, telecons and chats. Also, thank you for allowing me to come and work at BASF for three months. Whilst it was a pleasure to work with you and Simon, I'm sure I'll be having nightmares about the "Handschuhe" for years to come.

I would like to express my gratitude to Dr. Kristian Kempe for providing me with advice, solutions and ideas. Also, a special thank you goes to Dr. Paul Wilson. I cannot express enough thanks for your guidance, your incredible knowledge, your endless advice, and your willingness to help no matter how busy you were.

Of course, I would like to thank the members of the Haddleton group. Although most of you have now left, there are some whom I would particularly like to thank. Firstly, thank you to Chongyu and Nutt (Pink) for the lunches, for your support, and for making me laugh. Thank you to Rachel for putting up with my stressing and for your friendship. Thank you to Patrick for your help, the German lessons, the Doctor Who videos, and for making me smile. To Sam Lawton, thank you for the hugs, for the "ohrwurms", for making me laugh, and for the very weird conversations. Also, thank you to Jenny and Chris for helping me so much within the early years of my PhD.

I would also like to express my special thanks to Dr. Daniel Lester. There are so many things that I must thank you for; thank you for keeping our equipment running so smoothly, for your help, for reading this thesis, for your amusing stories, and for your friendship. Thank you to the technical staff (Dr. Ivan Prokes, Phil Aston and Dr. Lijiang Song) for keeping the instrumentation running to a high standard.

I would also like to thank Professor Steve Howdle and Dr. Simon Bassett at the University of Nottingham for your help with the depolymerisation work and for the use of their steel autoclaves. Speaking of the depolymerisation work, I must thank the return of Professor Perrier to the University of Warwick (and Perrier water) for inspiring that project.

My special thanks go to Dr. Kate Barwell and Dr. Simon Holder at the University of Kent. Without your influence and your support during my undergraduate degree, I would not be here today and I would not be submitting a PhD. thesis. An enormous thank you goes out to my friends who I have known since my undergrad. To Sam, Helen and Loz; you have provided endless amount of support, made me laugh, made sure I remembered to take a break, and you have listened to me panic with unending patience! Thank you so much.

Of course, I would like to thank “The Squad” (or alternatively, Ben, Jess and Josie). You guys have kept me (relatively) sane whilst I’ve been here. I cannot thank you enough for the countless tea breaks, the discussions, the guidance, the support and the ridiculous conversations (mini banana handles?!). These four years would have been very different without you and I will be forever thankful that you are in my life.

Having spent so much time there over the last few years, I would like to thank the people in the Department of Computer Science. Thank you to Charlie, Chris, Phil, Steve, Chester, Tim and Eleanor. I would also like to thank Sharon for letting me use one of the offices and for letting me pretend that I was a Computer Scientist.

Of course, there are many more Computer Scientists that I owe a great deal of thanks to. Firstly, I would like to thank Ali; for your friendship and for the enjoyable times and all the laughs we had as housemates. To Marchant, thank you for your constant support, your invaluable friendship, the hugs, the cat pictures, and the tea. Quite frankly, the things I must thank you for are endless. Thank you to Pete (or the other me) for convincing me that I could do this, for your words of inspiration, for the memes, and generally for everything. As with Marchant, it would take me too long to thank you for all the things. Then there's Archbold; thank you for welcoming me the second I came to Warwick. Thank you for introducing me to the great friends that I have made here. Thank you for your support, your friendship (8 years?!), for looking out for me, and for always making me laugh. Lastly, I would like to thank the most important of all the Computer Scientists, James Dickson. There are not enough words, nor are there ones which are adequately describe my appreciation for you. It would take me way too long to write all the ways in which you have made me happy, all the things you have done, all the support you have given me, and how much I value you. For now, I guess a "thank you" will have to suffice.

Thank you to the people who I can always count on to be nerdy with, and who help me to relax by playing Dungeons and Dragons. To Faiz (Sathariel/Soveliss), Leanne (Amber/Ilyana), Aimée (Moss/Tysha), Archbold (DM/Shaizeal) and Marchant (DM/Eliovar); you guys mean an awful lot to me and I am very thankful for your incredible friendships. Hopefully I'll channel my inner Aralaia and not Ytharra!

Finally, I would like to thank my family. To my Uncle, thank you for inspiring me to study Chemistry, for your guidance and patience within the early years, and for your endless love and support. To my parents, thank you for always believing in me, for being convinced that I could do this, and for loving me unconditionally. I could not have done this without you. This thesis is dedicated to you.

Declaration

Experimental work contained in this thesis is original research carried out by the author, unless otherwise stated, in the Department of Chemistry and the University of Warwick, between September 2013 and September 2017. No material contained herein has been submitted for any other degree, or at any other institution.

Results from other authors are references in the usual manner throughout the text.

Date:

Danielle Lloyd

Abstract

The overall aim of this work, sponsored by BASF, was to investigate the effect of the solvent, ligand and initiator, upon the $Cu^{(0)}$-mediated reversible deactivation radical polymerisation (RDRP) of water-soluble monomers. In addition to this, the simplicity and versatility of the aqueous methodology led to a secondary goal; the determination of reaction conditions that would allow for polymerisations to be conducted in an "off the shelf" manner.

As a starting point for this study, two bidendate and five multidentate ligands were screened as mediators for the controlled polymerisation of *N*-isopropylacrylamide (NIPAm) (Chapter 3). From these results, the polymerisations which involved tris[2-(dimethylamino)ethyl]amine (Me_6TREN) were deemed to be the most successful. However, as Me_6TREN was expensive and thus required synthesising, further investigation was carried out. Following characterisation by UV-Vis spectroscopy and the optimisation of reaction conditions, it was suggested that *N,N,N',N'',N''*-pentamethyldiethylenetriamine (PMDETA)) and (tris(2-aminoethyl)amine (TREN) were more suited to "off the shelf" polymerisations.

To continue the development of such a system, four initiators were employed for the synthesis of PNIPAm (Chapter 4). During this investigation, 2-bromo-*N*-(2-hydroxyethyl)-2-methylpropanamide (compound **(3)**) was identified as being the most appropriate initiator for a "*synthesis-free*" polymerisation.

In Chapter 2, a system for the well-controlled polymerisation and *in-situ* depolymerisation of acrylamides and acrylates was developed. In addition to this and following the reformation of monomer, deoxygenation of the resulting solution furnished high conversions and low dispersity polymers within 30 minutes.

Chapter 1: Introduction

From conventional free radical polymerisation to reversible deactivation radical polymerisation

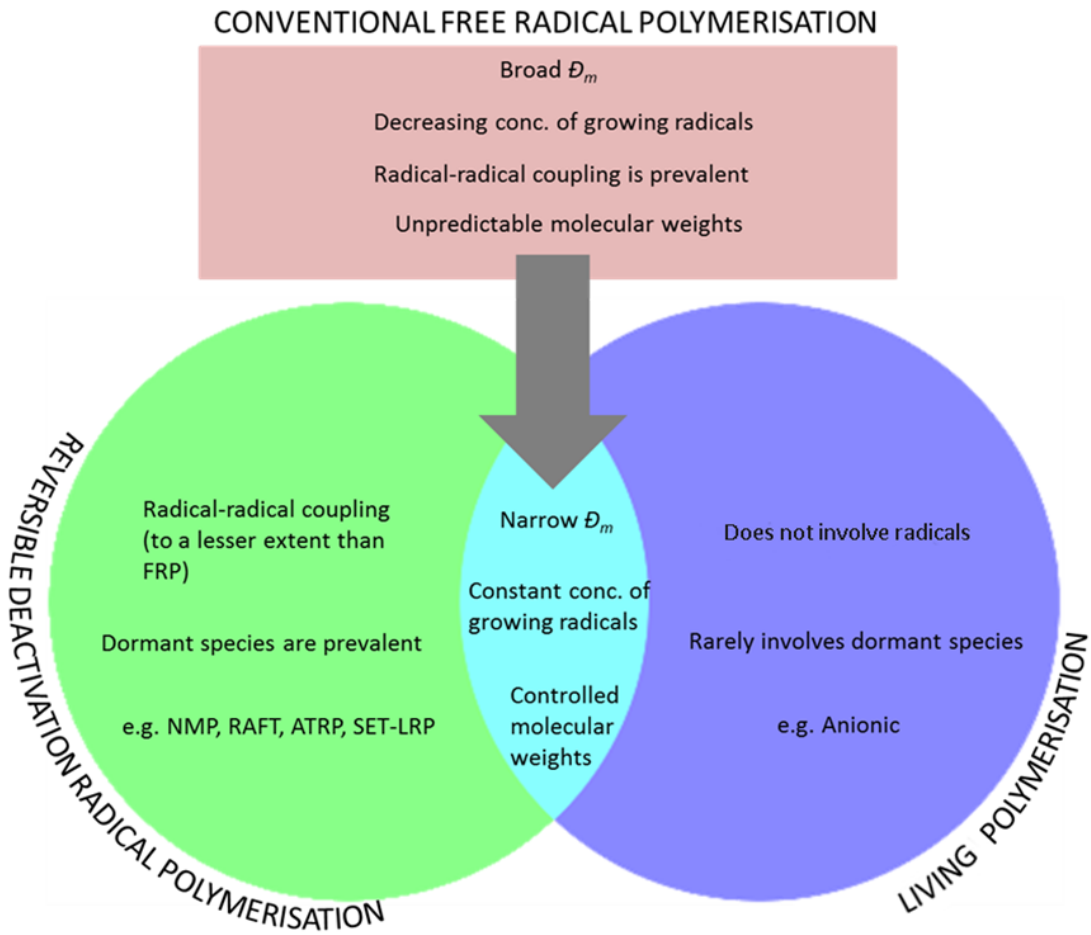

1.1. Introduction

Early polymer synthesis saw the production of Bakelite from the condensation polymerisation of formaldehyde and phenol in 1909.[1] Since then, polymer chemistry has evolved to include the development of free radical polymerisation and later, more sophisticated controlled or "living" radical techniques. Remarkably, this progression has enabled for the creation of a plethora of materials with tuneable properties that are viable for applications ranging from drug delivery and other bio-applications[2–6] to wastewater treatment.[7–10] Moreover, these advances have allowed polymer chemists to approach that which only nature can do; the synthesis of polymers with mono-dispersity.

This introduction aims to provide an overview of the techniques that are commonly used today for the synthesis of macromolecules. Preceded by a discussion on the reactivity of monomers, the mechanism and kinetics of conventional free radical polymerisation and controlled radical polymerisations will be covered. Beyond this, any information or background relating to a particular piece of work has been provided at the beginning of the relevant chapter.

1.2. The concept of the radical

Chemical species that possess an unpaired electron are known as "free" radicals.[11] Radicals, most commonly denoted by $R^{\bullet}$, are well known for their affinity towards vinyl-bonds, and upon their generation, will readily partake in radical addition. Radical addition can take place *via* two routes: "tail-addition" and "head-addition".[12,13] The former of these is most frequently observed and involves the preferential addition of a radical to the less sterically hindered end of a vinyl group (Scheme 1.1).[12]

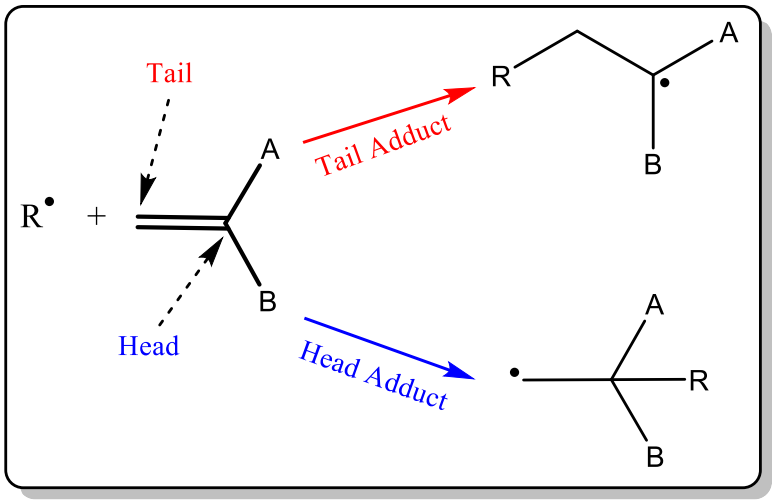

Scheme 1.1 – Depiction of the "head-addition" and "tail-addition" approach to radical addition.

The “head-addition” approach is not only less prevalent due to steric effects diminishing the rate of addition, but due to the subsequent formation of a relatively unstable primary radical.[14] The relative stability of radicals is determined by both hyperconjugation, and the extent to which the system is delocalised through resonance. Hyperconjugation causes stabilisation through the interaction of electrons in a σ–bond (for alkyl radicals this is an sp^3 hybrid) with a partially filled, or empty, adjacent π-orbital, and increases with the level of orbital overlap.[15–17] Thus, the order of radical stability follows methyl < primary < secondary < tertiary (Figure 1.1).[15,17]

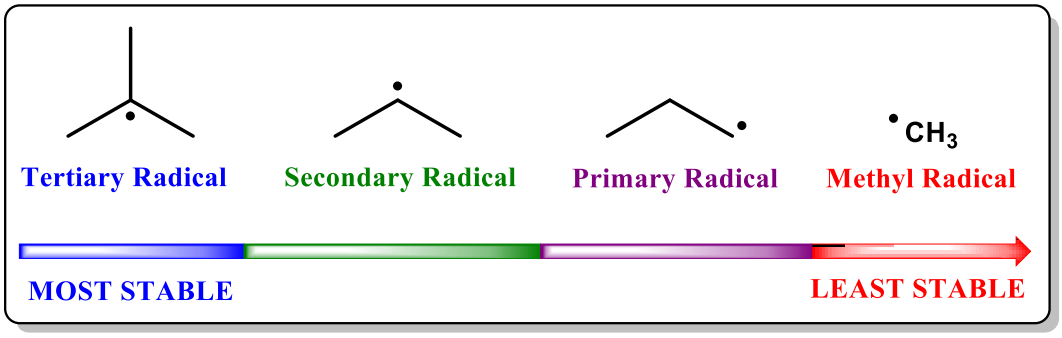

Figure 1.1 – A representation of the trend in radical stability.

In order to relate this to radical polymerisation systems, the trend in radical stability can be used to explain why the rates of polymerisation differ between acrylate and

methacrylate monomers. Upon radical addition, an acrylate monomer forms a secondary radical which, when compared to the tertiary radical formed from a methacrylate monomer, is less stable.[12,14] Resultantly, the polymerisation of acrylates occurs at much faster rate than methacrylates as less stable radicals more readily undergo propagation (*i.e.* the radical is more reactive). Indeed, this has been proven through the use of pulsed laser photolysis (PLP) which measures the relative propagation rate constants of these monomers.[15]

It is important to mention that polymerisation systems are highly complex and that the rate of polymerisation is influenced by more than just the stability of the radical (*e.g.* steric hindrance and polar substituents).[12,13,15] However, the effects of these factors will not be discussed as the purpose of this introduction is not to provide a comprehensive overview of radical reactivity but rather, a short summary.

The final pertinent piece of information which must be mentioned is the division of monomer activities into two categories: the “less activated” monomers (LAMs) and the “more activated” monomers (MAMs) (Figure 1.2).

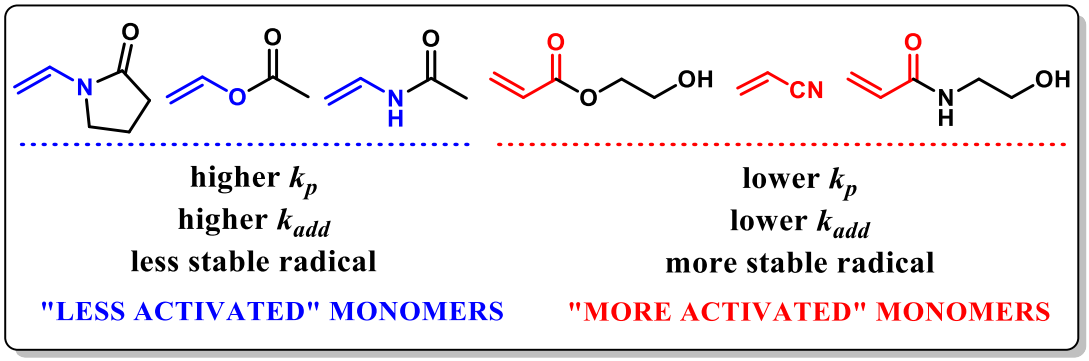

Figure 1.2 – A representation of the differences between "less activated" and "more activated" monomers.

LAMs, such as vinyl pyrrolidone and vinyl formamide, are characterised by their electron-rich double bonds and strong electron donating pendant groups.[18] Comparatively speaking, radical generation from LAMs is difficult due to the highly dense electron cloud which surrounds the vinyl bond. However, once formed, their

unconjugated nature and lack of resonance stabilisation, leads to the corresponding radical species being highly reactive.[14,19] As such, the polymerisation of LAMs is rapid, although without a means of regulating the interaction between radical species, is uncontrolled. Conversely, MAMs, which include (meth)acrylates and (meth)acrylamides are those which have a double bond conjugated to an electron withdrawing substituent such as a carbonyl or a nitrile group.[19,20] Radical formation from these monomers is consequently much easier, but the reactivity of the resulting species is much lower.

1.3. An introduction to polymerisation techniques: free radical polymerisation (FRP)

Perhaps the most well-known method for synthesising polymers by addition or chain growth to date is that of "conventional" free radical polymerisation (FRP).[21] Its high tolerance towards impurities, trace amounts of oxygen, and mild reaction conditions, make it an incredibly versatile and attractive technique.[22,23] Consisting of up to four main events (initiation, propagation, termination and chain transfer), the mechanism is relatively simple and in fact, forms the basis of several other polymerisation systems to date.[12,13,15]

1.3.1. Initiation

A FRP commences upon the generation of radicals from an initiating compound (typically an azo- or peroxide- species) such as 2,2'-azobis(2-methylproprionitrile) (AIBN) or dibenzoyl peroxide (BPO) (Scheme 1.2).[12,15,24]

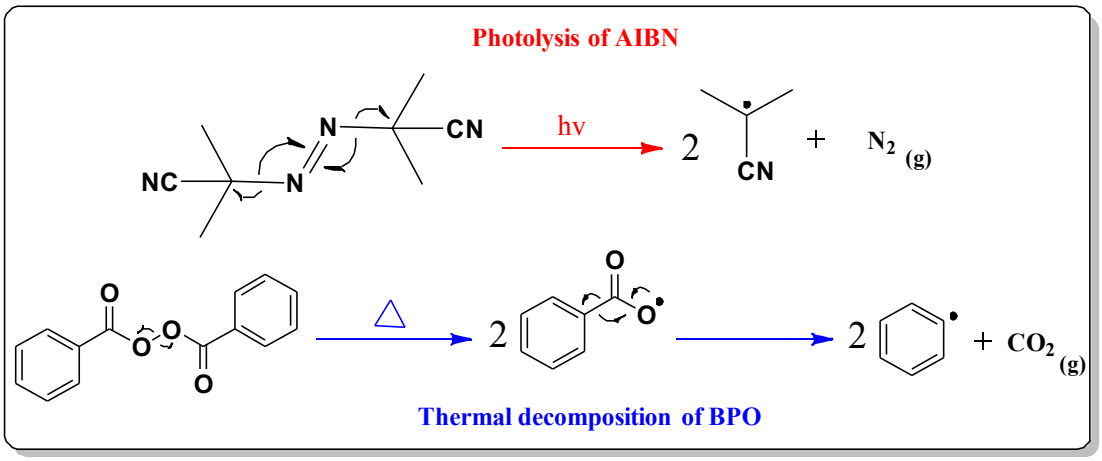

Scheme 1.2 - Decomposition of AIBN and BPO to form two primary radicals.

In most cases, radical formation is brought about through the decomposition of an initiating species *via* thermolysis, photolysis or a redox reaction.[12,15] The carbon centred, or primary oxygen centred radicals ($I^{\bullet}$) which are produced from this, subsequently undergo a radical addition to the carbon-carbon double bond of the monomer (M). This results in a chain initiating radical ($I\text{-}M^{\bullet}$) which is capable of participating in further monomer addition (Equations 1.1 and 1.2).[12,13,15] It is important to note that when speaking about initiation events, the term "primary radical" does not refer to a least substituted alkyl radical as described in Scheme 1.1 and Figure 1.1. Rather, it is another term for the "free" radicals which are generated upon the homolytic dissociation of an initiating compound.[15]

$$2I \xrightarrow{k_d} I^{\bullet} \qquad \textbf{(Equation 1.1)}$$

$$I^{\bullet} + M \xrightarrow{k_i} IM^{\bullet} \qquad \textbf{(Equation 1.2)}$$

Equations 1.1 and 1.2 - The initiation step in a FRP where k_i is the rate constant of initiation, k_d the rate constant of decomposition, $IM^{\bullet}$ the chain initiating radical, $I^{\bullet}$ the initiator radical, M the monomer and I the initiating species.

Since the addition of monomer to a primary radical is much faster than initiator dissociation, the rate determining step for this event is considered to be the latter (Equation 1.1).[12,13,15] As such, an expression for the rate of initiation (k_i) can be

derived based largely on the rate of initiator decomposition (k_d) and concentration of initiator prior to the formation of radicals ([I]) (Equations 1.3 and 1.4).

$$R_i = \frac{d[I^\bullet]}{dt} \quad \textbf{(Equation 1.3)}$$

$$R_i = 2k_d f[I] \quad \textbf{(Equation 1.4)}$$

Equations 1.3 and 1.4 – The expression for the rate of initiation where k_d is the rate of initiator decomposition, I the initiating species and f, the initiator efficiency.

The reactive nature of primary radicals means that they often participate in secondary reactions such as radical recombination, β-scission, hydrogen atom abstraction, rearrangements, and transfer to solvent.[15] Initiating radicals which are involved in these termination events cannot enable radical addition and therefore are not involved in the initiation process itself.[15] By comparing the amount of decomposed initiator with the number of polymer chains formed, this loss of initiating species can be compensated for in the rate equation. The inclusion of an additional factor, known as the initiator efficiency (f or I_{eff}), is a means of achieving this (Equation 1.5).[25]

$$I_{eff} = f = \frac{useful\ radicals\ giving\ successful\ initiation}{total\ number\ of\ radicals\ formed} \quad \textbf{(Equation 1.5)}$$

Equation 1.5 – An expression used for determining the efficiency of an initiator.

It is worth noting that polymerisation in any free radical (or indeed controlled radical) system is possible without an initiator.[12] Upon heating, monomers are capable of acting as their own initiating species and can produce polymers through a process which has been termed, auto-polymerisation (or alternatively, self-polymerisation). More often than not, this process is significantly less controlled when compared to a FRP conducted in the presence of an initiating species.

1.3.2. Propagation

The second event in a FRP is termed 'propagation' and begins with the initiating radical preferentially reacting with the least sterically hindered end of the monomers' double bond to yield an active polymer chain ($P_n^{\bullet}$) (Equation 1.6).[12,13,15]

$$\mathbf{IM^{\bullet} + M_1 \xrightarrow{k_p} P_1^{\bullet}} \qquad \textbf{(Equation 1.6)}$$

Equation 1.6 – A simplified expression for the production of a growing polymer chain, where k_p represents the rate constant of propagation, $IM^{\bullet}$ the chain initiating radical, $P_n^{\bullet}$ the propagating polymer chain, and M the monomer.

Providing that termination does not take place, these chains are capable of undergoing further addition until all of the monomer has been consumed (Equations 1.7 to 1.9). Thus, propagation exhibits a dependency upon the concentration of monomer ([M]) and active propagating radicals ([$P^{\bullet}$]) within the system.[15] Ultimately, this means the rate at which propagation occurs (R_p) can be derived by relating these factors to the sum of the rate constants for each monomer addition (k_p) (Equation 1.10).

$$\mathbf{P_1^{\bullet} + M_2 \xrightarrow{k_p} P_2^{\bullet}} \qquad \textbf{(Equation 1.7)}$$

$$\mathbf{P_2^{\bullet} + M_3 \xrightarrow{k_p} P_3^{\bullet}}_{\ldots etc.} \qquad \textbf{(Equation 1.8)}$$

$$\mathbf{P_n^{\bullet} + nM \xrightarrow{k_p} P_{n+1}^{\bullet}} \qquad \textbf{(Equation 1.9)}$$

Equations 1.7 to 1.9 - A simplified overview of the successive of monomers (propagation), where k_p represents the rate constant of propagation, $P_n^{\bullet}$ the propagating polymer chain, and M the monomer.

$$R_p = k_p[M][P^{\bullet}] \qquad \textbf{(Equation 1.10)}$$

Equation 1.10 – The expression for the rate of propagation where k_p represents the rate constant of propagation, $P_n^{\bullet}$ the propagating polymer chain, and M the monomer.

1.3.3. Termination

The reactive nature of radicals means that chain growth can be terminated at any point during a polymerisation (this statement holds true particularly for systems in which there is no way of regulating the interaction between active species).[12,13,15] As a consequence of this, the interaction between radicals with other components in the system results in the irrevocable loss of a chains' active centre and generates a "dead" polymer chain. Chains which are referred to as "dead" are incapable of undergoing further addition to monomer and as a result, can no longer propagate.[12]

Typically, termination occurs *via* two main routes: bimolecular termination (alternatively termed radical-radical coupling) and chain transfer termination.[12,13] Mechanistically speaking, bimolecular termination can arise through two different pathways; this is termination by combination or termination by disproportionation (Scheme 1.6).[12,13,15]

Termination $P_n^{\bullet} + P_m^{\bullet} \xrightarrow{k_t}$ "dead" polymer

Termination by combination $P_n^{\bullet} + P_m^{\bullet} \xrightarrow{k_{tc}} P_{n+m}$

Termination by disproportionation $P_n^{\bullet} + P_m^{\bullet} \xrightarrow{k_{td}} P_n + P_m$

Scheme 1.3 – A simplified scheme which demonstrates the two main mechanistic routes of bimolecular termination.

In the case of termination by combination, two propagating macro-radicals couple together to result in the formation of a higher molecular weight polymer chain that does not possess an active centre (Scheme 1.3). The rate (R_{tc}) at which this occurs is therefore determined solely by the rate at which the radicals interact with each other (Equation 1.11).

$$R_{tc} = k_{tc}[P^{\bullet}]^2 \quad \text{(Equation 1.11)}$$

Equation 1.11 – The expression for the rate of termination by combination where k_{tc} represents the rate constant of termination by combination, and P$^{\bullet}$ the propagating polymer chain.

In the case of termination *via* disproportionation, a nearby chain undergoes proton abstraction by a macro-radical to yield two ω-end capped polymers: one which is in possession of an unsaturated chain end and one which has a proton.[13,15] As the two routes of bimolecular termination are kinetically equivalent, the rate (R_{td}) at which disproportionation takes place is described by Equation 1.12.

$$R_{td} = k_{td}[P^{\bullet}]^2 \quad \text{(Equation 1.12)}$$

Equation 1.12 – The expression for the rate of termination by disproportionation where k_{td} represents the rate constant of termination by disproportionation, and P• the propagating polymer chain.

In instances where it is not necessary to distinguish between the two different reaction pathways, a more general term for the cessation of a polymerisation can be determined. Essentially, termination is the change in concentration of active species within the system as a function time (Equation 1.13). Therefore, combining Equations 1.11 and 1.12 allows for the rate of termination by radical-radical coupling to be expressed in a manner which is independent of the mechanistic pathway by which it is achieved (Equation 1.16).

$$R_t = \frac{-d[P^{\bullet}]}{dt} \quad \text{(Equation 1.13)}$$

Equation 1.13 – A general expression for termination, where –d[P•] represents the change in the concentration of propagating radicals, and dt represents the change in time.

$$R_t = R_{td} + R_{tc} \quad \text{(Equation 1.14)}$$

$$R_t = k_{td}[P^{\bullet}]^2 + k_{tc}[P^{\bullet}]^2 \quad \text{(Equation 1.15)}$$

$$R_t = 2k_t[P^{\bullet}]^2 \quad \text{(Equation 1.16)}$$

Equations 1.14 to 1.16 - Determination of the expression for the overall rate of termination. k_t represents the combined rate constants of termination, and P• the propagating polymer chain.

Determining the overall rate of a FRP (R_{polym}) is slightly more complex in comparison to determining the rates of the individual events themselves. This difficulty mainly arises due to the dependency of the rate upon the concentration of propagating radicals in a polymerisation system. Since most radicals are transient species,[15] they only exist within the reaction for a short period of time, and as such, measuring the concentration of them at any given moment is challenging. Nevertheless, electron paramagnetic resonance (EPR) spectroscopy is a technique which may be used to ascertain the absolute radical concentration as a function of conversion.[12,13,15] However, in practice, this is a very time-consuming method and as such is very rarely employed.

In the absence of EPR, a number of assumptions can be made to allow for the derivation of an overall rate equation for polymerisation. At the beginning of any reaction, the rate of radical formation exceeds the rate at which they are lost through termination events.[14] As the polymerisation proceeds, the concentration of $P^{\bullet}$ increases alongside the extent of termination until eventually, a steady state is reached whereby net radical formation is zero (Equation 1.17).

$$\frac{d[I^{\bullet}]}{dt} = \frac{-d[P^{\bullet}]}{dt} \qquad \textbf{(Equation 1.17)}$$

Equation 1.17 - An expression for the steady state assumption.

In short, a steady state, in which the rate of initiation is taken to be equal to the rate of termination (*i.e.* $R_i = R_t$), is the first assumption that is applied to this system. Doing so, allows for the concentration of all radical species within the system to be determined (Equations 1.18 to 1.19).

$$R_i = R_t = 2k_t[P^{\bullet}]^2 \qquad \textbf{(Equation 1.18)}$$

$$[P^{\bullet}] = \sqrt{\left(\frac{R_i}{2k_t}\right)} \qquad \textbf{(Equation 1.19)}$$

Equations 1.18 to 1.19 – The expression for the concentration of propagating radicals within a FRP system.

Assuming that only monomer is being consumed during the polymerisation,[14] Equation 1.19 can be combined with Equation 1.10 to produce a tentative expression for the rate of a FRP (Equation 1.20).

$$R_{polym} = k_p[M]\sqrt{\left(\frac{R_i}{2k_t}\right)} \quad \text{(Equation 1.20)}$$

Equation 1.20 - An expression for the rate of a FRP using the steady state assumption.

As this expression involves the rate of initiation, the limiting factor for this stage must be taken into account. Previously, the rate determining step for initiation was found to be the decomposition of the initiator molecule rather than the addition of this species to monomer.[14] Thus, substituting k_d into the rate equation generates a final expression for the rate of a FRP (Equation 1.22). At this point it is important to emphasise that this expression is only applicable to systems which are operating under steady state conditions.[14]

$$R_i = R_d = 2k_d f[I] \quad \text{(Equation 1.21)}$$

$$R_{polym} = k_p[M]\sqrt{\left(\frac{k_d f[I]}{k_t}\right)} \quad \text{(Equation 1.22)}$$

Equations 1.21 to 1.22 – The expression for the overall rate of a FRP using the steady state assumption.

1.3.4. Chain transfer

In addition to termination resulting from disproportionation and radical combination, a FRP often involves some form of side reaction, namely, chain transfer.[26] Through the extraction of an atom from another molecule within the system, chain transfer terminates the growth of an existing radical and results in the generation of a new active centre (Scheme 1.4).

Chain transfer	$P_n^{\bullet} + RY \xrightarrow{k_{tr}} P_nY + R^{\bullet}$
Chain transfer to initiator	$P_n^{\bullet} + IY \xrightarrow{k_{tr}} P_nY + I^{\bullet}$
Chain transfer to monomer	$P_n^{\bullet} + MY \xrightarrow{k_{tr}} P_nY + M^{\bullet}$
Chain transfer to ligand	$P_n^{\bullet} + LY \xrightarrow{k_{tr}} P_nY + L^{\bullet}$
Chain transfer to polymer	$P_n^{\bullet} + P_mY \xrightarrow{k_{tr}} P_nY + P_m^{\bullet}$
Chain transfer to solvent	$P_n^{\bullet} + SY \xrightarrow{k_{tr}} P_nY + S^{\bullet}$

Scheme 1.4 – A simplified demonstration of chain transfer events where k_{tr} represents the rate constant for chain transfer.

The new species may be then able to participate in further propagation events depending upon the radical formed (Scheme 1.5).[15]

$$\mathbf{R_n^{\bullet} + M \xrightarrow{k_r} R_nM^{\bullet} \xrightarrow{k_p}\xrightarrow{k_p}\xrightarrow{k_p} R_{nm}}$$

Scheme 1.5 – A simplified scheme illustrating re-initiation following chain transfer where R represents $I^{\bullet}$, $P_m^{\bullet}$ and $M^{\bullet}$.

If re-initiation occurs in this manner, then the rate of polymerisation may be altered. In instances where the rate of re-initiation (R_r) is equal to the rate of propagation (R_p) ($R_r = R_p$), there is little effect upon the rate of polymerisation.[13,15] However, when $R_r << R_p$, the rate of polymerisation decreases as it is suppressed by chain transfer events.[14]

Furthermore, as not all species can undergo propagation following abstraction, there is a decrease in the average molecular weight observed by size exclusion chromatography (SEC). Hence, in cases where a specific chain length is required, chain transfer agents (CTAs) can be intentionally added to FRPs as a means of providing some degree of control over the final molecular weight of the product.[26]

An example of a radical polymerisation technique which uses a CTA to control the molecular weight of a final product is catalytic chain transfer polymerisation (CCTP). CCTP combines the use of a highly efficient cobalt$^{(II)}$-macrocycle with FRP to synthesise low molecular weight polymers containing terminal vinyl end group functionality.[27–30]

Theoretically, how effective the CTA is at achieving this is determined by the ratio of the rate constant of chain transfer (k_{tr}) to the ratio of propagation (k_p) (Equation 1.23).

$$C_s = \frac{k_{tr}}{k_p} \quad \textbf{(Equation 1.23)}$$

Equation 1.23 – Expression for the chain transfer constant, C_s.

As this is difficult to measure experimentally, the effectiveness of a CTA can be determined by the Mayo equation (Equation 1.24), with the degree of polymerisation (DP_n) being easily calculated from ^{1}H nuclear magnetic resonance (NMR) spectroscopy.

$$\frac{1}{DP_n} = \frac{1}{DP_{n0}} + C_s \frac{[CTA]}{[M]} \quad \textbf{(Equation 1.24)}$$

Equation 1.24 – The Mayo equation where DP_n is the degree of depolymerisation of the product, DP_{n0} is the degree of polymerisation for the product obtained in the absence of chain transfer agent, [CTA] is the concentration of chain transfer agent and [M] is the concentration of monomer.

1.4. Living polymerisation

Although attaining any level of control over a conventional FRP is difficult, it remains one of the most robust and exploited methods in a chemist's arsenal for the synthesis of polymers. One of the biggest challenges that a polymer chemist faces with respect to FRPs, is the accurate prediction of molecular weight, architecture, composition, and end group functionality of the final product.[13] Indeed, it is not

atypical for systems based on FRP to produce polymers which vary greatly in their length and thus, often exhibit dispersities ($Đ_m$) within the region of 1.5 to 3.0.[31] As a way of circumventing these drawbacks, the concept of a "living" polymerisation was introduced and has since facilitated the accurate prediction, and more importantly the tailoring, of all aspects of a polymerisation.

1.4.1. Defining a "living" polymerisation

A truly "living" polymerisation is one in which termination reactions are completely absent. In 1992, Quirk and Lee proposed six key criteria which must be met in order for a polymerisation to be classed as "living".[32]

To be categorised as such a polymerisation must:

i) Have a constant concentration of active species within the system.

ii) Proceed until full monomer consumption has been achieved, with chains continuing to grow upon further addition of monomer.

iii) Maintain narrow molecular weight distributions (MWDs) throughout ($Đ_m$ < 1.2).

iv) Be capable of synthesising block co-polymers upon further monomer addition.

v) Produce polymers with high end group functionality.

vi) Possess a linear increase of molecular weight with conversion.

1.4.2. The kinetics of a "living" radical polymerisation

As outlined in Section 1.4.1., in a "living" radical polymerisation the concentration of radicals within a system should remain constant so long as termination and chain transfer events are kept to a minimum.[32] Providing that this is the case, the rate of

polymerisation can be simplified to the rate of monomer consumption with time (Equation 1.25).

$$\boldsymbol{R_p = \frac{-d[M]}{dt} = k_p[M][P^\bullet]} \quad \textbf{(Equation 1.25)}$$

Equation 1.25 – The expression for the rate of polymerisation for a "living" radical polymerisation.

Through a series of rearrangements and integrations, this equation yields $\ln([M]_0/[M]_t)$ (Equation 1.35) which, when plotted against time, exhibits a linear dependence for a “living” or controlled polymerisation. Furthermore, by applying a linear fit and determining the gradient of the line, this plot can be used to calculate the apparent value of k_p.

The derivation of this expression starts from Equation 1.26:

$$\boldsymbol{R_p = \frac{-d[M]}{dt} = k_p[M][P^\bullet]} \quad \textbf{(Equation 1.26)}$$

And is then shortened to two terms to yield Equation 1.27:

$$\boldsymbol{\frac{-d[M]}{dt} = k_p[M][P^\bullet]} \quad \textbf{(Equation 1.27)}$$

This is then rearranged to produce Equation 1.29:

$$\boldsymbol{\frac{-d[M]}{dt}\frac{1}{[M]} = k_p[P^\bullet]} \quad \textbf{(Equation 1.28)}$$

$$\boldsymbol{\frac{1}{[M]}d[M] = -k_p[P^\bullet]dt} \quad \textbf{(Equation 1.29)}$$

Normally dy/dx cannot be treated as a fraction because it is an operator. However, in this instance it is permissible to do so because of the chain rule.

Equation 1.29 is then integrated to provide Equation 1.31:

$$\int_{M_0}^{M_t} \frac{1}{[M]}\, d[M] = -k_p[P^\bullet] \int_0^t dt \qquad \textbf{(Equation 1.30)}$$

$$ln[[M]]_0^t = -k_p[P^\bullet][t]_0^t \qquad \textbf{(Equation 1.31)}$$

And then rearranged to yield Equation 1.32:

$$ln[M]_t - ln[M]_0 = -k_p[P^\bullet]t \qquad \textbf{(Equation 1.32)}$$

And then simplified to yield Equation 1.33:

$$ln\left(\frac{[M]_t}{[M]_0}\right) = -k_p[P^\bullet]t \qquad \textbf{(Equation 1.33)}$$

Which when substituted into Equation 1.26 results in Equation 1.34:

$$R_p = ln\left(\frac{[M]_t}{[M]_0}\right) = -k_p[P^\bullet]t \qquad \textbf{(Equation 1.34)}$$

And hence our final equation:

$$R_p = ln\left(\frac{[M]_0}{[M]_t}\right) \qquad \textbf{(Equation 1.2)}$$

Equation 1.35 – The expression showing that the rate constant of polymerisation for a "living" radical polymerisation can be derived from a plot of $ln([M]_0/[M]_t)$ versus time. $[M]_0$ is the concentration of monomer at time zero and $[M]_t$ is the concentration of monomer at any given time.

1.4.3. Living anionic polymerisation

The earliest examples of "living" polymerisation systems were that of anionic and cationic polymerisation.[33–37] Out of the two, the most frequently used ionic polymerisation technique is that of anionic polymerisation, which has allowed for the

precise design of polymers with controlled architectures and molecular weights.[38,39] Discovered by Szwarc and co-workers in 1956,[36] this technique employs organometallic bases such as *n*-butyllithium (*n*-BuLi), or electron transfer agents such as sodium naphthalenide, as initiators for the polymerisation of non-polar and polar electrophilic vinyl compounds.[36] Perhaps the most well-known example of such a polymerisation is that of the initial discovery; the polymerisation of styrene following electron transfer from sodium naphthalenide (Scheme 1.6).

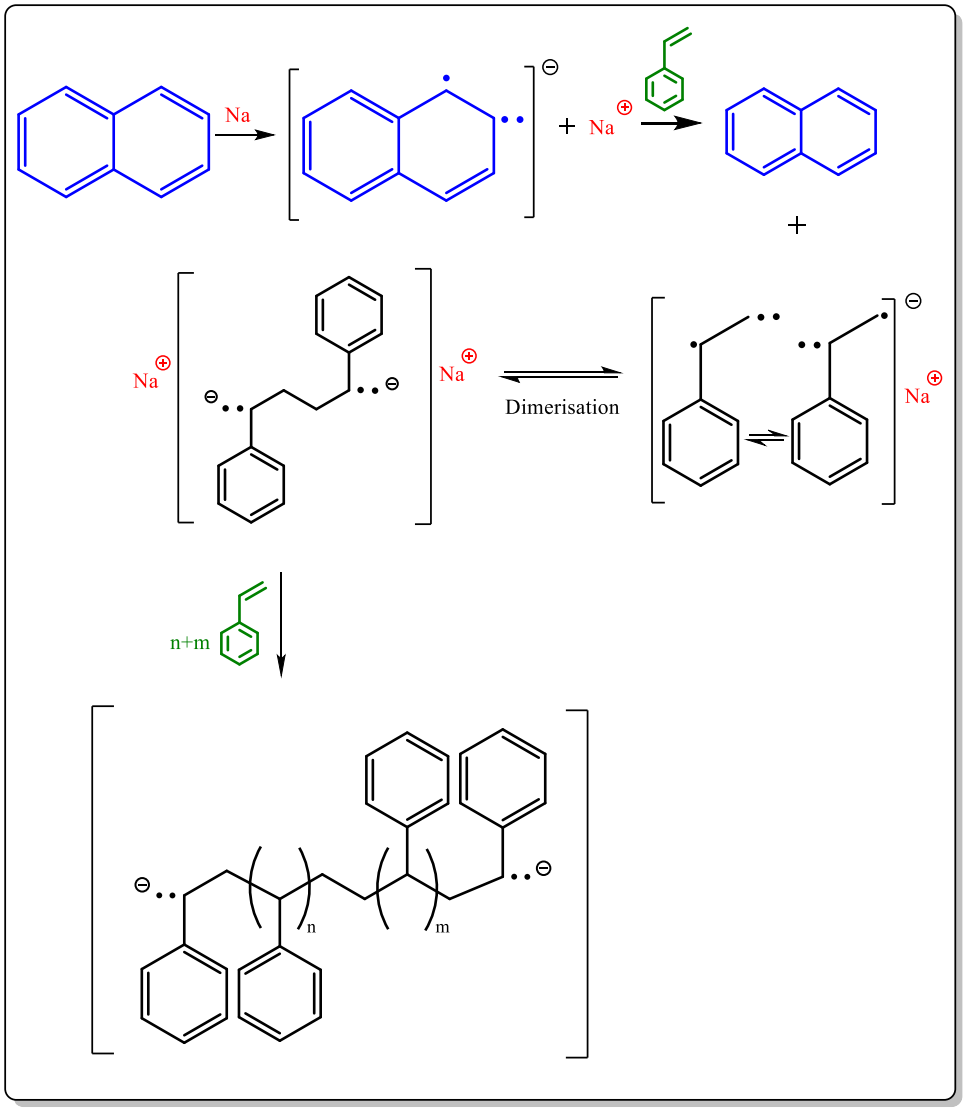

Scheme 1.6 – Mechanism for the anionic polymerisation of styrene using a naphthalene initiator.

Remarkably, unlike FRP and its counterpart cationic polymerisation, termination in anionic polymerisation is virtually non-existent.[14] The high nucleophilicity of the

initiators (and propagating chain ends) means that rigorous procedures for the removal of oxygen, water and protic impurities are a necessity.[40,41] Consequently, reactions are often conducted in aprotic solvents to prevent the propagating anionic centres from participating in proton transfer reactions and hence, reduces the occurrence of chain transfer events.[36] Moreover, the presence of anions at both ends of the polymer chain means that combination reactions are disfavoured due to electrostatic repulsion. This enables for propagation to proceed until the monomer has been exhausted.

Providing that appropriate measures have been taken, the removal of termination events allows for chemists to not only control the molecular weight of the resulting chains and achieve well-defined polymers but, through further monomer addition, the creation of block co-polymers.[38,42] Indeed, since its inception, anionic polymerisation has proven to be a highly reliable route for polymer synthesis both industrially, and academically.[38,40,43,44] Despite the low reaction temperatures (-78 °C) and the thorough purification/drying of reagents, it has been used industrially for the production of poly(butadiene), poly(styrene) and poly(isoprene).[43]

1.5. An introduction to polymerisation techniques: reversible deactivation radical polymerisation (RDRP)

Reversible deactivation radical polymerisation (RDRP) is an umbrella term that encompasses some of the techniques which have been developed as “living” alternatives to ionic polymerisation.[45] Currently, there are four main RDRP systems which exist: nitroxide mediated polymerisation (NMP), reversible addition – fragmentation chain transfer (RAFT), atom transfer radical polymerisation (ATRP), and single electron transfer – living radical polymerisation (SET-LRP).

The biggest barrier for developing a "living" polymerisation system is the high reactivity of radical species towards one another. RDRPs overcome this by establishing either a dynamic equilibrium (NMP,[46–48] ATRP,[49–51] and SET-LRP[52–54]) or using "degenerative chain transfer" (RAFT[55–57]) to regulate the concentration of propagating (macro)radicals within the system.

In systems where a dynamic equilibrium is established, transient species are reversibly "capped" through the introduction of a mediating component, such as a persistent radical. The inclusion of such a species provides temporary deactivation of the propagating (macro)radical and thus, reduces the concentration of active radicals within the system. Not only does this limit radical-radical coupling, it also ensures that all chains continue to propagate at the same rate. In the alternative approach, the reactivity of the propagating chains' active centre is altered when it is transferred to another species. Until this species is removed, the (macro)radical is unable to participate in further chain growth.

Although termination is not completely absent from RDRPs (the highly reactive nature of radicals means that some bimolecular termination will always be present in a radical polymerisation), the extent to which it occurs can be greatly reduced through careful optimisation of reaction conditions.[58–60] This means that if the criteria for a "living" polymerisation are strictly applied,[32] then the occurrence of termination events prevents these systems from being classed as such. Nevertheless, there are still many who choose to use the term "living" to describe RDRPs as they not only meet most of the requirements listed in Section 1.4.1., but are at the very least, close approximations of truly "living" systems.[61]

Regardless of their classification, RDRPs have revolutionised the field of polymer chemistry and have significantly expanded a chemist's toolbox for the synthesis of polymers. Amongst other things, the composition, end group, and molecular weight

of the final product can now be precisely controlled.[47,50,53,55–57,62–65] In addition to this, the facile modification of polymers can now be conducted *in-situ* or post-purification using a wide variety of synthetic pathways.[66,67]

1.5.1. Nitroxide mediated polymerisation (NMP)

Initially developed in 1985 by Solomon, Rizzardo and Cacioli,[68] nitroxide mediated polymerisation exploits the use of a stable and persistent free radical (such as a nitroxide, triazolinyl or dithiocarbamate) to afford control over the polymerisation.[12,13] As nitroxides are considered to be more efficient than other stable free radicals,[12] further discussion on NMP has referred to their involvement in the mechanism.

Following initiation, the nitroxide radical reacts rapidly to "trap" the propagating species and increase the concentration of dormant radicals within the system. In its "trapped" form, the end group is that of an alkoxyamine, and possesses a weak C-O bond which is capable of readily undergoing dissociation to regenerate the nitroxide and propagating chain.[69,70] This subsequently leads to the establishment of a dynamic equilibrium through the reversible trapping and release of propagating radicals (Scheme 1.7), which, providing that the formation of an alkoxyamine is favoured, generates a controlled polymerisation by minimising bimolecular termination.

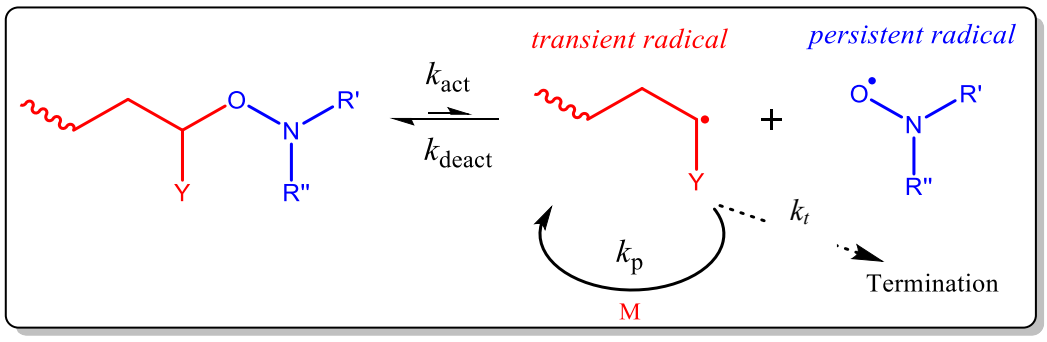

Scheme 1.7 – A condensed version of the mechanism of nitroxide mediated polymerisation (NMP), where the rate of activation k_{act}, rate of deactivation k_{deact}, and rate of termination k_t have been identified.

NMP is frequently used for the polymerisation of styrenic monomers[47,71,72] and is a desirable technique due to its simple purification procedures and absence of metal compounds. However, in contrast to others, it may be seen as an unattractive option; when NMP is conducted with 2,2,6,6-tetramethylpiperidinyl-1-oxy (TEMPO) acting as the persistent radical, high reaction temperatures (125 – 145 °C) and longer reaction times (1 – 3 days) are often required to obtain high yields when compared to other RDRP techniques.[12] Although the use of different alkoxyamines has helped to reduce the temperature down to ~40 °C,[73] other RDRP techniques are able to use reaction temperatures which are at ambient or below.[74,75]

1.5.2. Reversible addition–fragmentation chain transfer polymerisation and macromolecular design via interchange of xanthates (RAFT/MADIX)

One of the most versatile and refined RDRPs that currently exists is reversible addition fragmentation chain transfer (RAFT) polymerisation. First reported in 1998 by Moad, Rizzardo and Thang,[76] RAFT polymerisations have attracted considerable attention for the design of macromolecules comprising of an assortment of architectures (*i.e.* star polymers,[77–79] comb polymers,[77] multi-block co-polymers,[63,64,75,80] and bio-conjugates[4]) with predictable molecular weights and narrow MWDs.

Most commonly associated with the use of thiol-based compounds, the controlled nature of RAFT relies upon the establishment of a rapid equilibrium between the propagating radicals and a (polymeric) CTA.[55–57,76] RAFT polymerisations commence in a similar manner to “conventional” FRPs; with the generation of radicals ($I^{\bullet}$) from an initiating compound (Scheme 1.8). Upon their production, these radicals can either directly react with a CTA or react with a monomer (M) to form a propagating radical ($P_n^{\bullet}$). Once formed, the propagating radical is transferred to the

CTA to yield a polymeric CTA and another radical, R$^{\bullet}$. Through further reaction with monomer, this radical is then capable of reinitiating the polymerisation and upon doing so, forms a new propagating species ($P_m^{\bullet}$). The formation of $P_m^{\bullet}$ subsequently leads to the penultimate step of this mechanism; the establishment of a rapid equilibrium between the propagating radicals and the dormant polymeric RAFT agent.

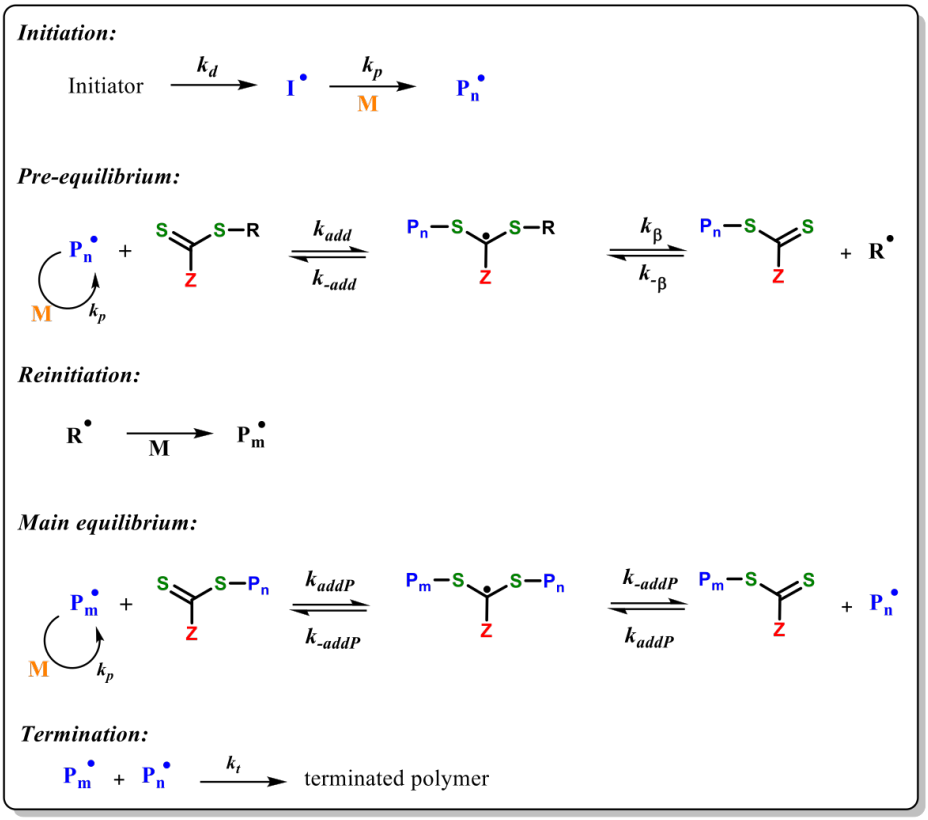

Scheme 1.8 – The proposed mechanism for RAFT where k_{add} is the addition rate constant, k_β is the β-scission rate constant, k_p the propagation rate constant, and k_t, the termination rate constant.

As with any polymerisation, chain growth will continue until either all of the monomer has been consumed, or until termination events (such as intentionally exposing the reaction to oxygen) arise. Importantly, the occurrence of radical-radical termination in RAFT polymerisations is low. This has enabled for high conversions and narrow MWDs to be readily obtained, as exemplified in the work conducted by Perrier and co-workers where complex and well-defined multiblock co-polymers have been synthesised in both aqueous and organic media.[63,64,75,81]

As a synthetic tool, RAFT is highly adaptable and can be used to polymerise a large pool of monomers which, unlike other techniques, is not restricted to the reactivity of the corresponding radical (*i.e.* whether they are formed from LAMs or MAMs). The accessibility of RAFT stems from being able to choose CTAs with activities that are appropriate to that of the propagating radical.[60,82,83] Usually, the highly "reactive" RAFT agents (such as the dithioesters or trithiocarbonates) are selected for the polymerisation of MAMs,[55–57] and the less "reactive" RAFT agents (those based on dithiocarbamates or xanthates) are selected for the polymerisation of LAMs.[84–88]

As most RAFT agents require a multistep synthesis, a polymer chemist is able to tailor its structure to their needs. When designing the CTA, the R group must, alongside remaining reactive with the polymeric CTA, be a sufficiently good leaving group to generate the formation (and re-initiation) of R$^{\bullet}$.[82,83,89] This ensures that the intermediate species in the pre-equilibrium can be re-established after reaction with monomer occurs. Likewise, the Z group (which acts in a similar manner) must balance possessing enough stability to ensure that radical addition to the C=S bond arises, without being too stable such that fragmentation from the intermediate species during the main equilibrium is hindered.[83,89] Resultantly, with the addition-fragmentation process limiting the number of active radicals present in the system, RAFT is characterised as a controlled radical polymerisation despite the free radical initiation.

Whilst RAFT is undoubtedly a sophisticated technique with clear advantages (its simplicity, the lack of metal catalyst, and compatibility towards a range of conditions being amongst them), there are still some pitfalls which need to be addressed. The most obvious of these is that despite the commercial availability of RAFT agents steadily increasing within recent years, many CTAs can only be acquired through a multistep synthesis.[89] As such, it is seen as an unattractive option to chemists who are averse to synthetic chemistry. Furthermore, the chosen CTA can introduce a

pink (in the case of dithioesters) or yellow (trithiocarbonates) discolouration to the final product and therefore, is problematic for some applications. In a similar way, the presence of a thioester group at the end of a polymerisation can be detrimental to industrial use (particularly for personal care applications) as its decomposition results in sulphur compounds with unpleasant odours.[12,13] Consequently, in comparison to other controlled radical techniques, an extra synthetic step (such as using AIBN to remove dithiobenzoate end groups from poly(methyl methacrylate) (PMMA)[67,83]) is required before the polymer is commercially viable. Recently, steps have been taken to develop a sulphur-free RAFT polymerisation[90,91] which, if commonly used, would negate this disadvantage.

1.5.3. Transition metal mediated–living radical polymerisation (TMM-LRP)

Transition metal species have found frequent use in organic chemistry as catalysts for the formation of carbon-carbon bonds and the addition of halogens to olefins in a reaction known as atom transfer radical addition (ATRA)[92]) (or the Kharasch reaction[93]). More recently, these metal species have also been employed as efficient mediators in a subset of RDRPs known as transition metal mediated-living radical polymerisations (TMM-LRPs). There are currently two main techniques which fall under this category: ATRP and SET-LRP.

Since their development, both of these systems have proven to be very effective synthetic tools due to their versatility, simple polymerisation procedures, and adaptability to a range of chemical environments. Indeed, the resourcefulness of ATRP and SET-LRP has allowed for the polymerisation of a wide variety of MAMs.[49,50] However, unlike other methods, the polymerisation of LAMs with TMM-LRPs is problematic due to the difficulty with respect to radical generation, and the instability of the resulting radical upon its formation.[94,95] Yet, despite this, transition

metal-mediated polymerisations are, particularly in the academic community, amongst two of the most widely employed methods for the synthesis of well-defined polymers.

1.5.4. Atom transfer radical polymerisation (ATRP)

The first technique to utilise transition metal complexes as a means of regulating polymerisations was that of ATRP, which was discovered independently by Sawamoto[96] and Matyjaszewski *et al.*[97] in 1995. In the initial work conducted by Sawamoto, ruthenium$^{(II)}$ based catalysts such as [$RuCl_2(PPh_3)_3$] were used for the successful and controlled polymerisation of methyl methacrylate.[96] In comparison, the alternative work by Matyjaszewski focused on the use of copper$^{(I)}$ based catalysts which, due to their success and relatively low cost, have been used almost ubiquitously in ATRP reactions to date.[50,97] Nevertheless, the catalytic system for ATRP has expanded since its conception and now includes a plethora of other transition metals which are capable of mediating the polymerisation; to a lesser degree of success when compared to copper, these include molybdenum,[98,99] palladium,[100] iron,[101–105] and nickel.[106,107]

In order to conduct a successful ATRP, an alkyl-halide initiator (I-X), a ligand (L), and a transition metal halide compound ($TM^{(n)}X$) are required, alongside a vinyl/acrylic monomer.[50] Once combined, the $TM^{(n)}X$ will co-ordinate with the ligand to form a transition metal complex, $TM^{(n)}X/L$. In its lowest oxidation state, this complex acts as an activating species to generate a propagating radical upon halogen abstraction (*via* an inner sphere electron transfer (ISET) mechanism) from I-X, and is in itself, oxidised ($TM^{(n+1)}X_2$). However, in its highest oxidation state, this complex takes the role of a deactivating species and works to render the propagating radical dormant by “capping” it with the abstracted halogen atom

following its reaction with monomer (k_p). This results in the reformation of the original complex and a species which can be re-activated by halogen transfer.[50] The "capping" and "uncapping" of the growing chain establishes a dynamic equilibrium between the dormant and active species which is critical to achieving a controlled polymerisation (Scheme 1.9).

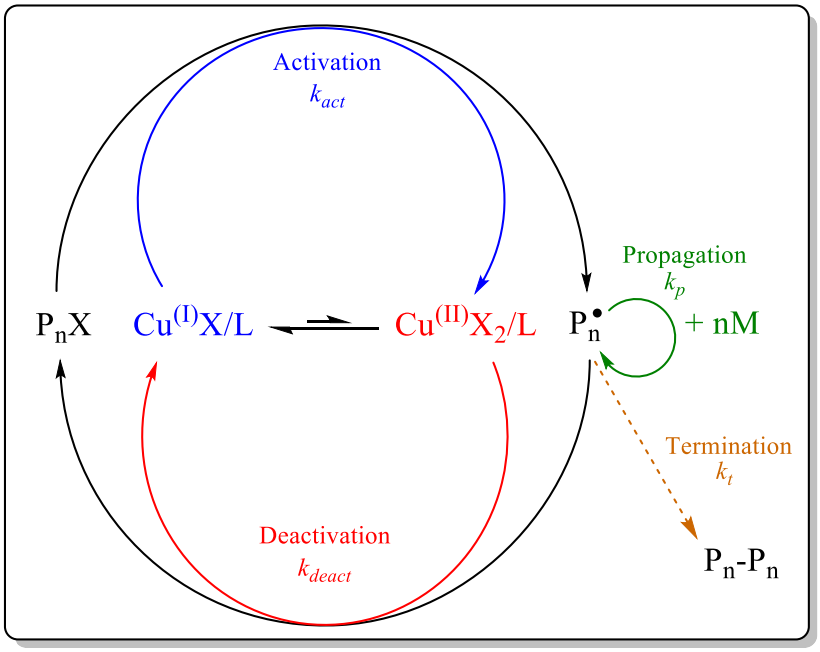

Scheme 1.9 – The posited mechanism for atom transfer radical polymerisation (ATRP) using a copper halide as the transition metal species. k_t represents the rate of termination, k_p the rate of propagation, k_{deact} the rate of deactivation, and k_{act}, the rate of activation.

Unlike a completely "living" system, termination events in RDRP techniques are inevitably present. In ATRP, bimolecular termination is likely to be encountered within the early stages of the reaction as a consequence of insufficient concentrations of the deactivating species. The resulting absence of radical trapping causes a slight excess of the deactivating species to be generated through a phenomenon known as the persistent radical effect (PRE) (Scheme 1.10).[108–110] Whilst a small amount of termination may sound undesirable, the PRE allows for greater control over the polymerisation as the equilibrium tends towards the formation of the dormant species. When combined with the ability for re-initiation through the retention of terminal-halide groups, ATRP is described as pseudo-living.

$$P_n\text{-}X + Cu^{(I)}X \underset{k_{deact}}{\overset{k_{act}}{\rightleftharpoons}} P_n^{\bullet} + Cu^{(II)}X_2$$

$$P_n^{\bullet} + nM \xrightarrow{k_p} P_{n+m}^{\bullet}$$

$$\mathbf{2P_n^{\bullet} + Cu^{(II)}X_2 \xrightarrow{k_t} P_n\text{-}P_n + (accumulation)\, Cu^{(II)}X_2}$$

Scheme 1.10 – Outline of the persistent radical effect (PRE) observed in the beginning of ATRP.

The main disadvantage of ATRP is generally accepted as being the use of a transition metal compound. This is particularly the case for copper-mediated ATRP where the potential/perceived toxicity and colour of this metal and its complexes make it unsuitable for a number of applications. To negate this issue, two low metal catalyst systems have been designed; these are initiators for continuous activator regeneration (ICAR-ATRP)[111] and activators regenerated by electron transfer (ARGET-ATRP).[112–114]

Along a similar vein is the recent metal-free ATRP system which was published by Hawker and Fors in 2014.[115] This approach uses light as an external stimulus for the activation and deactivation of propagating chains. The success of this system is attributed to a key component, 10-phenylphenothiazine (PTH), which adopts the same role as the $Cu^{(I)}$Br/ligand complex in conventional ATRP systems.

PTH is able to act as an effective mediator for the polymerisation as radicals can only be produced from this species when it is exposed to light. By utilising an "on-off" approach, narrowly disperse polymers with predictable molecular weights can be obtained. Whilst there is no mention of a method for removing PTH from the resulting polymers, the reaction conditions state that only 10 ppm of catalyst is required for the reaction to succeed.

1.5.5. Single electron transfer–living radical polymerisation (SET-LRP)

A second method through which a TMM-LRP can be conducted was developed by Percec *et al.* in 2006.[116] This system is based on his previous work with transition metal catalysed polymerisations of vinyl chloride (VC),[117] and single electron transfer – degenerative chain transfer living radical polymerisation (SET-DTLRP).[118] Termed single electron transfer – living radical polymerisation (SET-LRP), the "ultrafast" synthesis of PVC and poly(acrylates) at ambient temperature in polar media, were the first polymerisations to be reported using this technique.

SET-LRP bears many semblances to its predecessor, ATRP, in that it relies upon the foundation of a dynamic equilibrium amid the active and dormant chains in a reversible radical trapping process. However, unlike ATRP, the active catalyst is reported to be $Cu^{(0)}$ rather than $[Cu^{(I)}X/L]$ and, as such, a different mechanism for polymerisation was proposed (Scheme 1.11).[52]

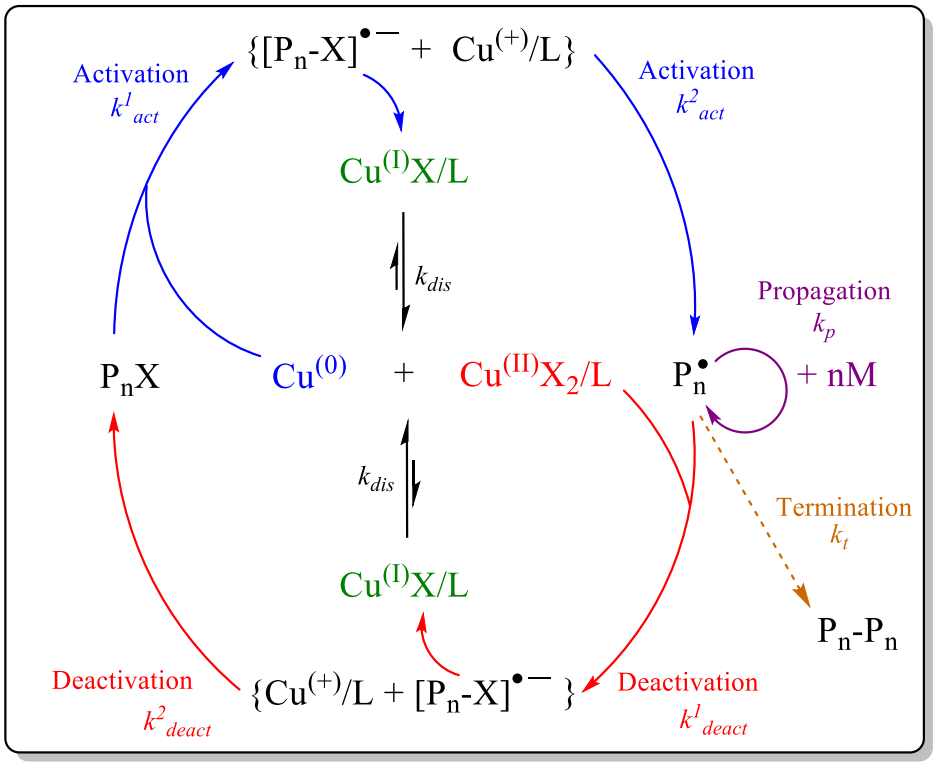

Scheme 1.11 – The mechanism for single electron transfer - living radical polymerisation (SET-LRP) as proposed in reference 52; where k_t represents the rate of termination, k_p the rate of propagation, k_{deact} the rate of deactivation, k_{act} the rate of activation and k_{dis} the rate of disproportionation.

In a manner not dissimilar to that of ATRP, $Cu^{(0)}$ (in the form of copper powder, copper wire, or indeed a copper coin)[119,120] reversibly extracts a halogen atom from the dormant species to form an active radical (which can directly propagate with monomer) and $[Cu^{(I)}X/L]$ (k_{act}). This abstraction occurs *via* an outer sphere electron transfer (OSET) process and subsequently results in the production of a radical anion intermediate prior to decomposition into $P_n^{\bullet}$. The formation of $[Cu^{(I)}X/L]$ following activation leads to the key step cited by this proposed mechanism; the spontaneous and fast disproportionation of "*in-situ*" $[Cu^{(I)}X/L]$ to generate "nascent" $Cu^{(0)}$ and the deactivating species, $[Cu^{(II)}X_2/L]$.[52,121] Reformation of the dormant chains (P_nX), due to the 'capping' of the propagating radical by the deactivating species, leads to the production of $[Cu^{(I)}X/L]$ and hence the continuous regeneration of the catalytic species.

As mentioned previously, a successful SET-LRP can only be achieved with the rapid disproportionation of $[Cu^{(I)}X/L]$ into $Cu^{(0)}$ and $[Cu^{(II)}X_2/L]$. In its absence, a polymerisation cannot be regulated due to an insufficient quantity of the deactivating species. It has been proposed by Percec that through disproportionation, 1/2 an equivalence of $Cu^{(II)}X_2$ and $Cu^{(0)}$ are regenerated for every equivalence of $Cu^{(I)}X$ and vice versa.[52] This regeneration subsequently removes the need for the PRE to infer control as $Cu^{(II)}X_2$ is formed instantaneously "*in-situ*".

There are a few factors which affect disproportionation, and by proxy, the polymerisation system as a whole. SET-LRP is a multicomponent technique and much like the selection of a CTA in RAFT, the choice of solvent, ligand, and monomer, are critical to its success.[52,53] Therefore, an understanding of the role that the individual components play upon this system is an important factor which needs to be discussed.

1.5.5.1. Factors affecting single electron transfer – living radical polymerisation (SET-LRP): choice of metal catalyst

An integral component of SET-LRP (and ATRP) is the choice of transition metal catalyst, as its main role is to establish a dynamic equilibrium between the dormant and active species within the system. In order for a TM catalyst to be effective there are three pre-requisites:[13]

1) It must have at least two readily available oxidation states which are separated by formal oxidation. This means that the metal centre is able to undergo redox reactions whereby it is oxidised from its lower state (Mt^n) to its higher state (Mt^{n+1}) and, following the acceptance of a halide, is then reduced back to its original form.

2) It needs to be able to form a reasonably strong complex with a ligand.

3) It must be capable of efficiently abstracting a halogen atom from the inactive polymer chains during the activation step.

Within the early years of SET-LRP, the choice of metal catalyst was restricted to zero-valent copper species and its derivatives. However, unfortunately, the perceived toxicity of copper meant that at the time of its development, the system was incompatible with biological and industrial applications. As a consequence of this, research focus shifted slightly to more “friendly” metal catalysts such as iron which is a relatively inexpensive, non-toxic, and biocompatible metal. To date, iron catalysts have been employed for the polymerisation of styrene,[122] acrylonitrile[123,124] and methyl methacrylate.[125] Impressively, the choice of catalyst does not end here; there have been reports of nickel,[126] ytterbium,[127] lanthanum,[128] gadolinium,[129] tin,[130] magnesium[131] and samarium[132] successfully mediating SET-LRP.

1.5.5.2. Factors affecting single electron transfer – living radical polymerisation (SET-LRP): choice of initiator

Initiators are primarily used in all of the aforementioned techniques to start the polymerisation process upon their decomposition to free radicals. In TMM-LRPs, the initiating species is also used to facilitate the chain growth of polymers at a constant rate from time zero. For RDRP systems, this is an especially important factor as an efficient initiator is imperative to obtaining narrow MWDs. Initiation should therefore be quantitative, with each unit propagating to the targeted degree of polymerisation. In RDRPs, the degree of polymerisation can easily calculated from ^{1}H NMR spectroscopy (Equations 1.36 to 1.38).

$$DP_n = \frac{concentration\ of\ consumed\ monomers}{concentration\ of\ polymer\ chains} \quad \textbf{(Equation 1.36)}$$

$$DP_n = \frac{[M]_0 - [M]_t}{[P]} \quad \textbf{(Equation 1.37)}$$

$$[P] = f[I]_0 \quad \textbf{(Equation 1.38)}$$

Equation 1.36 to 1.38 - An expression used to calculate the degree of polymerisation (DP_n) for a RDRP. Where $[M]_0$ is the concentration of monomer at time zero, $[M]_t$ the concentration of monomer at time t, [P] the concentration of polymer chains, f the initiator efficiency, and $[I]_0$ the concentration of initiator at time zero.

As with any contributing feature in a reaction, there are numerous factors which influence the effectiveness of an initiator and consequently, the polymerisation system itself. Perhaps the most important of these factors is that the rate of initiation must be greater than, or at an absolute minimum be equal to, the observed rate of propagation. This ensures that the active species are formed at the same time throughout the reaction and, as a result, minimises the difference between individual chain lengths.

In SET-LRP (or indeed ATRP), the initiator can be selected from a vast array of organic halogenated compounds. Typically, alkyl-halide initiators which possess a

bromine end group, such as methyl bromopropionate (MBP)[133–135] and ethyl 2-bromoisobutyrate (EBiB),[62,136–138] are those which are most commonly employed. The use of mono-functional initiators such as these has been well researched and, when used, frequently yield highly controlled polymers; however, there are numerous applications for which they are not suitable. For example, in cases where α,ω-telechelic polymers are desired, bifunctional initiators such as bis(2-bromopropionyl)ethane (BPE)[139–141] are utilised and allow for the synthesis to be conducted with relative simplicity. For alternative architectures to these, low dispersity star polymers can be produced through the use of a multi-armed initiator.[62,142–144]

The structure of a typical organic halide initiator is generally portrayed as R-X, where R is an alkyl group and X is a halide (predominantly Br or Cl).[52] In both TMM-LRPs, successful initiators have been shown to be those which have the C-X bond adjacent to an electron withdrawing moiety such as a carbonyl group. The presence of such a group helps to activate the C-X bond by delocalising the local electron cloud and increasing its polarity. As a consequence, a more stable radical is created upon the abstraction of a halogen.[11,17]

The stability of a radical following initiator decomposition plays an important role in determining the rate of a polymerisation. In the case of alkyl-halide initiators, radical stability can be directly correlated to the relative inductive effect of the R group adjacent to the electron withdrawing moiety. Substituents which have a greater inductive effect can more easily donate electron density to this group and hence make the corresponding radical more reactive (less stable) towards propagation. However, if the stabilisation effect of a substituent is too strong, the bond dissociation energy (BDE) for R-X is too high, and consequently results in poor initiator efficiency, or possibly, a complete lack of polymerisation.[145–147] BDE is the enthalpy change required to break a bond; the lower the BDE, the more easily a

radical ion pair is formed. To relate this in a practical example, the greater inductive effect of nitrogen when compared to oxygen explains why initiating (or in fact monomeric) species based on amides undergo propagation at a much faster rate when compared to their ester counterparts.

In addition to this, resonance effects can affect radical stability (Figure 1.3).

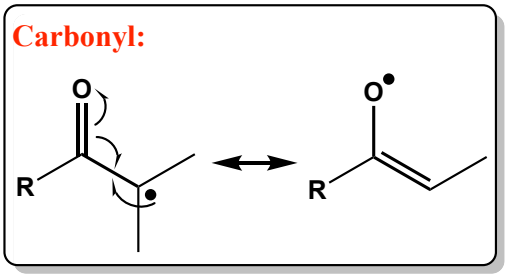

Figure 1.3 – The resonance structures for the carbonyl moiety with the radical species.

In the case of acrylamides and acrylates, lone pairs on the adjacent nitrogen and oxygen respectively can delocalise into the carbonyl moiety. The extent to which this occurs in amides is such that they are structurally planar (Figure 1.4).[11] For esters, owing to the great electronegativity of the oxygen, the preferred structure is over to the left hand side (Figure 1.4).[11]

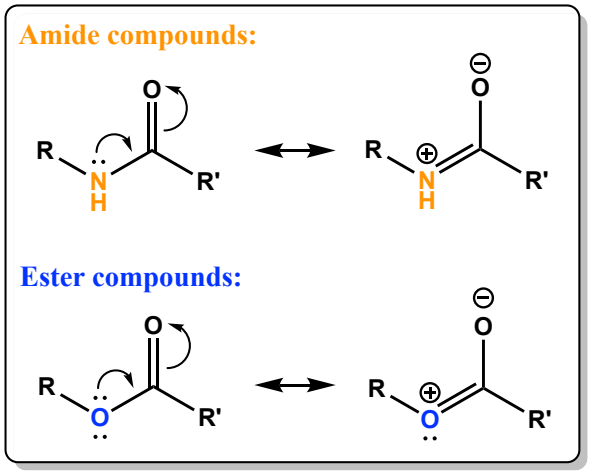

Figure 1.4 – The resonance structures for acrylamide and acrylate-based compounds.

As the carbonyl (or electron-withdrawing) moiety is in resonance with either the nitrogen or the oxygen, it is less available to stabilise the resulting radical through

resonance. Since this effect is more pronounced for amides, radicals that are generated from amide-based initiators propagate faster than those which are formed from esters.

When choosing an initiator for SET-LRP, the strength of the carbon-halogen bond is also a factor which should be taken into consideration. It has long been established that C-Cl bonds are stronger than C-Br bonds and thus have a higher BDE.[148] As a result, polymerisations which are initiated by alkyl-chlorides tend to have a slower k_i in comparison to those which are initiated by their comparable bromine derivative.[148] Therefore, in cases where $k_i > k_p$, a chloro-initiator may be used to regain control.

1.5.5.3. Factors affecting single electron transfer – living radical polymerisation (SET-LRP): choice of monomer

To date a large assortment of monomers have been successfully polymerised using SET-LRP. As with all radical polymerisations, suitable monomers are compounds which possess a vinyl group and are capable of forming free radicals upon initiation.[52,54] Typically, SET-LRP requires a monomer which has an electron withdrawing group conjugated to the vinyl group (MAM);[52,54] this ensures that radicals are formed with relative ease upon initiation and subsequent activation of dormant polymer chains. Radicals which are formed from MAMs have a low enough reactivity such that they can be rapidly "trapped" prior to radical-radical coupling.

Conversely, the polymerisation of monomers which are non-conjugated (LAMs) has proven to be a challenge for the same reasons as they have with ATRP; that is, a combination of the difficulty in forming the corresponding radical, and the reactivity that their radicals exhibit. Often, the activation of LAMs results in radicals which are highly reactive and therefore, readily undergo bimolecular termination or chain transfer to anything with an available transfer site.[149–151]

In addition, the polymerisation of electrolytic monomers (*i.e.* those with a pendant anionic or cationic group) has also proven to be problematic v*ia* TMM-LRPs.[53,54,152] Such monomers are capable of undergoing ligation to the metal centre, and result in the formation of a complex which tends towards the stabilisation of $Cu^{(I)}Br$.[153] This ultimately gives rise to catalyst deactivation and thus results in a loss of control over the polymerisation process. Similarly, as the monomer is often present in a large excess in comparison to the ligand, there is an insufficient quantity of catalyst which is able to effectively mediate the polymerisation. To a degree, it is possible to overcome this by using a salted form of the monomer; the addition of a counter-ion reduces the number of available binding sites on the monomer and consequently enables a complex to be formed between the metal centre and the preferred ligand.[153–155]

In a similar vein, TMM-LRPs cannot currently be conducted in the presence of significant amounts (> 10 %) of acid as the catalyst becomes poisoned without the use of a buffer.[156] This causes further problems when the polymerisation of electrolytic monomers is desired as they are often acidic in nature and can result in the dissociation of the copper/ligand complex through ligand protonation.[157,158] However, providing that the system is not at a low pH to begin with, using the salted form of the monomer prevents this from occurring as proton transfer reactions can no longer arise.

1.5.5.4. Factors affecting single electron transfer – living radical polymerisation (SET-LRP): choice of ligand

In SET-LRP, one of the main roles of the ligand is to create a metal complex which is soluble in the desired reaction medium such that efficient atom transfer and disproportionation is promoted.[52,53,59] As with the choice of solvent, the latter of

these is achieved through the use of ligands which do not promote the stabilisation of the $Cu^{(I)}X$ species. Through the careful selection of an appropriate ligand, the activation and deactivation processes can be adapted to suit the activity of the monomer and hence, enable regulated chain growth. When unsuccessful combinations of metal centres and ligands are used, undesirable chain termination events inevitably arise within the early stages of the polymerisation.[52,53,140,159]

The choice of an appropriate ligand relates to their relative reactivities as well as the overall reactivity of the metal complex. In TMM-LRPs, ligands are commonly divided into two categories: "less active", such as bipyridine (bpy) and pyridine-imines, and "more active", such as Me_6TREN, PMDETA and Cyclam. Catalysts which are described as being "active" are those which contain strong σ-donating ligands that preferentially stabilise the metal centre in its highest oxidation state ($Cu^{(II)}$).[160] These ligands are typically selected for the polymerisation of acrylates and acrylamides (*i.e.* high k_p monomers) (Table 1.1).[120,142,161–163]

In contrast to this, catalysts which are described as being "less active" are those which involve ligands that contain π-orbitals and are able preferentially stabilise the metal centre in its transitional state ($Cu^{(I)}$). When complexed, these ligands donate their σ-electron density into the metal centre in addition to accepting electron density into their low lying π^*-orbitals in a process known as back-bonding.[164] "Less active" ligands have been shown to be more suitable for the polymerisation of monomers with a low k_p (Table 1.1).[97,160,165] However, there are exceptions to this rule as the polymerisation of methacrylates and styrene has proven to be well controlled in the presence of "more active" ligands such as tris(2-pyridylmethyl)amine (TPMA)[113] and PMDETA (Table 1.1).[59,166,167]

Monomers → / Ligands ↓	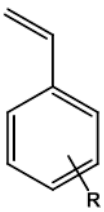	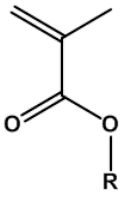	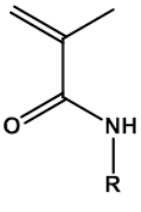	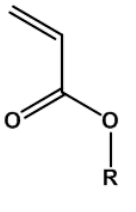	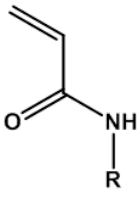
Cyclam derivatives					
PMDETA					
Me_6TREN					
HMTETA					
TPMA					
Bpy derivatives					
Pyridine-imine					

Table 1.1 - A summary of some of the successful (green) and unsuccessful (grey) ligand and monomer combinations used in TMM-LRPs. The ligands highlighted in blue represent σ-donors, those highlighted in red represent π-acceptors and those in orange represent both.

In a paper published in 2008, Matyjaszewski summarised the relative reactivities of the different ligands.[160] Whilst the exact values only hold true for ATRP polymerisations conducted in acetonitrile, the overall trend can still be applied to other solvent systems and to polymerisations which follow the SET-LRP protocol. In general, the reactivity of ligands decreases in the order of: tetradentate (cyclic-bridged) > tetradentate (branched) > tetradentate (cyclic) > tridentate > tetradentate (linear) > bidentate (Figure 1.5).[160]

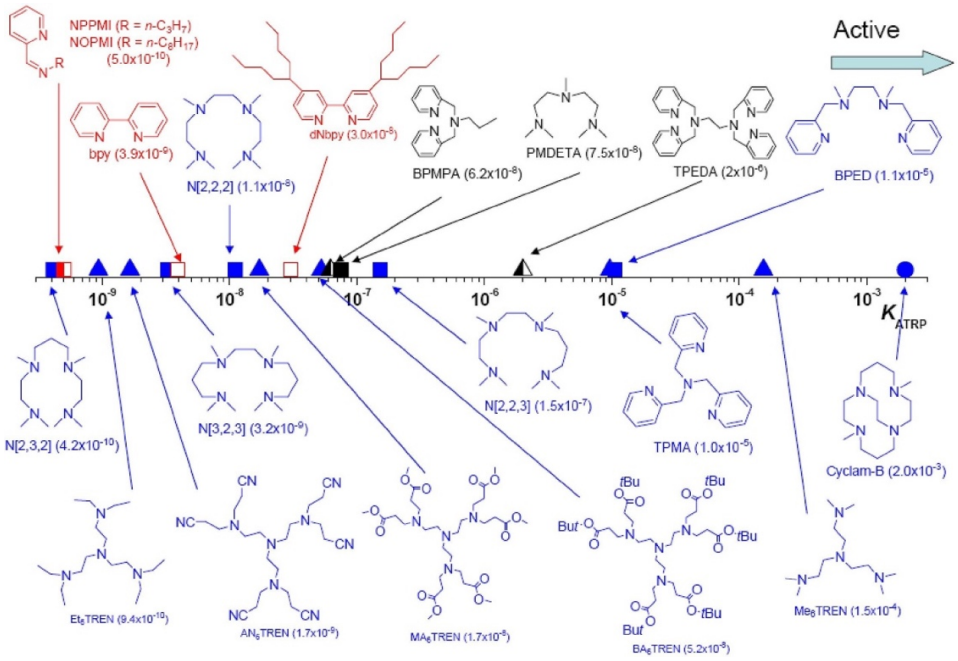

Figure 1.5 – A schematic representation of the change in catalyst activity as a result of ligand selection as shown in reference 160.

1.5.5.5. Factors affecting single electron transfer – living radical polymerisation (SET-LRP): choice of solvent

It has been claimed by Percec that the key step in SET-LRP is the disproportionation of $Cu^{(I)}Br$ generated during the activation of the alkyl-halide initiator by $Cu^{(0)}$.[52,121] In polar media, $Cu^{(I)}$ is highly unstable with respect to oxidation, and consequently rapidly undergoes disproportionation despite retaining a full complement of d-electrons (d^{10}). When combined with the correct choice of ligand and monomer, ideal SET-LRP conditions use a solvent which favours disproportionation and which does not stabilise the $Cu^{(I)}X$ species.[121]

Currently, the most common organic solvent used for SET-LRP is dimethyl sulfoxide (DMSO) which, due to its high polarity, makes it an attractive solvent choice for SET-LRP as it aids electron transfer.[54] Furthermore, DMSO is able to co-ordinate to, and stabilise, the $Cu^{(II)}$ species such that disproportionation is facilitated through a shifting of the equilibrium. Indeed, when polymerisations are conducted in this medium, first-order kinetics are obtained alongside the retention of near-quantitative end group functionality.[53,54]

As with most RDRP techniques, the choice of solvent in SET-LRP is not restricted to DMSO; alcohols such as isopropanol (IPA),[168] ethanol (EtOH),[169] and even fluorinated alcohols[133,134,170] have been successfully used as polymerisation media. It is worth mentioning that control over the polymerisation diminishes upon increasing the hydrophobicity of the reaction medium; an increase in the hydrophobic character of the solvent results in a decrease in the polarity of the medium, a reduction in the extent of disproportionation, and hence, a decrease in k_p.[52]

1.5.5.6. Single electron transfer – living radical polymerisation (SET-LRP) in aqueous media

A notable advancement to TMM-LRPs within recent years is the development of a protocol which enables SET-LRP to be conducted in aqueous media. Reported by Haddleton *et al.* in 2013, aqueous SET-LRP exploits the rapid and quantitative disproportionation of [$Cu^{(I)}Br/Me_6TREN$] into $Cu^{(0)}$ and [$Cu^{(II)}Br_2/Me_6TREN$] in water, prior to the addition of monomer and initiator (Scheme 1.12).[74] Reactions conducted under these conditions have been shown to proceed at a faster rate when compared to the alternative organic systems, and do so without any appreciable loss of control over the polymerisation process.[153,161,162,171]

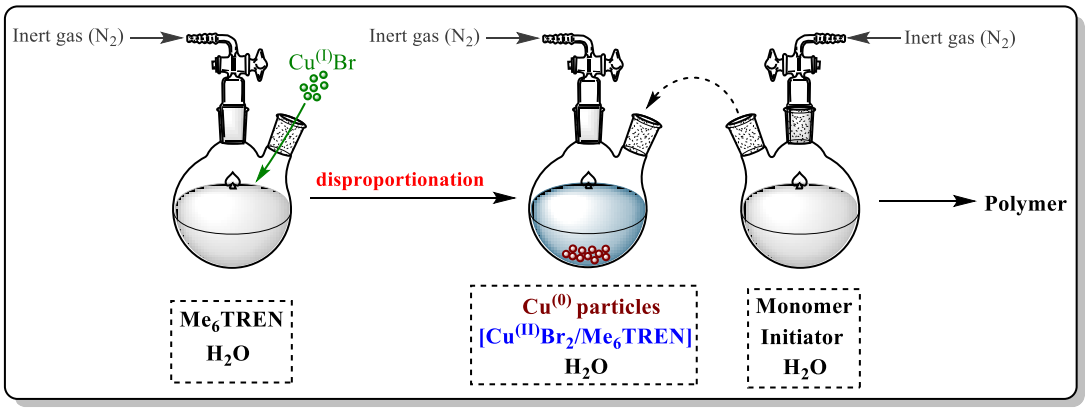

Scheme 1.12 – A diagrammatic representation of the aqueous single electron transfer - living radical polymerisation (SET-LRP) protocol.

Unlike SET-LRP conducted in organic media, a limitation of $Cu^{(0)}$-mediated aqueous polymerisations is the loss of chain end fidelity which arises from unwanted side reactions, and end group hydrolysis/substitution *via* a cyclic onium intermediate (Scheme 1.13).[171–174] The occurrence of these events, results in an increase in premature termination and as a consequence, leads to an increase in the dispersity of the final product. Through undertaking these polymerisations at low reaction temperatures, it has been found that these side reactions can be suppressed to such a degree whereby iterative and "*in-situ*" chain extensions can be facilely performed.[74,171]

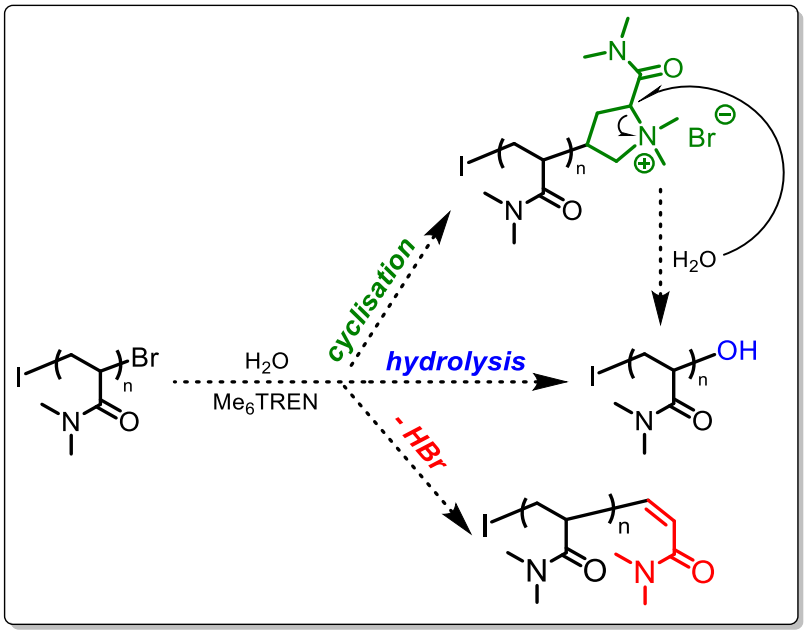

Scheme 1.13 – Modification of the halide end-group *via* cyclisation of the penultimate unit, hydrolysis and elimination of hydrobromic acid (HBr).

Despite the presence of side reactions, aqueous SET-LRP has proven to be a very robust tool for the synthesis of polymers through its application to more complex solvent systems including blood (sheep) serum,[175] phosphate-buffered saline (PBS),[74] and commercially available alcoholic beverages.[176] Remarkably, despite the presence of phenols, sugars and additives within this media, there is no noticeable diminishment in polymerisation control.

When the correct protocol is followed, aqueous SET-LRP permits a polymer chemist to polymerise (meth)acrylates[59,74,177] and acrylamides[74,162,171] to high conversion and narrow MWDs with relative ease; although a slight loss of control may still be observed for these monomers when there is an absence of external deactivating species.[59,166] Recently, it has been found that the addition of external halide salts such as sodium bromide (NaBr) can be used to combat this increase in dispersity.[166,178,179] In a similar way, the addition of tetraethylammonium bromide (TEABr) has been used to harness further control over a polymerisation when dissociation and/or denaturation of the copper/ligand complex occurs.[180]

Nevertheless, it is evident that copper-mediated LRPs are a powerful and resourceful synthetic tool. With regards to SET-LRP, the systems' tolerance towards impurities[176,181] and its adaptability to a range of conditions,[181] makes it a highly attractive option for the production of well-defined polymers. Indeed, through utilising this system, a vast range of monomers can be successfully polymerised.[52–54] For some of these, polymerisations can be conducted at low temperatures,[74] and in a variety of different vessels including UV nail lamps[178,182,183] and continuous flow reactors.[124,184,185]

1.5.5.7. Mechanistic debate

Conceptually, ATRP and SET-LRP are very similar to each other; they use the same components, polymerise the same monomers, and have similar limitations. Since the inception of the latter, these parallels have led to an ongoing debate which has dominated the literature and academic community.[186–196] The crux of this disagreement relates to the "true" mechanistic nature of the two techniques; or more specifically, whether or not SET-LRP is actually a variant of ATRP, or indeed if ATRP is actually a variant of SET-LRP known as supplemental activator and reducing agent – atom transfer radical polymerisation (SARA-ATRP). Currently, there are three main points of contention; these consist of the role of $Cu^{(0)}$ in the process, the route of activation, and the extent to which disproportionation occurs.

On one side of the argument, Percec and co-workers believe that the mechanism of SET-LRP follows activation by $Cu^{(0)}$, with the disproportionation of a $Cu^{(I)}$ species being key to providing control.[52] Matyjaszewski on the other hand, claims that the mechanism is closer to that of ATRP, with a $Cu^{(I)}$ species being the main activator, and $Cu^{(0)}$ being merely a supplementary activator in the early stages of the polymerisation.[194]

Considering the vast amounts of publications relating to this topic, it is clear that the "true" mechanism of polymerisation is complex, and may in fact prove to be an amalgamation of both concepts. Since the focus of this thesis is not to provide mechanism elucidation, the intricacies of the debate have not been covered in detail. Instead, an explanation of some of the key principles which are being disputed has been provided. Moreover, the specific mechanism of polymer formation is largely irrelevant to this thesis as ultimately, the polymers formed are the same; resultantly, for simplicities sake, the technique has been referred to as $Cu^{(0)}$-mediated RDRP throughout the following chapters.

1.5.5.7.1. Concept 1: supplemental activator and reducing agent – atom transfer radical polymerisation (SARA-ATRP)

At the very least, SARA-ATRP is considered to be a controlled radical polymerisation technique which is analogous to SET-LRP, as it is conducted using the same reagents: $Cu^{(0)}$, $[Cu^{(II)}X_2/L]$, a polar solvent, an alkyl-halide initiator, an amine ligand and a vinyl monomer.[197,198] The proposed mechanism however, differs to its counterpart in several fundamental aspects.

According to the postulated mechanism for SARA-ATRP (Scheme 1.14), polymerisation begins with the slow activation of an alkyl-halide initiator by $Cu^{(0)}$ in an ISET process, and results in the generation of an active radical. This radical is then capable of propagating with monomer, to generate an active polymer chain, before being reversibly "capped" with $[Cu^{(II)}X_2/L]$ to result in the formation of a dormant species. As with other RDRP mechanisms, this dormant species can then be re-activated and hence further polymerised, until either the monomer has been completely consumed or termination events arise.[194]

Additionally, the mechanism portrays disproportionation as having a minimal role in this system; instead, its reverse reaction (comproportionation) is said to be the prevalent process.[186,194] Providing that the ligand is present in excess, comproportionation of [$Cu^{(II)}X_2$/L] and $Cu^{(0)}$ dominates over the disproportionation of [$Cu^{(I)}$X/L]. This subsequently means that near exclusive activation of dormant chains is initiated by [$Cu^{(I)}$X/L] rather than $Cu^{(0)}$ in SARA-ATRP polymerisations.[194]

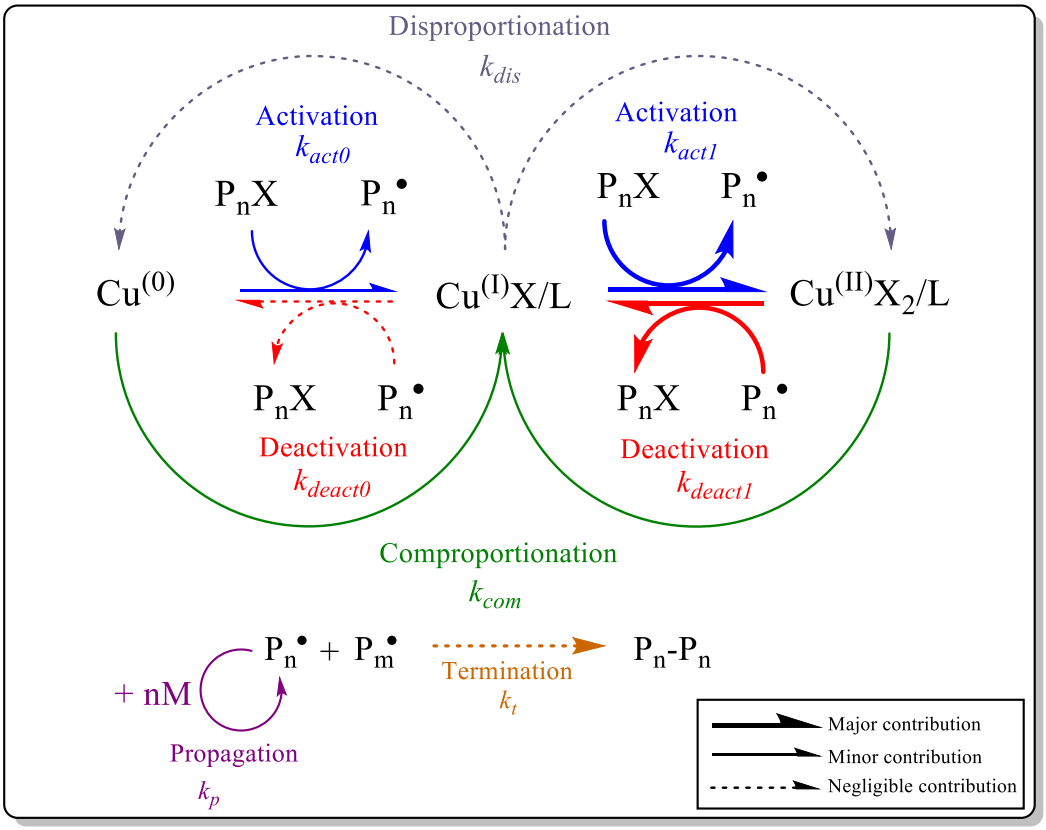

Scheme 1.14 – The proposed mechanism of supplemental activator and reducing agent – atom transfer radical polymerisation (SARA-ATRP) where k_t represents the rate of termination, k_p the rate of propagation, k_{deact} the rate of deactivation, k_{act} the rate of activation, k_{com} the rate of comproportionation and k_{dis} the rate of disproportionation.

As SARA-ATRP is a variation upon the "traditional" ATRP approach, the PRE effect is observed within the early stages of the reaction. This leads to an increase in the concentration of [$Cu^{(II)}X_2$/L] upon radical termination, and therefore means that all [$Cu^{(I)}$X/L] in the system is irreversibly oxidised.[190] At this point, the second and most important role of $Cu^{(0)}$ comes into play. Following the initial activation, $Cu^{(0)}$ acts as a reducing agent and converts [$Cu^{(II)}X_2$/L] into the main activator of polymer chains,

[$Cu^{(I)}X/L$].[190] The resulting production of [$Cu^{(I)}X/L$] means that activation by $Cu^{(0)}$ is no longer required, and as such, its role becomes solely that of a reducing agent.

For ease of comparison, a summary of the key differences between "traditional" ATRP, SARA-ATRP, and SET-LRP has been provided in Table 1.2.

Process	Traditional ATRP	SARA-ATRP	SET-LRP
Activation by $Cu^{(I)}$	Main activation pathway	Main activation pathway	Does not occur due to disproportionation
Activation by $Cu^{(0)}$	Does not occur	Supplemental	Exclusive
Activation mechanism	Inner sphere electron transfer (ISET)	Inner sphere electron transfer (ISET)	Outer sphere electron transfer (OSET)
Deactivation by $Cu^{(II)}$	Main deactivation pathway	Main deactivation pathway	Main deactivation pathway
Disproportionation of $Cu^{(I)}$	Minimal contribution	Minimal contribution	Instantaneous and complete
Comproportionation between $Cu^{(II)}$ and $Cu^{(0)}$	Does not occur	Occurs under certain conditions to compensate for termination	Does not occur
Radical termination	Occurs early on in the reaction	Occurs early on in the reaction	Minimal
Reagents	Same components used		

Table 1.2 – A comparison of "traditional" ATRP, SARA-ATRP and SET-LRP as proposed by the relevant inventors.[52,97,190]

1.5.5.7.2. Concept 2: electron transfer mechanisms

Electron transfer reactions are those which involve the relocation of an electron from one species to another. There are two routes through which this can occur: inner sphere electron transfer (ISET), and outer sphere electron transfer (OSET).[50] In

relation to ATRP and SET-LRP, the main distinction concerning the two mechanisms is determined by whether or not a halide species forms a bridge between the transition metal centre and the dormant chains.

In the case of ISET, electron transfer occurs in a concerted manner upon the activation of chains, and results in the formation of an active radical and an oxidised metal species.[50,164] Upon activation, the metal centre donates an electron to the dormant chain at the same time as a halogen atom is transferred to the metal centre (Scheme 1.15). This results in the formation of a transition state in which the two reactants are bridged by a halogen.

OSET on the other hand, comprises of an exchange of electrons between the metal centre and the dormant chains without the components interacting in any significant manner (Scheme 1.15).[50,164] As with ISET, this leads to the generation of an active radical and an oxidised metal species.

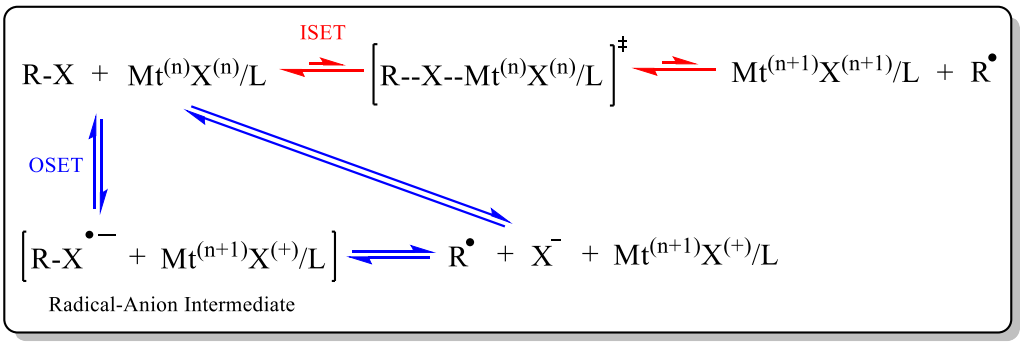

Scheme 1.15 - A summary of the OSET and ISET process.

In relation to the current proposed mechanisms for polymerisation, the alkyl-halide initiator and the dormant polymer chains in ATRP undergo ISET from the $Cu^{(I)}X/L$ complex to form the deactivator ($[Cu^{(II)}X_2/L]$), and a radical capable of propagating (Scheme 1.16).[50] In SET-LRP, the alkyl-halide initiator undergoes OSET from the $Cu^{(0)}$ activator to form a radical anion intermediate which rapidly decomposes into $[Cu^{(I)}X/L]$ (Scheme 1.16).[52] Subsequent disproportionation leads to the (re)generation of the deactivating and activating species.

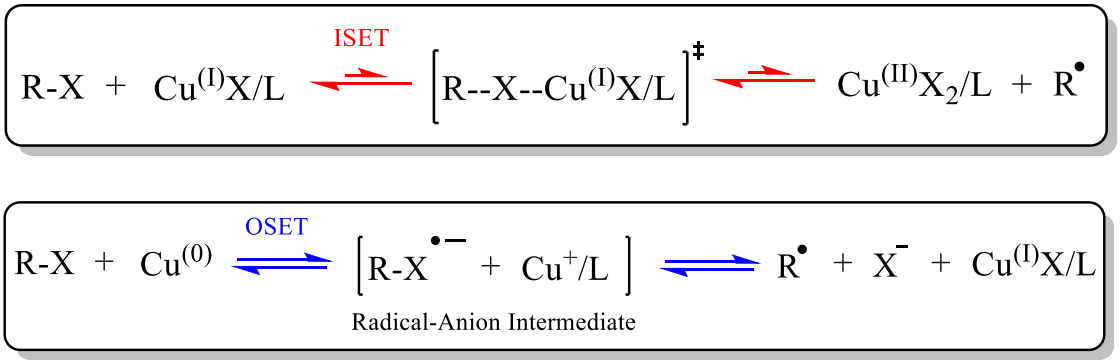

Scheme 1.16 - Outline of the ISET process as it relates to ATRP (above) and the OSET process as it should relate to SET-LRP (below).

1.5.5.7.3. Concept 3: disproportionation and comproportionation

$Cu^{(I)}X$ salts are generally considered to be unstable in aqueous solutions as they readily undergo a process known as disproportionation. Disproportionation is a redox reaction in which a species (in this case $Cu^{(I)}X$) is simultaneously oxidised and reduced by itself (Equation 1.39).[164]

$$2Cu^{(I)}X \overset{k_{dis}}{\rightleftharpoons} Cu^{(0)} + Cu^{(II)}X_2$$

Equation 1.39 – A representation of the key step in SET-LRP: the disproportionation (k_{dis}) of $[Cu^{(I)}X/L]$ into the activating species $Cu^{(0)}$ and the deactivating species $[Cu^{(II)}X_2/L]$ in polar solvents.

In the reverse reaction, termed comproportionation or symproportionation, the same element in two different oxidation states undergoes a redox reaction to form the element which has an intermediate (or transitional) oxidation state (Equation 1.40).[164]

$$Cu^{(0)} + Cu^{(II)}X_2 \overset{k_{com}}{\rightleftharpoons} 2Cu^{(I)}X$$

Equation 1.40 - Representation of the comproportionation (k_{com}) of $Cu^{(0)}$ and $[Cu^{(II)}X_2/L]$ into $[Cu^{(I)}X/L]$.

1.5.5.7.4. Concept 4: principle of halogen conservation (PHC)

One of the counter-arguments to the mechanism of SET-LRP is that it violates the principle of halogen conservation (PHC).[188,199] The PHC states that from the beginning to the end of the reaction, the quantity of halogens (X) must remain constant within the system.[199] Therefore, any loss of halogen functionality from a compound involved in a either of these two techniques must result in the transference of X to another species. Conversely, any formation of $[Cu^{(I)}X/L]$ or $[Cu^{(II)}X_2/L]$ must be accompanied by a loss of halogen-capped chain ends.

Experimentally, in both ATRP and SET-LRP, termination events inevitably arise as a result of bimolecular termination and other similar reactions. In ATRP, this is purported to occur at the beginning of a polymerisation and, as a result, leads to the PRE.[190] For this reason, ATRP obeys the PHC through an increase in the concentration of $[Cu^{(II)}X_2/L]$ upon the occurrence of termination and subsequent loss of halogen chain ends. Consequently, this enables the degree of termination to be quantified by simply following the change in concentration of the oxidised metal species.[199]

SET-LRP, on the other hand, is reported to contradict the PHC through claiming that a build-up of deactivating species does not occur upon the loss of chain end functionality.[190,199] The concentration of $[Cu^{(I)}X/L]$, and hence the concentration of $[Cu^{(II)}X_2/L]$, is therefore determined solely by the extent of disproportionation.

1.5.5.7.5. Concept 5: principle of microscopic reversibility (PMR)

The final point of disagreement is that SET-LRP contravenes the principle of microscopic reversibility (PMR). The PMR dictates that in a reversible reaction, the forward and the reverse pathways must be mirror images of each other.[200] Resultantly, activation of the dormant species must occur with the reduced form of

the deactivating species. ATRP abides by this rule as [$Cu^{(I)}X/L$] and [$Cu^{(II)}X_2/L$] are, respectively, the activating and deactivating components. If SET-LRP were to follow this rule, then activation with $Cu^{(0)}$ would result in deactivation with [$Cu^{(I)}X/L$]. Similarly, deactivation with [$Cu^{(II)}X_2/L$] would mean that activation occurred with [$Cu^{(I)}X/L$].

1.6. Summary

The main scope of this thesis is to conduct an in-depth investigation into the use of aqueous $Cu^{(0)}$-mediated RDRP for the synthesis of polymers. The majority of the following chapters focus on investigating the scope of this system through the polymerisation of a wide variety of water soluble monomers in the presence of differing initiators and ligands. The second chapter of this thesis focuses on the development of a depolymerisation system which is based on the aqueous $Cu^{(0)}$-mediated RDRP protocol and previous investigations into the use of commercial alcoholic beverages as solvents for these polymerisations.

1.8. References

1 L. H. Baekeland, *J. Ind. Eng. Chem.*, 1909, **1**, 149–161.

2 C. E. Wang, P. S. Stayton, S. H. Pun and A. J. Convertine, *J. Control. Release*, 2015, **219**, 345–354.

3 D. S. H. Chu, J. G. Schellinger, J. Shi, A. J. Convertine, P. S. Stayton and S. H. Pun, *Acc. Chem. Res.*, 2012, **45**, 1089–1099.

4 C. Boyer, V. Bulmus, T. P. Davis, V. Ladmiral, J. Liu and S. Perrier, *Chem. Rev.*, 2009, **109**, 5402–5436.

5 T.-H. Yang, *Recent Patents Mater. Sci.*, 2008, 1, 29–40.

6 P. C. B. and A. M. Grumezescu, *Curr. Med. Chem.*, 2014, 21, 3333–3374.

7 Y. Chen, W. Zhao and J. Zhang, *RSC Adv.*, 2017, **7**, 4226–4236.

8 C.-F. Huang, *Polym J*, 2016, 48, 341–350.

9 J. Zhang and Y. Chen, *RSC Adv.*, 2016, **6**, 69370–69380.

10 Y. Chen, M. He, C. Wang and Y. Wei, *J. Mater. Chem. A*, 2014, **2**, 10444–10453.

11 J. Clayden, N. Greeves and S. Warren, *Organic Chemistry*, OUP Oxford, 2nd edn., 2012.

12 G. G. Odian, *Principles of Polymerization*, Wiley-Interscience, Hoboken, N.J., 4th edn., 2004.

13 K. Matyjaszewski and T. P. Davis, *Handbook of Radical Polymerization*, 1st edn., 2003.

14 R. J. Young and P. A. Lovell, *Introduction to Polymers*, CRC Press, 3rd edn., 2011.

15 G. Moad and D. H. Solomon, *The Chemistry of Radical Polymerization*, Elsevier, 2nd edn., 2006.

16 IUPAC, *PAC*, 1994, **66**, 1077.

17 J. McMurry, *Organic Chemistry*, Cengage Learning, 8th edn., 2011.

18 S. Harrisson, X. Liu, J.-N. Ollagnier, O. Coutelier, J.-D. Marty and M. Destarac, *Polym.* , 2014, 6.

19 K. Nakabayashi and H. Mori, *Eur. Polym. J.*, 2013, **49**, 2808–2838.

20 D. J. Keddie, C. Guerrero-Sanchez, G. Moad, E. Rizzardo and S. H. Thang, *Macromolecules*, 2011, **44**, 6738–6745.

21 P. J. Flory, *J. Am. Chem. Soc.*, 1937, **59**, 241–253.

22 K. A. Davis and K. Matyjaszewski, *Statistical, Gradient, Block and Graft Copolymers by Controlled/Living Radical Polymerizations*, Springer Science & Business Media, 1st edn., 2002.

23 V. Chandrasekhar, *Inorganic and Organometallic Polymers*, Springer Science & Business Media, 1st edn., 2005.

24 X.-R. Li, X.-L. Wang and H. Koseki, *J. Hazard. Mater.*, 2008, **159**, 13–18.

25 M. Buback, H. Frauendorf, F. Günzler, F. Huff and P. Vana, *Macromol. Chem. Phys.*, 2009, **210**, 1591–1599.

26 J. Chiefari and E. Rizzardo, *Handbook of Radical Polymerization*, John Wiley & Sons, Inc., 2003.

27 A. A. Gridnev and S. D. Ittel, *Chem. Rev.*, 2001, **101**, 3611–3660.

28 A. Gridnev, *J. Polym. Sci. Part A Polym. Chem.*, 2000, **38**, 1753–1766.

29 J. P. A. Heuts, G. E. Roberts and J. D. Biasutti, *Aust. J. Chem.*, 2002, **55**, 381–398.

30 J. P. A. Heuts and N. M. B. Smeets, *Polym. Chem.*, 2011, **2**, 2407–2423.

31 C. L. Beyler and M. M. Hirschler, in *SFPE Handbook of Fire Protection Engineering*, 2002, pp. 110–131.

32 R. P. Quirk and B. Lee, *Polym. Int.*, 1992, **27**, 359–367.

33 S. Aoshima and S. Kanaoka, *Chem. Rev.*, 2009, **109**, 5245–5287.

34 M. Sawamoto and T. Higashimura, *Makromol. Chemie. Macromol. Symp.*, 1986, **3**, 83–97.

35 K. Matyjaszewski and M. Sawamoto, *Cationic Polymerizations; Mechanisms, Synthesis, and Appplications*, CRC Press, 1996.

36 M. Szwarc, M. Levy and R. Milkovich, *J. Am. Chem. Soc.*, 1956, **78**, 2656–2657.

37 M. Szwarc, *Nature*, 1956, **178**, 1168–1169.

38 N. Hadjichristidis, M. Pitsikalis, S. Pispas and H. Iatrou, *Chem. Rev.*, 2001, **101**, 3747–3792.

39 A. Hirao, R. Goseki and T. Ishizone, *Macromolecules*, 2014, **47**, 1883–1905.

40 H. Hsieh and R. P. Quirk, *Anionic Polymerization: Principles and Practical Applications*, CRC Press, 1st edn., 1996.

41 K. Ratkanthwar, N. Hadjichristidis and J. Mays, eds. N. Hadjichristidis and A. Hirao, Springer Japan, Tokyo, 2015, pp. 19–59.

42 G. Theodosopoulos and M. Pitsikalis, eds. N. Hadjichristidis and A. Hirao, Springer Japan, Tokyo, 2015, pp. 541–623.

43 R. P. Quirk, *Applications of Anionic Polymerization Research*, American Chemical Society, 1998, vol. 696.

44 J. Jagur-Grodzinski, *J. Polym. Sci. Part A Polym. Chem.*, 2002, **40**, 2116–2133.

45 D. J. Aubrey, G. J. Richard and G. Moad, *Pure Appl. Chem.*, 2009, **82**, 483.

46 G. Moad and E. Rizzardo, in *Nitroxide Mediated Polymerization: From Fundamentals to Applications in Materials Science*, The Royal Society of Chemistry, 2016, pp. 1–44.

47 J. Nicolas, Y. Guillaneuf, C. Lefay, D. Bertin, D. Gigmes and B. Charleux, *Prog. Polym. Sci.*, 2013, **38**, 63–235.

48 D. Gigmes and S. R. A. Marque, in *Encyclopedia of Radicals in Chemistry, Biology and Materials*, John Wiley & Sons, Ltd, 2012.

49 K. Matyjaszewski and J. Xia, *Chem. Rev.*, 2001, **101**, 2921–2990.

50 K. Matyjaszewski, *Macromolecules*, 2012, **45**, 4015–4039.

51 J. Xia and K. Matyjaszewski, *Macromolecules*, 1997, **30**, 7697–7700.

52 B. M. Rosen and V. Percec, *Chem. Rev.*, 2009, **109**, 5069–5119.

53 A. Anastasaki, V. Nikolaou, G. Nurumbetov, P. Wilson, K. Kempe, J. F. Quinn, T. P. Davis, M. R. Whittaker and D. M. Haddleton, *Chem. Rev.*, 2016, **116**, 835–877.

54 A. Anastasaki, V. Nikolaou and D. M. Haddleton, *Polym. Chem.*, 2016, **7**, 1002–1026.

55 G. Moad, E. Rizzardo and S. H. Thang, *Aust. J. Chem.*, 2006, 59, 669–692.

56 G. Moad, E. Rizzardo and S. H. Thang, *Aust. J. Chem.*, 2009, 62, 1402–1472.

57 G. Moad, E. Rizzardo and S. H. Thang, *Aust. J. Chem.*, 2012, 65, 985–1076.

58 N. V Tsarevsky, W. Tang, S. J. Brooks and K. Matyjaszewski, in *Controlled/Living Radical Polymerization*, American Chemical Society, 2006, vol. 944, pp. 5–56.

59 A. Simula, V. Nikolaou, F. Alsubaie, A. Anastasaki and D. M. Haddleton, *Polym. Chem.*, 2015, **6**, 5940–5950.

60 M. Destarac, *Polym. Rev.*, 2011, **51**, 163–187.

61 V. Percec and D. A. Tirrell, *J. Polym. Sci., Part A Polym. Chem.*, 2000, **38(10)**, 1705.

62 R. Aksakal, M. Resmini and C. R. Becer, *Polym. Chem.*, 2016, **7**, 171–175.

63 G. Gody, R. Barbey, M. Danial and S. Perrier, *Polym. Chem.*, 2015, **6**, 1502–1511.

64 G. Gody, T. Maschmeyer, P. B. Zetterlund and S. Perrier, *Macromolecules*, 2014, **47**, 3451–3460.

65 C. Boyer, N. A. Corrigan, K. Jung, D. Nguyen, T.-K. Nguyen, N. N. M. Adnan, S. Oliver, S. Shanmugam and J. Yeow, *Chem. Rev.*, 2016, **116**, 1803–1949.

66 A. Anastasaki, J. Willenbacher, C. Fleischmann, W. R. Gutekunst and C. J. Hawker, *Polym. Chem.*, 2017, **8**, 689–697.

67 H. Willcock and R. K. O'Reilly, *Polym. Chem.*, 2010, **1**, 149–157.

68 D. H. Solomon, E. Rizzardo, P. Cacioli, USPatent, 4581429 A, 1986.

69 C. J. Hawker, A. W. Bosman and E. Harth, *Chem. Rev.*, 2001, **101**, 3661–3688.

70 A. Studer and T. Schulte, *Chem. Rec.*, 2005, **5**, 27–35.

71 M. K. Georges, R. P. N. Veregin, P. M. Kazmaier and G. K. Hamer, *Macromolecules*, 1993, **26**, 2987–2988.

72 G. Moad, E. Rizzardo and D. H. Solomon, *Macromolecules*, 1982, **15**, 909–914.

73 C. Detrembleur, C. Jerome, J. De Winter, P. Gerbaux, J.-L. Clement, Y. Guillaneuf and D. Gigmes, *Polym. Chem.*, 2014, **5**, 335–340.

74 Q. Zhang, P. Wilson, Z. Li, R. McHale, J. Godfrey, A. Anastasaki, C. Waldron and D. M. Haddleton, *J. Am. Chem. Soc.*, 2013, **135**, 7355–7363.

75 L. Martin, G. Gody and S. Perrier, *Polym. Chem.*, 2015, **6**, 4875–4886.

76 J. Chiefari, Y. K. (Bill) Chong, F. Ercole, J. Krstina, J. Jeffery, T. P. T. Le, R. T. A. Mayadunne, G. F. Meijs, C. L. Moad, G. Moad, E. Rizzardo and S. H. Thang, *Macromolecules*, 1998, **31**, 5559–5562.

77 C. Barner-Kowollik, T. P. Davis, J. P. A. Heuts, M. H. Stenzel, P. Vana and M. Whittaker, *J. Polym. Sci. Part A Polym. Chem.*, 2003, **41**, 365–375.

78 J. Rosselgong, E. G. L. Williams, T. P. Le, F. Grusche, T. M. Hinton, M. Tizard, P. Gunatillake and S. H. Thang, *Macromolecules*, 2013, **46**, 9181–9188.

79 N. A. Hadjiantoniou, T. Krasia-Christoforou, E. Loizou, L. Porcar and C. S. Patrickios, *Macromolecules*, 2010, **43**, 2713–2720.

80 G. Gody, T. Maschmeyer, P. B. Zetterlund and S. Perrier, *Nat. Commun.*, 2013, **4**, 2505.

81 J. Zhang, G. Gody, M. Hartlieb, S. Catrouillet, J. Moffat and S. Perrier, *Macromolecules*, 2016, **49**, 8933–8942.

82 A. Favier and M.-T. Charreyre, *Macromol. Rapid Commun.*, 2006, **27**, 653–692.

83 S. Perrier and P. Takolpuckdee, *J. Polym. Sci. Part A Polym. Chem.*, 2005, **43**, 5347–5393.

84 S. Aroua, E. G. V Tiu, M. Ayer, T. Ishikawa and Y. Yamakoshi, *Polym. Chem.*, 2015, **6**, 2616–2619.

85 A. Guinaudeau, S. Mazieres, D. J. Wilson and M. Destarac, *Polym. Chem.*, 2012, **3**, 81–84.

86 I. J. Johnson, E. Khosravi, O. M. Musa, R. E. Simnett and A. M. Eissa, *J. Polym. Sci. Part A Polym. Chem.*, 2015, **53**, 775–786.

87 M. H. Stenzel, L. Cummins, G. E. Roberts, T. P. Davis, P. Vana and C. Barner-Kowollik, *Macromol. Chem. Phys.*, 2003, **204**, 1160–1168.

88 V. Mishra and R. Kumar, *J. Appl. Polym. Sci.*, 2012, **124**, 4475–4485.

89 D. J. Keddie, G. Moad, E. Rizzardo and S. H. Thang, *Macromolecules*, 2012, **45**, 5321–5342.

90 G. Nurumbetov, N. Engelis, J. Godfrey, R. Hand, A. Anastasaki, A. Simula, V. Nikolaou and D. M. Haddleton, *Polym. Chem.*, 2017, **8**, 1084–1094.

91 N. G. Engelis, A. Anastasaki, G. Nurumbetov, N. P. Truong, V. Nikolaou, A. Shegiwal, M. R. Whittaker, T. P. Davis and D. M. Haddleton, *Nat Chem*, 2017, **9**, 171–178.

92 W. T. Eckenhoff and T. Pintauer, *Dalt. Trans.*, 2011, **40**, 4909–4917.

93 L. A. van de Kuil, D. M. Grove, R. A. Gossage, J. W. Zwikker, L. W. Jenneskens, W. Drenth and G. van Koten, *Organometallics*, 1997, **16**, 4985–4994.

94 X. Lu, S. Gong, L. Meng, C. Li, S. Yang and L. Zhang, *Polymer (Guildf).*, 2007, **48**, 2835–2842.

95 P. Singh, A. Srivastava and R. Kumar, *J. Polym. Sci. Part A Polym. Chem.*, 2012, **50**, 1503–1514.

96 M. Kato, M. Kamigaito, M. Sawamoto and T. Higashimura, *Macromolecules*, 1995, **28**, 1721–1723.

97 J.-S. Wang and K. Matyjaszewski, *J. Am. Chem. Soc.*, 1995, **117**, 5614–5615.

98 F. Stoffelbach, D. M. Haddleton and R. Poli, *Eur. Polym. J.*, 2003, **39**, 2099–2105.

99 E. Le Grognec, J. Claverie and R. Poli, *J. Am. Chem. Soc.*, 2001, **123**, 9513–9524.

100 P. Lecomte, I. Drapier, P. Dubois, P. Teyssié and R. Jérôme, *Macromolecules*, 1997, **30**, 7631–7633.

101 Y. Wang, Y. Zhang, B. Parker and K. Matyjaszewski, *Macromolecules*, 2011, **44**, 4022–4025.

102 Y. Zhang, Y. Wang and K. Matyjaszewski, *Macromolecules*, 2011, **44**, 683–685.

103 D. Yang, D. He, Y. Liao, Z. Xue, X. Zhou and X. Xie, *J. Polym. Sci. Part A Polym. Chem.*, 2014, **52**, 1020–1027.

104 T. Ando, M. Kamigaito and M. Sawamoto, *Macromolecules*, 1997, **30**, 4507–4510.

105 K. Matyjaszewski, M. Wei, J. Xia and N. E. McDermott, *Macromolecules*, 1997, **30**, 8161–8164.

106 H. Uegaki, Y. Kotani, M. Kamigaito and M. Sawamoto, *Macromolecules*, 1998, **31**, 6756–6761.

107 H. Uegaki, Y. Kotani, M. Kamigaito and M. Sawamoto, *Macromolecules*, 1997, **30**, 2249–2253.

108 H. Fischer, *Macromolecules*, 1997, **30**, 5666–5672.

109 H. Fischer, *Chem. Rev.*, 2001, **101**, 3581–3610.

110 H. Fischer, *J. Polym. Sci., Part A Polym. Chem.*, 1999, **37**, 1885–1901.

111 D. Konkolewicz, A. J. D. Magenau, S. E. Averick, A. Simakova, H. He and K. Matyjaszewski, *Macromolecules*, 2012, **45**, 4461–4468.

112 P. Shivapooja, L. K. Ista, H. E. Canavan and G. P. Lopez, *Biointerphases*, 2012, **7**, 1–9.

113 A. Simakova, S. E. Averick, D. Konkolewicz and K. Matyjaszewski, *Macromolecules*, 2012, **45**, 6371–6379.

114 Y. Kwak, A. J. D. Magenau and K. Matyjaszewski, *Macromolecules*, 2011, **44**, 811–819.

115 N. J. Treat, H. Sprafke, J. W. Kramer, P. G. Clark, B. E. Barton, J. Read de Alaniz, B. P. Fors and C. J. Hawker, *J. Am. Chem. Soc.*, 2014, **136**, 16096–16101.

116 V. Percec, T. Guliashvili, J. S. Ladislaw, A. Wistrand, A. Stjerndahl, M. J. Sienkowska, M. J. Monteiro and S. Sahoo, *J. Am. Chem. Soc.*, 2006, **128**, 14156–14165.

117 V. Percec, A. V Popov, E. Ramirez-Castillo, M. Monteiro, B. Barboiu, O. Weichold, A. D. Asandei and C. M. Mitchell, *J. Am. Chem. Soc.*, 2002, **124**, 4940–4941.

118 V. Percec, T. Guliashvili, A. V Popov and E. Ramirez-Castillo, *J. Polym. Sci. Part A Polym. Chem.*, 2005, **43**, 1935–1947.

119 N. H. Nguyen, B. M. Rosen, G. Lligadas and V. Percec, *Macromolecules*, 2009, **42**, 2379–2386.

120 R. Aksakal, M. Resmini and C. R. Becer, *Polym. Chem.*, 2016, **7**, 6564–6569.

121 M. E. Levere, N. H. Nguyen, X. Leng and V. Percec, *Polym. Chem.*, 2013, **4**, 1635–1647.

122 L. Zhou, Z. Zhang, Z. Cheng, N. Zhou, J. Zhu, W. Zhang and X. Zhu, *Macromol. Chem. Phys.*, 2012, **213**, 439–446.

123 D. Liu, H. Chen, P. Yin, N. Ji, G. Zong and R. Qu, *J. Polym. Sci. Part A Polym. Chem.*, 2011, **49**, 2916–2923.

124 H. Chen, M. Zhang, M. Yu and H. Jiang, *J. Polym. Sci. Part A Polym. Chem.*, 2011, **49**, 4721–4724.

125 G. Wang and M. Lu, *Polym. Int.*, 2012, **61**, 1279–1283.

126 X.-H. Liu, Y.-H. Yu, D. Jia, B.-W. Cheng, F.-J. Zhang, H.-N. Li, P. Chen and S. Xie, *J. Polym. Sci. Part A Polym. Chem.*, 2013, **51**, 1559–1564.

127 D. Liu, J. Ma, H. Chen, P. Yin, N. Ji and G. Zong, *J. Polym. Sci. Part A Polym. Chem.*, 2011, **49**, 5109–5115.

128 Z. Hao, J. Zhang, H. Chen, D. Liu, D. Wang, H. Qu and J. Lang, *J. Polym. Sci. Part A Polym. Chem.*, 2013, **51**, 4088–4094.

129 D. Liu, H. Chen, P. yin, Z. Hao and L. Fan, *J. Polym. Sci. Part A Polym. Chem.*, 2012, **50**, 4809–4813.

130 Z. Hao, H. Chen, D. Liu and L. Fan, *J. Polym. Sci. Part A Polym. Chem.*, 2012, **50**, 4995–4999.

131 H. Chen, G. Lv, Y. Liang and J. Sun, *J. Polym. Sci. Part A Polym. Chem.*, 2013, **51**, 3328–3332.

132 H. Chen, G. Zong, L. Chen, M. Zhang, C. Wang and R. Qu, *J. Polym. Sci. Part A Polym. Chem.*, 2011, **49**, 2924–2930.

133 S. R. Samanta, A. Anastasaki, C. Waldron, D. M. Haddleton and V. Percec, *Polym. Chem.*, 2013, **4**, 5555–5562.

134 S. R. Samanta, M. E. Levere and V. Percec, *Polym. Chem.*, 2013, **4**, 3212–3224.

135 X. Jiang, S. Fleischmann, N. H. Nguyen, B. M. Rosen and V. Percec, *J. Polym. Sci. Part A Polym. Chem.*, 2009, **47**, 5591–5605.

136 L. Voorhaar, S. Wallyn, F. E. Du Prez and R. Hoogenboom, *Polym. Chem.*, 2014, **5**, 4268–4276.

137 X. Leng, N. H. Nguyen, B. van Beusekom, D. A. Wilson and V. Percec, *Polym. Chem.*, 2013, **4**, 2995–3004.

138 Q. Zhang, A. Anastasaki, G.-Z. Li, A. J. Haddleton, P. Wilson and D. M. Haddleton, *Polym. Chem.*, 2014, **5**, 3876–3883.

139 S. R. Samanta, R. Cai and V. Percec, *Polym. Chem.*, 2014, **5**, 5479–5491.

140 N. H. Nguyen, M. E. Levere and V. Percec, *J. Polym. Sci. Part A Polym. Chem.*, 2012, **50**, 35–46.

141 G. Lligadas and V. Percec, *J. Polym. Sci. Part A Polym. Chem.*, 2007, **45**, 4684–4695.

142 C. Waldron, A. Anastasaki, R. McHale, P. Wilson, Z. Li, T. Smith and D. M. Haddleton, *Polym. Chem.*, 2014, **5**, 892–898.

143 C. Boyer, A. Derveaux, P. B. Zetterlund and M. R. Whittaker, *Polym. Chem.*, 2012, **3**, 117–123.

144 M. R. Whittaker, C. N. Urbani and M. J. Monteiro, *J. Polym. Sci. Part A Polym. Chem.*, 2008, **46**, 6346–6357.

145 A. Kleine, C. L. Altan, U. E. Yarar, N. A. J. M. Sommerdijk, S. Bucak and S. J. Holder, *Polym. Chem.*, 2014, **5**, 524–534.

146 T. Guliashvili and V. Percec, *J. Polym. Sci. Part A Polym. Chem.*, 2007, **45**, 1607–1618.

147 M. B. Gillies, K. Matyjaszewski, P.-O. Norrby, T. Pintauer, R. Poli and P. Richard, *Macromolecules*, 2003, **36**, 8551–8559.

148 W. Tang and K. Matyjaszewski, *Macromolecules*, 2007, **40**, 1858–1863.

149 I. M. Heyns, R. Pfukwa and B. Klumperman, *Biomacromolecules*, 2016, **17**, 1795–1800.

150 T. Hatano, B. M. Rosen and V. Percec, *J. Polym. Sci. Part A Polym. Chem.*, 2010, **48**, 164–172.

151 H. Wu, Y. Wan, W. Wang, Y. Wang, N. Zhou, W. Zhang, X. Li, Z. Zhang and X. Zhu, *Polym. Chem.*, 2015, **6**, 2620–2625.

152 M. Fantin, A. A. Isse, A. Venzo, A. Gennaro and K. Matyjaszewski, *J. Am. Chem. Soc.*, 2016, **138**, 7216–7219.

153 V. Nikolaou, A. Simula, M. Droesbeke, N. Risangud, A. Anastasaki, K. Kempe, P. Wilson and D. Haddleton, *Polym. Chem.*, 2016.

154 G. Masci, L. Giacomelli and V. Crescenzi, *J. Polym. Sci. Part A Polym. Chem.*, 2005, **43**, 4446–4454.

155 E. J. Ashford, V. Naldi, R. O'Dell, N. C. Billingham and S. P. Armes, *Chem. Commun.*, 1999, 1285–1286.

156 S. Fleischmann and V. Percec, *J. Polym. Sci. Part A Polym. Chem.*, 2010, **48**, 4889–4893.

157 M. Fantin, A. A. Isse, A. Gennaro and K. Matyjaszewski, *Macromolecules*, 2015, **48**, 6862–6875.

158 R. Mincheva, D. Paneva, L. Mespouille, N. Manolova, I. Rashkov and P. Dubois, *J. Polym. Sci. Part A Polym. Chem.*, 2009, **47**, 1108–1119.

159 A. Anastasaki, C. Waldron, P. Wilson, R. McHale and D. M. Haddleton, *Polym. Chem.*, 2013, **4**, 2672–2675.

160 W. Tang, Y. Kwak, W. Braunecker, N. V Tsarevsky, M. L. Coote and K. Matyjaszewski, *J. Am. Chem. Soc.*, 2008, **130**, 10702–10713.

161 A. Anastasaki, A. J. Haddleton, Q. Zhang, A. Simula, M. Droesbeke, P. Wilson and D. M. Haddleton, *Macromol. Rapid Commun.*, 2014, **35**, 965–970.

162 G. R. Jones, Z. Li, A. Anastasaki, D. J. Lloyd, P. Wilson, Q. Zhang and D. M. Haddleton, *Macromolecules*, 2016, **49**, 483–489.

163 M. E. Levere, I. Willoughby, S. O'Donohue, P. M. Wright, A. J. Grice, C. Fidge, C. Remzi Becer and D. M. Haddleton, *J. Polym. Sci. Part A Polym. Chem.*, 2011, **49**, 1753–1763.

164 P. Atkins, *Inorganic Chemistry*, OUP Oxford, 5th edn., 2010.

165 D. M. Haddleton, C. B. Jasieczek, M. J. Hannon and A. J. Shooter, *Macromolecules*, 1997, **30**, 2190–2193.

166 A. Simula, A. Anastasaki and D. M. Haddleton, *Macromol. Rapid Commun.*, 2016, **37**, 356–361.

167 R. Whitfield, A. Anastasaki, V. Nikolaou, G. R. Jones, N. G. Engelis, E. H. Discekici, C. Fleischmann, J. Willenbacher, C. J. Hawker and D. M. Haddleton, *J. Am. Chem. Soc.*, 2017, **139**, 1003–1010.

168 A. Anastasaki, C. Waldron, V. Nikolaou, P. Wilson, R. McHale, T. Smith and D. M. Haddleton, *Polym. Chem.*, 2013, **4**, 4113–4119.

169 G. Lligadas and V. Percec, *J. Polym. Sci. Part A Polym. Chem.*, 2008, **46**, 2745–2754.

170 W. Wang, Z. Zhang, J. Zhu, N. Zhou and X. Zhu, *J. Polym. Sci. Part A Polym. Chem.*, 2009, **47**, 6316–6327.

171 F. Alsubaie, A. Anastasaki, P. Wilson and D. M. Haddleton, *Polym. Chem.*, 2015, **6**, 406–417.

172 J. T. Rademacher, M. Baum, M. E. Pallack, W. J. Brittain and W. J. Simonsick, *Macromolecules*, 2000, **33**, 284–288.

173 M. Teodorescu and K. Matyjaszewski, *Macromolecules*, 1999, **32**, 4826–4831.

174 A. Narumi, Y. Chen, M. Sone, K. Fuchise, R. Sakai, T. Satoh, Q. Duan, S. Kawaguchi and T. Kakuchi, *Macromol. Chem. Phys.*, 2009, **210**, 349–358.

175 Q. Zhang, Z. Li, P. Wilson and D. M. Haddleton, *Chem. Commun.*, 2013, **49**, 6608–6610.

176 C. Waldron, Q. Zhang, Z. Li, V. Nikolaou, G. Nurumbetov, J. Godfrey, R. McHale, G. Yilmaz, R. K. Randev, M. Girault, K. McEwan, D. M. Haddleton, M. Droesbeke, A. J. Haddleton, P. Wilson, A. Simula, J. Collins, D. J. Lloyd, J. A. Burns, C. Summers, C. Houben, A. Anastasaki, M. Li, C. R. Becer, J. K. Kiviaho and N. Risangud, *Polym. Chem.*, 2014, **5**, 57–61.

177 A. Simula, V. Nikolaou, A. Anastasaki, F. Alsubaie, G. Nurumbetov, P. Wilson, K. Kempe and D. M. Haddleton, *Polym. Chem.*, 2015, **6**, 2226–2233.

178 G. R. Jones, R. Whitfield, A. Anastasaki and D. M. Haddleton, *J. Am. Chem. Soc.*, 2016, **138**, 7346–7352.

179 J. Collins, S. J. Wallis, A. Simula, M. R. Whittaker, M. P. McIntosh, P. Wilson, T. P. Davis, D. M. Haddleton and K. Kempe, *Macromol. Rapid Commun.*, 2017, **38**, 1600534.

180 N. V Tsarevsky, T. Pintauer and K. Matyjaszewski, *Macromolecules*, 2004, **37**, 9768–9778.

181 D. J. Lloyd, V. Nikolaou, J. Collins, C. Waldron, A. Anastasaki, S. P. Bassett, S. M. Howdle, A. Blanazs, P. Wilson, K. Kempe and D. M. Haddleton, *Chem. Commun.*, 2016, **52**, 6533–6536.

182 A. Anastasaki, V. Nikolaou, G. S. Pappas, Q. Zhang, C. Wan, P. Wilson, T. P. Davis, M. R. Whittaker and D. M. Haddleton, *Chem. Sci.*, 2014, **5**, 3536–3542.

183 A. Anastasaki, V. Nikolaou, Q. Zhang, J. Burns, S. R. Samanta, C. Waldron, A. J. Haddleton, R. McHale, D. Fox, V. Percec, P. Wilson and D. M. Haddleton, *J. Am. Chem. Soc.*, 2014, **136**, 1141–1149.

184 N. Zhu, X. Hu, Y. Zhang, K. Zhang, Z. Li and K. Guo, *Polym. Chem.*, 2016, **7**, 474–480.

185 J. A. Burns, C. Houben, A. Anastasaki, C. Waldron, A. A. Lapkin and D. M. Haddleton, *Polym. Chem.*, 2013, **4**, 4809–4813.

186 D. Konkolewicz, Y. Wang, P. Krys, M. Zhong, A. A. Isse, A. Gennaro and K. Matyjaszewski, *Polym. Chem.*, 2014, **5**, 4396–4417.

187 S. Harrisson and J. Nicolas, *ACS Macro Lett.*, 2014, **3**, 643–647.

188 F. Alsubaie, A. Anastasaki, V. Nikolaou, A. Simula, G. Nurumbetov, P. Wilson, K. Kempe and D. M. Haddleton, *Macromolecules*, 2015, **48**, 5517–5525.

189 F. Alsubaie, A. Anastasaki, V. Nikolaou, A. Simula, G. Nurumbetov, P. Wilson, K. Kempe and D. M. Haddleton, *Macromolecules*, 2015, **48**, 6421–6432.

190 D. Konkolewicz, Y. Wang, M. Zhong, P. Krys, A. A. Isse, A. Gennaro and K.

Matyjaszewski, *Macromolecules*, 2013, **46**, 8749–8772.

191 C.-H. Peng, M. Zhong, Y. Wang, Y. Kwak, Y. Zhang, W. Zhu, M. Tonge, J. Buback, S. Park, P. Krys, D. Konkolewicz, A. Gennaro and K. Matyjaszewski, *Macromolecules*, 2013, **46**, 3803–3815.

192 M. Zhong, Y. Wang, P. Krys, D. Konkolewicz and K. Matyjaszewski, *Macromolecules*, 2013, **46**, 3816–3827.

193 Y. Wang, M. Zhong, W. Zhu, C.-H. Peng, Y. Zhang, D. Konkolewicz, N. Bortolamei, A. A. Isse, A. Gennaro and K. Matyjaszewski, *Macromolecules*, 2013, **46**, 3793–3802.

194 D. Konkolewicz, P. Krys, J. R. Góis, P. V Mendonça, M. Zhong, Y. Wang, A. Gennaro, A. A. Isse, M. Fantin and K. Matyjaszewski, *Macromolecules*, 2014, **47**, 560–570.

195 Y. Zhang, Y. Wang, C. Peng, M. Zhong, W. Zhu, D. Konkolewicz and K. Matyjaszewski, *Macromolecules*, 2012, **45**, 78–86.

196 F. Lorandi, M. Fantin, A. A. Isse and A. Gennaro, *Polymer (Guildf).*, 2015, **72**, 238–245.

197 C. Visnevskij and R. Makuska, *Macromolecules*, 2013, **46**, 4764–4771.

198 C. M. R. Abreu, A. C. Serra, A. V Popov, K. Matyjaszewski, T. Guliashvili and J. F. J. Coelho, *Polym. Chem.*, 2013, **4**, 5629–5636.

199 Y. Wang, M. Zhong, Y. Zhang, A. J. D. Magenau and K. Matyjaszewski, *Macromolecules*, 2012, **45**, 8929–8932.

200 R. L. Burwell and R. G. Pearson, *J. Phys. Chem.*, 1966, **70**, 300–302.

Chapter 2: Controlled polymerisation and *"in-situ"* depolymerisation of polyacrylamides and polyacrylates in the presence of dissolved CO_2

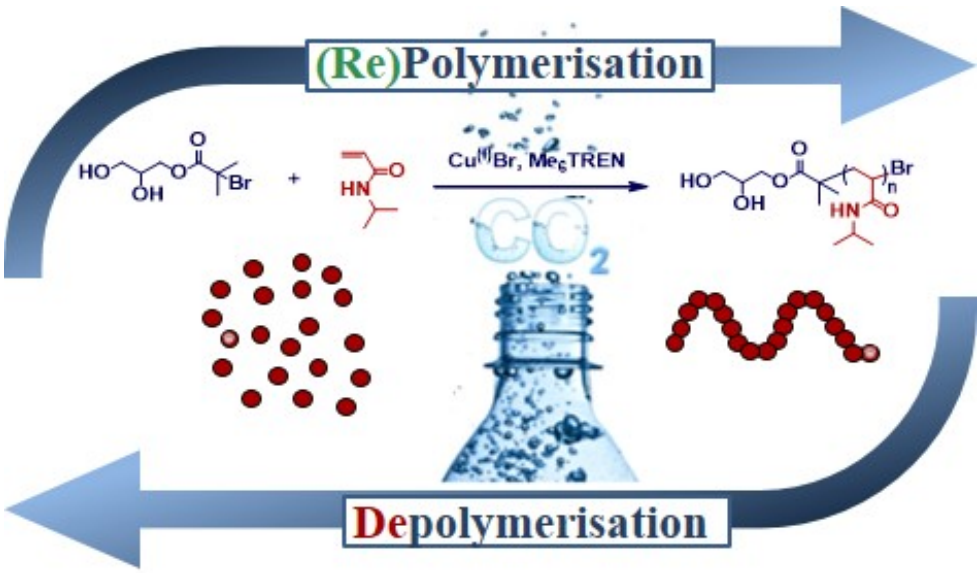

Well-controlled polymerisation and "in-situ" depolymerisation of acrylamides and acrylates in carbonated water using aqueous copper-mediated radical polymerisation is reported. After reaching high monomer conversions, maintaining formal polymerisation conditions resulted in the detection of well-defined lower molecular weight polymers/oligomers and the reformation of monomer. The identity of the monomer was confirmed analytically by GC-MS and experimentally following deoxygenation of the resulting solution which enabled for controlled polymerisation and the reformation of polymers that exhibited high conversions and low dispersities.

2.1. Introduction

2.1.1. The concept of depolymerisation

The term depolymerisation is used to describe the conversion of polymer into monomer and lower molecular weight polymeric species.[1] This occurs through a series of reactions that are typically induced by external stimuli. A polymer may undergo depolymerisation through a range of mechanisms; the two most commonly encountered of these being (1) random chain scission or (2) specific chain scission.[2–4]

In the case of random chain scission, the polymer is cleaved at random positions along the backbone in a statistical process (Scheme 2.1, Table 2.1).[4] When a polymer chain is broken in this method, it is typically referred to as degradation rather than depolymerisation.[2,5] This results from the process almost exclusively producing shorter polymer chains and infrequently generating monomeric species.[2,5] Whilst it is possible for degradation to occur in response to stimuli,[2] chain scission *via* this mechanism can occur at any time.

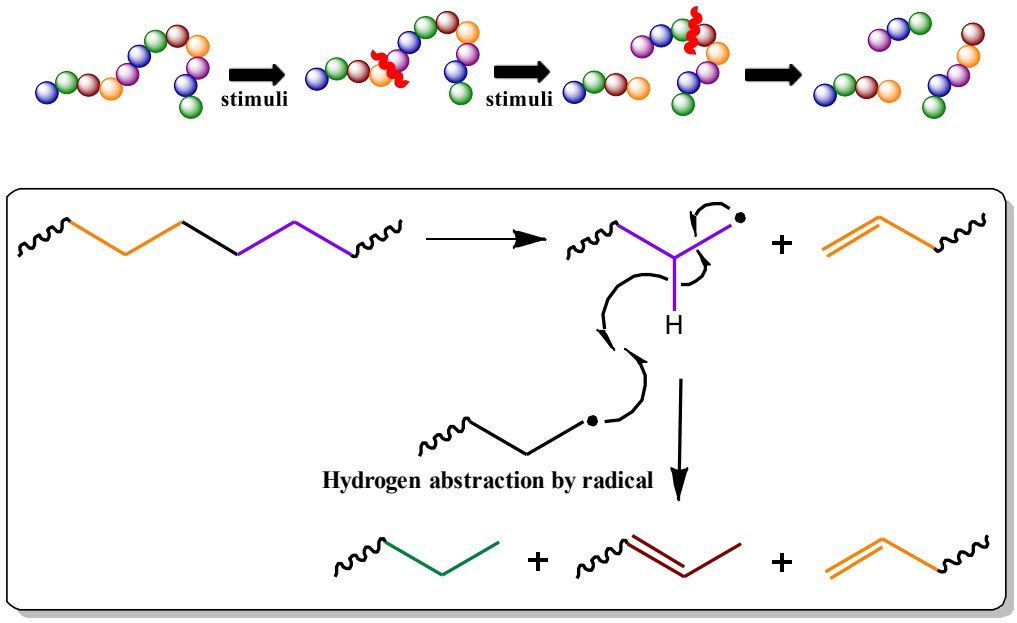

Scheme 2.1 - A representation of random chain scission.

On the other hand, depolymerisation that occurs *via* specific chain scission only results in the constituent monomer or, in the event of termination reactions such as radical-radical coupling or disproportionation, yields a combination of monomer and lower molecular weight polymers.[2–4] In this mechanism, depolymerisation can only arise when an external stimulus is used to trigger the systematic cleavage of the macromolecule from the chain end (Scheme 2.2, Table 2.1).[2–4,6]

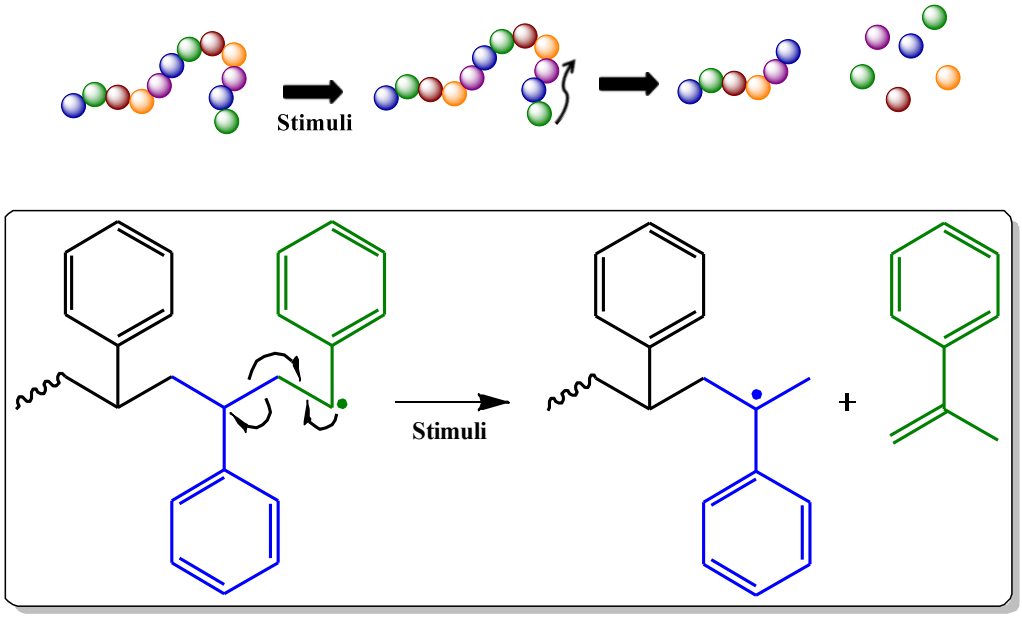

Scheme 2.2 - A representation of specific chain scission.

Specific Chain Scission	Random Chain Scission
Depolymerisation of polymer	Degradation of polymer
Needs initiation from stimuli	Any bond can break at any time but the process can be initiated by stimuli
Occurs through an unzipping mechanism	Occurs at random positions
Monomer concentration increases	Monomer production is minimal if at all
Steady decline in the average molecular weight of polymer chains (M_n)	Rapid decline in average molecular weight of polymer chains (M_n)
e.g. Poly (styrene)	e.g. Poly (ethylene)

Table 2.1 – A comparison between specific chain scission (depolymerisation)[6] and random chain scission (degradation).[2]

2.1.2. Self-immolative polymers

Whilst there are numerous examples of stimuli-responsive polymers that could be discussed within this chapter, perhaps the ones which are most relevant are those of the so-called "Self-Immolative Polymers" (SIPs). SIPs are formed when a macromolecule with an appropriate backbone (*i.e.* a polycarbamate, polyurethane, polyacetal or poly(benzyl ether)) is capped at the head-terminus with a specific protecting group.[7] When this group is cleaved, it triggers the sequential and complete fragmentation (*via* a head-to-tail mechanism) of the polymer into its constituent monomers (Scheme 2.3).[7–10]

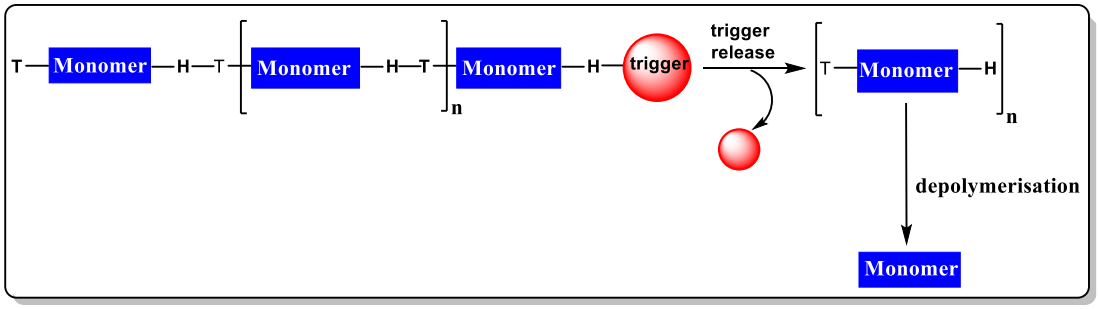

Scheme 2.3 - An illustration of the disassembly of a self-immolative polymer.

The cleavage of stimuli responsive polymers as a whole has been shown to occur with the application of temperature,[11–14] pH,[8,14,15] mechanical force,[16] and an electric/magnetic field.[17,18] As such, polymers of this type are considered to be highly versatile and have found frequent use within drug delivery systems,[8,19] as sensors and biosensors,[20] within environmental remediation processes,[21] and many other applications.[22,23]

2.1.3. Thermodynamics of depolymerisation

Unfortunately, the depolymerisation of polymers which are produced from radical chain growth polymerisations is much more problematic. This is not only due to the

expense, but as a result of the high kinetic energy barrier and low depropagation rate constants.[24]

As mentioned in the previous chapter, chain growth in radical polymerisations arises though the sequential addition of a free radical chain to monomer units during the propagation step.[24] However, in order for this process to occur, the reaction must be conducted below the ceiling temperature (T_c) of the given polymer; this is so that unwanted depolymerisation is avoided.[25,26] To give an example of this, PMMA is known to depolymerise at temperatures above 165 °C.[27]

According to the principle of microscopic reversibility, for every individual process within a system, a reverse reaction exists in a state of equilibrium.[28] Therefore, during the polymerisation process there is a counterpart to the propagation step (polymerisation) termed, depropagation (depolymerisation) (Equations 2.1 to 2.3).[24,25]

$$\mathbf{P_n^{\bullet} + M} \underset{k_{dp}}{\overset{k_p}{\rightleftharpoons}} \mathbf{P_{n+1}^{\bullet}} \qquad \textbf{(Equation 2.1)}$$

$$\textit{Propagation} \rightleftharpoons \textit{Depropagation} \qquad \textbf{(Equation 2.2)}$$

$$\textit{Polymerisation} \rightleftharpoons \textit{Depolymerisation} \qquad \textbf{(Equation 2.3)}$$

Equations 2.1 to 2.3 - Expressions showing the polymerisation/depolymerisation equilibria where $P_n^{\bullet}$ is a propagating polymer chain and M is monomer.

The position of this equilibrium, and hence whether depolymerisation occurs, is governed by the ceiling temperature and is thermodynamically controlled by Gibbs free energy (Equation 2.4).[24]

$$\Delta G_p = \Delta H_p - T_c \Delta S_p \qquad \textbf{(Equation 2.4)}$$

Equation 2.4 - The expression for the Gibbs free energy (ΔG_p) of a polymerisation where ΔH_p is the change in enthalpy, T_c the ceiling temperature and ΔS_p the change in entropy.

$$T_c = \frac{\Delta H_p}{\Delta S_p} \quad \textbf{(Equation 2.5)}$$

Equation 2.5 - A simplified thermodynamic expression for the ceiling temperature of a polymer.

As the driving force for a polymerisation is controlled by enthalpy, propagation is favoured when reactions are conducted at temperatures below the T_c ($\Delta H_p > T_c \Delta S_p$) (*i.e.* where the depropagation rate constant is low).[24,25] When the temperature is increased, this equilibrium is shifted towards depropagation. Until the temperature of the system reaches that of the ceiling temperature, and the rates of propagation and depropagation become equal, polymerisation is favoured. However, when it is at the ceiling temperature, the system enters a state of equilibrium ($\Delta H_p = T_c \Delta S_p$ = 0) and the net rate of polymerisation is zero.[24] Thus, when depolymerisation is desired, this threshold must be surpassed, and an environment created in which polymer formation is thermodynamically unfavourable ($T_c \Delta S_p > \Delta H_p$). To achieve this, most processes employ high reaction temperatures and as a result are often costly and energy intensive.[29,30]

2.1.4. Low temperature depolymerisation

In an attempt to overcome the need for high temperatures, Zhu *et al*. recently reported the low temperature (0 °C) depolymerisation of poly(*N*-isopropyl acrylamide) (PNIPAm) in aqueous media.[31] In this work, depolymerisation was achieved by the addition of TEMPO or 1,4-benzoquinone, and was proposed to proceed *via* abstraction of the terminal halide (Scheme 2.4). Unfortunately, both the polymerisation ($M_{n,experimental}$ = 106,900 g mol^{-1}; $Đ_m$ = 1.50) and depolymerisation ($M_{n,experimental}$ = 99,700 g mol^{-1}; $Đ_m$ = 1.48) processes exhibited a lack of control.

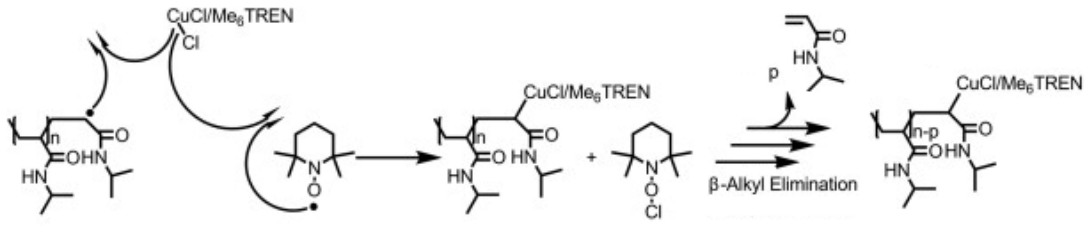

Scheme 2.4 – The proposed mechanism for the TEMPO-induced depolymerisation of PNIPAm (reproduced from reference 31).

The development of an aqueous $Cu^{(0)}$-mediated RDRP system[32] has allowed for the synthesis of well-defined water-soluble polymers (such as those based on acrylamides and acrylates) which were previously almost exclusively restricted to RAFT polymerisations.[33,34] The robustness of this technique has been demonstrated through the polymerisation of NIPAm in a variety of diverse media, including blood serum[35] and commercially available alcoholic beverages.[36] In the latter case, a proportion of the beverages contained carbon dioxide (CO_2), and it was subsequently theorised that conventional deoxygenation using an inert gas such as nitrogen (N_2) might be an unnecessary step in these reactions. To that end, CO_2 (an abundant, non-toxic and usually inert reagent) present in carbonated water was used as the solvent for the polymerisation of NIPAm, *N*-hydroxyethyl acrylamide (HEAm) and 2-hydroxyethyl acrylate (HEA).[37]

2.1.5. An introduction to the chemistry of carbon dioxide in water

Although CO_2 is a water soluble gas, the chemical species formed upon dissolution are relatively complex. As with most gases, the solubility of CO_2 follows Henry's Law (Section 2.1.6.), where its solubility will increase with a decrease in temperature.[38–41] When dissolved, CO_2 reversibly reacts to form carbonic acid (H_2CO_3) (Equation 2.7).[42] Carbonic acid is a diprotic, weak acid, which can undergo dissociation to form the bicarbonate ion (HCO_3^-) and later, through the dissociation of a second proton, the carbonate ion (CO_3^{2-}) (Equations 2.8 and 2.9).[43–45] The liberation of

protons to the surrounding medium through this dissociation gives rise to the partial acidity of carbonated water.

$$CO_2\,(g) \leftrightarrow CO_2\,(l) \quad \textbf{(Equation 2.6)}$$

$$CO_2\,(l) + H_2O\,(l) \leftrightarrow H_2CO_3(aq) \quad \textbf{(Equation 2.7)}$$

$$H_2CO_3(aq) + H_2O\,(l) \leftrightarrow H_3O^+(aq) + HCO_3^-(aq) \quad \textbf{(Equation 2.8)}$$

$$HCO_3^-(aq) + H_2O\,(l) \leftrightarrow H_3O^+(aq) + CO_3^{2-}(aq) \quad \textbf{(Equation 2.9)}$$

Equations 2.7 to 2.9 – Equations representing the behaviour of CO_2 in water.

2.1.6. Henry's Law

As indicated above, the solubility of a gas in a liquid is dependent upon two main factors: temperature and pressure.[41,46] For a given volume at a constant temperature, the concentration of any gas in solution is directly proportional to the partial pressure of gas above that solution.[47,48] Henry's Law (Equation 2.10) provides a relationship between these factors to form an expression for the distribution of gas between the solvent and the surrounding environment.[45]

$$p = K_H C \quad \textbf{(Equation 2.10)}$$

Equation 2.10 - The expression for Henry's Law where p represents the partial pressure of the solute above the solution, K_H Henry's Law constant and C, the concentration of solute in solution.

2.2. Results and discussion

2.2.1. Initial observations for the use of carbonated water as the solvent for the controlled polymerisation of N-isopropylacrylamide

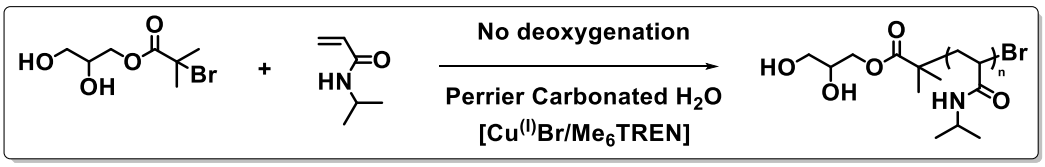

Scheme 2.5 – A schematic representation for the 0 °C polymerisation of NIPAm in carbonated water.

Initially, through utilising the "*in-situ"* disproportionation of [$Cu^{(I)}Br/Me_6TREN$] (Me_6TREN: tris[2-(dimethylamino)ethyl]amine) at 0 °C in carbonated water prior to the addition of monomer and initiator, a rapid (t < 10 minutes; > 99 % conversion) and controlled polymerisation of NIPAm (M_n = 3200 g mol^{-1}; $Đ_m$ = 1.16) (Figure 2.1) was achieved. Keeping the crude reaction mixture under formal polymerisation conditions for an hour resulted in a reduction in the molecular weight that was observed by SEC (M_n = 1600 g mol^{-1}; $Đ_m$ = 1.16) (Figure 2.1). Alongside this, there was a noticeable re-appearance of vinyl peaks in the ^1H NMR spectrum (Figure 2.1). Subsequent integration of the reformed vinyl protons (5.6 ppm) against the isopropyl methine proton present in the reformed monomer and remaining polymer (3.9 ppm), indicated that >50 % depolymerisation had occurred (% depolymerisation refers to the quantity of polymer which has undergone depolymerisation).

Crucially, after allowing the reaction to proceed for 24 hours, the extent of depolymerisation remained unchanged; indicating that depolymerisation had occurred over a relatively short time period and then ceased.

Scheme 2.6 – A schematic representation for the polymerisation/depolymerisation of NIPAm in carbonated water.

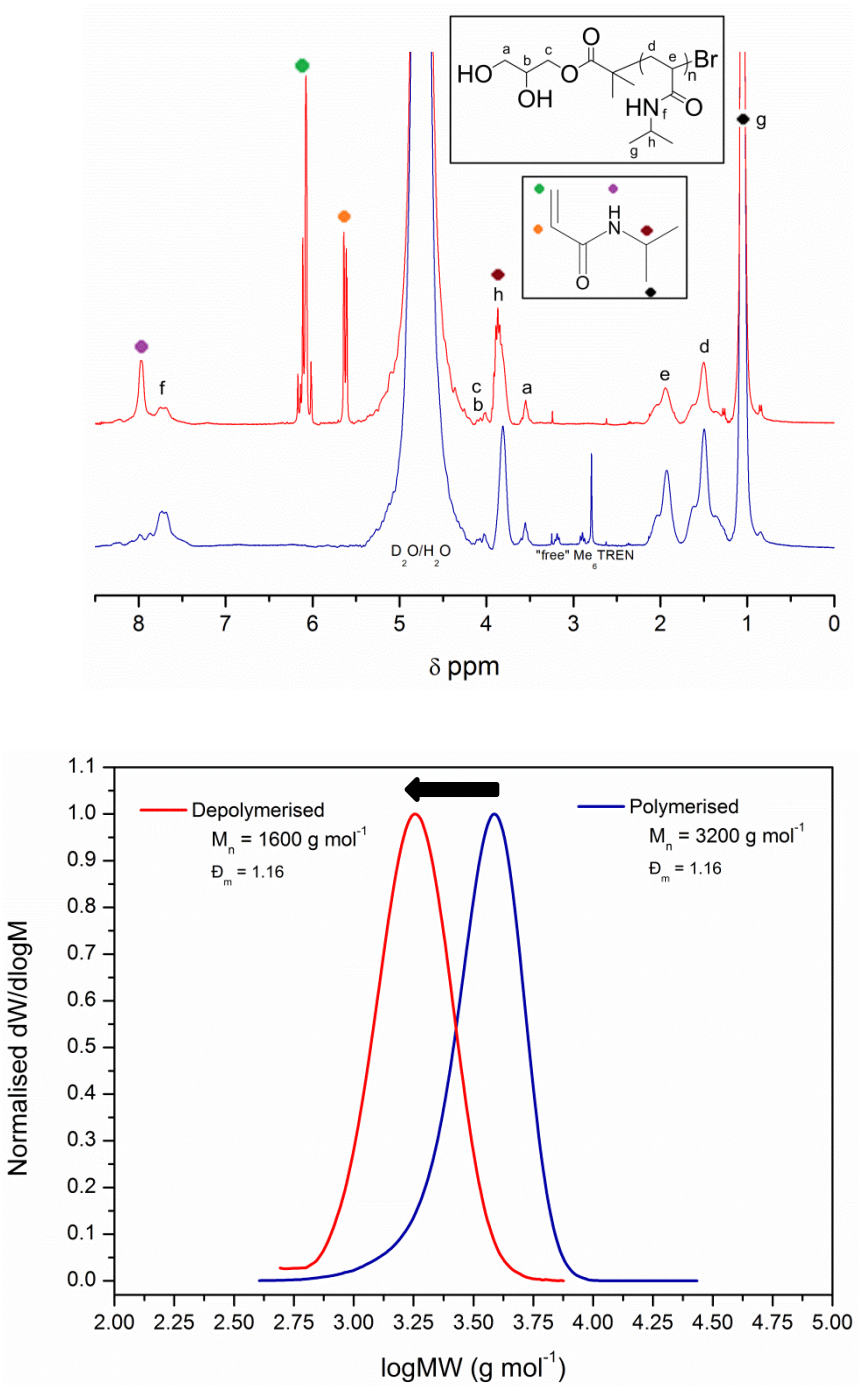

Figure 2.1 - ^{1}H NMR (above) and SEC chromatograms for the polymerisation (blue) and depolymerisation (red) of NIPAm in carbonated water at 0 °C.

Monitoring the reaction *via* a kinetic study revealed that complete monomer conversion had in fact been achieved within 60 seconds. After this point, the resulting polymer remained relatively stable for a further 30 minutes before undergoing depolymerisation (Figure 2.2).

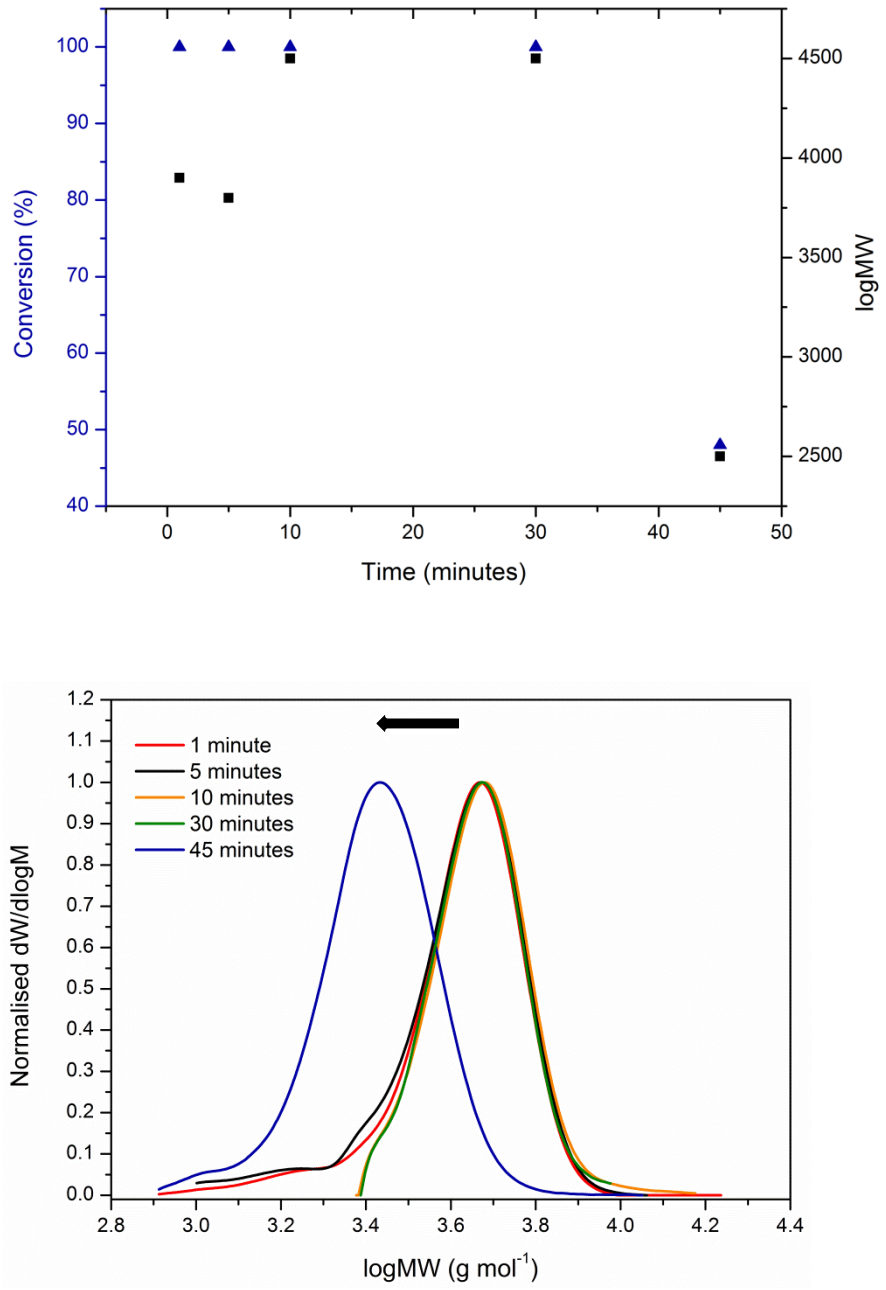

Figure 2.2 – Kinetic data (top) and SEC traces (bottom) for the polymerisation/depolymerisation process of PNIPAm in carbonated water.

The occurrence of "*in-situ*" depolymerisation was confirmed by analysing the resulting crude polymerisation solution by gas chromatography (GC) (Figure 2.3), and gas chromatography – mass spectrometry (GC-MS) (Figure 2.3). Upon comparing the data to that of a known standard, the NIPAm monomer ($[M+]_{exp}$ = 114.30; $[M+]_{th}$ = 114.09) was identified as being present. This therefore indicated that the controlled, low temperature depropagation of PNIPAm into NIPAm had arisen.

Code	Retention Time (minutes)
NIPAm standard	2.76
Depolymerised PNIPAm	2.75

Table 2.2 - Results for the GC analysis of depolymerised PNIPAm (green) and a NIPAm standard (black).

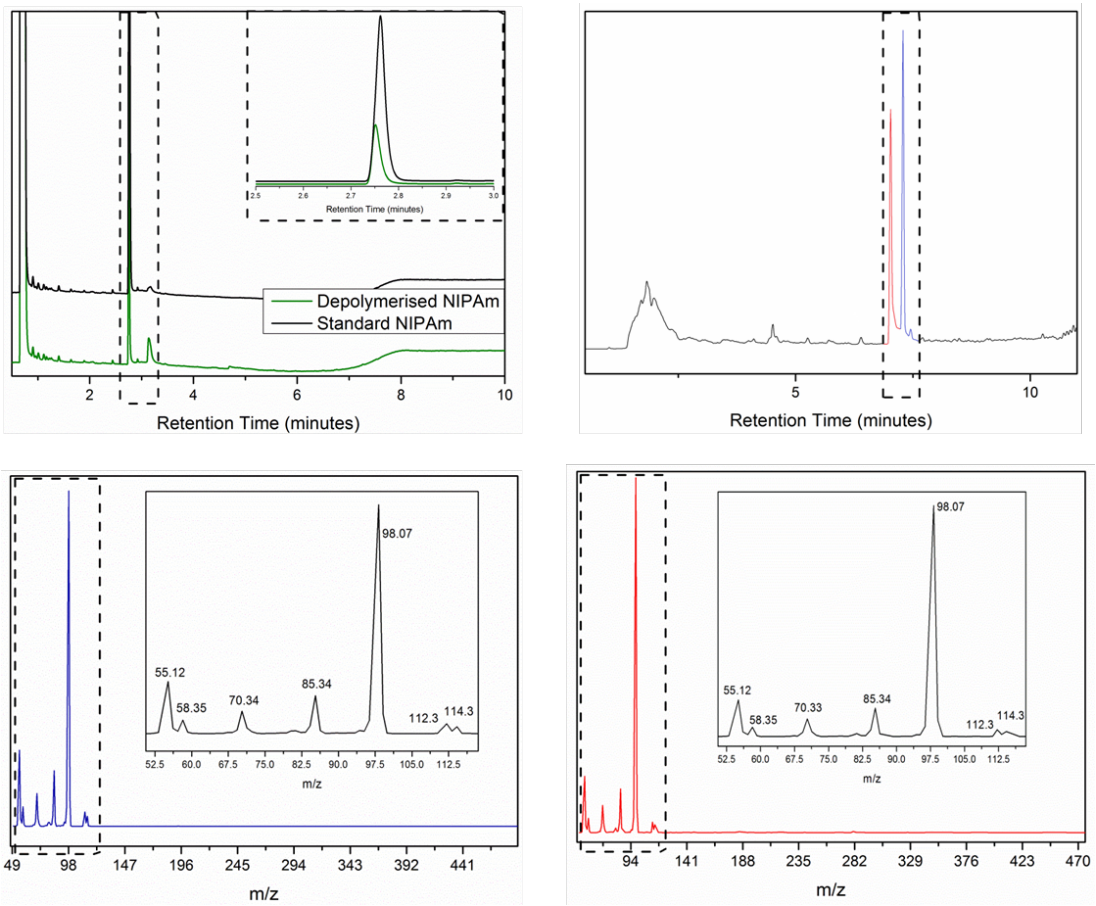

Figure 2.3 – GC and GC-MS traces for the reaction mixture post-depolymerisation; [NIPAm] : [I] : [$Cu^{(I)}Br$] : [Me_6TREN] = [20] : [1] : [0.4] : [0.4].

Fragmentation Structure	Theoretical m/z	Peak 1 m/z (rt = 7.02 minutes)	Peak 2 m/z (rt = 7.27 minutes)
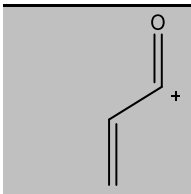	55.02	55.12	55.12
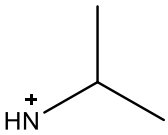	58.10	58.35	58.35
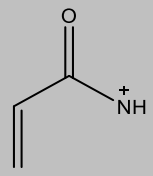	70.03	70.33	70.34
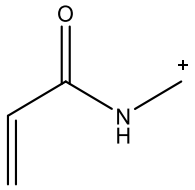	85.05	85.34	85.34
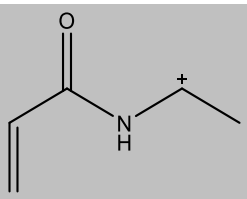	98.06	98.07	98.07
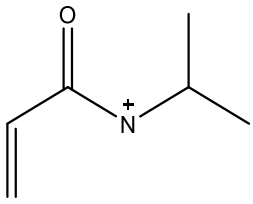	112.08	112.30	112.30
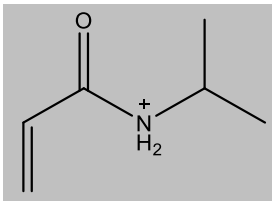	114.09	114.30*	114.30*

Table 2.3 - GC-MS analysis of the depolymerised PNIPAm reaction mixture where * denotes the molecular ion [M+].

Upon removing CO_2 from the system *via* N_2 purging post-depolymerisation (Scheme 2.7), the regenerated monomer was quantitatively repolymerised within 30 minutes (Figure 2.4) without sacrificing control over the process (M_n = 3500 g mol^{-1}; $Đ_m$ = 1.23) (Table 2.4, Figure 2.5). Notably, the final polymer remained stable against depolymerisation, with 100 % monomer conversion being maintained for at least 1 day; this further demonstrated the controlled nature of this system.

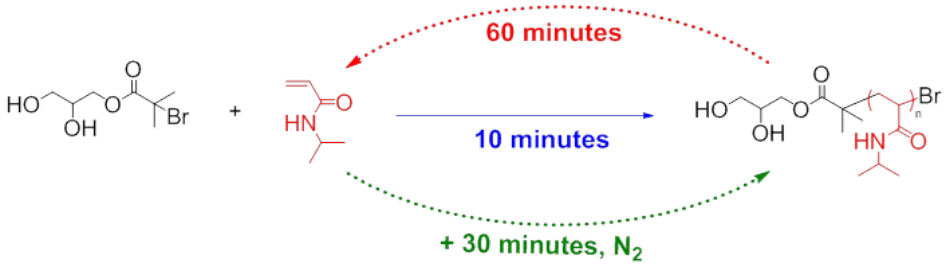

Scheme 2.7 – A schematic representation for the polymerisation/depolymerisation of NIPAm in carbonated water.

Monomer	Process	Conversion[b] (%)	M_n[a] (g mol^{-1})	$Đ_m$
NIPAm	Polymerisation	100	3200	1.16
	Depolymerisation	52	1600	1.16
	Repolymerisation	100	3500	1.23

Table 2.4 – A summary of the polymerisation, depolymerisation and repolymerisation of NIPAm in water in the presence of dissolved CO_2.

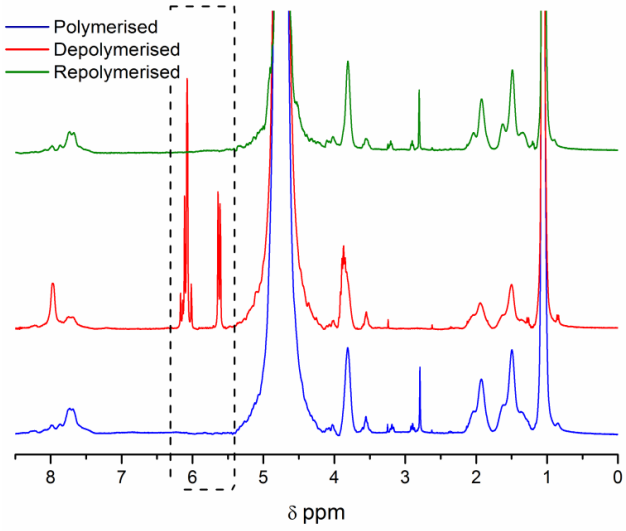

Figure 2.4 - ^{1}H NMR spectra for the polymerisation (blue), depolymerisation (red) and repolymerisation (green) of NIPAm in carbonated water at 0 °C; [NIPAm] : [I] : [Cu$^{(I)}$Br] : [Me$_6$TREN] = [20] : [1] : [0.4] : [0.4].

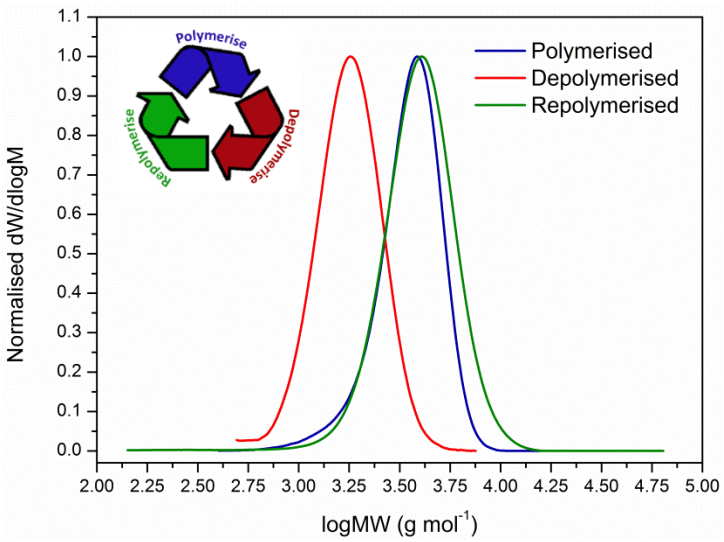

Figure 2.5 – Molecular weight distributions (MWDs) for the polymerisation (blue), depolymerisation (red) and repolymerisation (green) of NIPAm in carbonated water at 0 °C; [NIPAm] : [I] : [$Cu^{(I)}Br$] : [Me_6TREN] = [20] : [1] : [0.4] : [0.4].

It is important to note that when the polymerisation of NIPAm is conducted in HPLC grade water using N_2 deoxygenation as the source of O_2 removal, no depolymerisation occurs.[36,49]

2.2.2. Determining the effect of CO_2 upon depolymerisation

Considering the observation of depolymerisation in carbonated water but not in deoxygenated (N_2 sparging) HPLC grade water, an initial assessment of the two systems suggested that either CO_2, or the presence of dissolved minerals in the commercial carbonated water source, was a potential trigger for this phenomenon. To investigate the role of the former, HPLC grade water was carbonated using dry ice as the source of carbonation, and subsequently employed as the solvent for the polymerisation of NIPAm. Within 10 minutes, high conversion was obtained (94 %; M_n = 3600 g mol^{-1}) with depolymerisation arising after the reaction was allowed to proceed further (t = 24 hours; 34 % depolymerisation; M_n = 2800 g mol^{-1}; $Đ_m$ = 1.12) (Figure 2.6).

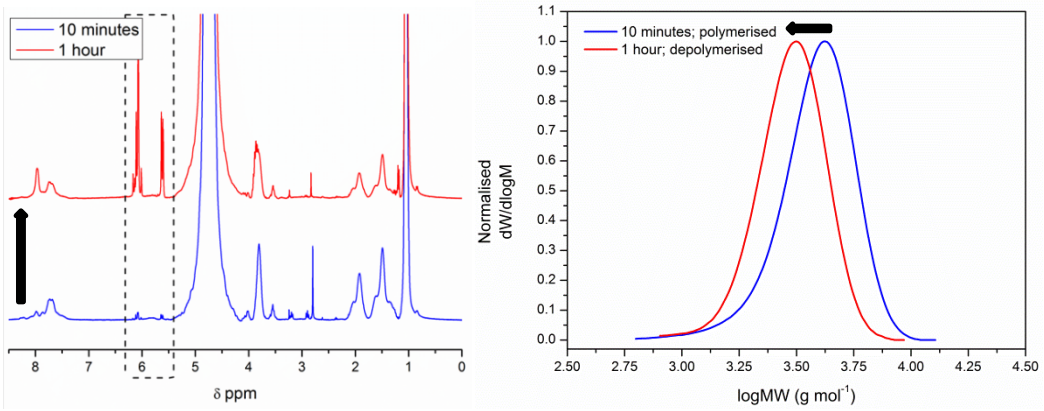

Figure 2.6 - ^{1}H NMR spectra for the polymerisation/depolymerisation of NIPAm in carbonated HPLC grade water (left). SEC traces for the polymerisation (blue) and depolymerisation (red) of NIPAm in carbonated HPLC grade water (right).

Despite the extent of depolymerisation being less than that which was previously observed, it was evident that dissolved CO_2 was the cause of depolymerisation. Furthermore, given the purity of HPLC grade water, it was deemed likely that the mineral additives present within carbonated water did not significantly contribute towards this phenomenon. In order to verify this, commercially available carbonated water was de-carbonated, and the polymerisation of NIPAm was conducted in the presence of air to yield 33 % conversion after 10 minutes, and 37 % after 24 hours.

When the polymerisation was conducted in the presence of N_2 however, 100 % conversion was attained after 10 minutes (M_n = 5300 g mol^{-1}; $Đ_m$ = 1.10) (Figure 2.7). After the reaction was left under formal polymerisation conditions for a further hour, no evidence of depolymerisation was observed by SEC or ^{1}H NMR (Figure 2.7). The stability of the polymer towards depropagation under this setup supported the theory that the presence of dissolved minerals within the commercial water had no noticeable influence upon the onset of depolymerisation.

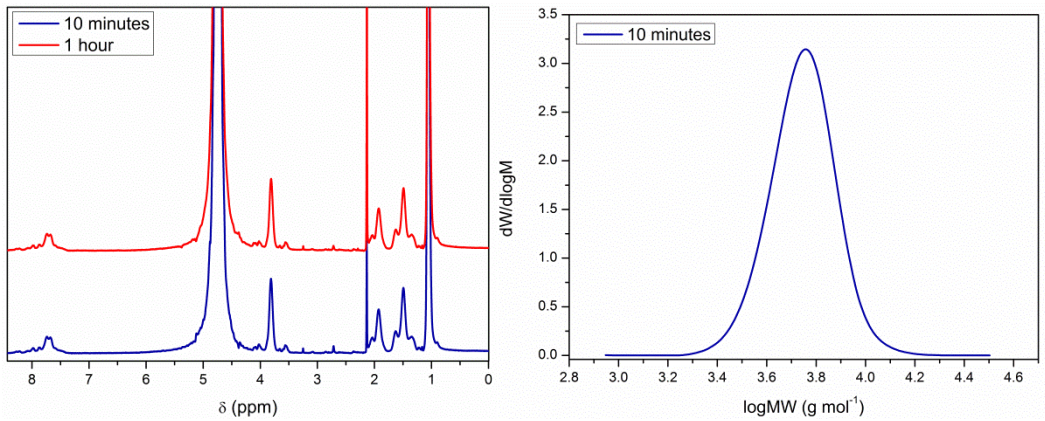

Figure 2.7 -^{1}H NMR spectra for the polymerisation of NIPAm in decarbonated commercially available carbonated water (left) and the SEC trace polymerisation of NIPAm in decarbonated commercially available carbonated water (right).

2.2.3. Investigation into the effect of pressure and temperature upon depolymerisation

An important factor to take into consideration when investigating this system was the carbonation process itself. Industrially, water is carbonated under pressures (between 1.5 and 2.5 bar)[50] that are higher than those which were most likely reached during the dry ice carbonation. For this reason, it was decided that the effect of pressure upon the polymerisation/depolymerisation system needed to be studied further.

It was theorised in accordance with Le Châtalier's Principle and Henry's Law, that in a closed system, an increase in pressure would result in an increase in the extent of depolymerisation by shifting the equilibrium to the right and increasing the concentration of CO_2 that was dissolved in the water (Equation 2.11).

$$\mathbf{CO_{2\,(g)} + H_2O_{(l)} \leftrightarrow CO_{2\,(aq)}} \qquad \textbf{(Equation 2.11)}$$

To assess this, the polymerisation of NIPAm in carbonated water was conducted at pressures ranging from 2 bar to 100 bar in a steel autoclave (typically used for conducting polymerisations in supercritical carbon dioxide ($scCO_2$)).[51,52] Upon

analysis of the results (Table 2.5) it was found that for all of the applied pressures, uncontrolled polymerisations ensued (Figure 2.8) alongside an absence of depolymerisation.

Pressure (bar)	10 minutes (% Conv.)	60 minutes (% Conv.)	$^{a}M_{n,\,SEC}$ (g mol^{-1})	$^{b}M_{n,\,SEC}$ (g mol^{-1})	$^{a}Đ_{m}$	$^{b}Đ_{m}$
10	100	100	3600	3300	2.85	1.89
100	100	98	6200	3400	4.74	1.91

Table 2.5 - ^{1}H NMR and SEC data for the polymerisation of NIPAm in carbonated deionised water under high pressures where "a" = 10 minutes and "b" = 60 minutes.

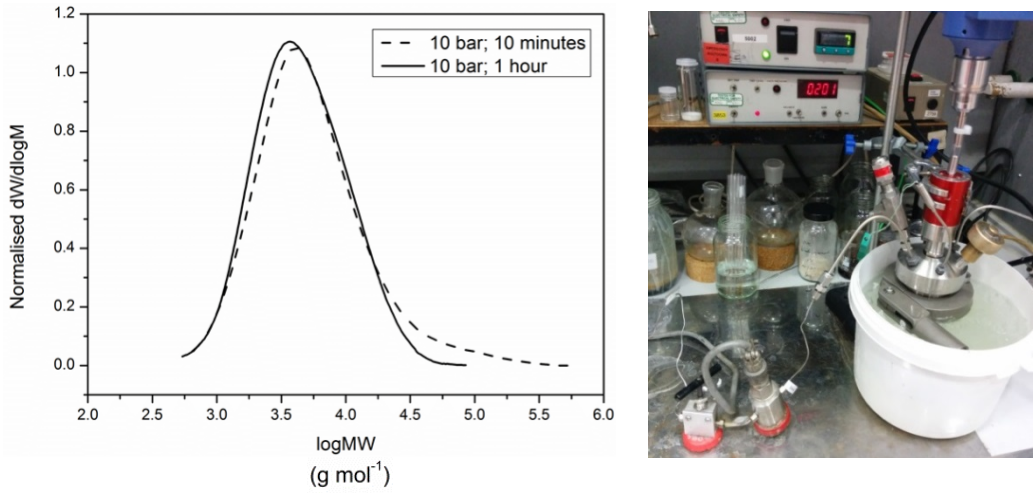

Figure 2.8 - Molecular weight distributions for the polymerisation of NIPAm in carbonated deionised water at 0 °C under a pressure of 10 bar (left). The setup for conducting the polymerisation of PNIPAm under a pressure of 10 bar (right).[52]

Currently it is unknown as to why depolymerisation was not achieved under increased pressure. It was postulated that there needed to be a thermodynamic change occurring through the loss of pressure over time in order for depropagation to take place. According to Henry's Law (Equation 2.10), in a closed system the concentration of CO_2 in the solution is directly proportional to the partial pressure of CO_2 in the headspace.[48] When there is a change in the pressure of the system, either through a leak or through being opened, CO_2 is lost from the solution over time. It was therefore plausible that whilst this could be observed in the conventional

setup *via* the gradual loss of CO_2 through a rubber septum and a glass vial, it was not possible in the steel autoclave.

In order to determine if this was the case, an "open top" polymerisation (in an unsealed vial under atmospheric conditions) of NIPAm was conducted. After 10 minutes, a maximum of 98 % conversion was achieved with analysis by SEC revealing the presence of a secondary high molecular weight peak (M_n = 4200 g mol^{-1}; $Đ_m$ = 2.25) (Figure 2.9) indicative of a loss of control over the polymerisation process. Further sampling of the reaction yielded a stable polymer; demonstrating that under these conditions there was an absence of depolymerisation.

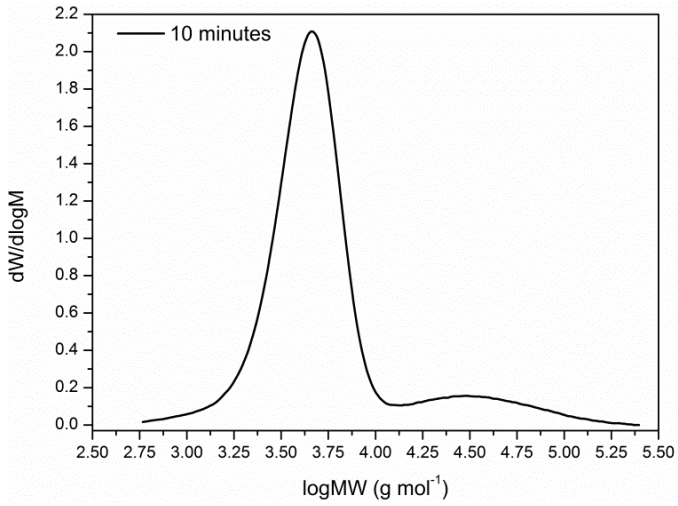

Figure 2.9 - Molecular weight distributions for the polymerisation of NIPAm in carbonated water at 0 °C in an unsealed vial.

Despite the stability of the polymer under "high" pressure, and given the absence of depolymerisation under "low" pressure, it is apparent that to some degree, pressure was a pre-requisite for depropagation.

Since depolymerisation is known to occur when a given polymer's T_c is reached, it was considered to be feasible that increasing the temperature of the system would result in a greater degree of depolymerisation. However, it should be noted that considering PNIPAm has a lower critical solution temperature (LCST) of 32 °C in water,[53–55] it seemed unlikely that at temperatures below this, where the polymer

was still soluble, would be close to the T_c. Nevertheless, in an attempt to demonstrate the validity of this hypothesis, the polymerisation of NIPAm in carbonated water was conducted at ambient temperature. Monitoring of the process through ^{1}H NMR and SEC characterisation revealed that whilst the polymerisation was rapid and controlled (> 99 % conversion, $Đ_m$ = 1.15) (Figure 2.10), the resulting polymer was stable towards depolymerisation.

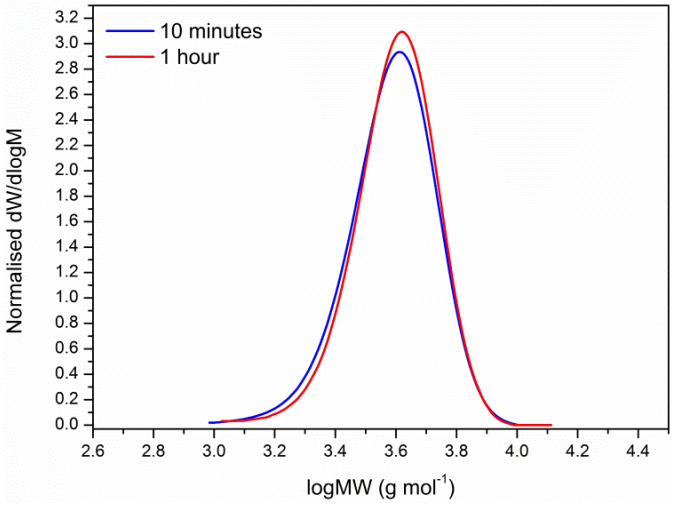

Figure 2.10 - Molecular weight distributions for the polymerisation of NIPAm in carbonated water at 25 °C.

It is clear that depropagation was reduced by an increase in temperature. As such, it was concluded that occurrence of depolymerisation in this system was not related to the T_c of the polymer. It is possible that the increase in temperature resulted in the concentration of dissolved CO_2 being insufficient to induce depolymerisation. However, this is merely a theory, and there is currently no evidence to support this.

2.2.4. Exploring the relationship between pH and depolymerisation

As previously mentioned, when CO_2 is dissolved in water it results in acidic conditions (pH = 4.72) when compared to water which has not been carbonated (pH = 6.28). Therefore, it was decided that the pH of the depolymerisation reaction media would be investigated as a function of time and conversion.

The data obtained from monitoring the process showed that upon the onset of depolymerisation (Figure 2.11) there was little change in pH during both the polymerisation (pH = 6.40) and depolymerisation (pH = 6.94) processes (ΔpH = 0.54) (Figure 2.11). This implied that depropagation was not induced by a change in pH, nor was there an event occurring which altered the pH of the polymerisation system.

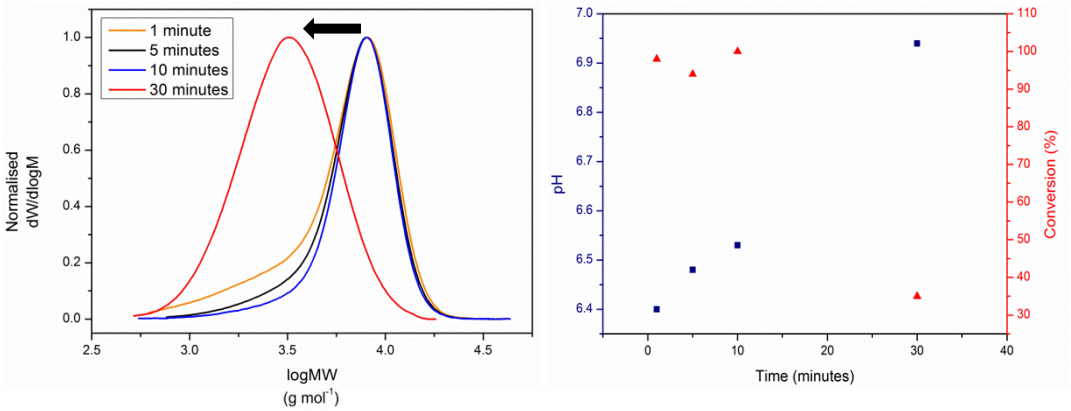

Figure 2.11 - SEC traces for the polymerisation/depolymerisation of DP = 40 PNIPAm (left). Plot of pH versus time (blue) and conversion versus time (red) for the polymerisation/depolymerisation of DP = 40 PNIPAm (right).

Despite only a slight change in pH being observed with the start of depolymerisation, its effect on this phenomenon was studied further. When the pH of carbonated water was adjusted to 8 using sodium hydrogen carbonate ($NaHCO_3$), near quantitative conversion was obtained, followed by an absence of depolymerisation after 48 hours (97 % conversion). This indicated that whilst there was no change in pH during the process, a pH < 8 was initially required for depolymerisation to occur. Although the reason for this is currently unclear, it is evident that the process was sensitive to pH when depolymerisation was conducted in the presence of CO_2.

When HPLC grade water was acidified to pH 5.55 and used as the solvent for a traditional aqueous $Cu^{(0)}$-mediated RDRP of NIPAm, a slow and incomplete reaction was observed (t = 24 hours; 73 % conversion; M_n = 1600 g mol^{-1}; $Đ_m$ = 1.25) (Figure

2.12). This was attributed to the protonation of the ligand in the $Cu^{(II)}Br_2/Me_6TREN$ complex and the occurrence of termination events.[56,57]

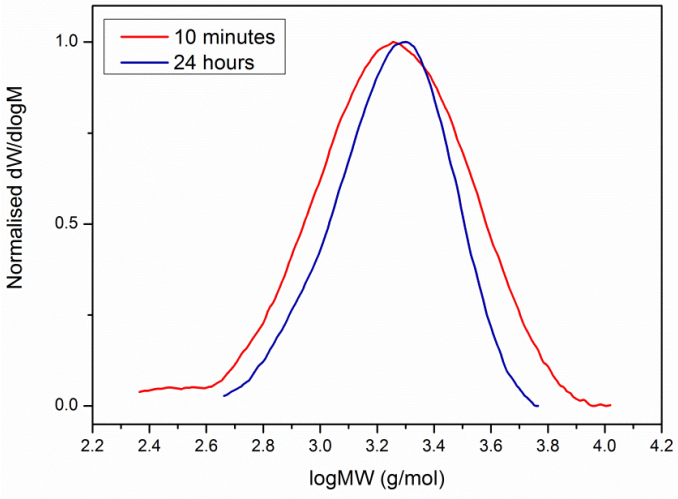

Figure 2.12 - Molecular weight distributions for the polymerisation of NIPAm in acidified HPLC grade water (pH 5.55) at 0 °C; [NIPAm] : [I] : [$Cu^{(I)}Br$] : [Me_6TREN] = [20] : [1] : [0.4] : [0.4].

Copper-amine complexes are affected by changes in pH through modification of the co-ordination sphere surrounding the metal centre. For example, $Cu^{(II)}$ complexes often have a preferred co-ordination number of 5. This means that in the presence of tetradentate ligands (such as Me_6TREN), at least one molecule of water or one halogen atom is bound to the copper centre.[58–60] In basic systems (pH > 8), ligand exchange will occur. During this process, OH^- ions displace the bound water or halogen atom to create a more stable complex.[42,61] Conversely, for systems that are operating at a low pH, the amine ligand undergoes a proton transfer reaction which ultimately leads to the complex becoming dissociated.[56,57,62] Considering this, it was hypothesised that depolymerisation was arising from modification of the $Cu^{(II)}Br_2/Me_6TREN$ complex as a consequence of a decrease in the ability of Me_6TREN to co-ordinate to the copper centre.

Probing the effect of pH on [$Cu^{(II)}Br_2/Me_6TREN$] by UV-Vis spectroscopy revealed the loss of the weak d-d transition at 680 nm[42] in both the acidified (pH 5.55) and carbonated water (pH 5.45) when compared to water with a pH of 8.89 (Figure

2.13). Interestingly, when carbonated water was deoxygenated with N_2 to mimic the treatment of the depolymerisation system prior to repolymerisation, the absorbance band reappeared and the spectra followed that of the $Cu^{(II)}Br_2/Me_6TREN$ complex in HPLC grade water (Figure 2.13).

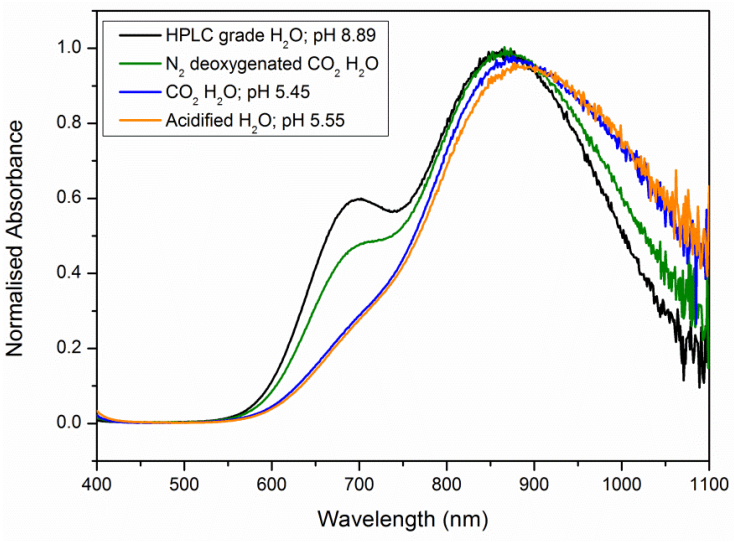

Figure 2.13 - UV-Vis spectra for [$Cu^{(II)}Br_2/Me_6TREN$] in HPLC grade water (black), N_2 deoxygenated carbonated water (green), carbonated water (blue) and acidified HPLC grade water (orange).

To determine the role of the copper complex upon this system, 100 µL concentrated hydrochloric acid (HCl) was added to the reaction prior to depolymerisation (t = 10 minutes; 100% conversion; $Đ_m$ = 1.22) (Figure 2.15); this was in order to reduce the concentration of the $Cu^{(II)}$ complex through ligand protonation. Upon addition, a noticeable colour change from blue to colourless was observed. As this was accompanied by a decrease in the absorbance recorded by UV-Vis spectroscopy and a further loss of the weak d-d transition, this indicated that dissociation of the complex had indeed occurred (Figure 2.14).

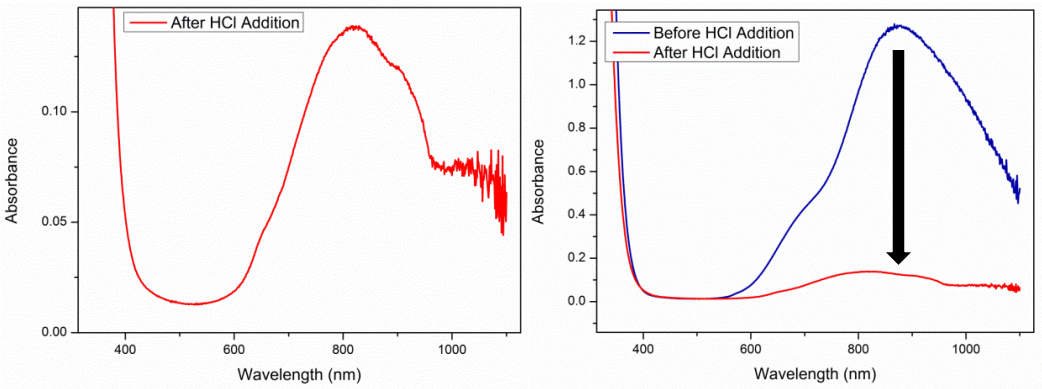

Figure 2.14 – UV-Vis data showing the effect of adding concentrated HCl to the reaction.

According to SEC measurements, allowing the reaction to proceed resulted in the onset of depolymerisation without any noticeable increase in dispersity (t = 60 minutes; 54 % depolymerisation; $Đ_m$ = 1.17) (Figure 2.15). Importantly, these results demonstrated that controlled depolymerisation could take place following the loss of [$Cu^{(II)}Br_2$/Me_6TREN]. With that in mind, it was decided that the effect of changing the co-ordination sphere around copper needed to be studied further.

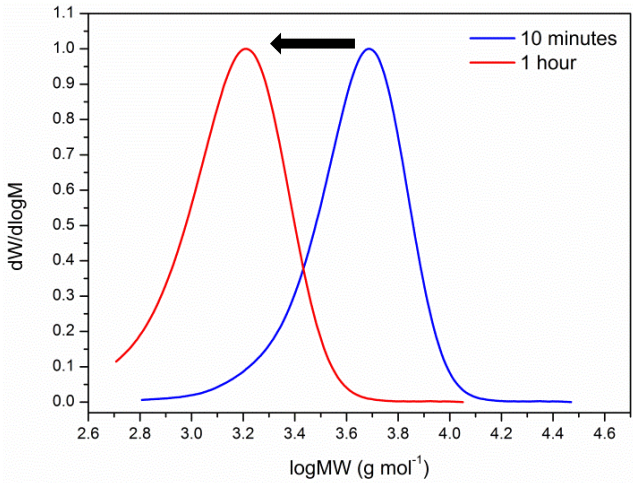

Figure 2.15 - SEC data for the effect of adding concentrated HCl to the crude reaction mix prior to depolymerisation.

2.2.5. Studying the effect of changing ligands on depolymerisation

Whilst there is very little in the literature regarding the depolymerisation of acrylic/vinyl-based polymers, it is well established that nitrogen based ligands and their copper complexes can aid the depolymerisation of compounds such as lignin

(a natural, highly amorphous co-polymer formed of three different monomer units, *para*-coumaryl alcohol, coniferyl alcohol and sinapyl alcohol, most commonly found in the second cell wall of plants).[63,64]

N,N,N',N'',N''-Pentamethyldiethylenetriamine (PMDETA) is an *N*-donating tridentate ligand which co-ordinates to copper in a different manner than the tetradentate Me_6TREN ligand.[65,66,67] During the development of the aqueous $Cu^{(0)}$-mediated RDRP protocol, it was screened as the ligand for the polymerisation of NIPAm in HPLC grade water ([M] : [I] : [L] : [$Cu^{(I)}$Br] = [80] : [1] : [0.4] : [0.8]).[32] In this work it was found that 95 % conversion could be achieved within 3 hours (M_n = 9600 g mol^{-1}; $Đ_m$ = 1.51)).

When used as the ligand for the polymerisation of NIPAm in carbonated water, a multimodal MWD was attained with a loss of control over the average molecular weight observed by SEC (88 % conversion; M_n = 6100 g mol^{-1}; $Đ_m$ = 1.62). With the resulting polymer remaining stable after 1 hour (82 % conversion) (Figure 2.16), it was theorised that altering the co-ordination sphere around copper prevented depolymerisation from occurring and thus, supported the earlier theory of a modified complex being a pre-requisite for depropagation to occur.

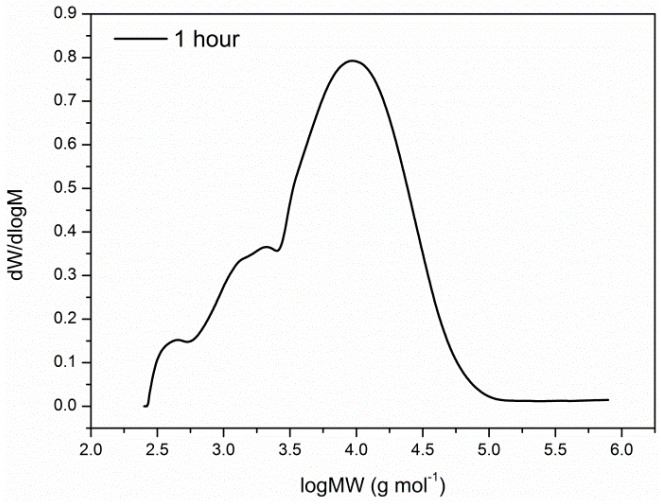

Figure 2.16 - Molecular weight distributions for the polymerisation of PNIPAm in carbonated water at 0 °C; [NIPAm] : [I] : [$Cu^{(I)}$Br] : [PMDETA] = [20] : [1] : [0.4] : [0.4].

2.2.6. Expanding the scope of the system

In order to further probe the constraints of this system, the depolymerisation of higher molecular weight PNIPAm (> 12,800 g mol^{-1}) was also examined. When polymers with a targeted DP = 120 were polymerised with 0.4 eq. of Me_6TREN and $Cu^{(I)}Br$, low conversions (< 10 %) arose. However, by increasing the $Cu^{(I)}Br$/ligand concentration (and hence that of $Cu^{(II)}Br_2$ and $Cu^{(0)}$) to 2.4 eq., 100 % conversion was achieved within 10 minutes (M_n = 20,600 g mol^{-1}; $Đ_m$ = 1.18). This was followed by 43 % depolymerisation after 1 hour (M_n = 12,400 g mol^{-1}; $Đ_m$ = 1.11) (Figure 2.17).

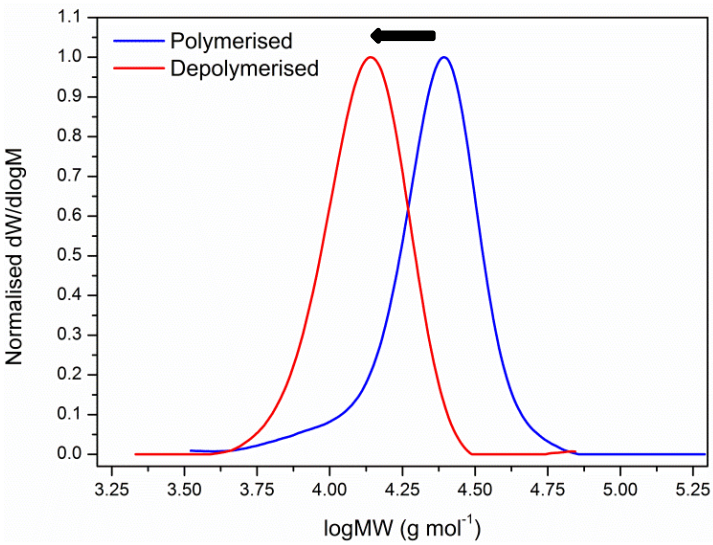

Figure 2.17 - Molecular weight distributions for the polymerisation of NIPAm in carbonated water in the presence of excess $Cu^{(I)}Br$ and Me_6TREN at 0 °C; [NIPAm] : [I] : [$Cu^{(I)}Br$] : [Me_6TREN] = [120] : [1] : [2.4] : [2.4].

Interestingly, the polymers that were produced from both stages had a significantly lower dispersity than when the same concentration of Me_6TREN and $Cu^{(I)}Br$ was used for the polymerisation of NIPAm in HPLC grade water (100 % conversion; M_n = 22,000 g mol^{-1}; $Đ_m$ = 1.79) (Figure 2.18).

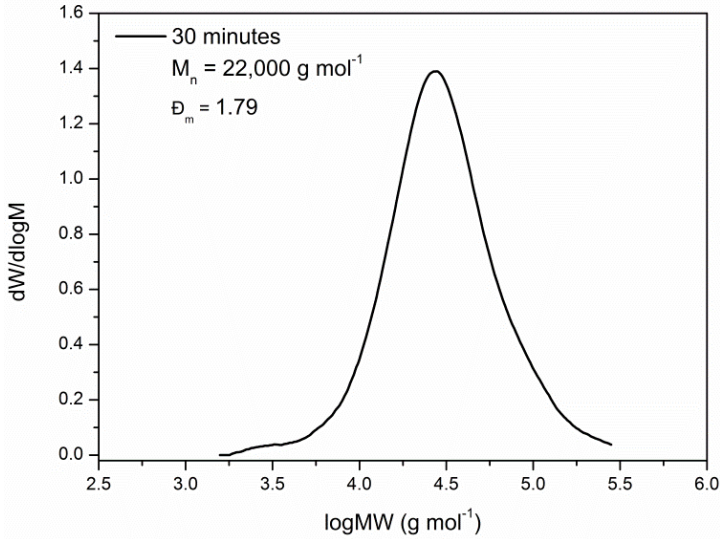

Figure 2.18 - Molecular weight distribution for the polymerisation of NIPAm in HPLC Grade water in the presence of excess $Cu^{(I)}Br$ and Me_6TREN at 0 °C; [NIPAm] : [I] : [$Cu^{(I)}Br$] : [Me_6TREN] = [120] : [1] : [2.4] : [2.4].

Targeting high PNIPAm DP values (n = 240 and 360) required a further increase in the concentration of $Cu^{(I)}Br$ and Me_6TREN. Unlike the synthesis of DP = 120 PNIPAm, this resulted in a loss of control over the process with undesirable radical-radical coupling occurring as evidenced by the noticeable bimodality observed in the SEC chromatograms (Figure 2.19).

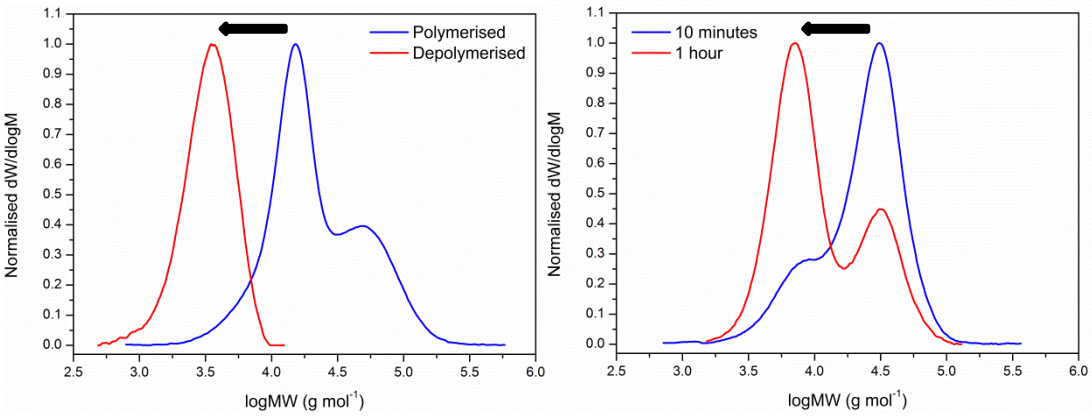

Figure 2.19 - Molecular weight distributions for the polymerisation of NIPAm in carbonated water in the presence of excess $Cu^{(I)}Br$ and Me_6TREN at 0 °C; [NIPAm] : [I] : [$Cu^{(I)}Br$] : [Me_6TREN] = [240] : [1] : [4.8] : [4.8] (left) and [NIPAm] : [I] : [$Cu^{(I)}Br$] : [Me_6TREN] = [360] : [1] : [7.2] : [7.2] (right).

Based on these findings, it was subsequently hypothesised that when 0.4 eq. of $Cu^{(I)}Br/Me_6TREN$ was employed for the high molecular weight polymerisations, the

concentration of activating species was not sufficient enough for polymerisation to occur. It is possible that this related to ligand protonation and the dissociation of the $Cu^{(II)}$ complex in acidic conditions, although there is currently no additional evidence beyond the UV-Vis study reported earlier.

It was also believed that conducting polymerisations in the presence of excess ligand concentrations alone could enable for the synthesis of high molecular weight polymers. However, when the polymerisation was conducted with 0.4 eq. of $Cu^{(I)}Br$ and 2.4 eq. Me_6TREN, 0 % conversion was achieved after 1 hour, thus indicating that this was not the case (Figure 2.20).

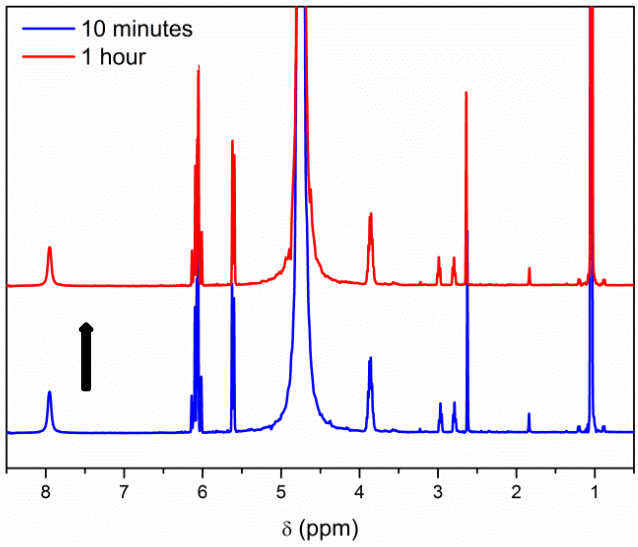

Figure 2.20 – ^1H NMR spectra for the polymerisation of NIPAm in carbonated water in the presence of excess ligand. [NIPAm] : [I] : [$Cu^{(I)}Br$] : [Me_6TREN] = [20] : [1] : [0.4] : [2.4].

It was evident from the SEC results that depolymerisation arose for each of the high molecular weight polymerisations when an excess of $Cu^{(I)}Br$/ligand was employed. Pleasingly, this was reflected in the results that were obtained from ^1H NMR spectroscopy (Table 2.6 and Figure 2.21).

Target DP	$Cu^{(I)}Br/Me_6TREN$ (eq.)	Time (mins)	Conversion (%)	Deconversion (%)	$M_{n,SEC}$ g mol^{-1}	$Đ_m$
120	2.4	10	100	-	20,600	1.18
120	2.4	60	57	43	12,400	1.11
240	4.8	10	98	-	15,500	2.04
240	4.8	60	13	87	2,900	1.23
360	7.2	10	98	-	14,600	1.96
360	7.2	60	4	96	8,300	1.90

Table 2.6 – A summary of results for the depolymerisation of high molecular weight PNIPAm.

For PNIPAm with a targeted DP = 120, utilising 2.4 eq. of $Cu^{(I)}Br$/ligand resulted in 43 % depolymerisation within 1 hour. It is worth noting that this result was similar to those which were obtained for DP = 20 PNIPAm in the presence of 0.4 eq. $Cu^{(I)}Br$ and ligand. However, for the other molecular weights, a significantly greater extent of depropagation was observed. Following 1 hour, it was found that 87 % and 96 % depolymerisation occurred for DP = 240 and DP = 360 respectively (Figure 2.21).

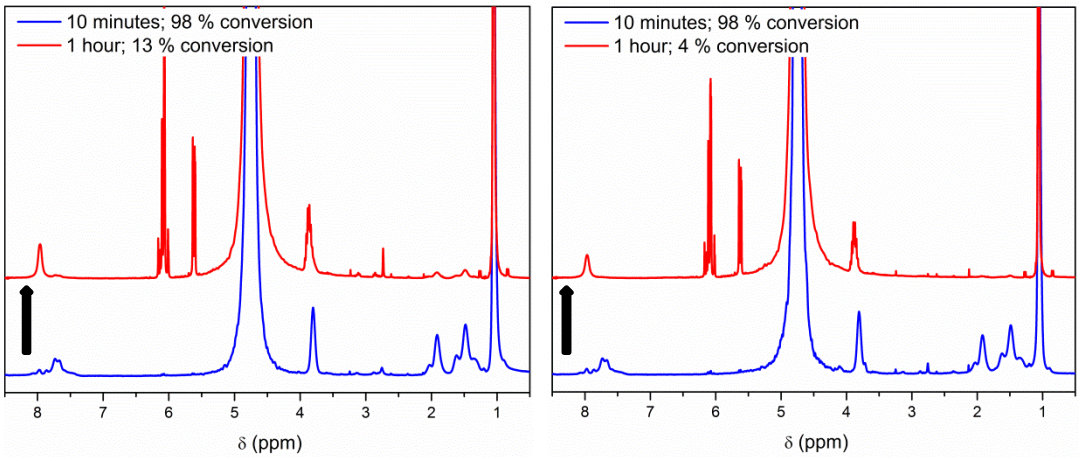

Figure 2.21 – ^1H NMR spectra for the polymerisation of NIPAm in carbonated water in the presence of excess $Cu^{(I)}Br$ and Me_6TREN at 0 °C; [NIPAm] : [I] : [$Cu^{(I)}Br$] : [Me_6TREN] = [240] : [1] : [4.8] : [4.8] (left) and [NIPAm] : [I] : [$Cu^{(I)}Br$] : [Me_6TREN] = [360] : [1] : [7.2] : [7.2] (right).

Earlier it was hypothesised that a modified copper complex was the cause of depolymerisation. Within Table 2.6 it can be seen that there was an increase in monomer reformation with an increase in chain length and the concentration of copper and ligand. Currently, there is not enough evidence to determine the reason

behind the increase in depolymerisation. However, given the previous findings, it was theorised that an increase in the concentration of the modified copper complex contributed to its occurrence. If this were indeed the case, then the cessation of depolymerisation for DP = 120 and DP = 20 PNIPAm could be as a result of an insufficient amount of the required copper complex. Further to this, it could mean that by increasing the concentration of copper and ligand to 2.4 eq., that a greater extent of depolymerisation could be attained.

To that end, 2.4 eq. of $Cu^{(I)}Br$ and ligand was used for the depolymerisation of DP = 20 PNIPAm. Unfortunately, the results that were obtained from ^{1}H NMR spectroscopy revealed an absence of depolymerisation. Moreover, characterisation by SEC revealed a deviation from the symmetrical Poisson-like distribution and controlled molecular weights that were previously achieved in this system (Figure 2.22). According to the proposed mechanisms for $Cu^{(0)}$-mediated RDRPs (the mechanism is currently under debate in the literature[68–70]), the addition of excess copper results in a loss of control over the polymerisation and an increase in termination. Similarly, free ligand (that which is not bound to the copper centre) results in chain transfer and quarternisation of the ligand onto the ω–end of the polymer to result in a loss of end group fidelity.[71,72]

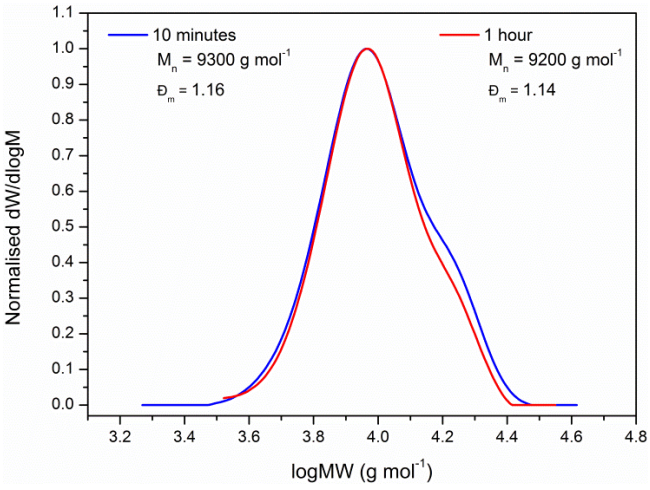

Figure 2.22 – Molecular weight distributions for the polymerisation of NIPAm in carbonated water in the presence of excess $Cu^{(I)}Br$ and Me_6TREN at 0 °C.

2.2.7. Investigating the end group fidelity

For any polymerisation to be classed as "living" or "controlled", the end group fidelity of the polymers must be retained. Hence, the synthesised polymers should possess the ability to chain extend to full conversion or be capable of undergoing multi-block copolymerisation *via* iterative monomer addition.[73]

Previous reports have highlighted the difficulty in maintaining high end group functionality in aqueous media due to an increased rate of hydrolysis of the terminal bromide.[32,49,74] Nevertheless, to test the "livingness" of this system during the polymerisation stage, an "*in-situ*" chain extension was attempted prior to depolymerisation. This involved adding an aliquot of NIPAm to the reaction mixture after near quantitative conversion had been reached (t = 10 minutes, 100 % conversion).

Within 30 minutes, 74 % conversion of the second monomer had been achieved (M_n = 7200 g mol^{-1}, $Đ_m$ = 1.18) (Figure 2.23) without the need for any purification steps prior to the addition. The data obtained from monitoring the process by SEC suggested that the polymers possessed a high level of chain end functionality with a clear increase in their average molecular weight and only small amount of tailing being visible within the low molecular weight region (Figure 2.23).

Interestingly, allowing the reaction to proceed for 24 hours under formal polymerisation conditions resulted in 87 % depolymerisation and a significant shift to lower molecular weights according to SEC (Figure 2.23). Although this suggestee that the chain extended PNIPAm underwent depolymerisation, the process was less controlled and resulted in a much broader MWD when compared to the original system.

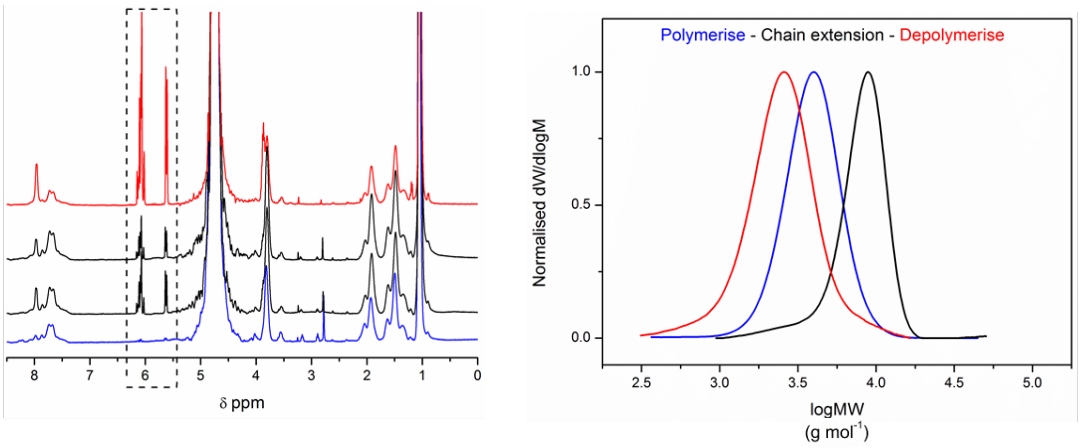

Figure 2.23 – ^{1}H NMR (left) and SEC (right) data for the chain extension of PNIPAm prior to depolymerisation.

Whilst the retention of high end group functionality from polymers produced from the first step of this system has been shown, the same has not yet been determined for the reverse reaction. Accordingly, the "livingness" of the depolymerisation step was tested through the addition of an aliquot of NIPAm post-depropagation. As expected, 98 % conversion of the initial monomer was observed after 10 minutes (M_n = 3700 g mol^{-1}, $Đ_m$ = 1.17), with 20 % depolymerisation (M_n = 3300 g mol^{-1}, $Đ_m$ = 1.15) occurring after 1 hour (Figure 2.24). Upon the second addition of NIPAm, no chain extension was observed *via* ^{1}H NMR or SEC, but rather a further 42 % of the initial polymer depolymerised (M_n = 1800 g mol^{-1}, $Đ_m$ = 1.78) (Figure 2.24).

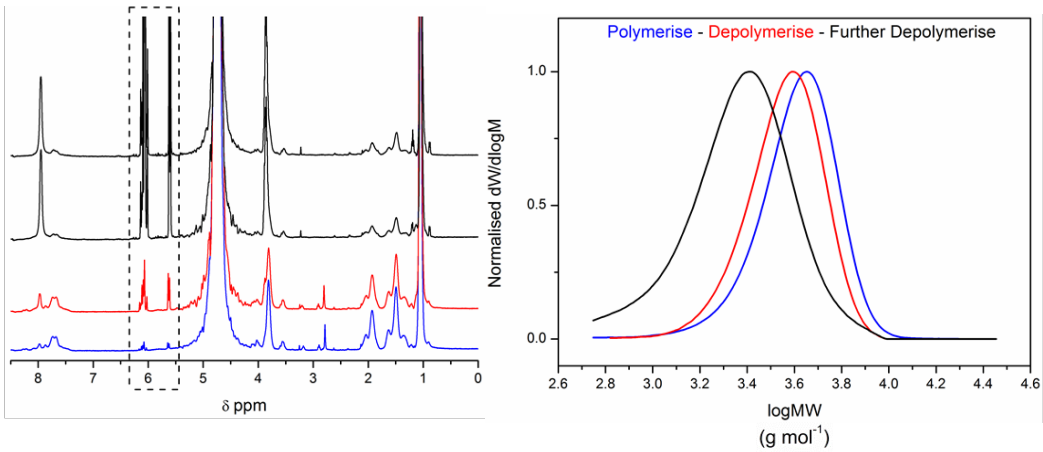

Figure 2.24 – ^{1}H NMR (left) and SEC data (right) for the attempted chain extension of PNIPAm post depolymerisation.

There were several possible explanations for the lack of chain extension following depolymerisation; the most notable of these being that by the time the second aliquot was introduced, polymer formation was thermodynamically unfavourable as the rate of depolymerisation had exceeded the rate of polymerisation. Alternatively, the absence could have been caused by a loss of end group fidelity following depropagation; however, as it has previously been shown that the regenerated monomer can be controllably repolymerised, this seemed unlikely.

2.2.8. Exploring the requirement for a bromine end group

In order to test whether a relationship between the bromine end group and depolymerisation existed, silver acetate (AgOAc) was introduced into the reaction upon high monomer conversion (90 % conversion; M_n = 3200 g mol^{-1}; $Đ_m$ = 1.27). This was in a 1:1 molar equivalence with respect to the total quantity of bromine.

Silver ions readily form ionic bonds with bromine to produce silver bromide (AgBr), a compound which is highly insoluble in water. This was evident when a grey precipitate (AgBr) formed upon the addition of AgOAc to the polymerisation. When analysed by SEC and ^{1}H NMR, the data revealed that depolymerisation had occurred despite the loss of bromine (58 % depolymerisation; M_n = 1400 g mol^{-1}, $Đ_m$ = 1. 48) (Figure 2.25). However, it had done so at the expense of control over the resulting polymer.

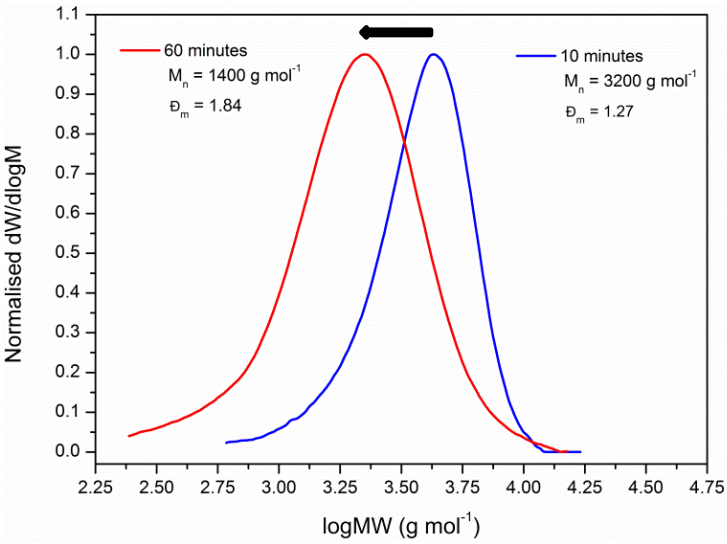

Figure 2.25 – SEC data for the polymerisation (blue) and depolymerisation (red) of DP = 20 PNIPAm in the presence of silver acetate.

To eliminate the possibility that the broad molecular weight distribution was due to an alternative factor, a conventional depolymerisation reaction was run concurrently as a control. Following quantitative conversion after 10 minutes, a decrease to 33 % was observed after 1 hour with the final polymer remaining narrowly disperse (M_n = 2500 g mol^{-1}, $Đ_m$ = 1.23).

It is apparent that the presence of silver acetate had a detrimental effect upon the system. If the mechanism for depolymerisation related in part to that of $Cu^{(0)}$-mediated RDRP, this was possibly due to the decrease in the concentration of polymers with bromine end groups and a decrease in the concentration of the deactivating species. This consequently implied that whilst a bromine end group was not required for depolymerisation to occur, it was required for the process to be controlled.

2.2.9. Depolymerisation of N-hydroxyethyl acrylamide (HEAm)

In an attempt to further investigate the scope of this system, the polymerisation of *N*-hydroxyethyl acrylamide (HEAm) was conducted in carbonated water. As with the

previous reactions, rapid and near-quantitative conversion was achieved within 1 minute (~ 98 %; M_n = 6400 g mol^{-1}; $Đ_m$ = 1.10). The resulting polymer was therefore left under formal polymerisation conditions for 1 hour.

Integration of the reformed vinyl protons (5.7 ppm) against the methylene protons present in the regenerated monomer and remaining polymer (3.9 ppm), indicated that 71 % depolymerisation had occurred within this time (t = 60 minutes; M_n = 3200 g mol^{-1}; $Đ_m$ = 1.10) (Figure 2.26). Interestingly, the rate of both polymerisation and depolymerisation was much faster than that which was observed for NIPAm. Further to this, a greater extent of depropagation was also furnished.

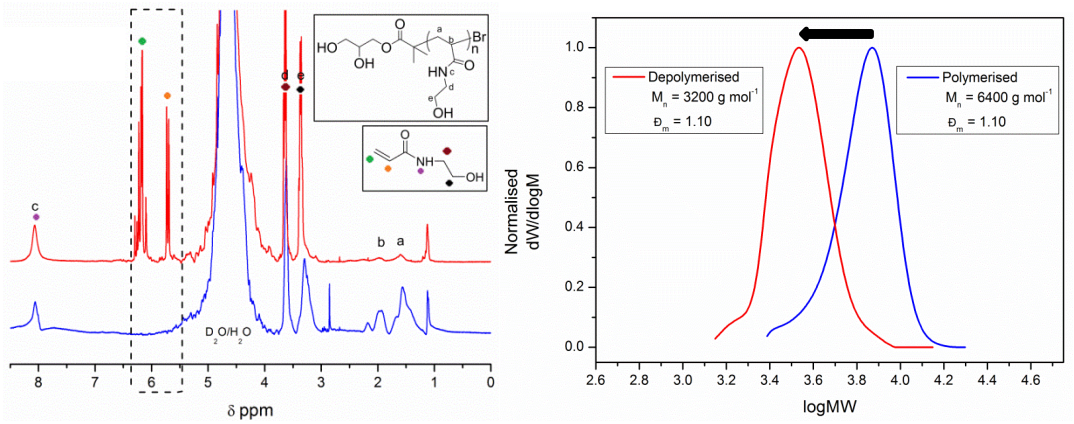

Figure 2.26 – ^{1}H NMR spectra (left) and SEC chromatograms (right) for the polymerisation (blue) and depolymerisation (red) of PHEAm in carbonated water at 0 °C; [HEAm] : [I] : [Cu$^{(I)}$Br] : [Me$_6$TREN] = [20] : [1] : [0.4] : [0.4].

Monitoring the reaction as a function of time revealed the absence of the induction period that was seen for NIPAm before the onset of depolymerisation. In addition to this, it was found that quantitative conversion and narrowly disperse polymers were achieved within 30 seconds. Pleasingly, the depolymerisation process remained highly controlled throughout with a maximum point being reached after 1 hour (Figure 2.27).

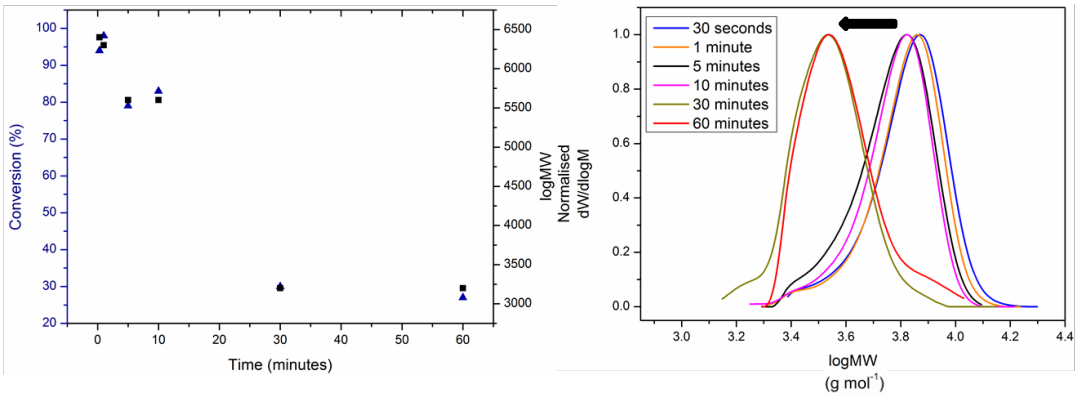

Figure 2.27 – The kinetic data (left) and the SEC traces (right) that were obtained for the polymerisation/depolymerisation process of PHEAm in carbonated water.

2.2.10. Depolymerisation of 2-hydroxyethyl acrylate (HEA)

Thus far, only the depolymerisation of polyacrylamides has been described. Therefore, for the purposes of establishing whether this system was only viable for one monomer class, 2-hydroxyethyl acrylate (HEA) was polymerised in carbonated water (t = 1 minute; 93% conversion; M_n = 7100 g mol^{-1}; $Đ_m$ = 1.16) (Figure 2.28). Encouragingly, as with the acrylamides, depolymerisation reached a maximum point after 1 hour (34 % depolymerisation; M_n = 5800 g mol^{-1}; $Đ_m$ = 1.13) with the resulting polymer remaining stable towards depropagation (Figure 2.28).

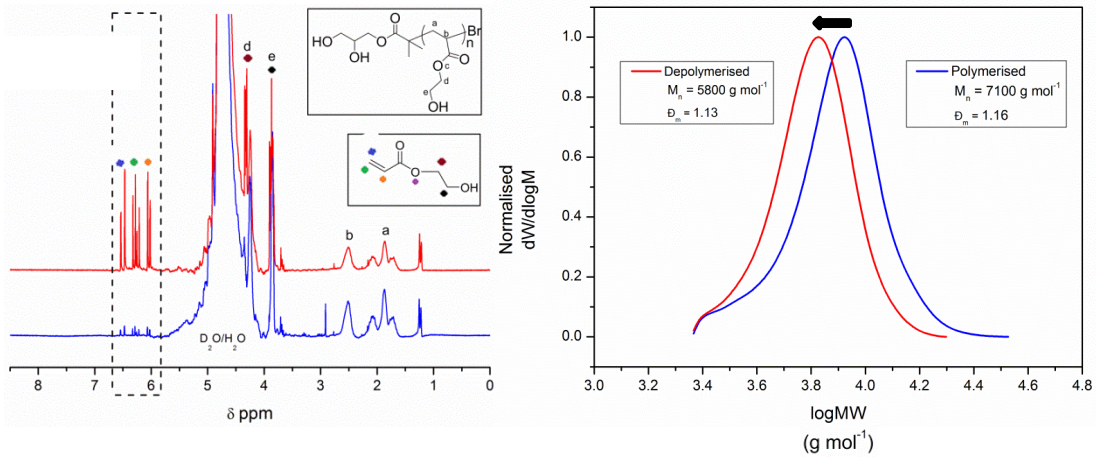

Figure 2.28 – ^{1}H NMR spectra (left) and molecular weight distributions (right) for the polymerisation (blue) and depolymerisation (red) of PHEA in carbonated water at 0 °C; [HEA] : [I] : [Cu$^{(I)}$Br] : [Me$_6$TREN] = [20] : [1] : [0.4] : [0.4].

In a similar manner to that of the original system, undertaking a small kinetic study revealed the presence of an induction period before the onset of depolymerisation. During this time, quantitative conversion and highly controlled polymers were achieved within 1 minute and remained relatively stable for 10 minutes (Figure 2.29). Moreover, as with the acrylamides, polymers with low dispersities were produced throughout the reaction (t = 60 minutes; M_n = 5800 g mol^{-1}; $Đ_m$ = 1.13) (Figure 2.29).

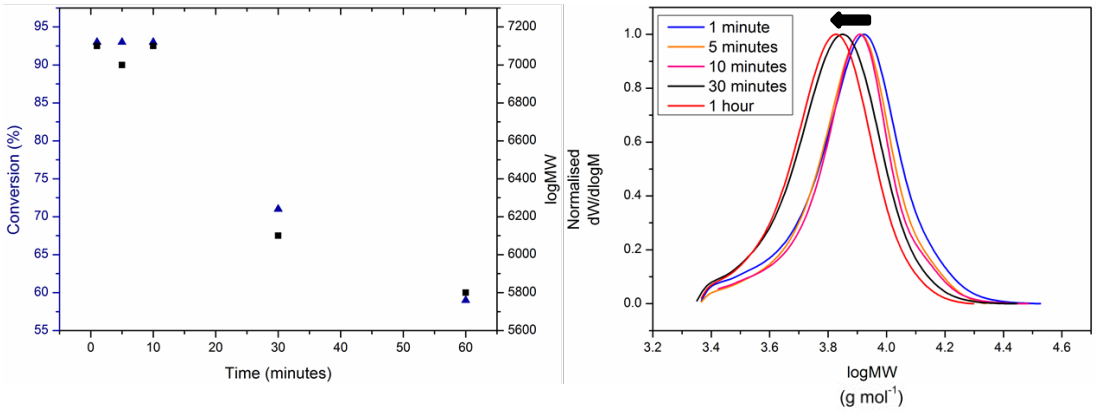

Figure 2.29 – The kinetic data (left) and the SEC traces (right) that were obtained for the polymerisation/depolymerisation process of PHEA in carbonated water.

With the depolymerisation of PHEA being observed, it has been shown that both acrylamides and acrylates can undergo depolymerisation. If this system applied exclusively to acrylamides, a potential explanation for depolymerisation could be the formation of a carbamate linkage between the –NH group and CO_2. When CO_2 is dissolved in aqueous media and an amine is introduced into the system, the formation of a carbamate species can be observed.[44,75–77] The generation of such a species is increasingly favoured in the order tertiary << secondary < primary amines.[78] However, as acrylate monomers do not possess the required –NH group, no such link can be formed with HEA.

Pleasingly, the absence of a carbamate species was supported by a lack of any noticeable change (other than the reformation of vinyl signals) in the ^{1}H NMR spectra for both NIPAm (Figure 2.1) and HEAm (Figure 2.26). In addition to this,

when the ^{1}H NMR spectrum of NIPAm in HPLC grade water was compared to that of NIPAm in carbonated water, there was no apparent shifting of the –NH peak (Figure 2.30).

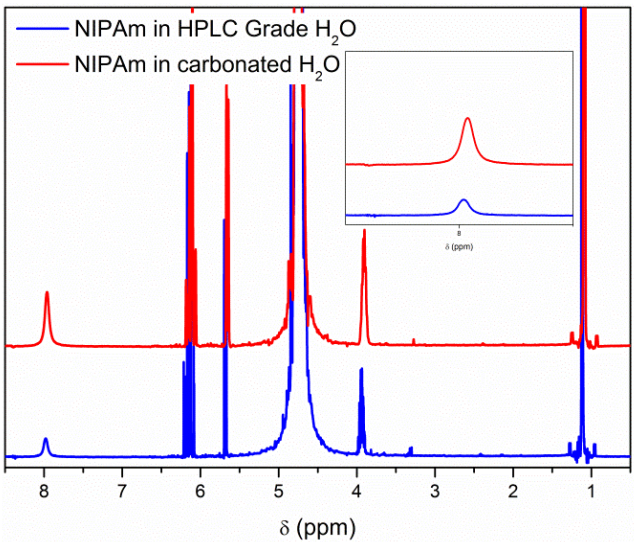

Figure 2.30 – A comparison of the ^{1}H NMR spectra obtained from stirring NIPAm in HPLC grade water (blue) and in carbonated water (red)

2.2.11. Attempting to depolymerise poly(2-hydroxyethylacrylate) synthesised by photo-induced living radical polymerisation

Given the potential industrial applications for this system, PHEA made by an alternative synthetic route was assessed for depolymerisation. As the importance of the –Br end group was not able to be dismissed, it was deemed to be important that the resulting polymer possessed a high level of end group functionality.

Recently, Haddleton *et al.*, reported a sophisticated photo-induced living radical polymerisation system which has allowed for the controlled synthesis of acrylates with remarkable end group fidelity.[79,80] Through utilising this system, PHEA (M_n = 6400 g mol^{-1}; $Đ_m$ = 1.15) was synthesised in DMSO, placed under a variety of conditions (Table 2.7), and monitored over a period of 4 days in an attempt to induce depolymerisation.

Conditions	Depolymerisation after 24 hours	Depolymerisation after 4 days
In CO_2 water only	0 %	0 %
With initiator and CO_2 water	0 %	0 %
With $Cu^{(I)}Br$, Me_6TREN and CO_2 water	0 %	0 %
Standard depolymerisation conditions	0 %	0 %

Table 2.7 – A summary of results for the attempted depolymerisation of PHEA.

Unfortunately, as indicated by Table 2.7, the ^1H NMR results from this study indicated that monomer regeneration did not occur under any of the conditions that were attempted. This was further demonstrated by the molecular weight of the polymer remaining unchanged. As a consequence of this, it was concluded that PHEA synthesised in a different system cannot currently be depolymerised.

2.2.12. Disproving a potential mechanism: β-alkyl elimination

It is clear that this system is complex, and that there are many factors which contributed towards the occurrence of depolymerisation. Existing literature suggested that the mechanism may have been based on β-alkyl elimination. However, as this would have resulted in the formation of hydrobromic acid (HBr),[31] and given that only a slight change in pH was observed with the onset of depolymerisation (Section 2.2.4; Figure 2.11), this was considered to be unlikely. Moreover, this mechanism would only have allowed for the release of one monomer unit and thus, would not have resulted in any significant amount of depolymerisation.

Nevertheless, to rule out the possibility of β-alkyl elimination, a small molecule (2-bromo-*N*-(2-hydroxyethyl)propanamide) was synthesised and placed under standard reaction conditions. If the proposed mechanism was correct, then the HEAm monomer would have formed upon the loss of HBr. Following this, as 2-

bromo-*N*-(2-hydroxyethyl)propanamide was able to act as an initiator for $Cu^{(0)}$-mediated RDRPs, polymerisation would have commenced (Scheme 2.8). Alternatively, if for some reason polymerisation could not be achieved, then HEAm would remain in solution. Regardless, both of these outcomes would have produced characteristic peaks in the ^1H NMR spectrum.

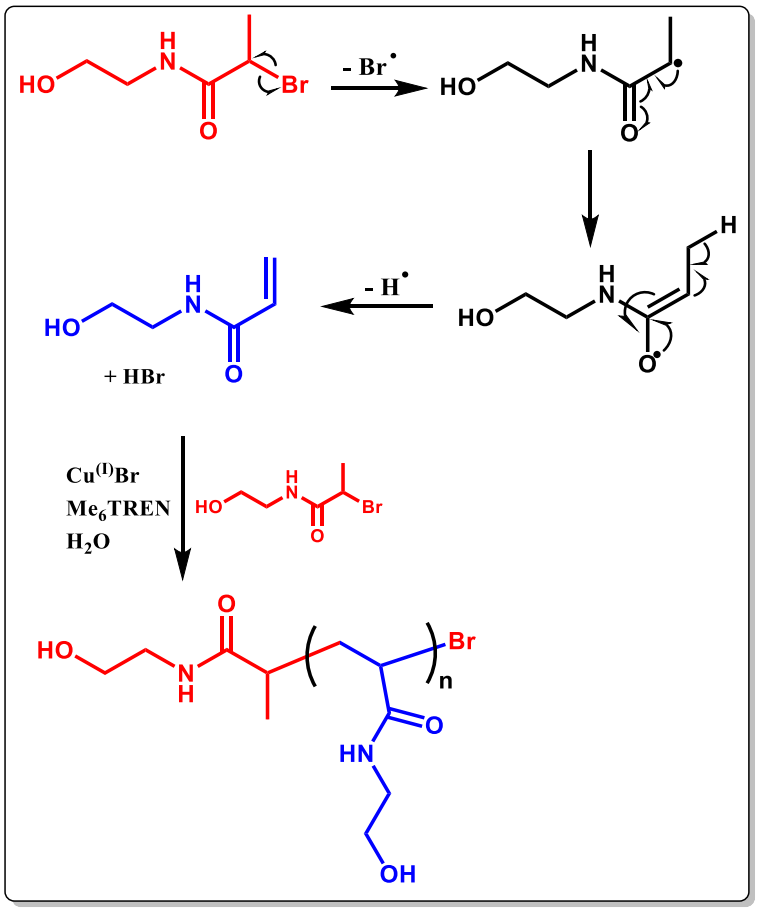

Scheme 2.8 - Mechanism for the β-alkyl elimination of 2-bromo-*N*-(2-hydroxyethyl)propanamide.

Unfortunately, after 24 hours, no polymer or monomer was observed and the crude reaction mixture remained largely unchanged (Figure 2.31 and Section 2.4.3). It is worth highlighting that a significant decrease in the concentration of "free ligand" (2.89 ppm and 3.19 ppm) was seen with time as a result of the ligand binding to $Cu^{(I)}Br$. Nevertheless, this confirmed that the mechanism of depolymerisation was not β-alkyl elimination.

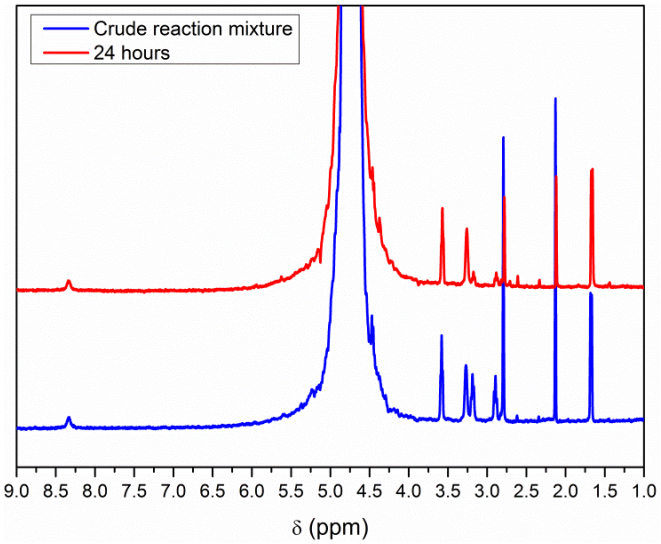

Figure 2.31 - A comparison of the ^{1}H NMR spectra that resulted from the investigation into β-alkyl elimination as the mechanism for depolymerisation.

2.2.13. Control experiments

A crucial part of any mechanism elucidation is the conduction of control experiments. Thus, to rule out the possibility of CO_2 binding to the initiator or the monomer, these compounds were allowed to stir in both HPLC grade water and carbonated water for 24 hours prior to analysis by ^{1}H NMR spectroscopy. In both cases, no significant difference between the ^{1}H NMR spectra was observed (Figure 2.32). This implied that no structural alterations were occurring to either the initiator or the monomer in the presence of CO_2.

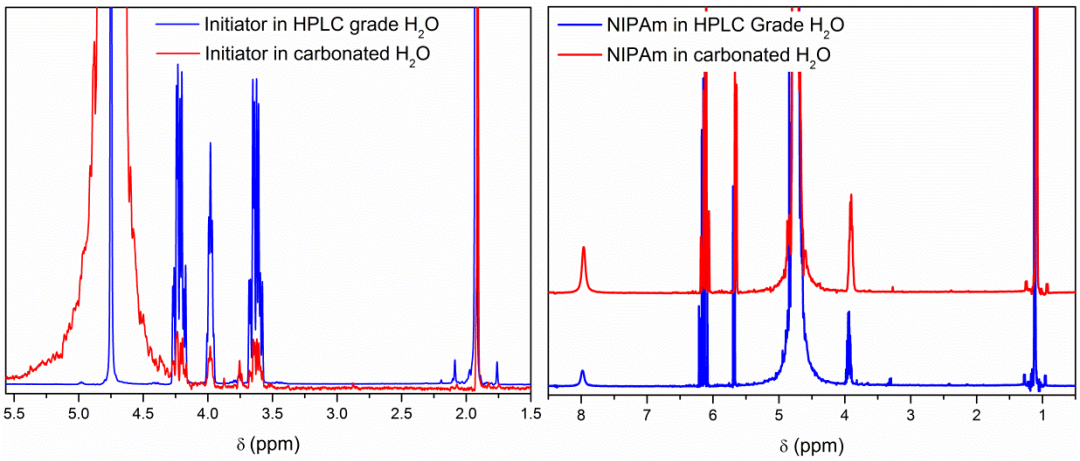

Figure 2.32 - A comparison of the ^{1}H NMR spectra that were obtained from allowing the initiator (left) and the monomer (right) to stir overnight in HPLC grade water (blue) and carbonated water (red).

In addition to this, different combinations of the polymerisation components were stirred overnight in the presence of CO_2 (Table 2.8) and subsequently analysed by ^1H NMR spectroscopy. This was in an effort to determine whether any changes were being made to the individual species as a result of being in the presence of each other. It is important to note that as $Cu^{(I)}Br$ is insoluble in water without a ligand, there were some arrangements which were not investigated.

Control #	Monomer	Initiator	Ligand	$Cu^{(I)}X$	CO_2
1	✓	✗	✗	✗	✓
2	✗	✓	✗	✗	✓
3	✗	✗	✓	✗	✓
4	✓	✓	✓	✗	✓
5	✓	✗	✓	✗	✓
6	✗	✓	✓	✗	✓
7	✗	✗	✓	✓	✓
8	✓	✓	✓	✗	✓
9	✓	✗	✓	✓	✓

Table 2.8 – An overview of the different combination of reagents that were analysed by ^1H NMR spectroscopy; where the tick represents those that were present and the cross represents those that were omitted.

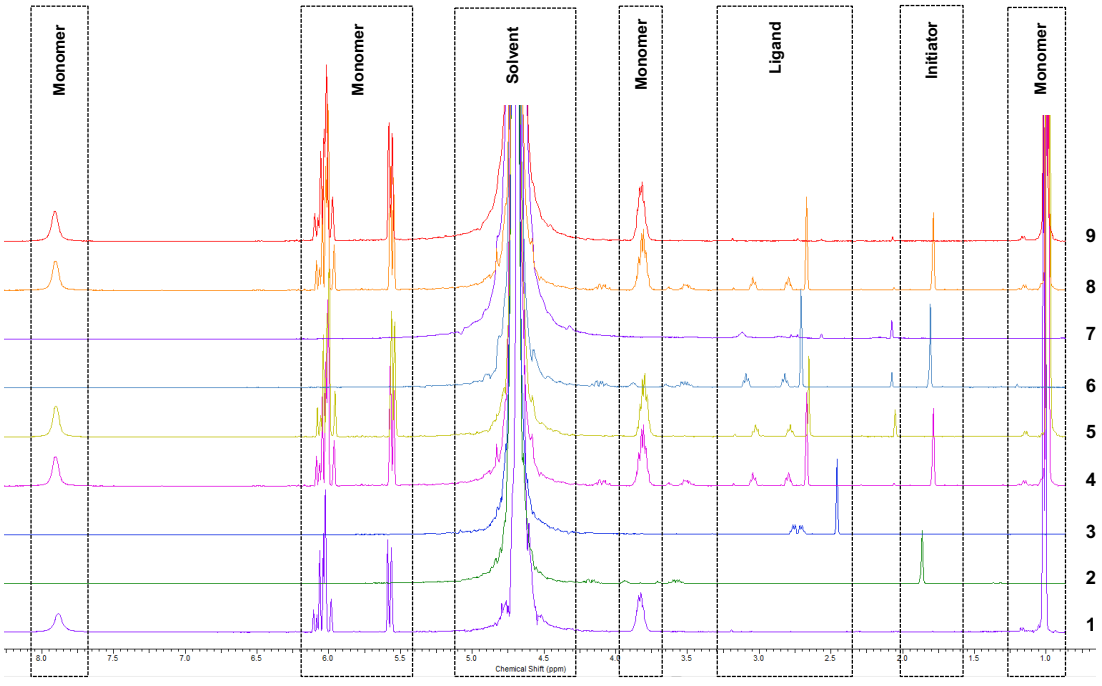

Figure 2.33 – A comparison of the ^1H NMR spectra that were obtained from the control experiments.

Analysis of the resulting solutions *via* ^{1}H NMR spectroscopy revealed that there was a change in the chemical shift for the peaks which correspond to the ligand (between 2.4 and 3.3. ppm).[32,81] In Figure 2.33 it can be seen that the ligand peaks moved downfield when in the presence of other compounds. Given that this shift was the same no matter what components the ligand was combined with, it seemed unlikely that this hinted towards the cause of depolymerisation. As there was no other difference between the spectra, these findings implied that the trigger for depolymerisation was either not observable *via* ^{1}H NMR, or that there was no correlation between its occurrence and the individual components of the reaction.

2.2.14. Further studies into the role of CO_2

Finally, with the knowledge that CO_2 was a pre-requisite for depolymerisation, it was important to rule out the possibility of its incorporation into the polymer backbone. As such, four PNIPAm samples were synthesised and isolated for comparison (Table 2.9). These were: PNIPAm post-polymerisation, PNIPAm post-depolymerisation, PNIPAm post-repolymerisation and finally, PNIPAm synthesised by traditional aqueous $Cu^{(0)}$-mediated RDRP.

Name	Conversion (%)	Depolymerisation (%)	M_n g mol^{-1}	$Đ_m$
Pre-depolymerisation	96	-	3200	1.16
Post-depolymerisation	46	50	1600	1.16
Post- repolymerisation	100	-	3500	1.23
Traditional	100	-	4500	1.11

Table 2.9 - A summary of the results obtained from ^{1}H NMR and SEC analysis of the isolated PNIPAm samples.

As a means of further investigating whether there was any change to the polymer backbone, the four PNIPAm samples were analysed using matrix-assisted laser desorption/ionisation – time of flight mass spectrometry (MALDI-ToF MS).

Interestingly, when the MALDI spectrum of the PNIPAm sample obtained *via* traditional aqueous $Cu^{(0)}$-mediated RDRP was directly compared to that of the pre-depolymerisation sample (Figure 2.34), the two distributions were seen to closely mimic one another (Figure 2.34). In fact, the only observable difference between the two spectra was the intensity of the peaks and the presence of species within the low molecular weight region. This indicated that the polymer was structurally the same, and therefore implied that there had been no incorporation of CO_2 or any other species into the polymer backbone.

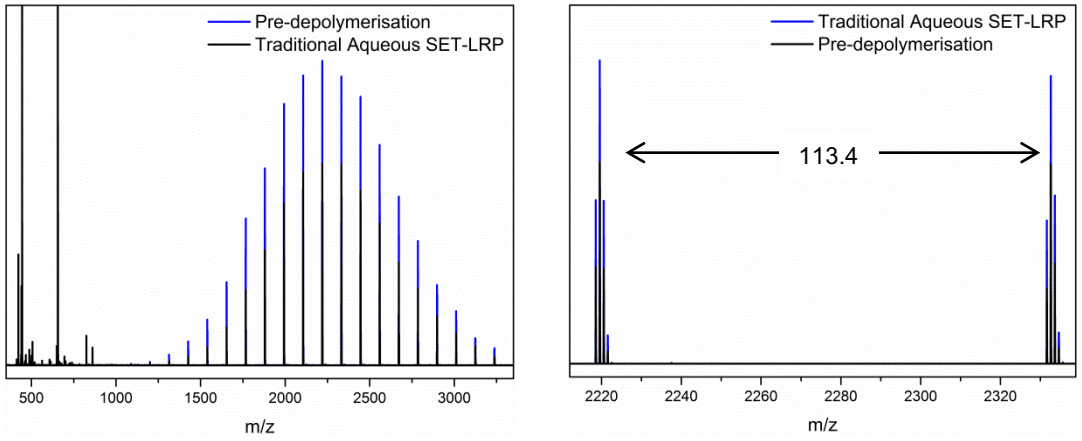

Figure 2.34 - A comparison of the MALDI-ToF MS spectra obtained for PNIPAm that was isolated pre-depolymerisation (blue) and following synthesis *via* traditional aqueous $Cu^{(0)}$-mediated RDRP (black).

In addition to this, other than a slight shifting of the average molecular weight and an increase in the intensity of the spectra, there was no deviation between the distributions that were produced from analysing the post-repolymerisation PNIPAm sample and that of the pre-depolymerisation PNIPAm sample (Figure 2.35). This therefore supported the conclusion that the polymerisation of the reformed NIPAm monomer had occurred a controlled manner.

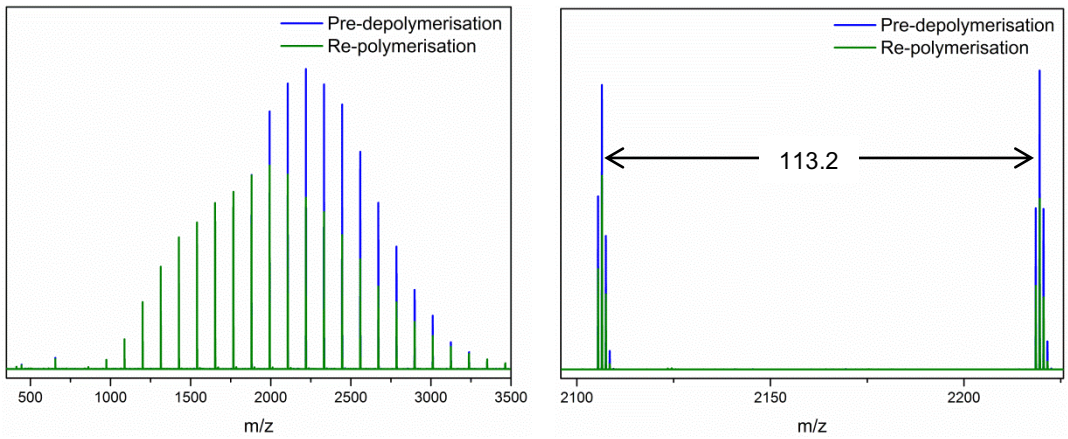

Figure 2.35 – A comparison of the MALDI-ToF MS spectra obtained for PNIPAm that was isolated pre-depolymerisation (blue) and post-repolymerisation (green).

Overall, the MALDI-ToF MS analysis of the four isolated PNIPAm samples (Figures 2.34 to 2.35) revealed the presence of only a single distribution which corresponded to PNIPAm initiated by 3-dihydroxypropyl 2-bromo-2-methylpropanoate and terminated by elimination (loss of HBr as seen in Scheme 2.9). Additionally, with the repeat unit ranging from 113.1 to 113.4 Da (NIPAm Theo. = 113.2 Da), the data suggested that the PNIPAm backbone was not altered by the incorporation of CO_2 or through any other modification.

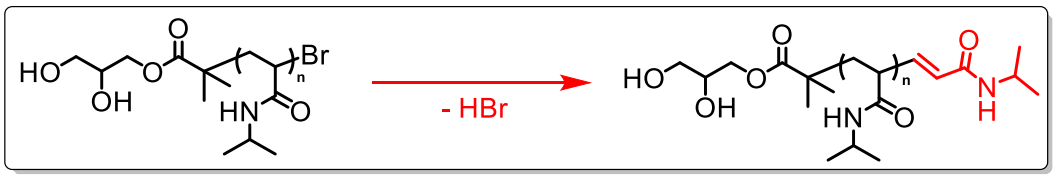

Scheme 2.9 – A schematic representation of a terminated PNIPAm chain end *via* elimination.

Finally, the lack of backbone modification was further confirmed by fourier transform infrared spectroscopy (FT-IR). Characterisation *via* this technique revealed no noticeable or significant difference between the four PNIPAm samples (Figure 2.36).

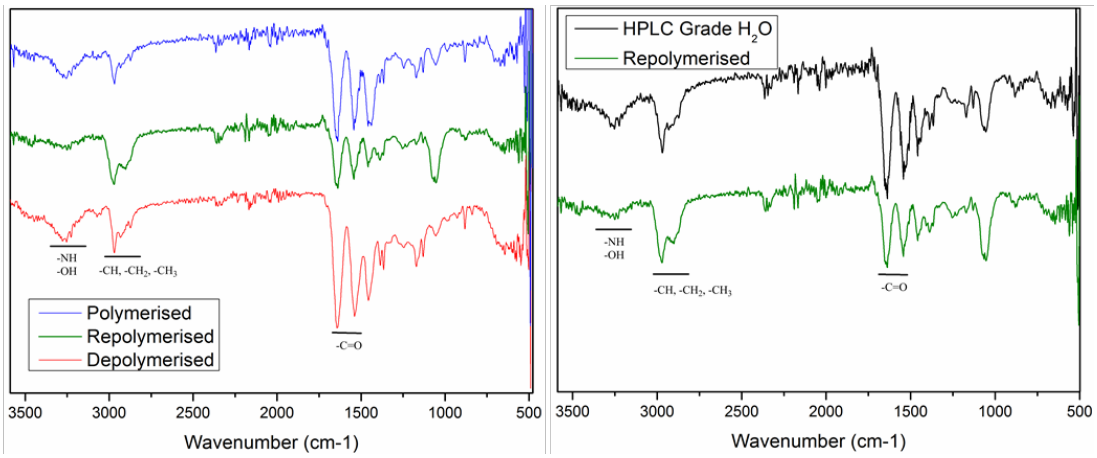

Figure 2.36 – FT-IR analysis of the four different PNIPAm samples isolated for comparison.

2.3. Conclusion

Overall, this investigation has described the low temperature depolymerisation of water-soluble polyacrylamides and polyacrylates in the presence of dissolved CO_2. Whilst a mechanism was not completely established, this study has provided some key insight into the potential causes for this phenomenon and has enabled for several mechanistic routes to be discounted. One of the more notable examples of this was the lack of depolymerisation when reactions were conducted at ambient temperature. It is possible that this was due to a decrease in the concentration of dissolved CO_2, although there is not currently evidence to suggest that this is the case. Further to this, depolymerisation was not observed when a bromine ω-terminated polymer was subjected to the standard CO_2 reaction conditions. This could potentially suggest that a key component in this mechanism is being formed during the polymerisation process.

Another plausible explanation for depolymerisation is the modification of the $Cu^{(II)}Br_2$/Me_6TREN co-ordination complex in the presence of dissolved CO_2. However, a mechanism based on this observation cannot currently be provided, and doing so would be purely speculation.

Unlike previously reported systems, narrowly disperse, low molecular weight polymers were produced following depolymerisation. This was accompanied by the regeneration of monomer in a reversible process. Notably, through switching CO_2 with N_2, the controlled repolymerisation of reformed monomer was achieved without sacrificing the attainment of desired molecular weight or the size of the mass distribution. Moreover, the ability to conduct "*in-situ*" chain extension post-polymerisation without the need for purification, further exemplified the controlled nature of this system. Ultimately, this investigation has led to the development of a low temperature aqueous system with conceivable potential, both commercially and environmentally, for the controlled reversal of acrylic/vinyl polymerisations.

2.4. Experimental

2.4.1. Materials

N-Isopropylacrylamide (NIPAm, Sigma-Aldrich, 97 %), copper$^{(II)}$bromide ($CuBr_2$, Sigma-Aldrich, 99 %), water (HPLC grade, VWR), deionised water (RO grade), hydrochloric acid (HCl, Sigma-Aldrich, 37 %), ethanolamine (Sigma-Aldrich, ≥ 99.5 %), anhydrous tetrahydrofuran (THF, Sigma-Aldrich, ≥ 99.9 %), 2-bromopropionyl bromide (97 %, Sigma-Aldrich), magnesium sulphate ($MgSO_4$, Fisher Scientific), dichloromethane (DCM, ≥ 99.8 %, Sigma-Aldrich), hexane (≥ 95 %, Sigma-Aldrich) MilliQ water (18.2 MΩcm), silver acetate (Sigma-Aldrich, 99.99 %), dimethyl sulphoxide (DMSO, Fisher, > 99.7 %), ethyl α-bromo-isobutyrate (EBiB, Sigma-Aldrich, 98 %) and sodium hydrogen carbonate ($NaHCO_3$, Fisher Scientific, 99.7 %) were used without further purification. Cuprisorb™ resin was purchased from Seachem. Commercially bought carbonated water (Highland Spring sparkling and Perrier water) was used as received (Table 2.10).

	Highland Spring Carbonated Water	Highland Spring Still Water	Perrier Carbonated Water
Bicarbonate	150	150	390
Calcium	40.5	40.5	147.3
Chloride	6.1	6.1	21.5
Magnesium	10.1	10.1	3.4
Nitrates	3.1	3.1	4.3
Potassium	0.7	0.7	0.6
Sodium	5.6	5.6	9.0
Sulphates	5.3	5.3	33
pH	4.72	7.8	5.46

Table 2.10 - Average mineral analysis at the source (mg/L) for Highland Spring carbonated and still water and Perrier water.

N,N,N',N'',N''-Pentamethyldiethylenetriamine (PMDETA, Sigma-Aldrich, 99 %) was distilled under reduced pressure (55 °C, 10^{-1} mbar), deoxygenated, and stored in an

ampule under nitrogen protection at 4 °C prior to use. 2-Hydroxyethyl acrylate (HEA, BASF, 96 %) and *N*-hydroxyethyl acrylamide (HEAm, Sigma-Aldrich, 97 %) were uninhibited using basic alumina prior to use in the polymerisations. Copper$^{(I)}$bromide ($Cu^{(I)}Br$, Aldrich, > 98 %) was purified according to the method detailed by Keller and Wycoff.[82]

3-Dihydroxypropyl 2-bromo-2-methylpropanoate was synthesised according to the literature procedure.[83] *N,N,N',N'',N''*-Hexamethyl-[tris(aminoethyl)amine] (Me_6TREN) was synthesised according to the literature procedure, deoxygenated, and stored in an ampoule at 4 °C under nitrogen protection.[81]

2.4.2. Characterisation and instrumentation

^{1}H NMR spectra were recorded on Brüker AV-250, DPX-400, and HD-500 spectrometers using deuterated solvents obtained from Sigma-Aldrich. The percentage conversion of NIPAm was determined *via* ^{1}H NMR through integration of the vinyl group (5.6 ppm, 1H, d) and integration of the C$\underline{H}(CH_3)_2$ proton (3.9 ppm, 1H, m). The conversion of HEAm was calculated by ^{1}H NMR through integration of the vinyl group (5.65 ppm, 1H, d) and integration of the C$\underline{H_2}$NH peak (3.93 ppm, 2H, q). For HEA, the conversion was calculated *via* ^{1}H NMR through integration of the vinyl group (6.95 ppm, 1H, d) and integration of the C$\underline{H_2}$OH peak (3.75 ppm, 2H, q). The following abbreviations were used to describe multiplicities; s = singlet, d = doublet, t = triplet, q = quartet and m = multiplet.

IR spectra were collected on a Brüker VECTOR-22 FT-IR spectrometer using a Golden Gate diamond attenuated reflection cell.

GC-FID was performed using a Varian 450 fitted with a FactorFourTM capillary column VF-1ms, of 15 m x 0.25 mm I.D. and film thickness 0.25 µm, utilising methanol as the sample solvent. The oven temperature was programmed as

follows: 40 °C (allowed to hold for 1 minute) then increased by 25 °C min^{-1} to 200 °C. The injector was operated at 200 °C with the FID at 220 °C and nitrogen was used as the carrier gas at a flow rate of 1 mL min^{-1}.

Gas chromatography – mass spectrometry (GC-MS) was conducted on a Varian 4000 GC equipped with an ion trap mass spectrometer and a non-polar column (Varian Factor Four VF5, 30 m x 0.25 mm x 0.25 μm) with a splitless injector operated at 325 °C.

Size exclusion chromatography (SEC) measurements were performed on an Agilent PL50 equipped with 2 Agilent Polargel L Columns eluting with dimethylformamide containing 0.1 M LiBr as an additive at 50°C. The flow rate was 1 mL min^{-1} and detection was achieved using simultaneous refractive index (RI) and UV (λ = 280 nm) detectors. Molecular weights were calculated relative to narrow PMMA standards. All samples were stirred in the presence of Cuprisorb™ resin to remove residual copper species, dissolved in the appropriate eluent and filtered through disposable 0.45 μm PTFE filters before analysis. Molecular weight data was analysed using Agilent SEC software and plotted using OriginPro 8.5.

UV-Vis spectra were recorded on an Agilent Technologies Cary 60 UV-Vis in the range of 200 – 1100 nm using a cuvette with a 10 mm optical path length. The source of UV light for the synthesis of PHEA was a UV nail gel curing lamp (commercially available from a range of suppliers) (λ_{max} ~ 360 nm) equipped with four 9W bulbs.

MALDI-ToF mass spectrometry was carried out using a Bruker Daltonics Ultraflex II MALDI-ToF mass spectrometer, equipped with a nitrogen laser delivering 2 ns laser pulses at 337 nm. Positive ion ToF detection was conducted using an accelerating voltage of 25 kV. Saturated solutions of trans-2-[3-(4-tert-butylphenyl)-2-methyl-2-propylidene] malonitrile (DCTB) and α-cyano-4-hydroxycinnamic acid (CHCA) in 50

μL of tetrahydrofuran (THF) were used as the matrices with sodium iodide as a cationisation agent (1.0 mg/mL). 1.0 mg/mL of sample was mixed with a matrix and the cationisation agent. 0.7 μL of this was solution was applied to the target plate. Spectra were recorded in reflector mode with PEG 2500 kDa used as a calibrant.

All pH measurements were conducted using a SevenGo™ pH – SG2 meter (Fisher Scientific) equipped with a pH semi-micro tip electrode (Thermo Scientific Orion).

2.4.3. General experimental procedures

Synthesis of *N,N,N',N',N'',N''*-hexamethyl-[tris(aminoethyl)amine] (Me_6TREN)

Formaldehyde 37% v/v (270.9 mL, 3.64 mol) and formic acid (320 mL, 8.15 mol) were charged to a 1 L RBF and placed in an ice bath. Whilst being vigorously stirred, tris-(2-aminoethyl)amine (50 mL, 0.33 mol) was added dropwise, over the period of 1h, to this mixture. The resulting solution was then refluxed at 120°C for 24h and left to cool; after which the volatile fractions were removed *in vacuo*, producing a yellow/orange oil. A saturated sodium hydroxide solution was then used to adjust the pH to pH 10 in an ice bath, which resulted in the formation of an orange/brown oily layer. This was then extracted with 3 x 150 mL aliquots of chloroform, 100 mL of water, and finally a further 50 mL of chloroform. The resulting organic layers were combined, dried using $MgSO_4$, and the volatiles removed *in vacuo* to yield a brown oil. Under reduced pressure (75°C, 10^{-3} mbar), the oil was distilled yielding a colourless oil (47.41 g, 62% yield.)

^{1}H NMR ($CDCl_3$, 400 MHz), δ (ppm): 2.55 and 2.32 (t, J = 5.84 Hz and 4.14 Hz) 12 H, $((CH_3)_2$-N-C$\underline{H_2}$-C$\underline{H_2}$-N-R), 2.17 (s, 18 H, $((C\underline{H_3})_2$-N-R). **^{13}C NMR ($CDCl_3$, 400 MHz), δ (ppm):** 57.5 $((CH_3)_2$-N-$\underline{C}H_2$-CH_2-N-R), 53.1$((CH_3)_2$-N-CH_2-$\underline{C}H_2$-N-R), 45.9 $((\underline{C}H_3)_2$-N-R). **IR (cm^{-1}):** 1035, 1124. **ESI-MS (*m/z*):** [M+] 231.25 (*230.39 Th*eo.)

Synthesis of 2-bromo-*N*-(2-hydroxyethyl)propanamide

To a 3-neck RBF in ice, ethanolamine (19.8 mL, 0.33 mol, 3.3 eq.) was dissolved in anhydrous tetrahydrofuran (200 mL) under a nitrogen atmosphere. To the cooled solution, 2-bromopropionyl bromide (10.5 mL, 0.10 mol, 1.0 eq.) was added dropwise *via* a dropping funnel. After complete addition, the reaction was stirred rapidly, allowed to warm to ambient temperature and left to react for 4 hours. The reaction mix was subsequently filtered to remove the white salt and the THF evaporated *in vacuo.* The resulting residue was dissolved in dichloromethane, washed with brine water three times and dried over anhydrous $MgSO_4$. Any remaining volatiles were removed *in vacuo* and the resulting product purified by recrystallisation in hexane to yield a white powder (0.22 g, yield = 1 %).

^{1}H NMR (D_2O, 300 MHz), δ (ppm): 1.74 (d, J = 6.80 Hz, 3 H, C*H*$_3$-CH-Br-R), 3.33 (m, 2 H, R-C*H*$_2$-CH_2-OH), 3.64 (m, 2 H, R-CH_2-C*H*$_2$-OH), 4.52 (q, J = 6.70 Hz, 1 H, CH_3-C*H*-Br-R **^{13}C NMR (D_2O, 300 MHz), δ (ppm):** 21.3 (*C*H_3-CH-Br-R), 41.6 (R-*C*H_2-CH_2-OH), 43.2 (CH_3-*C*H-Br-R), 59.4 (R-CH_2-*C*H_2-OH), 172.9 (CH_3-CH-Br-*C*O-R) (**IR (cm^{-1}):** 1035, 1124. **ESI-MS (*m/z*):** [M+] 231.20 (*230.39 Th*eo.)

Typical procedure for the polymerisation and depolymerisation of NIPAm

Ligand was added to a 14 mL glass vial containing Highland Spring carbonated water (3 mL), sealed with a rubber septum and stirred at 250 rpm for 1 minute. The glass vial was then placed into an ice/water bath to regulate the temperature and supress the rate of hydrolysis. $Cu^{(I)}Br$ (12.7 mg, 0.09 mmol, 0.4 eq.) was rapidly added to the ligand-water mix and the vial was re-sealed. Upon addition of $Cu^{(I)}Br$ to the ligand-water mix, a coloured solution formed and red/brown $Cu^{(0)}$ particles were visible. The solution was allowed to stir and disproportionate whilst 3-dihydroxypropyl 2-bromo-2-methylpropanoate (53.3 mg, 0.22 mmol, 1.0 eq.) and NIPAm (500 mg, 4.42 mmol, 20 eq.) were dissolved in Highland Spring carbonated

water (2 mL), sealed with a rubber septum, and stirred at 250 rpm for 10 minutes. At the end of this period, the initiator-monomer solution was transferred *via* a syringe and needle into the glass vial containing the disproportionated ligand and $Cu^{(I)}Br$.

The relevant quantities for ligands were: Me_6TREN (23.6 μL, 0.09 mmol, 0.4 eq.) and PMDETA (18.5 μL, 0.09 mmol, 0.4 eq.).

Typical procedure for the polymerisation, depolymerisation and repolymerisation of NIPAm in the presence of Me_6TREN

Initially, the typical procedure for the polymerisation and depolymerisation of NIPAm in the presence of Me_6TREN was followed. However, after depolymerisation (1 hour), the crude reaction mix was bubbled with N_2 for 30 minutes and the reaction allowed to stir for a further 30 minutes, after which a sample was taken.

Typical procedure for the aqueous $Cu^{(0)}$-mediated RDRP of NIPAm

To a Schlenk tube equipped with a magnetic stirring bar, HPLC grade water (3 mL) and ligand were added and purged of oxygen *via* nitrogen (N_2) bubbling for 2 minutes. The mixture was placed into an ice/water bath to regulate the temperature (0 °C) after which $Cu^{(I)}Br$ (12.7 mg, 0.09 mmol, 0.4 eq.) was added under an N_2 atmosphere. Upon addition of $Cu^{(I)}Br$ to the ligand-water mix, a coloured solution formed and red/brown $Cu^{(0)}$ particles were visible. The resulting solution was allowed to stir and disproportionate whilst 3-dihydroxypropyl 2-bromo-2-methylpropanoate (53.3 mg, 0.22 mmol, 1.0 eq.) and NIPAm (500 mg, 4.42 mmol, 20 eq.) were dissolved in water (2 mL) and bubbled with nitrogen for 15 minutes. At the end of the deoxygenation period the initiator-monomer solution was transferred *via* a nitrogen purged syringe and needle into the Schlenk tube. Samples for ^1H NMR spectroscopy and SEC were taken using a nitrogen purged syringe, filtered through an alumina column, and diluted in the appropriate solvents.

The relevant quantities for ligands were: Me_6TREN (23.6 µL, 0.09 mmol, 0.4 eq.) and PMDETA (18.5 µL, 0.09 mmol, 0.4 eq.).

Procedure for the polymerisation and depolymerisation of PNIPAm conducted in HPLC grade water carbonated with dry ice

Dry ice (0.5 g) was charged to a vial containing water (20 mL, HPLC grade) and sealed with a latex balloon. After complete dissolution of the dry ice pellet, the balloon was removed and the carbonated water used as a solvent for the polymerisation of DP = 20 NIPAm. The typical procedure for the polymerisation and depolymerisation of NIPAm in the presence of Me_6TREN was then followed.

Procedure for the polymerisation of PNIPAm conducted in de-carbonated carbonated water

Highland Spring carbonated water (20 mL) was subjected to three rigorous freeze-thaw cycles, followed by 30 minutes of sonication to ensure that complete removal of CO_2 had been achieved. The typical procedure for the aqueous $Cu^{(0)}$-mediated RDRP of NIPAm in the presence of Me_6TREN was then followed using the de-carbonated, carbonated water as the solvent.

Typical procedure for the high pressure polymerisation DP = 20 NIPAm in carbonated water

$Cu^{(I)}Br$ (12.7 mg, 0.09 mmol, 0.4 eq.), Me_6TREN (23.6 µL, 0.09 mmol, 0.4 eq.) and deionised water (3 mL) were charged to a high-pressure steel autoclave. The vessel was partially sealed and placed into an ice/water bath. The resulting catalytic solution was subsequently degassed *via* CO_2 purging at 2 bar for 10 minutes. During this time, deionised water (2 mL), NIPAm (500 mg, 4.42 mmol, 20.0 eq.), and 3-dihydroxypropyl 2-bromo-2-methylpropanoate (53.3mg, 0.22 mmol, 1.0 eq.)

were degassed in a sealed vial with carbon dioxide. After 10 minutes the monomer-initiator solution was transferred *via* a degassed syringe to the autoclave. At this point, the vessel was fully sealed and a range of pressures (10 bar, 24 bar, 48 bar and 100 bar) were applied. The reaction mixture was then stirred at 250 rpm for 10 minutes after which the reaction was terminated by freezing the solution in an acetone/dry ice bath. When completely frozen, the pressure was reduced by venting the autoclave over a period of ~ 30 minutes, and a sample was removed and thawed. The reaction was repeated with the polymerisation being left for 1 hour before termination. All samples were diluted in an appropriate solvent and analysed by ^{1}H NMR spectroscopy and SEC.

Procedure for the open top polymerisation of DP = 20 NIPAm in carbonated water

The typical procedure for the polymerisation and depolymerisation of NIPAm in the presence of Me_6TREN was followed. However, instead of sealing the vials with a rubber septum, they were left unsealed for the duration of the experiment.

Procedure for the ambient temperature polymerisation and depolymerisation of NIPAm in the presence of Me_6TREN

The typical procedure for the polymerisation and depolymerisation of NIPAm in the presence of Me_6TREN was followed. However, rather than placing the vials in an ice/water bath, the polymerisation was conducted at ambient temperature.

Procedure for monitoring the pH of the polymerisation and depolymerisation process

The typical procedure for the polymerisation and depolymerisation of NIPAm in the presence of Me_6TREN was followed. The pH of the reaction mix was monitored

immediately upon sampling of the reaction, with all samples being frozen and thawed for ^{1}H NMR spectroscopy following the measurements.

Procedure for the aqueous $Cu^{(0)}$-mediated RDRP of NIPAm in the presence of Me_6TREN at pH 5.55

The typical procedure for the aqueous $Cu^{(0)}$-mediated RDRP of NIPAm in the presence of Me_6TREN was followed. However, acidified HPLC grade water (pH 5.55) was used as the solvent rather than the standard HPLC grade water.

Procedure for the polymerisation and depolymerisation of DP = 20 NIPAm in the presence of Me_6TREN at pH 8

The typical procedure for the polymerisation and depolymerisation of NIPAm in the presence of Me_6TREN was followed. However, the pH of Highland Spring carbonated water was adjusted to 8 with $NaHCO_3$ and used as the solvent rather than the standard Highland Spring carbonated water.

Procedure for the polymerisation and depolymerisation of NIPAm in the presence of Me_6TREN with addition of HCl *prior* to depolymerisation

Initially, the typical procedure for the polymerisation and depolymerisation of NIPAm in the presence of Me_6TREN was followed. However, after 10 minutes, concentrated hydrochloric acid (HCl) (100 µL, 3.00 mmol) (37 %, Sigma Aldrich) was added to the reaction mix. Samples for ^{1}H NMR spectroscopy and SEC were taken using a syringe, frozen in liquid nitrogen, thawed, and diluted in the appropriate solvents.

Typical procedure for the polymerisation and depolymerisation of high molecular weight (DP = 120, 240 & 360) NIPAm in the presence of Me_6TREN

Me_6TREN was added to a 14 mL glass vial containing Highland Spring carbonated water (3 mL), sealed with a rubber septum and stirred at 250 rpm for 1 minute. The glass vial was then placed into an ice/water bath to regulate the temperature and supress the rate of hydrolysis. $Cu^{(I)}Br$ was rapidly added to the ligand-water mix and the vial was re-sealed. Upon addition of $Cu^{(I)}Br$ to the ligand-water mix, a coloured solution formed and red/brown $Cu^{(0)}$ particles were visible. The solution was allowed to stir and disproportionate whilst 3-dihydroxypropyl 2-bromo-2-methylpropanoate and NIPAm were dissolved in Highland Spring carbonated water (2 mL), sealed with a rubber septum, and stirred at 250 rpm for 10 minutes. At the end of this period the initiator-monomer solution was transferred *via* a syringe and needle into the glass vial containing the disproportionated ligand and $Cu^{(I)}Br$. Samples for ^{1}H NMR spectroscopy and SEC were taken using a syringe, frozen in liquid nitrogen, thawed, and diluted in the appropriate solvents.

The quantities and equivalents of the reagents for the polymerisations are provided in Table 2.11.

Targeted DP	Monomer (mg)	Initiator (eq.)	Initiator (mg)	Ligan (eq.)	Ligand (µL)	$Cu^{(I)}Br$ (eq.)	$Cu^{(I)}Br$ (mg)
120	500.0	1.0	8.9	0.4	3.9	0.4	2.1
120	500.0	1.0	8.9	2.4	23.6	2.4	12.7
240	500.0	1.0	4.4	2.4	23.6	4.8	12.7
360	500.0	1.0	3.0	2.4	23.6	7.2	12.7

Table 2.11 - Conditions used to synthesise PNIPAm in carbonated water to different degrees of polymerisation (DP).

Procedure for the polymerisation and depolymerisation of NIPAm in the presence of excess Me_6TREN and $Cu^{(I)}Br$

The typical procedure for the polymerisation and depolymerisation of NIPAm in the presence of Me_6TREN was followed. However, the quantities of Me_6TREN and $Cu^{(I)}Br$ were changed to: Me_6TREN (141.7 µL, 0.53 mmol, 2.4 eq.) and $Cu^{(I)}Br$ (76.0 mg, 0.53 mmol, 2.4 eq.)

Procedure for the polymerisation and depolymerisation of NIPAm in the presence of excess Me_6TREN only

The typical procedure for the polymerisation and depolymerisation of NIPAm in the presence of Me_6TREN was followed. However, the quantity of Me_6TREN was changed to: 141.7 µL, 0.53 mmol, 2.4 eq.

Procedure for the chain extension of PNIPAm *prior* to depolymerisation in the presence of Me_6TREN

Initially, the typical procedure for the polymerisation and depolymerisation of NIPAm in the presence of Me_6TREN was followed. However, after 10 minutes, NIPAm (500 mg, 4.42 mmol, 20.0 eq.) dissolved in Highland Spring carbonated water (2 mL) was added to the crude reaction mix.

Procedure for the chain extension of PNIPAm *post* depolymerisation in the presence of Me_6TREN

Initially, the typical procedure for the polymerisation and depolymerisation of NIPAm in the presence of Me_6TREN was followed. However, after 60 minutes, NIPAm (500 mg, 4.42 mmol, 20.0 eq.) dissolved in Highland Spring carbonated water (2 mL) was added to the crude reaction mix.

Procedure for the addition of silver acetate prior to the depolymerisation of DP = 20 PNIPAm in carbonated water

Initially, the typical procedure for the polymerisation and depolymerisation of NIPAm in the presence of Me_6TREN was followed. However, after 10 minutes, silver acetate (50.1 mg, 0.30 mmol, 0.8 eq.) was rapidly added to the crude reaction mix and the vial re-sealed.

Typical procedure for the polymerisation and depolymerisation of other monomers *N*-hydroxyethyl acrylamide (HEAm) in the presence of Me_6TREN

Me_6TREN (23.2 µL, 0.09 mmol, 0.4eq.) was added to a 14 mL glass vial containing Highland Spring carbonated water (3 mL), sealed with a rubber septum and stirred at 250 rpm for 1 minute. The glass vial was then placed into an ice/water bath to regulate the temperature and supress the rate of hydrolysis. $Cu^{(I)}Br$ (12.5 mg, 0.09 mmol, 0.4 eq.) was rapidly added to the ligand-water mix and the vial was re-sealed. Upon addition of $Cu^{(I)}Br$ to the ligand-water mix, a coloured solution formed and red/brown $Cu^{(0)}$ particles were visible. The solution was allowed to stir and disproportionate whilst 3-dihydroxypropyl 2-bromo-2-methylpropanoate (52.4 mg, 0.22 mmol, 1.0 eq.) and uninhibited HEAm (500 mg, 4.34 mmol, 20 eq.) was dissolved in Highland Spring carbonated water (1 mL), sealed with a rubber septum, and stirred at 250 rpm for 10 minutes. At the end of this period the initiator-monomer solution was transferred *via* a syringe and needle into the glass vial containing the disproportionated ligand and $Cu^{(I)}Br$. Samples for ^{1}H NMR spectroscopy and SEC were taken using a syringe, frozen in liquid nitrogen, thawed, and diluted in the appropriate solvents.

Typical procedure for the polymerisation and depolymerisation of 2-hydroxyethyl acrylate (HEA) in the presence of Me_6TREN

Me_6TREN (23.0 µL, 0.09 mmol, 0.4eq.) was added to a 14 mL glass vial containing Highland Spring carbonated water (3 mL), sealed with a rubber septum and stirred at 250 rpm for 1 minute. The glass vial was then placed into an ice/water bath to regulate the temperature and supress the rate of hydrolysis. $Cu^{(I)}Br$ (12.3 mg, 0.09 mmol, 0.4 eq.) was rapidly added to the ligand-water mix and the vial was re-sealed. Upon addition of $Cu^{(I)}Br$ to the ligand-water mix, a coloured solution formed and red/brown $Cu^{(0)}$ particles were visible. The solution was allowed to stir and disproportionate whilst 3-dihydroxypropyl 2-bromo-2-methylpropanoate (51.9 mg, 0.22 mmol, 1.0 eq.) and uninhibited HEA (500 mg, 4.31 mmol, 20 eq.) were dissolved in Highland Spring carbonated water (1 mL), sealed with a rubber septum, and stirred at 250 rpm for 10 minutes. At the end of this period the initiator-monomer solution was transferred *via* a syringe and needle into the glass vial containing the disproportionated ligand and $Cu^{(I)}Br$. Samples for ^{1}H NMR spectroscopy and SEC were taken using a syringe, frozen in liquid nitrogen, thawed, and diluted in the appropriate solvents.

Procedure for investigating the depolymerisation of PHEA synthesised by photo-induced living radical polymerisation

Filtered monomer (DP 20), EBiB (1 eq.), $CuBr_2$ (0.04 eq.), Me_6TREN (0.24 eq.) and DMSO (2 mL) were added to a vial sealed with a rubber septum and degassed *via* purging with nitrogen for 15 minutes at ambient temperature. Polymerisation commenced upon placement of the degassed reaction mixture under the UV lamp. Samples were taken for analysis by ^{1}H NMR spectroscopy and SEC using a degassed syringe and diluted in the appropriate solvents. The resulting polymer was divided and placed in the presence of a varying combination of components and left

to stir for a minimum of 24 hours before sampling and dilution in the appropriate solvents for ^{1}H NMR and SEC analysis.

Procedure for the investigating the potential β-alkyl elimination of 2-bromo-N-(2-hydroxyethyl)propanamide under standard depolymerisation conditions

The typical procedure for the polymerisation and depolymerisation of NIPAm in the presence of Me_6TREN was followed. However, 2-bromo-N-(2-hydroxyethyl)propanamide (43.3 mg, 0.22 mmol, 1.0 eq.) was added to the reaction instead of 3-dihydroxypropyl 2-bromo-2-methylpropanoate.

Procedure for the control experiments in Section 2.2.13

The components used for the control experiments were: NIPAm (500 mg, 4.42 mmol, 20 eq.), 3-dihydroxypropyl 2-bromo-2-methylpropanoate (53.3. mg, 0.22 mmol, 1 eq.), $Cu^{(I)}Br$ (12.7 mg, 0.09 mmol, 0.4 eq.), Me_6TREN (23.0 µL, 0.09 mmol, 0.4 eq.), carbonated water (5 mL) and HPLC grade water (5 mL).

Depending upon the combination, these compounds were mixed together in a glass vial that was rapidly sealed with a rubber septum. Following this, the resulting solutions were allowed to stir overnight. Samples for ^{1}H NMR spectroscopy were taken using a syringe, frozen in liquid nitrogen, thawed, and diluted in the appropriate solvents.

2.5. References

1 IUPAC, A. D. Jenkins, P. Kratochvil, R. F. T. Steptop and U. W. Suter, *Pure Appl. Chem.*, 1996, **68**, 2287–2311.

2 R. J. Meier and J. M. Chalmers, *Molecular Characterization and Analysis of Polymers*, Elsevier, 1st edn., 2008.

3 J. G. Speight, *Handbook of Industrial Hydrocarbon Processes*, Gulf Professional Publishing, 1st edn., 2010.

4 H. H. G. Jellinek, *The Effects of Polymer Degradation on Flow Properties of Fluids and Lubricants Containing Polymers*, ASTM International, 1st edn., 1965.

5 C. L. Beyler and M. M. Hirschler, in *SFPE Handbook of Fire Protection Engineering*, 2002, pp. 110–131.

6 G. Madras, J. M. Smith and B. J. McCoy, *Polym. Degrad. Stab.*, 1997, **58**, 131–138.

7 A. Sagi, R. Weinstain, N. Karton and D. Shabat, *J. Am. Chem. Soc.*, 2008, **130**, 5434–5435.

8 M. Gisbert-Garzaran, D. Lozano, M. Vallet-Regi and M. Manzano, *RSC Adv.*, 2017, **7**, 132–136.

9 G. I. Peterson, M. B. Larsen and A. J. Boydston, *Macromolecules*, 2012, **45**, 7317–7328.

10 B. Fan and E. R. Gillies, in *Encyclopedia of Polymer Science and Technology*, John Wiley & Sons, Inc., 2002.

11 F. Liu and M. W. Urban, *Prog. Polym. Sci.*, 2010, **35**, 3–23.

12 M. Wei, Y. Gao, X. Li and M. J. Serpe, *Polym. Chem.*, 2017, **8**, 127–143.

13 H. Zou and W. Yuan, *Polym. Chem.*, 2015, **6**, 2457–2465.

14 D. Schmaljohann, *Adv. Drug Deliv. Rev.*, 2006, **58**, 1655–1670.

15 S. Dai, P. Ravi and K. C. Tam, *Soft Matter*, 2008, **4**, 435–449.

16 D. A. Davis, A. Hamilton, J. Yang, L. D. Cremar, D. Van Gough, S. L. Potisek, M. T. Ong, P. V Braun, T. J. Martinez, S. R. White, J. S. Moore and N. R. Sottos, *Nature*, 2009, **459**, 68–72.

17 J. Thevenot, H. Oliveira, O. Sandre and S. Lecommandoux, *Chem. Soc. Rev.*, 2013, **42**, 7099–7116.

18 T. Tanaka, I. Nishio, S.-T. Sun and S. Ueno-Nishio, *Science (80-.).*, 1982, **218**, 467–469.

19 A. K. Bajpai, S. K. Shukla, S. Bhanu and S. Kankane, *Prog. Polym. Sci.*, 2008, **33**, 1088–1118.

20 J. Hu and S. Liu, *Macromolecules*, 2010, **43**, 8315–8330.

21 D. Parasuraman and M. J. Serpe, *ACS Appl. Mater. Interfaces*, 2011, **3**, 2732–2737.

22 H. Koerner, G. Price, N. A. Pearce, M. Alexander and R. A. Vaia, *Nat Mater*, 2004, **3**, 115–120.

23 F. Wang, Y.-H. Lai and M.-Y. Han, *Macromolecules*, 2004, **37**, 3222–3230.

24 G. G. Odian, *Principles of Polymerization*, Wiley-Interscience, Hoboken, N.J., 4th edn., 2004.

25 F. S. Dainton and K. J. Ivin, *Nature*, 1948, **162**, 705–707.

26 H. W. McCormick, *J. Polym. Sci.*, 1957, **25**, 488–490.

27 L. E. Manring, *Macromolecules*, 1991, **24**, 3304–3309.

28 R. C. Tolman, *Proc. Natl. Acad. Sci.*, 1925, **11**, 436.

29 H. Nishida, *Polym J*, 2011, **43**, 435–447.

30 W. Kaminsky and F. Hartmann, *Angew. Chemie Int. Ed.*, 2000, **39**, 331–333.

31 L. Li, X. Shu and J. Zhu, *Polymer (Guildf).*, 2012, **53**, 5010–5015.

32 Q. Zhang, P. Wilson, Z. Li, R. McHale, J. Godfrey, A. Anastasaki, C. Waldron and D. M. Haddleton, *J. Am. Chem. Soc.*, 2013, **135**, 7355–7363.

33 W. Bai, L. Zhang, R. Bai and G. Zhang, *Macromol. Rapid Commun.*, 2008, **29**, 562–566.

34 A. B. Lowe and C. L. McCormick, *Prog. Polym. Sci.*, 2007, **32**, 283–351.

35 Q. Zhang, Z. Li, P. Wilson and D. M. Haddleton, *Chem. Commun.*, 2013, **49**, 6608–6610.

36 C. Waldron, Q. Zhang, Z. Li, V. Nikolaou, G. Nurumbetov, J. Godfrey, R. McHale, G. Yilmaz, R. K. Randev, M. Girault, K. McEwan, D. M. Haddleton, M. Droesbeke, A. J. Haddleton, P. Wilson, A. Simula, J. Collins, D. J. Lloyd, J. A. Burns, C. Summers, C. Houben, A. Anastasaki, M. Li, C. R. Becer, J. K. Kiviaho and N. Risangud, *Polym. Chem.*, 2014, **5**, 57–61.

37 D. J. Lloyd, V. Nikolaou, J. Collins, C. Waldron, A. Anastasaki, S. P. Bassett, S. M. Howdle, A. Blanazs, P. Wilson, K. Kempe and D. M. Haddleton, *Chem. Commun.*, 2016, **52**, 6533–6536.

38 R. Wiebe and V. L. Gaddy, *J. Am. Chem. Soc.*, 1940, **62**, 815–817.

39 W. S. Dodds, L. F. Stutzman and B. J. Sollami, *Ind. Eng. Chem. Chem. Eng. Data Ser.*, 1956, **1**, 92–95.

40 R. L. Madan, *Physical Chemistry*, McGraw Hill Education Private Limited, 1st edn., 2015.

41 S. C. A. A. S. Negi, *A Textbook of Physical Chemistry*, New Age International, 1st edn., 1985.

42 P. Atkins, *Inorganic Chemistry*, OUP Oxford, 5th edn., 2010.

43 B. H. G. and J. T. Edsall, *J. Biol. Chem.*, 1963, **238**, 3502.

44 N. McCann, D. Phan, X. Wang, W. Conway, R. Burns, M. Attalla, G. Puxty and M. Maeder, *J. Phys. Chem. A*, 2009, **113**, 5022–5029.

45 Q. M. Zhang, A. Ahiabu, Y. Gao and M. J. Serpe, *J. Mater. Chem. C*, 2015, **3**, 495–498.

46 N. Ghasem, *Computer Methods in Chemical Engineering*, CRC Press, 1st edn., 2011.

47 R. Chang, *Physical Chemistry for the Chemical and Biological Sciences*, University Science Books, 3rd edn., 2000.

48 D. W. B. Daniel L. Reger, Scott R. Goode, *Chemistry: Principles and Practice*, Cengage Learning, 3rd edn., 2009.

49 F. Alsubaie, A. Anastasaki, P. Wilson and D. M. Haddleton, *Polym. Chem.*, 2015, **6**, 406–417.

50 *Highland Spring*, Unpublished Data, 2014.

51 A. R. Goddard, S. Perez-Nieto, T. M. Passos, B. Quilty, K. Carmichael, D. J. Irvine and S. M. Howdle, *Green Chem.*, 2016, **18**, 4772–4786.

52 K. J. Thurecht, A. Heise, M. deGeus, S. Villarroya, J. Zhou, M. F. Wyatt and S. M. Howdle, *Macromolecules*, 2006, **39**, 7967–7972.

53 K. Jain, R. Vedarajan, M. Watanabe, M. Ishikiriyama and N. Matsumi, *Polym. Chem.*, 2015, **6**, 6819–6825.

54 P. Shivapooja, L. K. Ista, H. E. Canavan and G. P. Lopez, *Biointerphases*, 2012, **7**, 1–9.

55 Q. Duan, Y. Miura, A. Narumi, X. Shen, S.-I. Sato, T. Satoh and T. Kakuchi, *J. Polym. Sci. Part A Polym. Chem.*, 2006, **44**, 1117–1124.

56 K. Matyjaszewski and J. Xia, *Chem. Rev.*, 2001, **101**, 2921–2990.

57 N. V Tsarevsky, T. Pintauer and K. Matyjaszewski, *Macromolecules*, 2004, **37**, 9768–9778.

58 F. Thaler, C. D. Hubbard, F. W. Heinemann, R. van Eldik, S. Schindler, I. Fábián, A. M. Dittler-Klingemann, F. E. Hahn and C. Orvig, *Inorg. Chem.*, 1998, **37**, 4022–4029.

59 B. M. Rosen and V. Percec, *J. Polym. Sci. Part A Polym. Chem.*, 2007, **45**, 4950–4964.

60 K. Matyjaszewski, B. Göbelt, H. Paik and C. P. Horwitz, *Macromolecules*, 2001, **34**, 430–440.

61 F. A. Cotton, G. Wilkinson and P. L. Gaus, *Basic Inorganic Chemistry*, John Wiley & Sons, Inc., 3rd edn., 1995.

62 K. Matyjaszewski, W. Jakubowski, K. Min, W. Tang, J. Huang, W. A. Braunecker and N. V Tsarevsky, *Proc. Natl. Acad. Sci.* , 2006, **103**, 15309–15314.

63 J. Dai, S. Nanayakkara, T. C. Lamb, A. J. Clark, S.-X. Guo, J. Zhang, A. F. Patti and K. Saito, *New J. Chem.*, 2016.

64 M. P. Pandey and C. S. Kim, *Chem. Eng. Technol.*, 2011, **34**, 29–41.

65 L. Chu, K. I. Hardcastle and C. E. MacBeth, *Inorg. Chem.*, 2010, **49**, 7521–

7529.

66 G. Kickelbick, T. Pintauer and K. Matyjaszewski, *New J. Chem.*, 2002, **26**, 462–468.

67 O. Bertrand, P. Wilson, J. A. Burns, G. A. Bell and D. M. Haddleton, *Polym. Chem.*, 2015, **6**, 8319–8324.

68 F. Alsubaie, A. Anastasaki, V. Nikolaou, A. Simula, G. Nurumbetov, P. Wilson, K. Kempe and D. M. Haddleton, *Macromolecules*, 2015, **48**, 6421–6432.

69 B. M. Rosen and V. Percec, *Chem. Rev.*, 2009, **109**, 5069–5119.

70 D. Konkolewicz, Y. Wang, P. Krys, M. Zhong, A. A. Isse, A. Gennaro and K. Matyjaszewski, *Polym. Chem.*, 2014, **5**, 4396–4417.

71 A. Anastasaki, C. Waldron, P. Wilson, R. McHale and D. M. Haddleton, *Polym. Chem.*, 2013, **4**, 2672–2675.

72 C. Boyer, P. B. Zetterlund and M. R. Whittaker, *J. Polym. Sci. Part A Polym. Chem.*, 2014, **52**, 2083–2098.

73 R. P. Quirk and B. Lee, *Polym. Int.*, 1992, **27**, 359–367.

74 J. T. Rademacher, M. Baum, M. E. Pallack, W. J. Brittain and W. J. Simonsick, *Macromolecules*, 2000, **33**, 284–288.

75 N. McCann, M. Maeder and H. Hasse, *J. Chem. Thermodyn.*, 2011, **43**, 664–669.

76 G. H. Lorimer, *Trends Biochem. Sci.*, 2016, **8**, 65–68.

77 M. Horiguchi and Y. Ito, *Tetrahedron*, 2007, **63**, 12286–12293.

78 D. C. Thomas and S. M. Benson, *Carbon Dioxide Capture for Storage in Deep Geologic Formations*, Elsevier, 1st edn., 2005.

79 A. Anastasaki, V. Nikolaou, Q. Zhang, J. Burns, S. R. Samanta, C. Waldron, A. J. Haddleton, R. McHale, D. Fox, V. Percec, P. Wilson and D. M. Haddleton, *J. Am. Chem. Soc.*, 2014, **136**, 1141–1149.

80 A. Anastasaki, V. Nikolaou, G. S. Pappas, Q. Zhang, C. Wan, P. Wilson, T. P. Davis, M. R. Whittaker and D. M. Haddleton, *Chem. Sci.*, 2014, **5**, 3536–3542.

81 M. Ciampolini and N. Nardi, *Inorg. Chem.*, 1966, **5**, 41–44.

82 H. D. Keller, R. N.; Wycoff, *Inorg. Synth.*, 1946, **2**, 1–4.

83 S. Perrier, S. P. Armes, X. S. Wang, F. Malet and D. M. Haddleton, *J. Polym. Sci. Part A Polym. Chem.*, 2001, **39**, 1696–1707.

Chapter 3: Towards "off the shelf" polymerisation: screening of ligands for $Cu^{(0)}$-mediated RDRP in aqueous media

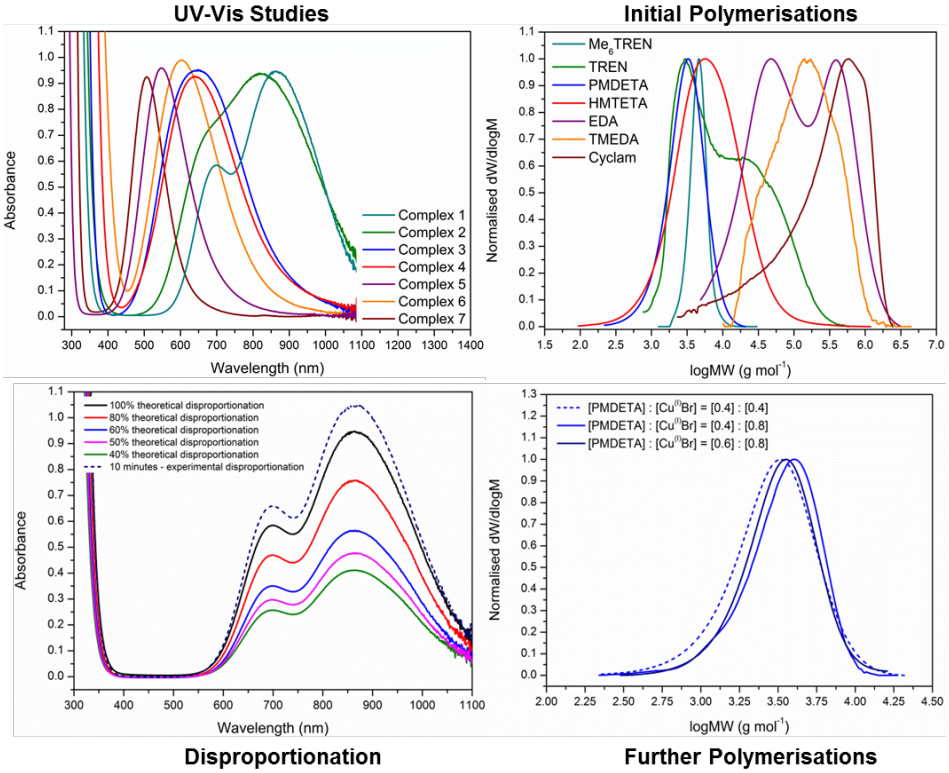

In a step towards developing an "off the shelf" facile polymerisation system, six ligands were screened as alternatives to Me_6TREN. Out of those ligands, TREN, PMDETA, HMTETA and Cyclam were found to facilitate disproportionation. Upon further investigation, PMDETA and TREN were identified as the two ligands which exhibited the most promise. However, after optimising the reaction conditions, it was found that neither of the ligands were ideal. Polymerisations conducted in the presence of TREN produced varying results, and PMDETA was unable to yield the same level of polymerisation control as Me_6TREN. Nevertheless, due to their commercial availability and the relatively controlled polymerisations, they were both deemed to be suitable replacements for Me_6TREN in "off the shelf" polymerisations.

3.1. Introduction

Amongst some of the most commonly employed water-soluble polymers are those which are based on acrylamides and acrylates. To date, they have been used in a vast range of industrial applications including: tissue engineering,[1,2] drug delivery,[3–5] personal care products,[6] paper and wastewater treatment,[7] and enhanced oil recovery (EOR).[8,9] However, their employment in applications which involve direct contact with animals and humans is almost always accompanied by some degree of apprehension over their toxicity.[10,11]

The main cause of concern does not always arise from the polymers themselves, but rather, from their constituent residual monomers and *in-vivo* degradation products. In most cases, the polymers have been shown to be non-toxic to humans, animals and plants.[10] Thus, their presence in any application is not considered to be a problem providing that they do not degrade.[12] Conversely, many monomers are considered to be highly toxic (carcinogens and neurotoxins). As such, their existence within applications has the potential to cause harm upon the general populous.

In order to minimise the damage to living organisms, companies must adhere to strict guidelines with regards to the levels of residual monomer. Typically, a limit of parts per million (ppm) is set as the maximum concentration that is allowed within any given product.[13] Whilst purification steps can be performed in order to reduce the monomer content, it is generally much simpler and faster to use polymerisation techniques that can afford quantitative conversions.

Although FRP remains a widely used polymerisation technique in industry, its high rates of reaction can lead to a lack of molecular weight predictability and moderately high dispersity values.[14] Due to these limitations, FRP is considered a sub-optimal

synthetic tool for applications that require precise molecular weights and narrow dispersities (*i.e.* calcium carbonate dispersion).[15,16]

Fortunately, the design of precise macromolecules is not unachievable, as the existence of RDRP techniques (such as RAFT,[17–19] NMP,[20] ATRP[21] and those mediated by $Cu^{(0)}$)[22–25] makes it possible to synthesise polymers with predictable and desirable characteristics. Despite RDRPs becoming routinely employed for the polymerisation of a vast array of monomers, the controlled polymerisation of acrylamide and its derivatives was, until recently, almost exclusively restricted to RAFT.[26–28]

Prior to 2013, the synthesis of polyacrylamides *via* copper-mediated RDRPs proved to be problematic, with the majority of polymerisations resulting in low conversions, broad MWDs, or unpredictable molecular weights.[29–32] Whilst there had been some degree of success for the polymerisation of NIPAm, the majority of reactions were conducted in either non-aqueous media or binary mixtures of water and organic solvents.[33,34,35] Not only was this a significant disadvantage for industrial scale-up, but considering the expanding interest in water-soluble and bio-compatible polymers, this was a substantial drawback for the polymerisation technique.

During a publication relating to the attempted ATRP of *N,N*-dimethylacrylamide (DMAm),[30] Brittain *et al.* highlighted two key reasons for a lack of polymerisation control. Firstly, complexation of the amide group onto the ω-end of the polymers was causing the stabilisation of propagating radicals. This led to an unacceptably high concentration of radicals at any given moment and thus, resulted in high levels of radical-radical coupling. The second reason was that a loss of end group functionality had occurred as a consequence of cyclisation involving the nucleophilic displacement of the halogen end group by the penultimate amide nitrogen.

To further illustrate the lack of control, Shen *et al.* reported the polymerisation of DMAm *via* ATRP at high temperatures (100°C).[36] Within this work, the use of *N*,*N'*-di(3-hexoxo-3-oxopropyl)-*N*,*N'*-bis(2-pyridylmethyl)ethane-1,2-diamine (BPED) as the ligand enabled for relatively low dispersities ($Đ_m$ = 1.27) and good agreement between the experimental and theoretical molecular weights to be obtained. However, the rate of polymerisation was quite slow, with only 66 % conversion being reached after 4 hours. Although high conversions were achieved with longer reaction times (17 hours), this was at the expense of a broadening MWD ($Đ_m$ = 1.60).

Perhaps one of the most successful examples of an acrylamide based polymerisation *via* copper-mediated RDRP techniques was conducted by Kakuchi *et al.* in 2009.[37] Through utilising a mixture of ethanol and water as the solvent, HEAm was polymerised to high conversions (maximum 80 %) and narrow MWDs ($Đ$ < 1.21) within 1 hour. Subsequent successful chain extensions with *N*-acryloylmorpholine (NAM) and *N*-[3-(dimethylamino)propyl]acrylamide (DMAPAA), highlighted that, not only were the polymerisations controlled, but the polymers retained a high level of end group functionality throughout the process.

The synthesis of acrylamide-based polymers *via* alternative techniques to RAFT has become considerably easier by the introduction of the aqueous $Cu^{(0)}$-mediated RDRP methodology.[22,38–40] Relying upon the complete disproportionation of a $Cu^{(I)}X$/L complex prior to the addition of monomer and initiator, this procedure allows for the polymerisation of acrylamides[38,40] (and other water-soluble monomers[39,41–47]) with near-quantitative conversions and narrow MWDs.

To re-iterate, the difficulties in obtaining well-defined polymers *via* copper-mediated techniques have largely been attributed to the occurrence of undesirable side reactions (such as the reversible dissociation and substitution of the ligand from the

$Cu^{(II)}$ complex[22,48]) and the loss of end group fidelity resulting from hydrolysis.[30,31,37] Fortunately, by regulating the polymerisation temperature close to 0 °C, the latter of these difficulties can be supressed for the duration of the reaction.

The aqueous $Cu^{(0)}$-mediated RDRP methodology itself is relatively straightforward, and can be divided into two steps: the disproportionation of a $Cu^{(I)}X$ species in the presence of a *N*-donating ligand, and the addition of monomer and initiator to this solution (Scheme 3.1).

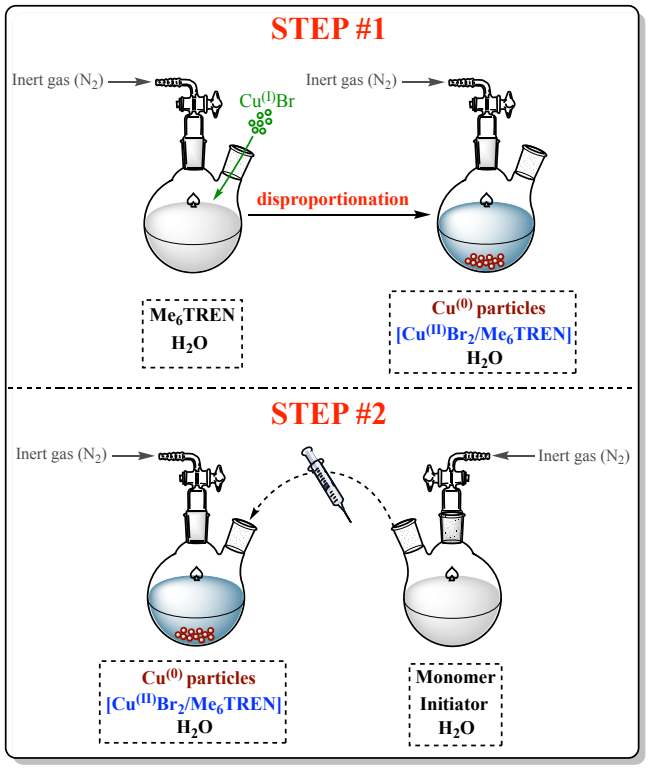

Scheme 3.1 – A schematic outline of the two steps in the aqueous $Cu^{(0)}$-mediated RDRP protocol.

Irrespective of this systems' simplicity and that of the technique as a whole, $Cu^{(0)}$-mediated RDRPs have yet to find widespread commercial use. One of the main reasons behind this is the use of copper and its associated/perceived toxicity.[49,50] Despite it being possible to remove such species during the "work-up" stage *via* the use of alumina or Cuprisorb™, the potential for small quantities to remain in the final product causes some degree of concern. In an effort to minimise this drawback,

progress has been made to not only reduce the levels of catalyst loading,[51–53] but to find suitable transition metal alternatives.[51,54]

Even though advances have been made with respect to the presence of copper within the system, there are still drawbacks which hinder both the implementation and research into TMM methodologies. For example, out of the five components which are required for the aqueous protocol, only three can be purchased for a relatively low price and from a variety of vendors ($Cu^{(I)}Br$, monomer and solvent). Acquiring the initiator or ligand can therefore either prove to be costly (Me_6TREN costs ~£125 per mL from Sigma-Aldrich), or may require the user to perform extensive synthesis and rigorous purification (the initiator[55] and Me_6TREN[56]). To a non-synthetic chemist, or those who find organic synthesis unappealing, the need to conduct small molecule synthesis and prepare ligands may deter them from utilising this technique.

There are further issues that are associated with these compounds, specifically with regards to their storage. Me_6TREN and many other *N*-containing ligands are highly susceptible to degradation and oxidation.[57] In order to extend their longevity, they are usually kept under cold, dark, dry and inert conditions. If either oxidation or degradation occurs, then the ligand must undergo further purification (such as distillation) prior to its use. Alongside this, $Cu^{(I)}Br$ must be kept under oxygen free conditions to avoid its oxidation into $Cu^{(II)}Br_2$. Since the frequent use of this compound makes interaction with air difficult to avoid, purification is almost always a pre-requisite. In fact, it is often found that even newly purchased $Cu^{(I)}Br$ with a stated purity of >99 % is green. Given that $Cu^{(I)}$ retains a full complement of d-electrons (d^{10}) and therefore should be colourless, it is evident why treatment is needed.

3.1.1. The selection of appropriate ligands for "off the shelf" polymerisation

In order to expand the scope of $Cu^{(0)}$-mediated RDRPs, the issue of reagent preparation is one which needs to be addressed. One potential way to achieve this is through the creation of an "off the shelf" polymerisation system; that is, one which exclusively employs commercially available materials.

At the beginning of this project, the aqueous $Cu^{(0)}$-mediated RDRP protocol was in the early stages of its development. There were only a few publications relating to its optimisation,[38,39,58] and the focus of these was largely based around expanding the range of suitable monomers.[42,59] Unsurprisingly, as the system enables for unprecedented control over the polymerisation of acrylamide based monomers, there has since been a substantial amount of papers relating to its use a synthetic tool.

Nevertheless, despite the emphasis which is placed upon the complete and full disproportionation of a $Cu^{(I)}X/L$ complex,[22] there has been very little investigation into the use of different ligands. It is, however, worthwhile mentioning that whilst there have not been many studies for $Cu^{(0)}$-mediated RDRP mechanisms as a whole,[58,60–63] there have been investigations into the selection of ligands for ATRP.[21,64–67]

Currently, the majority of acrylamide and acrylate polymerisations *via* $Cu^{(0)}$-mediated RDRPs employ Me_6TREN as the ligand, with adaptations being made for their respective methyl derivatives.[58,61] Whilst it has been shown that the resulting copper complexes are highly capable of facilitating the controlled polymerisation of these monomers, the price of Me_6TREN makes it unsuitable for use in an "off the shelf" manner. To that end, six alternative ligands were selected for screening as

mediators for the synthesis of PNIPAm in aqueous media. These were: tris(2-aminoethyl)amine (TREN), *N,N,N′,N″,N‴*-pentamethyldiethylenetriamine (PMDETA), 1,1,4,7,10,10-hexamethyltriethylenetetramine (HMTETA), ethylenediamine (EDA), *N,N,N′,N′*-tetramethylethylenediamine (TMEDA), and 1,4,8,11-tetraazacyclotetradecane (Cyclam) (Table 3.1). Importantly, to provide a direct comparison to the proposed alternatives, the use of Me_6TREN as the ligand for the aqueous $Cu^{(0)}$-mediated RDRP of NIPAm was also investigated.

Ligand	Structure	Cost per mL	Supplier
Me_6TREN	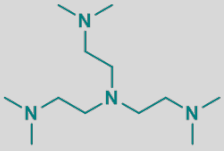	£125.50	Sigma-Aldrich
TREN	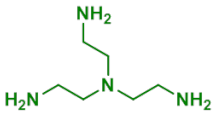	£2.80	Sigma-Aldrich
PMDETA	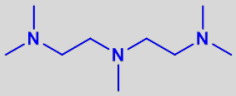	£0.30	Sigma-Aldrich
HMTETA	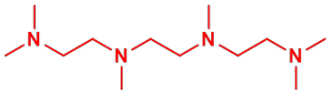	£15.14	Sigma-Aldrich
EDA		£0.17	VWR International Ltd.
TMEDA	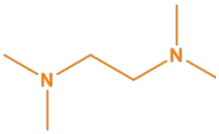	£0.67	Fisher Scientific
Cyclam	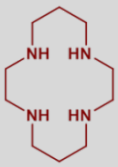	£43.50	Fisher Scientific

Table 3.1 – An overview of the cost of each ligand screened during the development of "off the shelf" polymerisation system.

Finally, it is worth mentioning that the chosen ligands varied in their denticity and the geometry that they prefer to adopt upon binding. For ease of access, this information has been summarised in Table 3.2.[62,66]

Ligand	Denticity	Geometry of the $Cu^{(I)}$ complex	Geometry of the $Cu^{(II)}Br_2$ complex
Me_6TREN	"Claw-like" Tetradentate	Trigonal bipyramidal*	Distorted trigonal bipyramidal**
TREN	"Claw-like" Tetradentate	Trigonal bipyramidal*	Trigonal bipyramidal*
PMDETA	Tridentate	-	Square pyramidal**
HMTETA	Tetradentate	-	Distorted square pyramidal**
EDA	Bidentate	Tetrahedral*	Square pyramidal*
TMEDA	Bidentate	Tetrahedral*	Square pyramidal*
Cyclam	Cyclic Tetradentate	Square planar*	Square pyramidal*

Table 3.2 – A summary of the denticity and the preferred geometries of the $Cu^{(I)}$Br/ligand and $Cu^{(II)}$Br/ligand complexes. The information denoted * was obtained from [62] and ** from [66].

3.2. Results and discussion

Considering the complexity of TMM-RDRP systems, it was not expected that each (or in fact any) of the selected ligands would mediate the controlled polymerisation of acrylamides and acrylates. Nonetheless, as most of the ligands that were screened in this work have not been previously employed for aqueous $Cu^{(0)}$-mediated RDRPs, it was deemed important to obtain preliminary data for all of the chosen compounds. This was done regardless of whether the inherent nature and activities of the complexes prevented them from being applicable to the targeted monomers.[43,68–70]

A simple and reliable reaction that can be performed within the aqueous system is the synthesis of PNIPAm. As a means of pinpointing which of the copper/ligand complexes warranted further investigation, initial polymerisations of NIPAm were conducted, alongside a series of disproportionation studies.

3.2.1. Initial polymerisations

3.2.1.1. $Cu^{(0)}$-mediated RDRP in the presence of multidentate ligands

The polymerisation of NIPAm using Me_6TREN as a ligand under standard $Cu^{(0)}$-mediated RDRP conditions ([M] : [I] : [L] : [$Cu^{(I)}$Br] = [20] : [1.0] : [0.4] : [0.4] resulted in a well-defined PNIPAm homopolymer, as expected.[22,38] Pleasingly, ^{1}H NMR spectroscopy indicated that quantitative monomer conversion (>99 %) had been attained within 30 minutes.

Upon subsequent analysis of the resulting polymer by SEC, a narrow and monomodal distribution ($Đ_m$ = 1.09; Figure 3.1) was revealed. In addition to this, there was a relatively good agreement between the theoretical (M_n = 2500 g mol^{-1}) and experimental (M_n = 4300 g mol^{-1}) molecular weights.

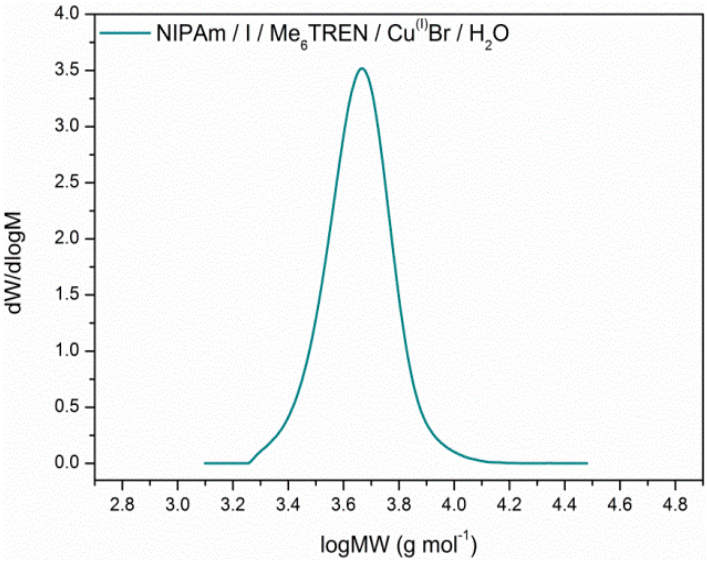

Figure 3.1 – The MWD resulting from the aqueous $Cu^{(0)}$-mediated RDRP of NIPAm in the presence of Me_6TREN. Conditions: [M] : [I] : [L] : [$Cu^{(I)}$X] = [20] : [1.0] : [0.4] : [0.4]. $Đ_m$ = 1.09 and M_n = 4300 g mol^{-1}.

Various reasons can explain why discrepancies in molecular weight values arise, these include: poor initiator efficiency, a lack of polymerisation control, the presence of "free ligand",[63] and differences in hydrodynamic volume (V_h) between the chosen

SEC calibrant and the analysed sample. However, at this point, there is not enough evidence to determine which of these factors was the cause of the disagreement.

It should also be noted that in order to enable for an accurate comparison of the various tetradentate ligands in a standard $Cu^{(0)}$-mediated RDRP, a 1:1 exchange with Me_6TREN and either TREN, HMTETA or Cyclam was tested. This assumed that each ligand occupied the same number of binding sites on the metal centre which, due to the metal complex geometry, was believed to be accurate. Although PMDETA is a tridentate, rather than a tetradentate ligand, an equimolar ratio of $Cu^{(I)}$Br to ligand was also employed in this instance. Finally, as EDA and TMEDA are both bidentate ligands, their concentration within the polymerisation media was doubled in order to ensure that the co-ordination shell of copper was complete ([M] : [I] : [L] : [$Cu^{(I)}$Br] = [20] : [1.0] : [0.8] : [0.4]).

The substitution of Me_6TREN for its synthetic precursor TREN[71,72] has previously been attempted for the polymerisation of NIPAm *via* aqueous $Cu^{(0)}$-mediated RDRP ([M] : [I] : [L] : [$Cu^{(I)}$Br] = [80] : [1.0] : [0.4] : [0.8]).[22] However, whilst Haddleton *et al.,* successfully synthesised PNIPAm to near-quantitative conversion (99 %) within 1 hour, the polymerisation process lacked dispersity control ($Đ_m$ = 1.49).

When TREN was employed as the ligand herein, the polymerisation of NIPAm proceeded to 100% conversion within the same time-frame. Although it was possible to attain complete monomer conversion, the presence of a bimodal distribution in the SEC chromatogram (Figure 3.2) highlighted a substantial loss of polymerisation control ($Đ_m$ = 5.38). Nevertheless, the recorded molecular weight values ($M_{n,theoretical}$ = 2500 g mol^{-1} and $M_{n,SEC}$ = 5300 g mol^{-1}) were similar to those that were obtained for the polymerisation conducted with Me_6TREN ($M_{n,theoretical}$ = 2500 g mol^{-1} and $M_{n,SEC}$ = 4300 g mol^{-1}).

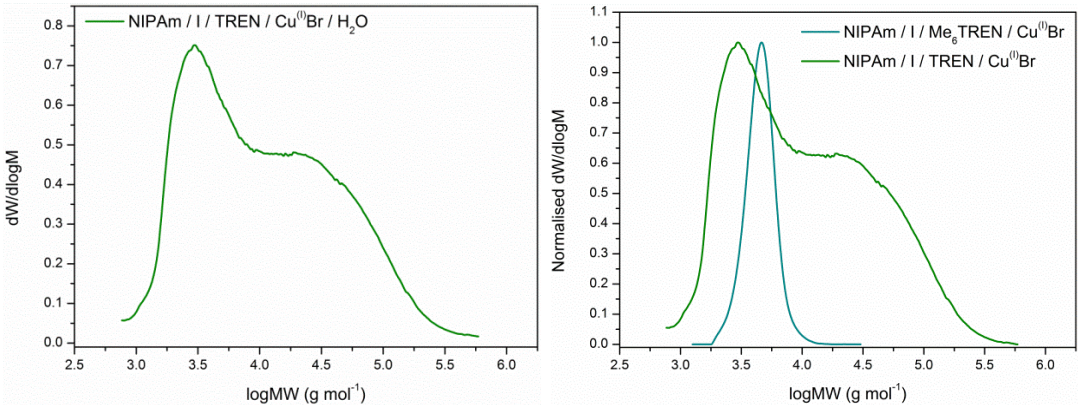

Figure 3.2 - The MWD resulting from the aqueous $Cu^{(0)}$-mediated RDRP of NIPAm in the presence of TREN. Conditions: [M] : [I] : [L] : [$Cu^{(I)}$X] = [20] : [1.0] : [0.4] : [0.4]. $Đ_m$ = 5.38 and M_n = 5300 g mol^{-1} (left); Comparison of the MWDs resulting from the polymerisation of NIPAm in the presence of Me_6TREN and TREN (right).

The presence of a high molecular weight shoulder implied that uncontrolled chain growth had occurred during propagation. Considering that the polymerisation of NIPAm with Me_6TREN was deemed to be controlled, it was concluded that the initiator used for this polymerisation was relatively efficient. As such, it was believed that poor initiator efficiency was not the reason for the lack of polymerisation control.

It is possible that the bimodality stemmed from either the inefficient deactivation of the propagating radicals, or a lack of deactivating species. However, given the degree of disagreement between the theoretical and experimental molecular weights, free radical chain growth was not considered to be the dominant cause of the high dispersity. Regardless of the reason, it is evident that under these conditions, copper/TREN complexes are not suitable mediators for the polymerisation of NIPAm.

The next ligand screened was PMDETA; a tridentate ligand which has a lower rate constant of activation (k_{act}) in comparison to Me_6TREN.[73] It is perhaps worth noting that PMDETA has previously been screened (to varying degrees of success) as the ligand for the polymerisation of NIPAm *via* alternative copper-mediated RDRP techniques[74,75] and during the development of the aqueous protocol.[22] In addition to this, it has also been exploited within the aqueous $Cu^{(0)}$-mediated RDRP

methodology for the controlled polymerisation of methacrylate based monomers.[58] When used for the polymerisation of NIPAm in this study, high conversions (~ 96 %) were obtained within 30 minutes. Importantly, in the ensuing characterisation by SEC, there was a lack of noticeable bimodality within the chromatogram; instead, a broad ($Đ_m$ = 1.54; Figure 3.3) but monomodal MWD was detected.

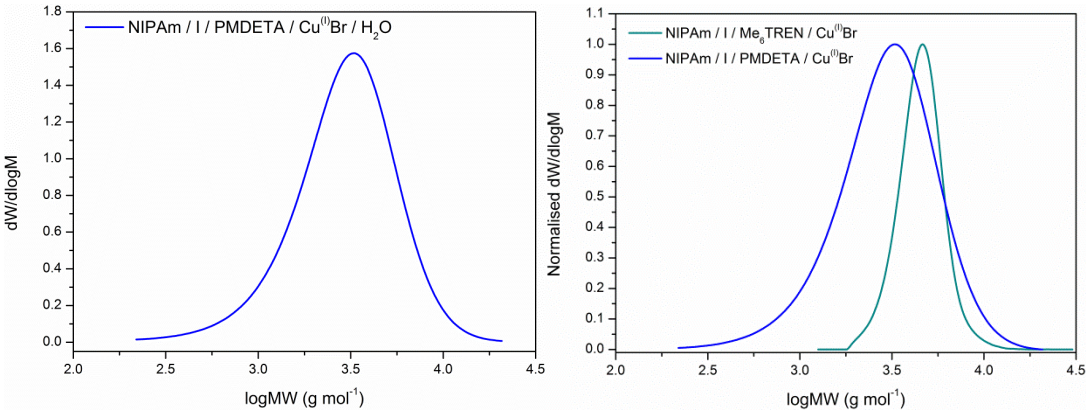

Figure 3.3 - The MWD resulting from the aqueous $Cu^{(0)}$-mediated RDRP of NIPAm in the presence of PMDETA. Conditions: [M] : [I] : [L] : [$Cu^{(I)}$X] = [20] : [1.0] : [0.4] : [0.4]. $Đ_m$ = 1.54 and M_n = 2300 g mol^{-1} (left); Comparison of the MWDs resulting from the polymerisation of NIPAm in the presence of Me_6TREN and PMDETA (right).

Generally speaking, a system which produces a dispersity of <1.5 can be categorised as controlled.[76] Yet, the propensity of copper-mediated techniques to produce highly narrow MWDs means that there is hesitation around following this particular criterion. Given that there was a slight amount of tailing in the low molecular weight region, it was deemed likely that some degree of chain termination had occurred during the polymerisation process. Notably, although different conditions were used, these results were found to be similar to those within the existing literature.[22,77]

The SEC measurements showed that the experimental (M_n = 2300 g mol^{-1}) and theoretical (M_n = 2400 g mol^{-1}) molecular weights were in close agreement with one another. Given that the only difference between this and the earlier polymerisations was the ligand type, it did not seem likely that the previously observed lack of molecular weight agreement resulted from a difference in V_h between the chosen

calibrant and the sample. Perhaps more importantly, the SEC data suggested that PMDETA enabled for more control over the polymerisation of NIPAm than TREN.

When PMDETA was exchanged for HMTETA,[78–81] the polymerisation of NIPAm was found to be slow and incomplete. Unlike the previous reactions, when a sample was taken after 30 minutes and analysed by ^{1}H NMR spectroscopy, it was found that only 81 % conversion had been achieved (Figure 3.4). Upon further monitoring of the reaction it was determined that no further polymerisation had occurred (t = 24 hours; 78 % conversion).

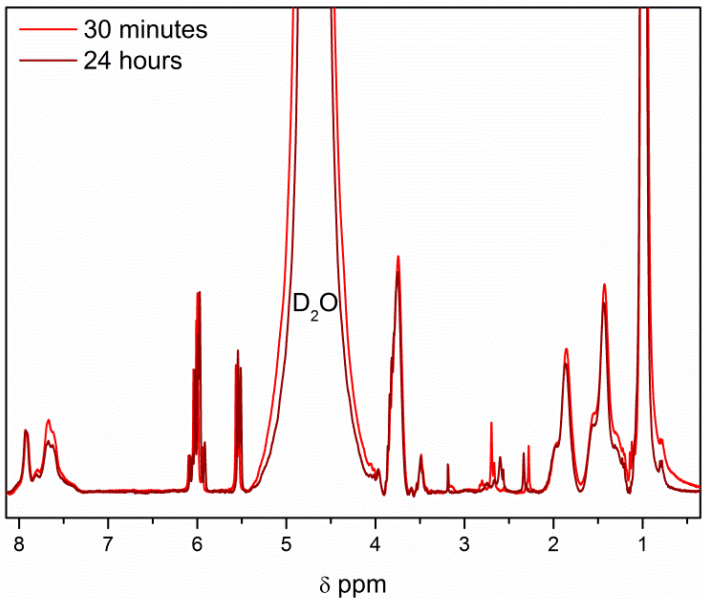

Figure 3.4 – A comparison of the ^{1}H NMR spectra obtained for the polymerisation of NIPAm in the presence of HMTETA. Conditions: [M] : [I] : [L] : [$Cu^{(I)}$X] = [20] : [1.0] : [0.4] : [0.4].

The limited conversion obtained during the polymerisation was attributed to irreversible chain termination events. As with PMDETA and TREN, this was ascribed to the slow deactivation of propagating species giving a broad but symmetrical MWD ($Đ_m$ = 3.53; Figure 3.5). The combination of the limited conversion and high dispersity values subsequently led to the conclusion that HMTETA could not adequately facilitate the controlled polymerisation of NIPAm under these conditions.

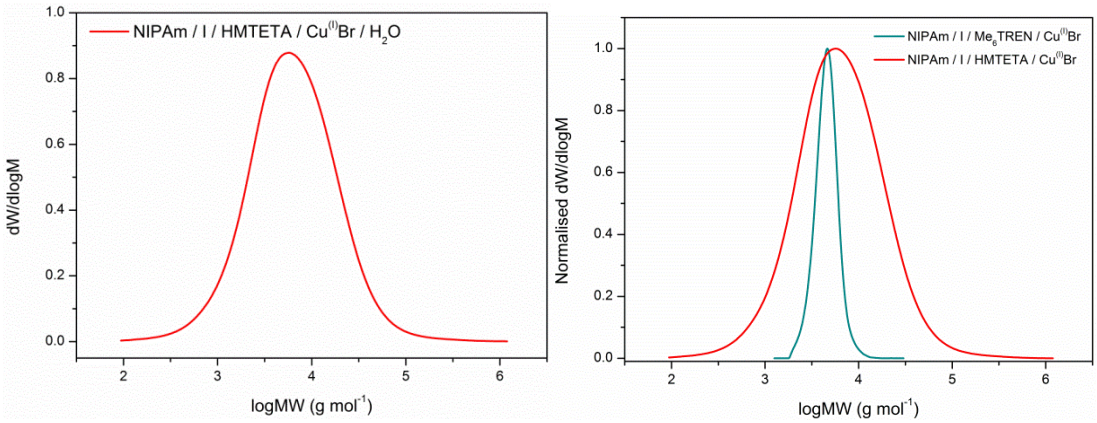

Figure 3.5 - The MWD resulting from the aqueous $Cu^{(0)}$-mediated RDRP of NIPAm in the presence of HMTETA. Conditions: [M] : [I] : [L] : [$Cu^{(I)}$X] = [20] : [1.0] : [0.4] : [0.4]. $Đ_m$ = 3.53 and M_n = 3400 g mol^{-1} (left); Comparison of the MWDs resulting from the polymerisation of NIPAm in the presence of Me_6TREN and HMTETA (right).

The final multidentate ligand that was screened as part of this work was Cyclam. Cyclam is a macrocyclic tetradentate ligand which, based on existing studies conducted for alternative copper-mediated techniques, is considered to be one of the more "active" ligands.[73] In its least substituted form, Cyclam has not previously been investigated for the synthesis of polymers *via* copper-mediated RDRP techniques, however, its tetramethyl- (Me_4Cyclam, 1,4,8,11-tetramethyl-1,4,8,11-tetraazacyclotetradecane) and hexamethyl- (Me_6Cyclam, 5,5,7,12,12,14-hexamethyl-1,4,8,11-tetraazacyclotetradecane) derivatives on the other hand, have frequently been exploited for the polymerisation of LAMs.[82–85]

When Cyclam was employed as the ligand for the aqueous $Cu^{(0)}$-mediated RDRP of NIPAm, quantitative monomer conversion (100 %) was attained within 30 minutes. Unfortunately, and perhaps unsurprisingly given the activity of the ligand,[69] the results from SEC (Figure 3.6) indicated that the polymerisation process was highly uncontrolled ($Đ_m$ = 8.50).

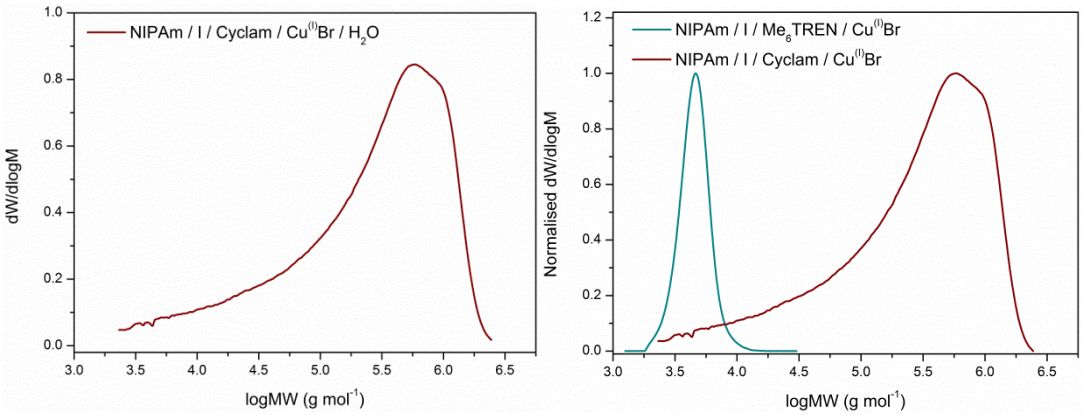

Figure 3.6 - The MWD resulting from the aqueous $Cu^{(0)}$-mediated RDRP of NIPAm in the presence of Cyclam. Conditions: [M] : [I] : [L] : [$Cu^{(I)}$X] = [20] : [1.0] : [0.4] : [0.4]. $Đ_m$ = 8.50 and M_n = 54,400 g mol^{-1} (left); Comparison of the MWDs resulting from the polymerisation of NIPAm in the presence of Me_6TREN and Cyclam (right).

The most prevalent feature within the SEC trace itself was the large amount of tailing within the low molecular weight region (Figure 3.6). Typically, this is taken to be indicative of a large amount of termination occurring during the polymerisation process. To that end, the appearance of this tail was attributed to radical-radical coupling resulting from the inefficient deactivation of propagating species.

Although high monomer conversions were obtained, the large discrepancy between molecular weight values ($M_{n,theoretical}$ = 2500 g mol^{-1} and $M_{n,SEC}$ = 54,400 g mol^{-1}) was not entirely unexpected. Given the high levels of bimolecular termination, the uncontrolled chain growth was subsequently ascribed to the addition of an undesirable number of monomer units onto the remaining active chains. Additionally, based on these findings, it was concluded that the polymerisation of NIPAm in the presence of Cyclam could not be regulated under these conditions.

3.2.1.2. $Cu^{(0)}$-mediated RDRP in the presence of bidentate ligands

There are numerous literature reports detailing the use of bidentate ligands for copper-mediated RDRPs.[68,86–88] However, there is very little evidence of EDA or its derivatives being employed within these methodologies.[81,89–91] More importantly,

there are no known reports that involve the use of EDA or TMEDA as the ligand for an aqueous $Cu^{(0)}$-mediated RDRP. Thus, it was decided that EDA would be screened as the ligand for the polymerisation of NIPAm in aqueous media.

Following sampling of the reaction mixture after 30 minutes, analysis by ^{1}H NMR spectroscopy revealed that the polymerisation of NIPAm had proceeded to full monomer conversion but with broad and complex MWDs (Figure 3.7).

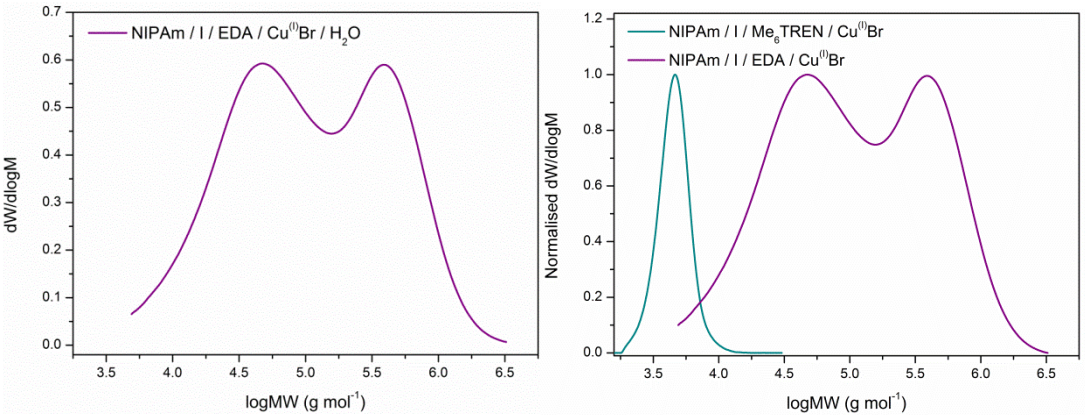

Figure 3.7 - The MWD resulting from the aqueous $Cu^{(0)}$-mediated RDRP of NIPAm in the presence of EDA. Conditions: [M] : [I] : [L] : [$Cu^{(I)}$X] = [20] : [1.0] : [0.8] : [0.4]. $Đ_m$ = 5.29 and M_n = 48,500 g mol^{-1} (left); Comparison of the MWDs resulting from the polymerisation of NIPAm in the presence of Me_6TREN and EDA (right).

In the resulting SEC trace (Figure 3.7), a bimodal and broad distribution ($Đ_m$ = 5.29) was visible alongside a large disagreement between the experimental (M_n = 2500 g mol^{-1}) and theoretical (M_n = 48,500 g mol^{-1}) molecular weights. It was believed that the bimodality was most likely caused by a combination of two events: free radical chain growth and undesirable bimolecular termination. As a result, EDA was concluded to be an incompatible ligand for this system.

In a similar manner to the polymerisation with EDA, using TMEDA for the polymerisation of NIPAm resulted in high conversions within 30 minutes (~ 98 %), large dispersity values ($Đ_m$ = 2.50; Figure 3.8) and unpredictable molecular weights ($M_{n,\ theoretical}$ = 2500 g mol^{-1}; $M_{n,SEC}$ = 84,700 g mol^{-1}). Regardless of the cause, it is

clear that TMEDA based copper complexes cannot be employed as facilitators for the polymerisation of NIPAm *via* aqueous $Cu^{(0)}$-mediated RDRP.

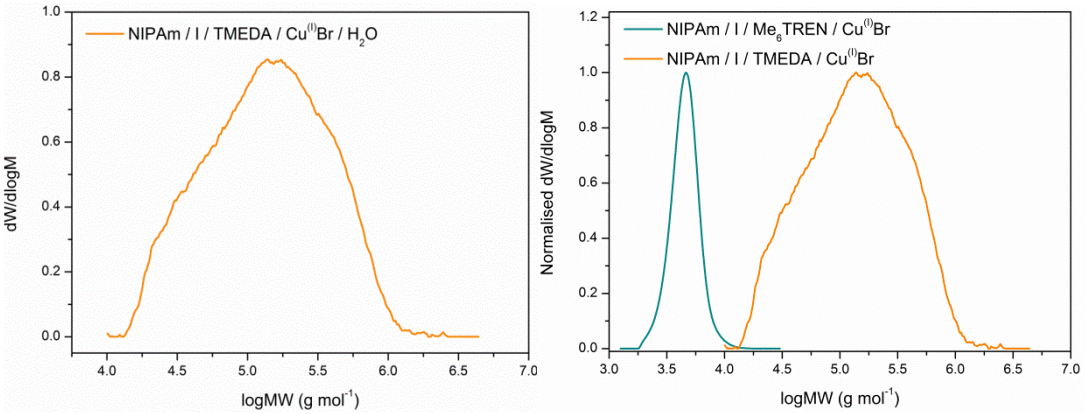

Figure 3.8 - The MWD resulting from the aqueous $Cu^{(0)}$-mediated RDRP of NIPAm in the presence of TMEDA. Conditions: [M] : [I] : [L] : [$Cu^{(I)}$X] = [20] : [1.0] : [0.8] : [0.4]. $Đ_m$ = 2.50 and M_n = 84,700 g mol^{-1} (left); Comparison of the MWDs resulting from the polymerisation of NIPAm in the presence of Me_6TREN and TMEDA (right).

3.2.1.3. Summary of the initial polymerisations

For the development of an "off the shelf" polymerisation system, six ligands were tested for the controlled synthesis of PNIPAm in aqueous media *via* the $Cu^{(0)}$-mediated RDRP technique. ^{1}H NMR spectroscopy measurements indicated that near-quantitative conversion had occurred within an acceptable time frame (< 1 hour) for five out of the six polymerisations (using TREN, PMDETA, Cyclam, EDA and TMEDA) (Table 3.3). In the case of HMTETA however, only 78 % conversion was achieved within 24 hours (Table 3.3).

SEC measurements showed that each of the polymerisations lacked control; broad MWDs, and in some cases polymers with unpredictable molecular weights, were obtained (Figure 3.9). The narrowest dispersity value of ~ 1.5 was obtained for PNIPAm synthesised using PMDETA as an alternative ligand to Me_6TREN (Table 3.3). Given that there was at least some level of control over the polymerisation process, it was theorised that it might be possible to lower the dispersity value through the optimisation of reaction conditions. However, it should be mentioned

that as most of these ligands have not previously been utilised in the aqueous system, there may not be any conditions under which a controlled polymerisation can be realised.

Ligand	Time (hours)	Conversion (%)	$M_{n,th}$ (g mol^{-1})	$M_{n,SEC}$ (g mol^{-1})	$Đ_m$
Me_6TREN	0.5	100	2500	4300	1.09
TREN	1	100	2500	5300	5.38
PMDETA	0.5	96	2400	2300	1.54
HMTETA	24	81	2000	3400	3.53
EDA	0.5	100	2500	39,000	2.98
TMEDA	0.5	98	2500	84,800	2.50
Cyclam	0.5	100	2500	54,400	8.50

Table 3.3 - A comparison of the data resulting from the aqueous $Cu^{(0)}$-mediated RDRP of NIPAm in the presence of each ligand.

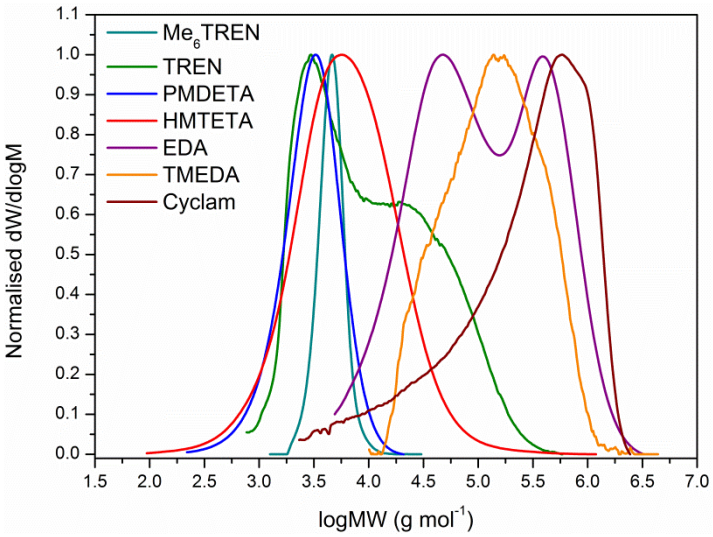

Figure 3.9 - A comparison of the MWDs resulting from the aqueous $Cu^{(0)}$-mediated RDRP of NIPAm in the presence of each ligand.

3.2.2. Studying the ligand/$Cu^{(I)}$Br complexes in aqueous media via UV-Vis spectroscopy

The chemistry of copper is well known; the electron shell of $Cu^{(II)}$ is incomplete (d^9), its complexes undergo d-d transitions, give rise to intense absorbances within the UV-Vis region, and produce solutions which are deeply coloured.[92,93] $Cu^{(I)}$ on the

other hand, retains a full complement of d-electrons (d^{10}), and its complexes do not participate in d-d transitions.[92,93]

As a means of further investigating the behaviour of the ligands and their respective copper complexes, the UV-Vis spectra of each $Cu^{(II)}$/ligand complex was recorded, their relevant transitions were assigned, and the λ_{max} and their extinction coefficients (ε) were determined from the gradient of the calibration curve (Figures 3.10 to 3.12 and Table 3.4).

Ligand	d-d transition (nm)	λ_{max} (nm)	ε for λ_{max} (L mol^{-1} cm^{-1})
Me_6TREN	696 and 861	861	794
TREN	664 and 819	819	208
PMDETA	642	642	315
HMTETA	642	642	351
EDA	549	549	91
Cyclam	507	507	154
TMEDA	602	602	148

Table 3.4 – The UV-Vis spectral data obtained from placing $Cu^{(II)}Br_2$ with each ligand in H_2O.

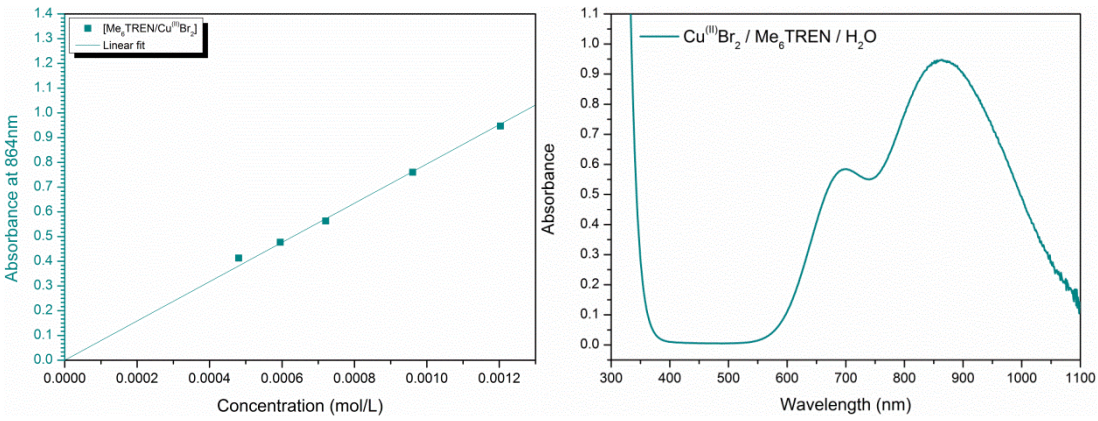

Figure 3.10 – The calibration plot that was used for calculating the ε of $Cu^{(II)}Br_2$/Me_6TREN (cyan) at λ_{max} (left). The UV-Vis spectrum obtained from placing $Cu^{(II)}Br_2$/Me_6TREN in H_2O (cyan) (right).

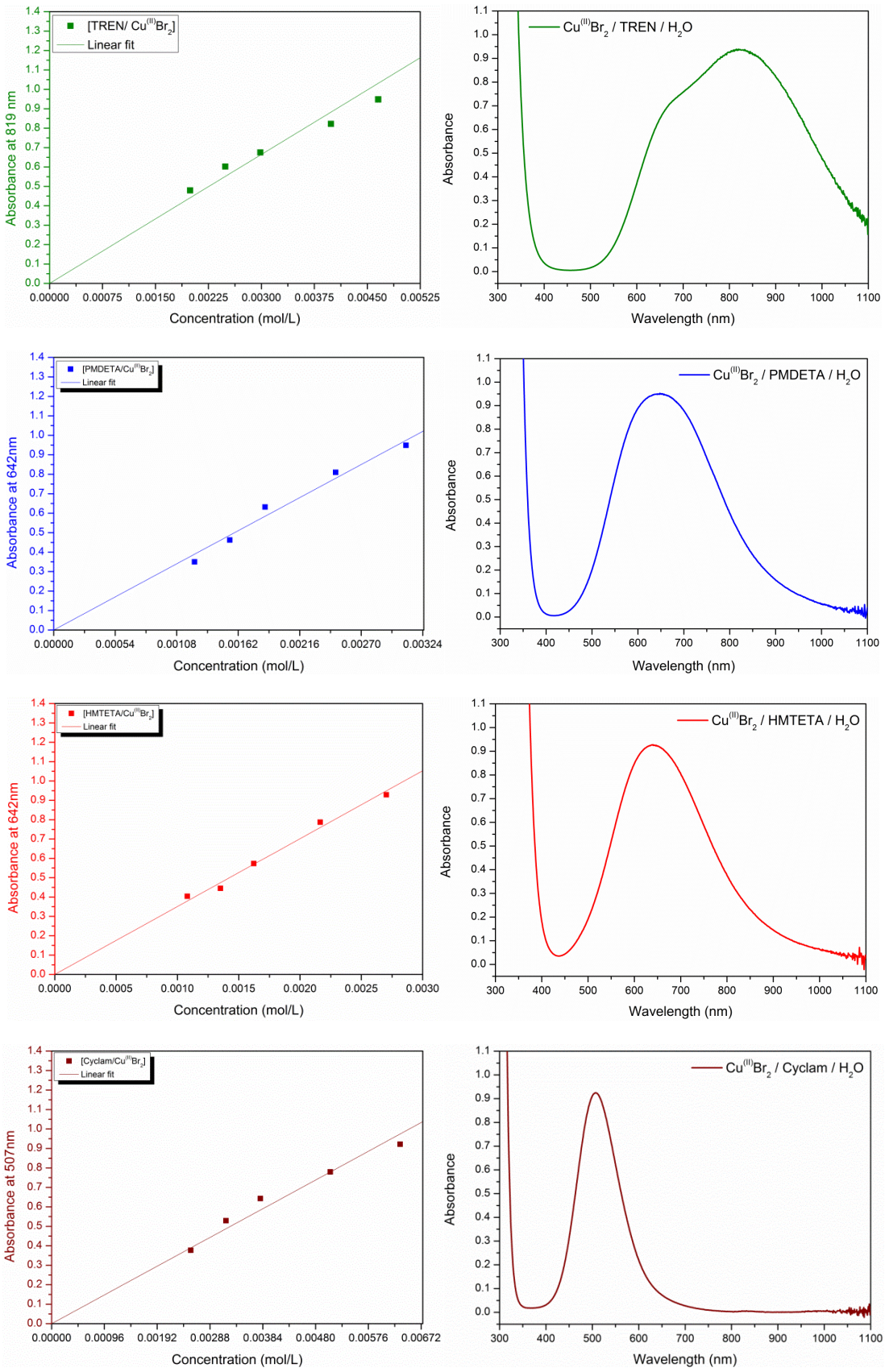

Figure 3.11 - The calibration plot that was used for calculating the ε of $Cu^{(II)}Br_2$/TREN (green), $Cu^{(II)}Br_2$/PMDETA (blue), $Cu^{(II)}Br_2$/HMTETA (red), and $Cu^{(II)}Br_2$/Cyclam (burgundy) at λ_{max} (left). The UV-Vis spectrum obtained from placing $Cu^{(II)}Br_2$/TREN (green), $Cu^{(II)}Br_2$/PMDETA (blue), $Cu^{(II)}Br_2$/HMTETA (red), and $Cu^{(II)}Br_2$/Cyclam (burgundy) in H_2O (right).

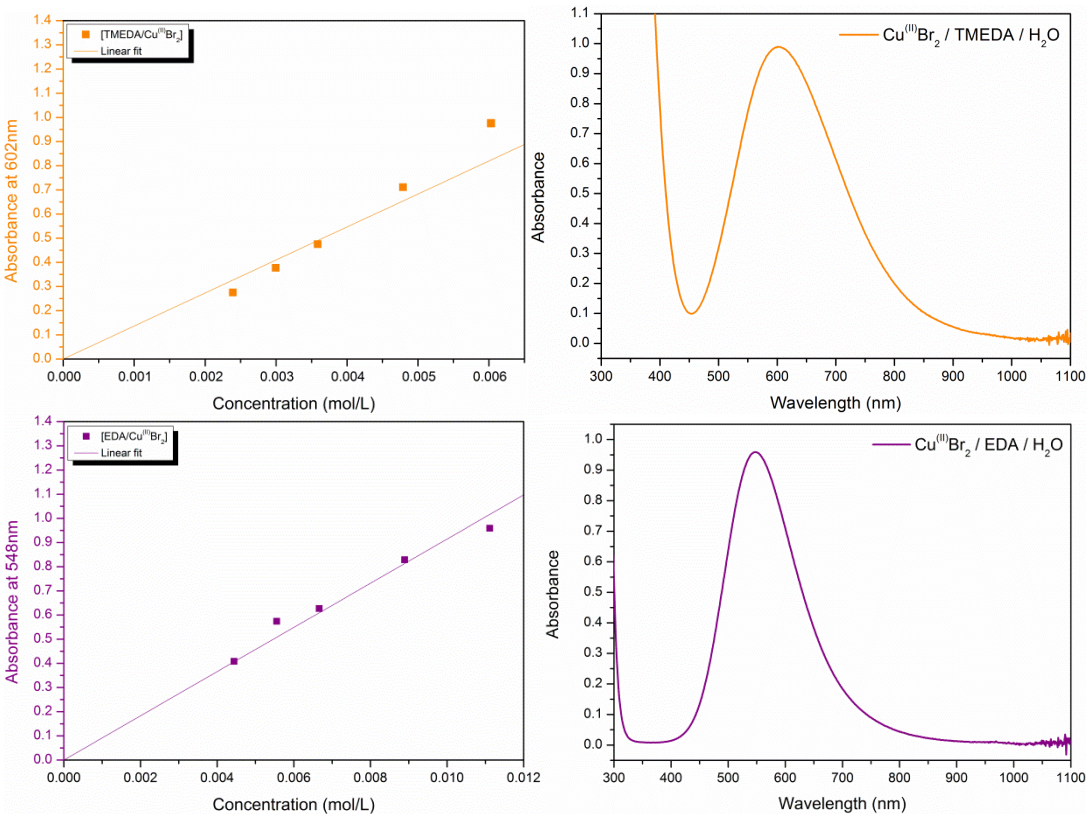

Figure 3.12 - The calibration plot that was used for calculating the ε of $Cu^{(II)}Br_2$/TMEDA (orange) and $Cu^{(II)}Br_2$/EDA (purple) at λ_{max} (left). The UV-Vis spectrum obtained from placing $Cu^{(II)}Br_2$/TMEDA (orange) and $Cu^{(II)}Br_2$/EDA (purple) in H_2O (right).

Control experiments were also performed to rule out the formation of the hexaqua complex ($[Cu^{(II)}/H_2O)_6]Br_2$.[92] Dissolving $Cu^{(II)}Br_2$ in water gave rise to a d-d transition with λ_{max} = 805 nm (Figure 3.13). Pleasingly, since the generated spectrum did not mimic any of those which were obtained from the $Cu^{(II)}Br_2$/ligand complexes, it was surmised that the hexaqua complex was not responsible for the absorbance bands.

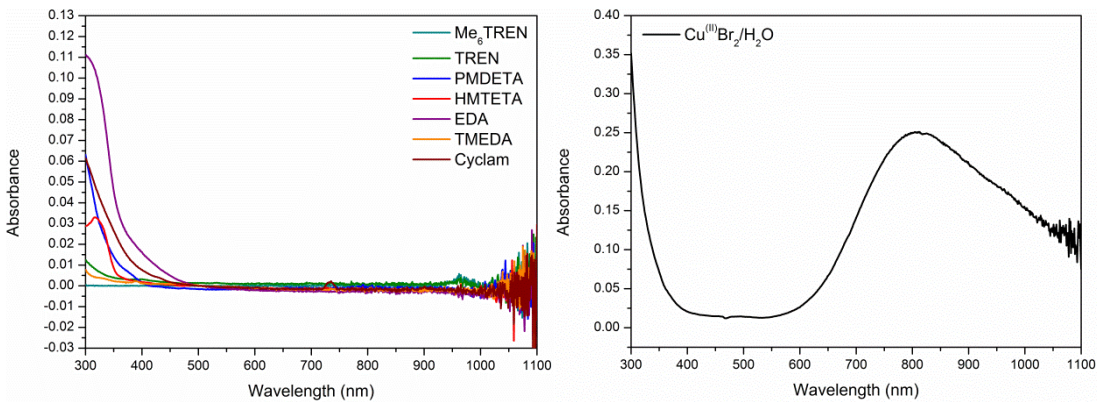

Figure 3.13 – The UV-Vis spectra resulting from adding each ligand to 3 mL H_2O (left). The UV-VIs spectrum resulting from adding $Cu^{(II)}Br_2$ to 3 mL H_2O (right).

In addition to this, no d-d transition was observed for the ligands in water. However, there were absorption bands which were recorded in the far UV region (Figure 3.13). This suggested that the recorded d-d transitions did not arise from the ligands themselves but rather, resulted from copper complexes with the ligands.

Direct comparison of the UV-Vis spectra for each $Cu^{(II)}Br_2$/ligand complex (Figure 3.14) enabled the rationalisation of the relative ligand field strengths. For the ligands employed within this work, the relative field strengths were found to increase in the order of Me_6TREN > TREN > PMDETA ~ HMTETA > TMEDA > EDA > Cyclam.

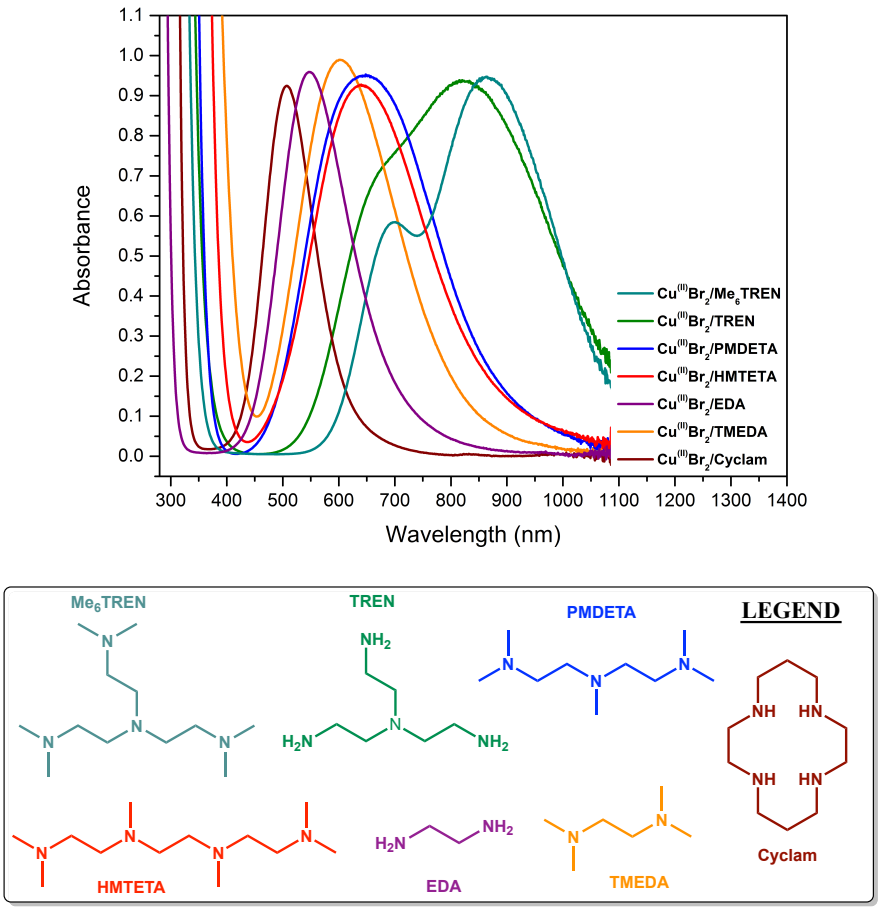

Figure 3.14 – A comparison of the UV-Vis spectra obtained for each of the $Cu^{(II)}Br_2$/ligand complexes.

Unfortunately, by combining the spectral data in Figure 3.14 with the observations made during the initial polymerisations (Table 3.3; Figure 3.9), it was concluded that characterisation by UV-Vis spectroscopy was not sufficient to enable the

polymerisation efficiency classification of the co-ordination complexes. In addition to this, it was found that λ_{max} could not be utilised in a predictive manner at this stage. However, given that the absorbance bands differed in widths, it was deemed possible that with further study, this feature may be utilised for the selection of appropriate ligands.

3.2.3. Investigating the extent of disproportionation via UV-Vis spectroscopy

The complete disproportionation of $Cu^{(I)}$ is considered to be crucial to the success of the aqueous $Cu^{(0)}$-mediated RDRP protocol. As such, it is important to select a ligand which does not preferentially stabilise the $Cu^{(I)}$ species.[96] The tendency of a ligand to stabilise $Cu^{(I)}$ relates in part to the geometry that the resulting complex adopts upon co-ordination.[62] For example, complexes with bidentate ligands prefer to be (distorted) tetrahedral; complexes with cyclic tetradentate ligands tend to be square planar; and "claw-like" tetradentate ligands tend to be (distorted) trigonal bipyramidal or (distorted) square pyramidal.[62] Out of these geometries, the stabilisation of $Cu^{(I)}$ decreases in the order of tetrahedral > trigonal bipyramidal ~ square pyramidal > square planar.[62] Relating this back to Section 3.1.1., it was expected that EDA and TMEDA would less readily undergo disproportionation compared to the other ligands; in particular, that of Cyclam.

It is possible to easily gauge the stability of a $Cu^{(I)}$ halide and its corresponding complex by monitoring the change in absorbance of $[Cu^{(II)}Br_2/L]$ and comparing it to known standards.[94,95] Unfortunately, this is not so easily achieved during the polymerisation process, as disruptions to the system (such as the introduction of oxygen or the removal of copper particles[97]) can affect molecular weight predictability and control.

As a means of overcoming this, separate disproportionation experiments, which only involved the addition of $Cu^{(I)}Br$ to ligand, were conducted in water. To provide a point of comparison, a calibration plot was generated for each of the complexes based on five pre-determined concentrations of $Cu^{(II)}Br_2$. In ascending order, these represented a theoretical disproportionation of 40 %, 50 %, 60 %, 80 % and 100 %.

The UV-Vis spectra were recorded for each of the copper/ligand complexes after 10 minutes. This time-period was chosen as it represented the level of disproportionation following deoxygenation of the $Cu^{(I)}Br$/ligand solution. For complexes that did not reach 100 % disproportionation within this time-frame, another spectrum was measured after 20 minutes to calculate the extent of disproportionation at the point when most polymerisations began.

The disproportionation of $Cu^{(I)}Br$ in the presence of Me_6TREN was found to be close to 100 % for the "standard" aqueous $Cu^{(0)}$-mediated RDRP protocol.[22] In a subsequent mechanistic study conducted by Haddleton Group, it was found that 99 % of [$Cu^{(I)}Br$/Me_6TREN] underwent disproportionation within 15 minutes.[95] Pleasingly, similar data was gathered during this work (Figure 3.15).

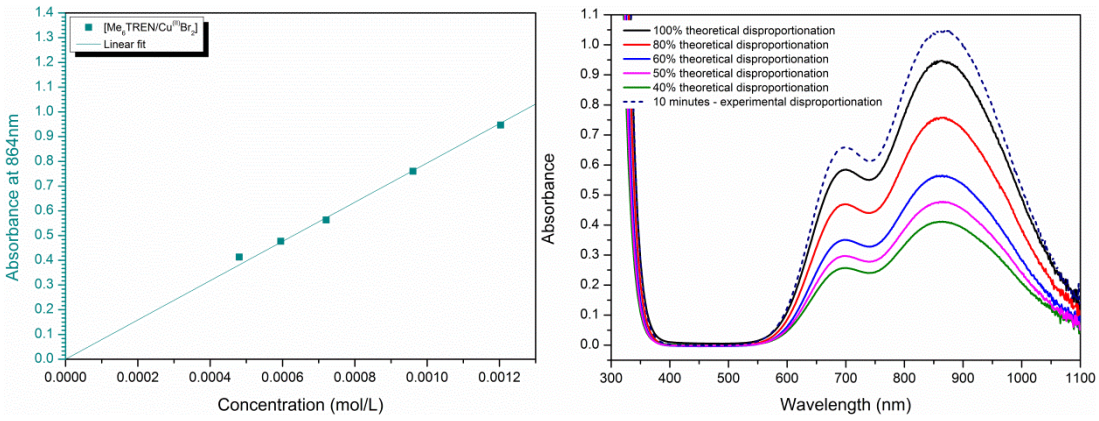

Figure 3.15 – A plot showing the absorbance at λ_{max} (864 nm) for each of the calibration samples with Me_6TREN (left) and the UV-Vis traces resulting from monitoring the disproportionation of $Cu^{(I)}Br$ in the presence of Me_6TREN (right). The solid lines —, —, —, —, —, represent the 40 %, 50 %, 60 %, 80% and 100% theoretical extent of disproportionation respectively and the dashed line (----) represents the extent of disproportionation after 10 minutes.

However, the absorbance of $Cu^{(II)}Br_2$ was recorded as being greater than the theoretical maximum (~110 %). To some extent this has previously been reported;[22] although no obvious reasoning was given for its occurrence, it is believed that this was due to the interaction of the solution with oxygen during sample preparation.

The presence of $Cu^{(0)}$ particles within the disproportionation solution (Section 3.2.5.) necessitated sample filtration prior to characterisation (Scheme 3.2). This was conducted in an effort to avoid light scattering and hence, inaccurate UV measurements.[98] It was therefore speculated that if any of the remaining $Cu^{(I)}$ species had been oxidised by air, it would have transpired during this process. Importantly, as the sample was analysed directly after filtration, the amount of $Cu^{(II)}Br_2$ resulting from undesirable oxidation was considered to be minimal.

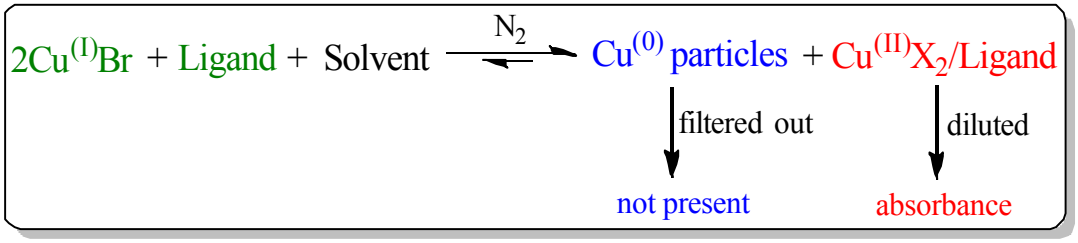

Scheme 3.2 - A generalised scheme for the UV-Vis studies.

It has been reported that TREN and PMDETA readily promote disproportionation in water.[22] Indeed, this certainly seemed to be the case visually as a colour change was noticed almost immediately upon the addition of $Cu^{(I)}Br$ (Section 3.2.5.). When the resulting solutions were analysed by UV-Vis spectroscopy, it was noted that in each instance, the evolution of $Cu^{(II)}$ was found to surpass the 100 % mark (Figure 3.16). As was the case with Me_6TREN, this was provisionally ascribed to the interaction of air with the sample.

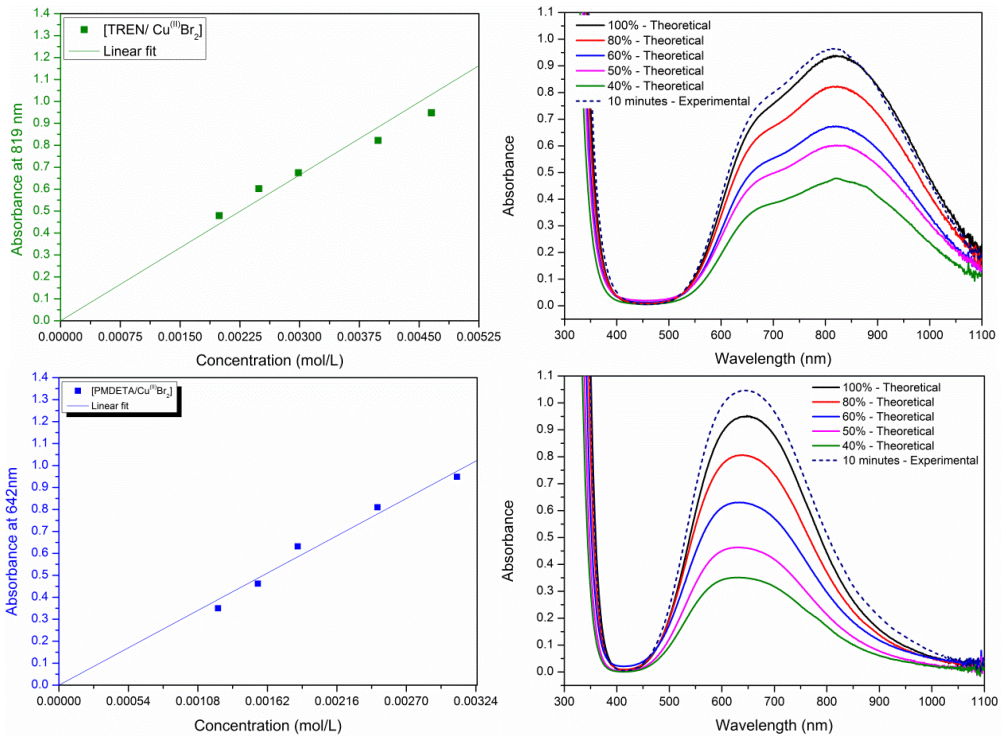

Figure 3.16 – A plot showing the absorbance at λ_{max} for each of the calibration samples with TREN (top left) and PMDETA (bottom left). The UV-Vis traces resulting from monitoring the disproportionation of $Cu^{(I)}Br$ in the presence of TREN (top right) and PMDETA (bottom right). The solid lines —, —, —, —, —, represent the 40 %, 50 %, 60 %, 80% and 100% theoretical disproportionation and the dashed line (----) represents disproportionation after 10 minutes.

Since Cyclam is believed to stabilise $Cu^{(I)}Br$ the least,[62] it was theorised that disproportionation performed in the presence of this ligand would rapidly reach completion. Indeed, after 10 minutes, it was found that complete disproportionation had arisen (as determined *via* UV-Vis spectroscopy; measured value = 110%) (Figure 3.17).

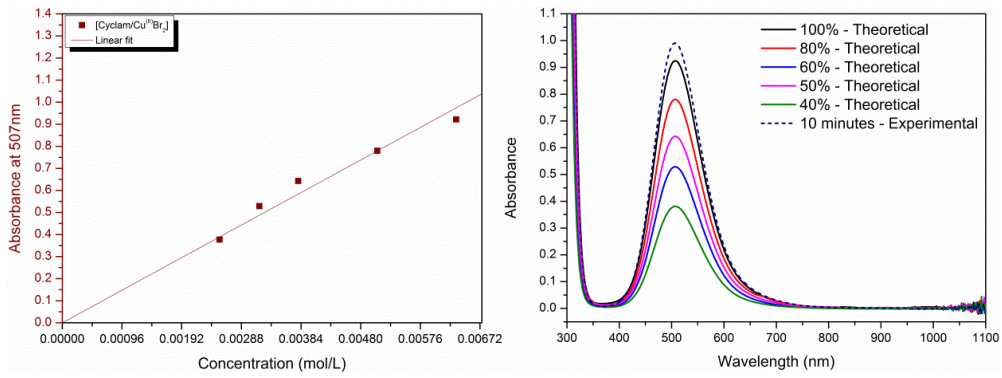

Figure 3.17 - A plot showing the absorbance at λ_{max} (507 nm) for each of the calibration samples with Cyclam (left). Also, the UV-Vis traces resulting from monitoring the disproportionation of $Cu^{(I)}Br$ in the presence of Cyclam (right). The solid lines —, —, —, —, —, represent the 40 %, 50 %, 60 %, 80% and 100% theoretical extent of disproportionation and the dashed line (- - -) represents the extent of disproportionation after 10 minutes.

As expected, TREN, PMDETA and Cyclam formed weakly stabilised co-ordination complexes with $Cu^{(I)}$ (as determined from the disproportionation studies). HMTETA was also predicted to form weakly stabilised complexes, however, disproportionation was not reached within the allotted time-frame (Figure 3.18). Instead, <50 % disproportionation was observed after 20 minutes.

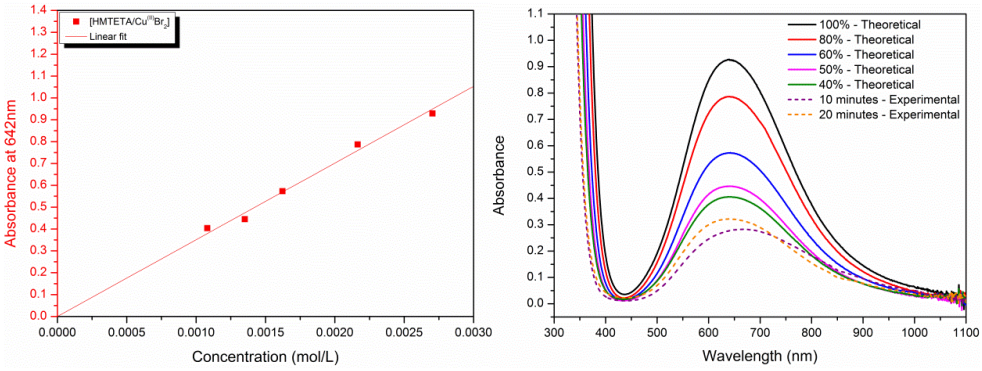

Figure 3.18 – A plot showing the absorbance at λ_{max} (642 nm) for each of the calibration samples with HMTETA (left). The UV-Vis traces resulting from monitoring the disproportionation of $Cu^{(I)}Br$ in the presence of HMTETA (right). The solid lines —, —, —, —, —, represent the 40 %, 50 %, 60 %, 80% and 100% theoretical extent of disproportionation and the dashed lines (- - -) (- - -) represent the extent of disproportionation after 10 and 20 minutes, respectively.

Unlike HMTETA, the results from combining $Cu^{(I)}Br$ with both EDA and TMEDA were as hypothesised. After 20 minutes "disproportionation time", very low levels of $Cu^{(II)}$ were observed, with EDA leading to ~ 75 % (Figure 3.19) and TMEDA ~ 5 % disproportionation (Figure 3.20) respectively.

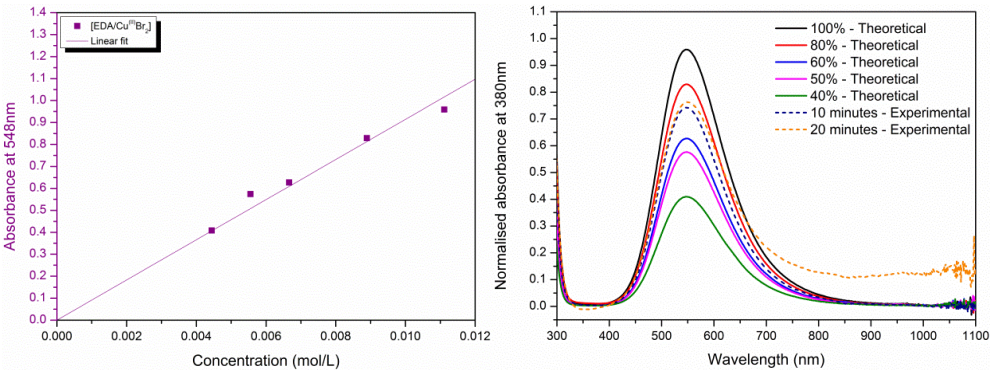

Figure 3.19 - A plot showing the absorbance at λ_{max} for each of the calibration samples with EDA (left). Also, the UV-Vis traces resulting from monitoring the disproportionation of $Cu^{(I)}Br$ in the presence of EDA (right). The solid lines —, —, —, —, —, represent the 40 %, 50 %, 60 %, 80% and 100% theoretical extent of disproportionation and the dashed lines (- - -) (- - -) represent the extent of disproportionation after 10 and 20 minutes, respectively.

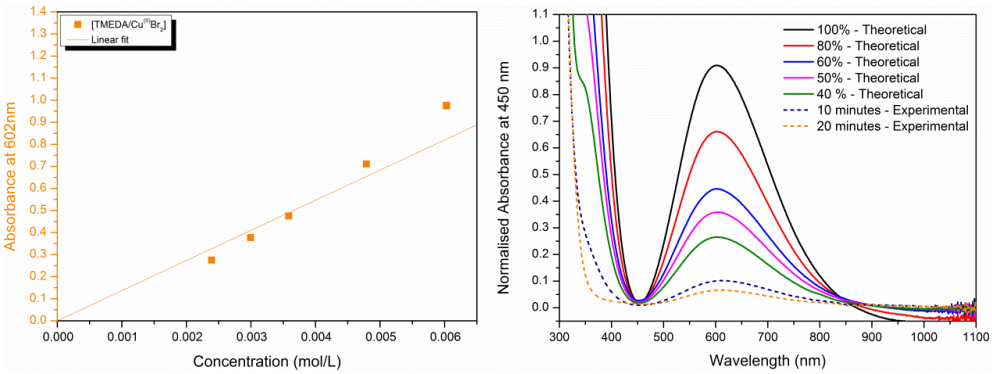

Figure 3.20 – A plot showing the absorbance at λ_{max} for each of the calibration samples with (left). Also, the UV-Vis traces resulting from monitoring the disproportionation of $Cu^{(I)}Br$ in the presence of TMEDA (right). The solid lines —, —, —, —, —, represent the 40 %, 50 %, 60 %, 80% and 100% theoretical extent of disproportionation and the dashed lines (- - -) (- - -) represent the extent of disproportionation after 10 and 20 minutes, respectively.

At the beginning of this section it was suggested that $Cu^{(I)}$ complexes with TREN, PMDETA, Cyclam and HMTETA would more readily undergo disproportionation than those with EDA or TMEDA. Indeed, this was found to be the case for most of the ligands. With respect to the multidentate ligands, TREN, PMDETA, and Cyclam all afforded 100% disproportionation within 10 minutes. However, when the disproportionation of $Cu^{(I)}Br$ was conducted in the presence of HMTETA, the evolution of $Cu^{(II)}Br_2$ was recorded as being incomplete after 20 minutes. Conversely, each of the bidentate ligands acted as expected, that is, they were found to be less efficacious at promoting the evolution of $Cu^{(II)}$ than the multidentate ligands. This was exhibited by the extent of disproportionation remaining incomplete after 20 minutes.

3.2.4. The effect of oxygen exposure on the extent of disproportionation

$Cu^{(I)}$ complexes with either Me_6TREN, TREN, PMDETA or Cyclam as the ligand, rapidly resulted in 100 % disproportionation. Given the ease at which $Cu^{(I)}$ species undergo oxidation into $Cu^{(II)}$, this phenomenon was provisionally ascribed to the introduction of oxygen into the UV-Vis sample.

Although the disproportionation step itself was conducted under an inert atmosphere (N_2), it is possible that the solution was exposed to oxygen upon preparing the sample. Unfortunately, due to the presence of copper particles, all solutions required filtering prior to analysis; this was subsequently achieved *via* the use of an air-tight glass syringe.

Importantly, care was taken to limit the amount of time between disproportionation, filtration and characterisation. Therefore, the extent to which oxygen influenced the level of disproportionation was considered to be minimal. If this assumption held true, then an absence of deoxygenation prior to filtration would result in a much higher level of disproportionation than that which was observed in Section 3.2.3.

To that end, $Cu^{(I)}Br$ was added to Me_6TREN under air and allowed to stir for 10 minutes. Following filtration and characterisation by UV-Vis spectroscopy, a much greater (~ 2.5 times) absorbance was recorded for the sample which did not involve deoxygenation procedures (Figure 3.21). As this was the only difference between the two setups, it is apparent that only a small amount of oxygen was introduced into the samples discussed in Section 3.2.3. (Note: since this test was intended to be a "proof of concept", this process was not repeated with the other ligands.)

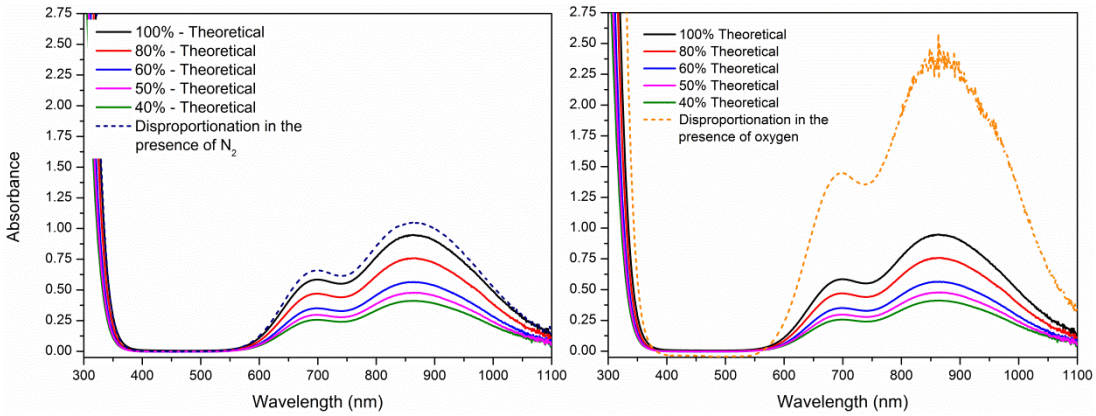

Figure 3.21 – UV-Vis traces showing the effect of oxygen upon disproportionation, where the solid lines —, —, —, —, —, represent the 40 %, 50 %, 60 %, 80% and 100% theoretical extent of disproportionation in the presence of N_2 and the dashed line ----- represents the extent of disproportionation in the presence of O_2 (right) and the dashed line ----- represents the extent of disproportionation in the presence of N_2 (left).

In addition to acting as a "proof of concept", this study highlighted the importance of deoxygenation upon these systems. Based on the differences in the extent of disproportionation, it was concluded that in the presence of N_2, not all of the $Cu^{(I)}$ species underwent oxidation. However, when there was a significant amount of oxygen within in the system, a greater proportion of $Cu^{(I)}$ was converted into $Cu^{(II)}$. Theoretically, this could have a detrimental effect upon the amount of polymerisation control. If 100 % of $Cu^{(I)}$ species were to be oxidised, this would prevent the regeneration of both the $Cu^{(I)}$ complex and the copper particles. Regardless of the mechanism for $Cu^{(0)}$-mediated RDRP, this would consequently prevent the re-activation of dormant chains.

It is perhaps worth noting that as well as affecting disproportionation, oxygen can efficiently bind to carbon centred radicals (*i.e.* those of the initiator or propagating species).[99] This essentially retards the polymerisation or, through the generation of peroxy- radicals, increases the occurrence of chain transfer. Therefore, whilst oxygen promotes disproportionation, it is detrimental to the polymerisation process as it leads to events which either hinder propagation or result in a loss of control.

3.2.5. Visually observing the behaviour of the ligand/$Cu^{(I)}$Br complexes in aqueous media

By observing the colour of $Cu^{(II)}Br_2$ complexes in solution, it is possible to not only conclude whether disproportionation has occurred, but to make a tentative evaluation upon its extent. To that end, 3 mL HPLC grade water was charged to a vial and bubbled with N_2 for 30 seconds. Following this, $Cu^{(I)}$Br was added under an inert atmosphere and the resulting solution was deoxygenated for 10 minutes. To visually assess the extent of disproportionation, observations were recorded at t = 0 minutes, t = 10 minutes, t = 20 minutes and t = 24 hours (Table 3.5).

For all ligands except HMTETA and TMEDA, deeply coloured solutions and dark precipitates were observed 10 minutes after their addition to $Cu^{(I)}Br$ and water (Table 3.5). Comparing these solutions to their respective $Cu^{(II)}$ controls (Figure 3.22; Table 3.6), enabled for the colouration to be ascribed to the formation of the $Cu^{(II)}Br_2$/L complex, and for the precipitate to be attributed to the formation of copper particles.[22,39,100] In addition to this, since the intensity of these colours closely mimicked that of the controls; it was deemed likely that a high extent of disproportionation had occurred within at least 20 minutes.

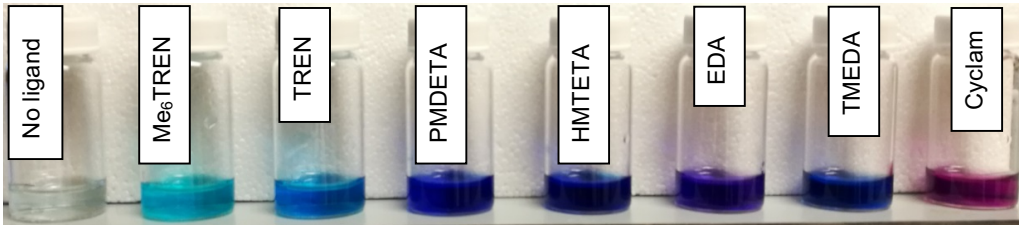

Figure 3.22 – A comparison of the colours produced by each $Cu^{(II)}Br_2$/L complex in 3 mL water.

In the case of HMTETA, the resulting solution was only pale after 20 minutes. When this was compared to the highly intense colour of its control sample, it was reasoned that disproportionation had not reached its fullest extent. However, after leaving the solution overnight, it was found that a deep blue solution had formed. This led to the tentative conclusion that it was perhaps possible to achieve 100 % disproportionation of a $Cu^{(I)}Br$/HMTETA complex within 24 hours. Interestingly, the same observation was also recorded for both TMEDA (the pale blue solution was masked by the high quantity of orange precipitate) and EDA (the pale purple solution was hidden by the dark brown precipitate).

Perhaps more importantly, it was concluded that the ligands most likely to have promoted full disproportionation within a polymerisation time-scale were Me_6TREN, TREN, PMDETA and Cyclam. Pleasingly, as this correlated with the results that were obtained by UV-Vis spectroscopy, it was deemed reasonable for visual observations to be utilised as a preliminary tool for assessing disproportionation.

Ligand	t = 0 minutes	t = 10 minutes	t = 20 minutes	t = 24 hours	Summary of Observations
No ligand ($Cu^{(I)}Br$ control)	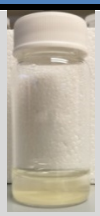	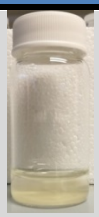	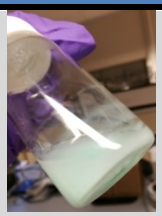	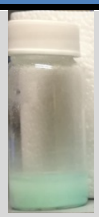	Insoluble white solid after 10 mins Insoluble green solid after 20 mins and 24h
Me_6TREN	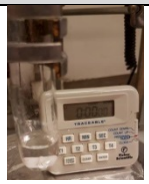				Cyan solution with dark brown particles after 10 and 20 mins No particles after 24h
TREN	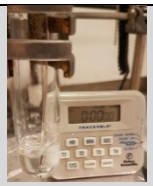		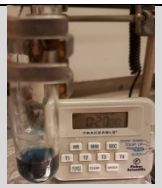		Deep cyan solution with dark brown particles after 10 and 20 mins No particles after 24h
PMDETA	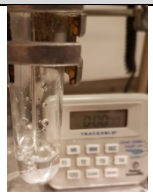				Deep blue solution with dark brown particles after 10 and 20 mins No particles after 24h
HMTETA	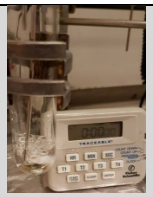				Pale blue solution with some orange particles after 10 and 20 mins Deep blue solution but no particles after 24h
EDA		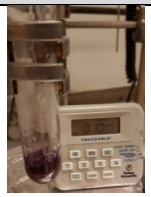			Purple solution with dark brown particles after 10 and 20 mins Deep purple solution with no particles after 24h
TMEDA					Very pale blue solution with many orange particles after 10 and 20 minutes Deep blue solution with no particles after 24h
Cyclam		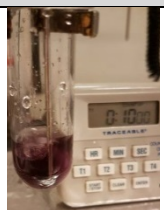		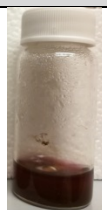	Deep red solution with dark brown particles after 10 and 20 mins Particles still visible after 24h

Table 3.5 - A summary of the visual observations resulting from combining $Cu^{(I)}Br$ with Me_6TREN, TREN, PMDETA, HMTETA, EDA, TMEDA and Cyclam in water.

Ligand	$Cu^{(II)}Br_2$	$Cu^{(II)}Br_2$ and $Cu^{(I)}Br$ t = 20 minutes	$Cu^{(II)}Br_2$ and $Cu^{(I)}Br$ t = 24 hours	Summary of Comparison
No ligand (control)		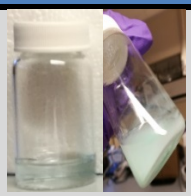		No formation of $Cu^{(II)}Br_2$ Disproportionation did not occur under these conditions
Me_6TREN				Similarly coloured solution to $Cu^{(II)}$ control Likely a high amount of disproportionation occurred after 20 minutes
TREN			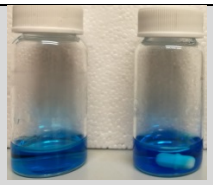	Similarly coloured solution to $Cu^{(II)}$ control Likely a high amount of disproportionation occurred after 20 minutes
PMDETA			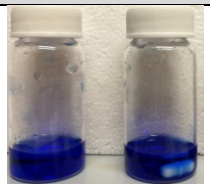	Similarly coloured solution to $Cu^{(II)}$ control Likely a high amount of disproportionation occurred after 20 minutes
HMTETA			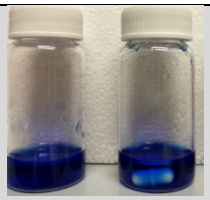	Pale solution after 20 minutes. Likely a low extent of disproportionation Similarly coloured solution after 24 hours. Likely a high extent of disproportionation
EDA			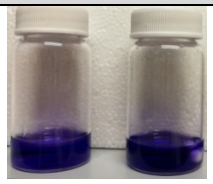	Similarly coloured solution to $Cu^{(II)}$ control Likely a high amount of disproportionation occurred after 20 minutes
TMEDA	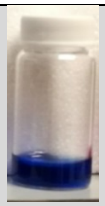		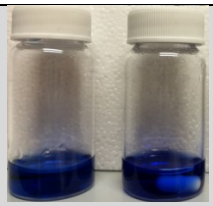	Pale solution after 20 minutes. Likely a low extent of disproportionation Similarly coloured solution after 24 hours. Likely a high extent of disproportionation
Cyclam			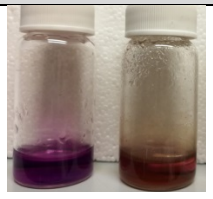	Similarly coloured solution to $Cu^{(II)}$ control Likely a high amount of disproportionation occurred after 20 minutes

Table 3.6 – A comparison of the observations from combining $Cu^{(II)}Br_2$ (left images) and $Cu^{(I)}Br$ (right images) with Me_6TREN, TREN, PMDETA, HMTETA, EDA, TMEDA and Cyclam in water.

3.2.6. Further investigation into the disproportionation of HMTETA, EDA and TMEDA

It has been shown that complexes which involve HMTETA, EDA and TMEDA are incapable of reaching 100 % disproportionation within the usual aqueous $Cu^{(0)}$-mediated RDRP time-frame (10 – 20 minutes).[22,101] In Section 3.2.5., it was theorised that it was possible to achieve near-complete disproportionation after overnight stirring of the solution. Accordingly, as there appeared to be a close relationship between the visual observations and the UV-Vis data, it was hypothesised that higher absorbances would be observed if scans were taken overnight.

For this reason, the disproportionation of $Cu^{(I)}Br$ in the presence of HMTETA, EDA and TMEDA was monitored *via* UV-Vis spectroscopy overnight. To identify the time at which disproportionation reached its fullest extent, kinetic studies were conducted whereby scans were taken every 10 minutes for the first 60 minutes, and then every 30 minutes in the time that followed. It should be noted that as with the previous disproportionation experiments, samples were filtered through PTFE membranes prior to analysis in order to minimise light scattering.

The UV-Vis traces (Figure 3.23) showed that the disproportionation of [$Cu^{(I)}Br$/HMTETA] increased with time. Notably, after 2 hours, the absorbance of [$Cu^{(II)}Br_2$/HMTETA] was recorded as being greater than the theoretical maximum. As was the case with some of the earlier experiments, the excess oxidation was ascribed to the interaction of air with the sample (Section 3.2.4.).

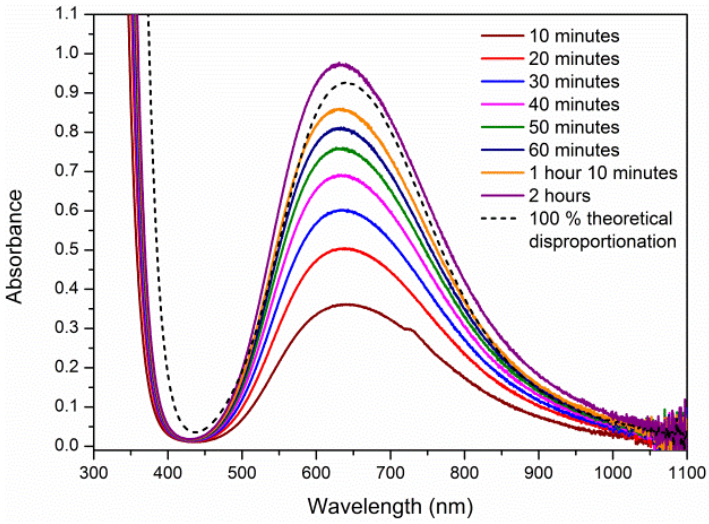

Figure 3.23 – The UV-Vis traces resulting from the kinetic monitoring of the disproportionation of $Cu^{(I)}Br$ in the presence of HMTETA (—) compared to the 100 % theoretical disproportionation from the calibration of [$Cu^{(II)}Br_2$/HMTETA] (- - -). The sample for this set of data was filtered.

However, when the evolution of [$Cu^{(II)}Br_2$/TMEDA] was kinetically monitored by UV-Vis spectroscopy, the results disagreed with the visual observations. Rather than achieving complete disproportionation overnight, it was found that only 15 % of the $Cu^{(I)}$ complex had been converted into $Cu^{(II)}$ (Figure 3.24).

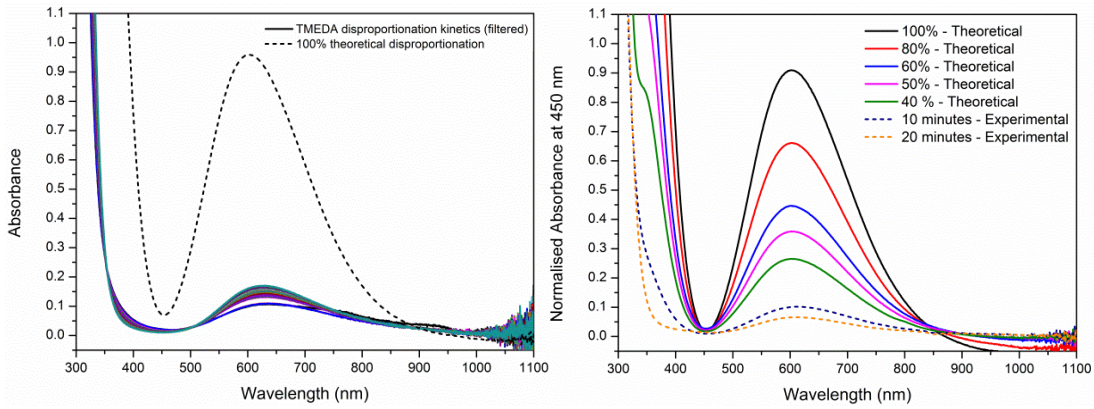

Figure 3.24 – The UV-Vis traces resulting from the kinetic monitoring of the disproportionation of $Cu^{(I)}Br$ in the presence of TMEDA (—) compared to the 100 % theoretical disproportionation from the calibration of [$Cu^{(II)}Br_2$/TMEDA] (- - -) (left). The UV-Vis traces resulting from the disproportionation of $Cu^{(I)}Br$ in the presence of TMEDA after 10 and 20 minutes (- - -) compared to the calibration of [$Cu^{(II)}Br_2$/TMEDA] (—) (right). Samples for this set of data were filtered.

It is worthwhile mentioning that the UV-Vis absorbance for [$Cu^{(II)}Br_2$/TMEDA] after 20 minutes was similar to that which was observed during the first

disproportionation experiment (where the level of disproportionation in this instance was ~ 5 % (Figure 3.20)).

Although there was a gradual increase in the absorbance of [$Cu^{(II)}Br_2$/EDA] from the disproportionation of $Cu^{(I)}Br$ and EDA, only 55 % rather than the earlier 75 % disproportionation was achieved within 20 minutes (Figure 3.25). As a result, it was deemed to be unlikely that any of the observed $Cu^{(II)}$ absorbance arose from the interaction of $Cu^{(I)}Br$ with air.

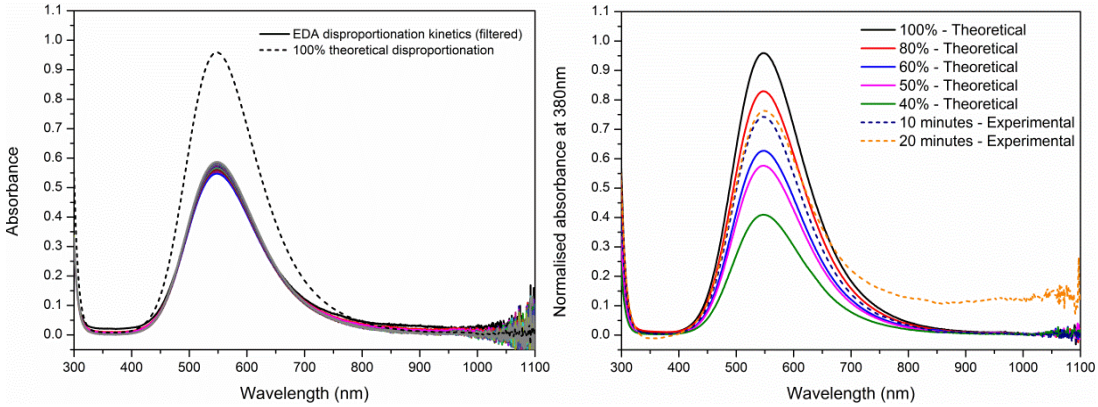

Figure 3.25 - The UV-Vis traces resulting from the kinetic monitoring of the disproportionation of $Cu^{(I)}Br$ in the presence of EDA (—) compared to the 100 % theoretical disproportionation from the calibration of [$Cu^{(II)}Br_2$/EDA] (- - -) (left). The UV-Vis traces resulting from the disproportionation of $Cu^{(I)}Br$ in the presence of EDA after 10 and 20 minutes (- - -) compared to the calibration of [$Cu^{(II)}Br_2$/EDA] (—) (right). Samples for this set of data were filtered.

To investigate whether sample filtration was the cause of the observed discrepancies, the disproportionation experiments of [$Cu^{(II)}Br_2$/HMTETA], [$Cu^{(II)}Br_2$/EDA] and [$Cu^{(II)}Br_2$/TMEDA] were repeated, and UV-Vis spectra were collected without passing the sample through a PTFE membrane.

In Section 3.2.5., it was found that that only a few particles were formed during the disproportionation of $Cu^{(I)}Br$ in the presence of HMTETA. Therefore, it was expected that there would be minimal scattering and little problem with obtaining UV-Vis data. Indeed, when the solutions were characterised by UV-Vis spectroscopy, there was only a slight broadening of the traces when compared to those from the calibration plot (Figure 3.26). Moreover, the complete formation of [$Cu^{(II)}Br_2$/HMTETA] was

observed to occur on a similar time-scale to that of the previous experiment (~ 2 hours). As a result, it was concluded that HMTETA was capable of efficiently facilitating the disproportionation of $Cu^{(I)}Br$.

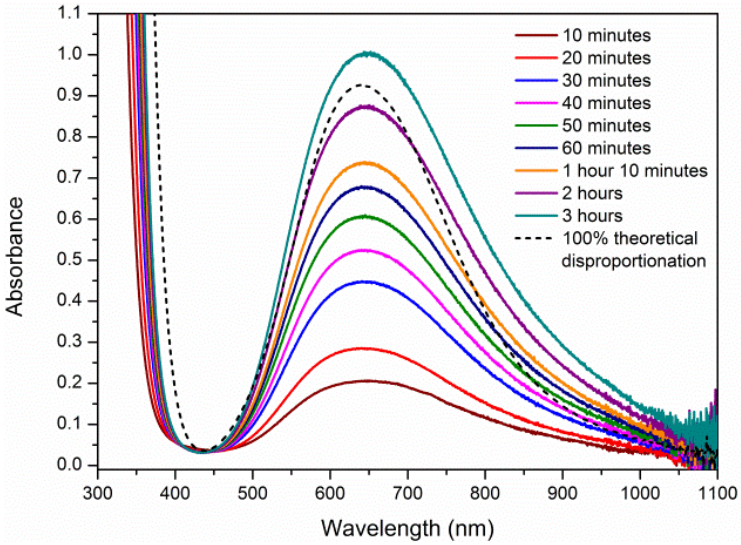

Figure 3.26 – The UV-Vis traces resulting from the kinetic monitoring of the disproportionation of $Cu^{(I)}Br$ in the presence of HMTETA (——) compared to the 100 % theoretical disproportionation from the calibration of [$Cu^{(II)}Br_2$/HMTETA] (- - -). The sample for this set of data was not filtered.

Furthermore, due to the close agreement between $Cu^{(II)}$ absorbances (Figure 3.27), it was determined that the findings for the filtered sample were a relatively accurate representation of the ability of HMTETA to promote this phenomenon.

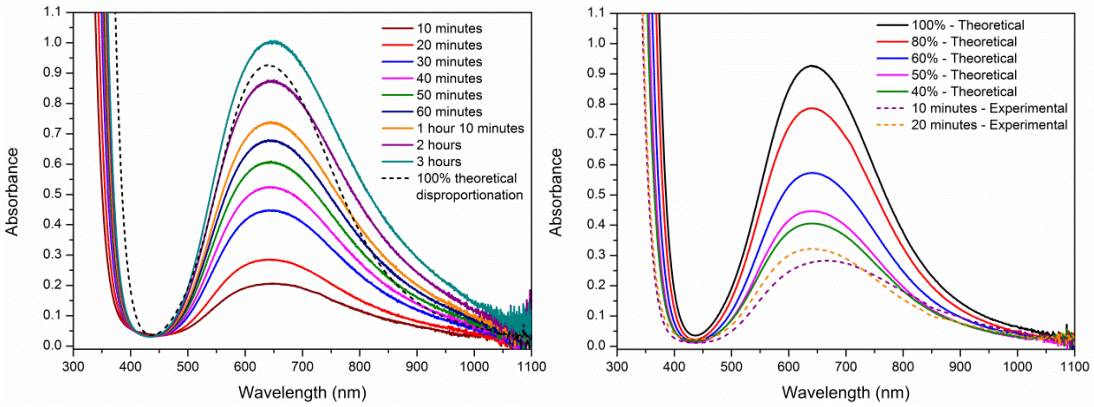

Figure 3.27 - The UV-Vis traces resulting from the kinetic monitoring of the disproportionation of $Cu^{(I)}Br$ in the presence of HMTETA (——) compared to the 100 % theoretical disproportionation from the calibration of [$Cu^{(II)}Br_2$/HMTETA] (- - -). Samples for this set of data were not filtered (left) The UV-Vis traces resulting from the disproportionation of $Cu^{(I)}Br$ in the presence of HMTETA after 10 and 20 minutes (- - -) compared to the calibration of [$Cu^{(II)}Br_2$/HMTETA] (——). Samples for this set of data were filtered (right).

For EDA and TMEDA, the effect of scattering was much more prevalent due to the higher quantity of copper particles (Figure 3.28 - Figure 3.29). With regards to EDA (Figure 3.28), the baseline readings exhibited a fairly high absorbance (the highest absorbance is represented by the black line and corresponds to the first scan that was taken during the kinetic monitoring). As this was when the particles were in their most agitated state, the absorbance was accredited to a high degree of light scattering. This conclusion was further supported by a decrease in the absorbance with time as the particles settled. Alongside this, normalising the spectra inferred that greater than 100 % disproportionation had arisen overnight (Figure 3.28). However, given that light scattering leads to an increase in UV absorbance, it was decided that little weight would be placed on this data.

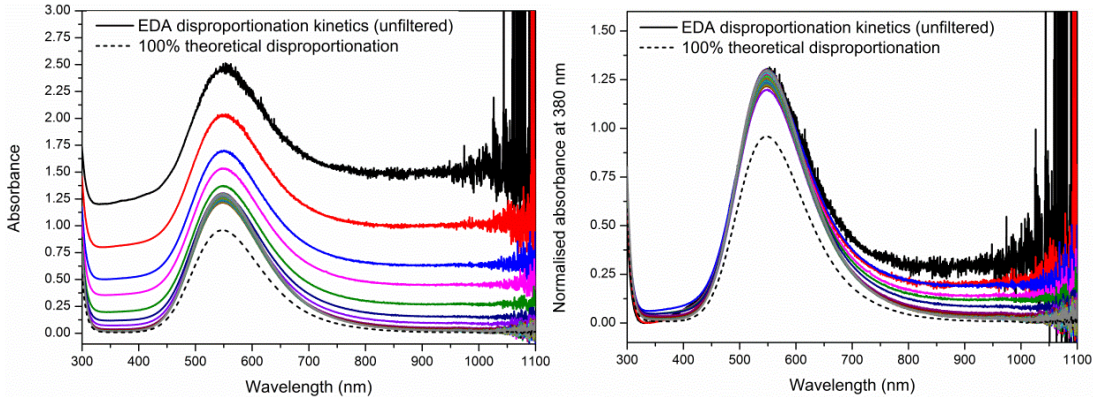

Figure 3.28 – The UV-Vis traces resulting from the kinetic monitoring of the disproportionation of $Cu^{(I)}Br$ in the presence of EDA (—) compared to the 100 % theoretical disproportionation from the calibration of [$Cu^{(II)}Br_2$/EDA] (- - -) (left). The offset UV-Vis traces resulting from the kinetic monitoring of the disproportionation of $Cu^{(I)}Br$ in the presence of EDA (—) compared to the 100 % theoretical disproportionation from the calibration of [$Cu^{(II)}Br_2$/EDA] (- - -) (left). Samples for this set of data were not filtered.

In contrast to this, upon offsetting the UV-Vis spectra produced by the disproportionation of [$Cu^{(I)}$Br/TMEDA], there was only a slight change in the intensity of the absorbance from that which was previously documented (Figure 3.29). This implied that the effect of filtration upon the disproportionation of this complex was minimal.

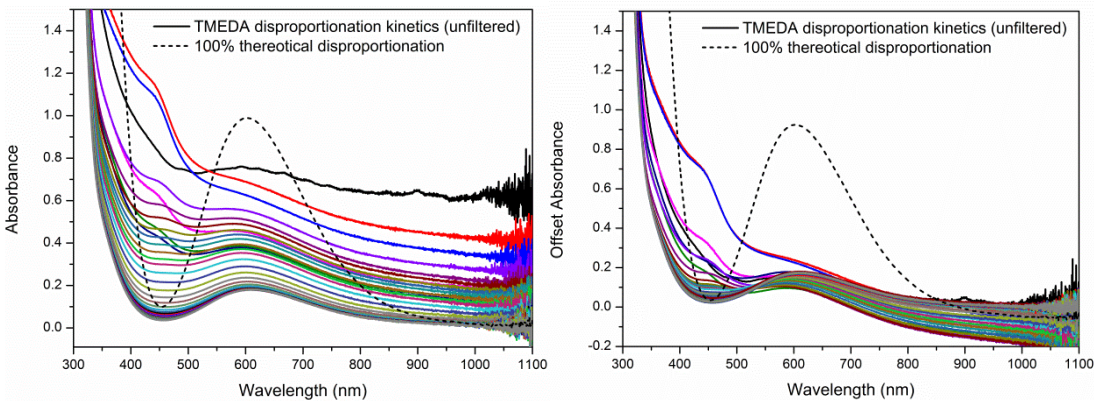

Figure 3.29 - The UV-Vis traces resulting from the kinetic monitoring of the disproportionation of $Cu^{(I)}Br$ in the presence of TMEDA (—) compared to the 100 % theoretical disproportionation from the calibration of [$Cu^{(II)}Br_2$/TMEDA] (- - -) (left). The offset UV-Vis traces resulting from the kinetic monitoring of the disproportionation of $Cu^{(I)}Br$ in the presence of TMEDA (—) compared to the 100 % theoretical disproportionation from the calibration of [$Cu^{(II)}Br_2$/TMEDA] (- - -) (left). Samples for this set of data were not filtered.

Filtering of samples is a necessary requirement for the UV-Vis characterisation of disproportionated solutions. In the case of EDA and TMEDA, the presence of particles resulted in scattering and hence, led to the collection of inaccurate UV data. Therefore, to draw final conclusions relating to their disproportionation, the spectra for the filtered samples were used.

From this data it was surmised that EDA and TMEDA were not suitable ligands for the aqueous $Cu^{(0)}$-mediated RDRP protocol as it was not possible to achieve 100 % disproportionation. As such, it is clear why the polymerisation of NIPAm in the presence of these ligands was not controlled (Section 3.2.1.1).

Conversely, as HMTETA was able to promote the complete evolution of $Cu^{(II)}Br_2$ within 3 hours, further investigation into its use as the ligand for the polymerisation of NIPAm was warranted. When it was previously used as the ligand for the polymerisation of NIPAm, the disproportionation step was only conducted for 20 minutes. However, at this time-point, the UV-Vis data suggests that only 25 - 30 % disproportionation had been achieved. The subsequent lack of deactivating species, and the presence of $Cu^{(I)}$ complexes with a very high k_{act} at the start of the polymerisation, might explain why the resulting MWD was very broad.

3.2.7. Polymerisation of NIPAm with HMTETA after 3 hours of disproportionation

To probe whether it was possible to improve the polymerisation of NIPAm in the presence of HMTETA, [$Cu^{(I)}$Br/HMTETA] was allowed to disproportionate for 3 hours prior to the addition of monomer and initiator. Unlike the initial reaction conducted with this ligand (Section 3.2.1.1.), characterisation by ^{1}H NMR spectroscopy revealed that high monomer conversion had been attained within 30 minutes (Figure 3.30).

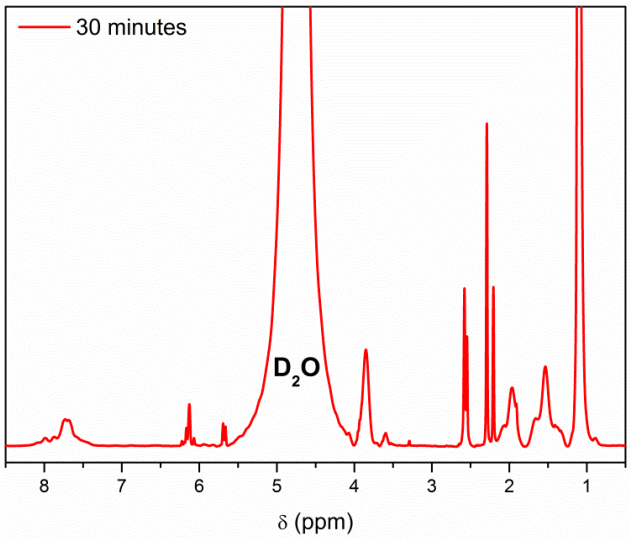

Figure 3.30 - The ^{1}H NMR spectrum obtained for the polymerisation of NIPAm in the presence of HMTETA following 3 hours' disproportionation. Conditions: [M] : [I] : [L] : [$Cu^{(I)}$X] = [20] : [1.0] : [0.4] : [0.4].

Nevertheless, when the reaction mixture was analysed by SEC, it was found that the polymerisation process lacked control ($Đ_m$ = 3.74) (Figure 3.31). Interestingly, the SEC results were worse than those which were obtained in Section 3.2.1.1. In addition to a broader MWD, a loss of symmetry and a small amount of tailing was visible in the low molecular weight region (Figure 3.31). Further to this, a shift in the average molecular weight was recorded, and a greater disagreement between the experimental (5500 g mol^{-1}) and theoretical (2300 g mol^{-1}) molecular weight was observed (Table 3.7).

Length of disproportionation (minutes)	Conversion (%)	$M_{n,th}$ (g mol^{-1})	$M_{n,SEC}$ (g mol^{-1})	$Đ_m$
20	81	2000	3400	3.53
180	92	2300	5500	3.74

Table 3.7 – A comparison of the results obtained for the polymerisation of NIPAm in the presence of HMTETA. Conditions: [M] : [I] : [L] : [$Cu^{(I)}$X] = [20] : [1.0] : [0.4] : [0.4].

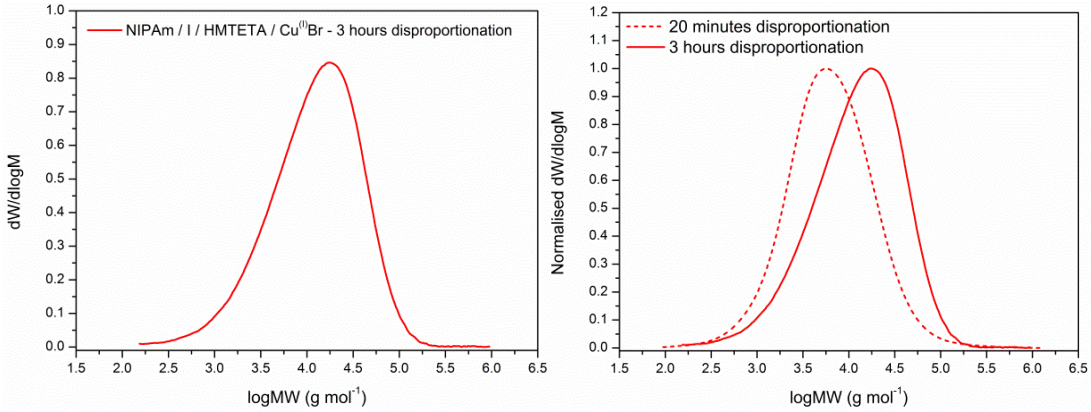

Figure 3.31 – The SEC trace obtained for the polymerisation of NIPAm in the presence of HMTETA following 3 hours disproportionation (left). A comparison of the SEC traces obtained for the polymerisation of NIPAm in the presence of HMTETA after 20 minutes disproportionation (- - -) and 3 hours disproportionation (——). Conditions: [M] : [I] : [L] : [$Cu^{(I)}$X] = [20] : [1.0] : [0.4] : [0.4] (right).

Following the initial synthesis of PNIPAm with HMTETA, it was hypothesised that the lack of polymerisation control was caused by inefficient deactivation of the propagating species (Section 3.2.1.1.). However, given that the extent of disproportionation was found to be incomplete for this polymerisation, it was more likely that an insufficient concentration of [$Cu^{(II)}Br_2$/HMTETA] resulted in the free radical addition of monomeric species to the active radicals.

Due to the nature of disproportionation, it was reasoned that a greater concentration of deactivating species was present in the catalyst solution after 3 hours. Irrespective of this, there was no improvement in polymerisation control following the extended disproportionation period. Thus, it seemed unlikely that a low concentration of [$Cu^{(II)}Br_2$/HMTETA] was responsible for the broad MWD observed in Figure 3.31. Rather, it is more plausible that the high dispersity value resulted from the dissociation of the $Cu^{(II)}$-Br bonds, as a consequence of prolonged

exposure of the copper/ligand complexes to water during the disproportionation stage.[22,48]

Nevertheless, as polymerisations involving HMTETA required 3 hours to reach full disproportionation, and as there were no signs of improvement upon polymerisation control, it was decided that HMTETA would not be studied further in this work.

3.2.8. Selection of appropriate ligands for further investigation

Based on the results that were gathered within the previous sections, HMTETA, EDA and TMEDA were deemed to be inadequate substitutes for Me_6TREN. In addition to this, despite promoting full disproportionation, the initial polymerisations with the remainder of the ligands (TREN, PMDETA and Cyclam) were found to be uncontrolled (Section 3.2.1.1.). In the case of Cyclam, it was originally theorised that inefficient deactivation and radical-radical coupling were the cause of the broad MWD ($Đ_m$ = 8.50) and large molecular weights (54,400 g mol^{-1}). Since the observation of complete disproportionation implied that enough of the deactivating species was produced prior to the start of the polymerisation, this claim was supported. Perhaps more importantly, the magnitude of the molecular weight disagreement suggested that a large proportion of monomer addition had occurred *via* a free radical process. It was therefore speculated that optimising reaction conditions would not aid its ability to provide polymerisation control.

Conducting the polymerisation of NIPAm in the presence of PMDETA, however, gave rise to the targeted molecular weight (2300 g mol^{-1}) and a dispersity value that was comparatively low ($Đ_m$ = 1.54). Due to the Poisson-like distribution and the lack of any tailing or molecular weight discrepancy, it was subsequently decided that the use of PMDETA based complexes required further investigation.

3.2.8.1. Optimising the polymerisation of NIPAm in the presence of PMDETA

The role of the deactivating species in copper-mediated RDRP techniques is crucial; it acts to minimise the occurrence of termination events by shifting the polymerisation equilibrium towards the dormant species.[21,68] To achieve low dispersity values, not only must the deactivator be efficient, but it must be present in a sufficient quantity. Given that PMDETA complexes have previously showed promise as capable deactivators, attempts were made to optimise the reaction conditions.

Working on the assumption that an increase in $Cu^{(I)}Br$ would provide a higher concentration of deactivating species, the polymerisation conditions were initially modified to [M] : [I] : [PMDETA] : [$Cu^{(I)}Br$] = [20] : [1] : [0.4] : [0.8]. Whilst the resulting MWD was narrower ($Đ_m$ = 1.38; Figure 3.32), the polymerisation process was found to be slow and incomplete (t = 24 hours; 79 % conversion).

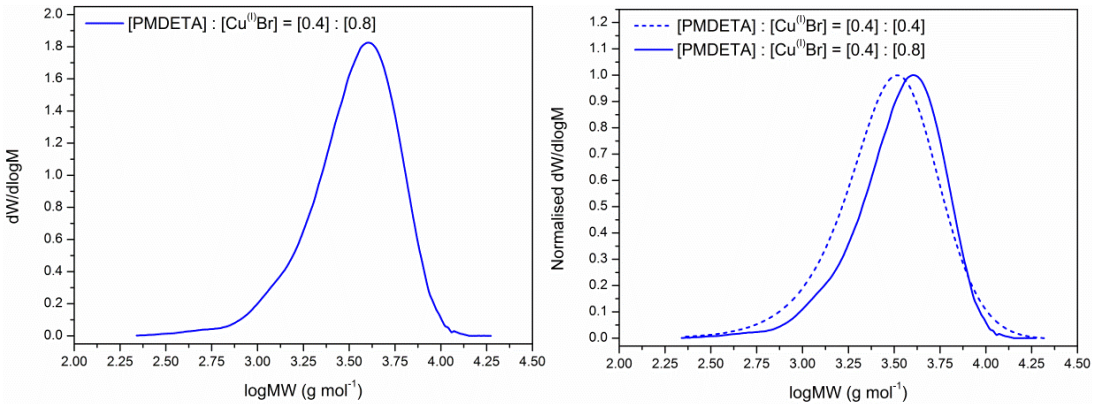

Figure 3.32 – The MWD resulting from the aqueous $Cu^{(0)}$-mediated RDRP of NIPAm in the presence of PMDETA. Conditions: [M] : [I] : [L] : [$Cu^{(I)}X$] = [20] : [1.0] : [0.4] : [0.8]. $Đ_m$ = 1.38 and M_n = 2800 g mol^{-1} (left); Comparison of the MWDs resulting from the polymerisation of NIPAm in the presence of PMDETA (right).

In an attempt to increase the rate of polymerisation whilst retaining the improved control, the concentration of ligand was subsequently increased (conditions: [M] : [I] : [PMDETA] : [$Cu^{(I)}Br$] = [20] : [1] : [0.6] : [0.8]). Upon doing so, quantitative conversion was achieved within 1 hour. Notably, there was no significant increase in

chain termination ($Đ_m$ = 1.40; $M_{n,theoretical}$ = 2500 g mol^{-1}; $M_{n,experimental}$ = 2700 g mol^{-1}; Figure 3.33) when the SEC data was compared to that of [M] : [I] : [PMDETA] : [$Cu^{(I)}Br$] = [20] : [1] : [0.4] : [0.8] (Figure 3.33).

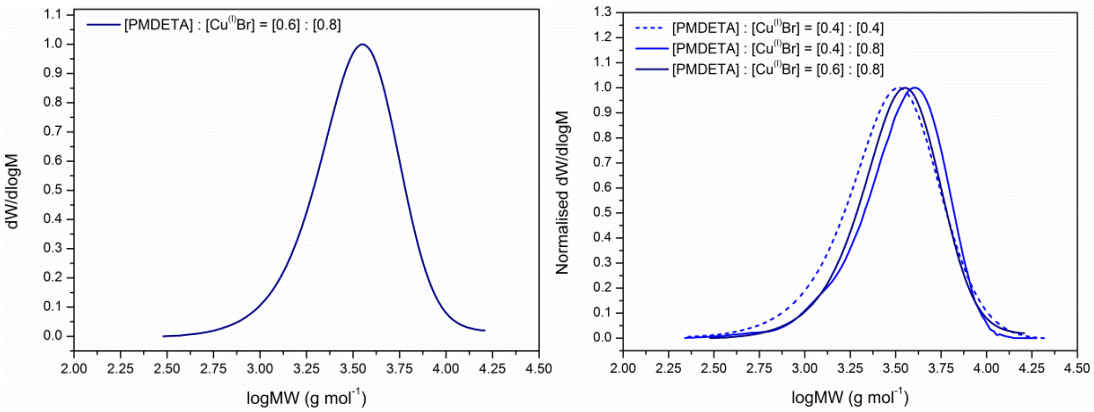

Figure 3.33 - The MWD resulting from the aqueous $Cu^{(0)}$-mediated RDRP of NIPAm in the presence of PMDETA. Conditions: [M] : [I] : [L] : [$Cu^{(I)}X$] = [20] : [1.0] : [0.6] : [0.8]. $Đ_m$ = 1.40 and M_n = 2700 g mol^{-1} (left); Comparison of the MWDs resulting from the polymerisation of NIPAm in the presence of PMDETA (right).

Fine-tuning both the $Cu^{(I)}Br$ and ligand concentrations can have a positive impact upon the polymerisation process. Yet, despite the enhanced control, the final dispersity value was still considered to be high. Fortunately, previous literature studies suggested that the addition of external halide salts could narrow the MWD.[101–103] The polymerisation of NIPAm was therefore repeated under the optimised conditions except this time with the addition of 1.0 M NaBr during the disproportionation stage.

Haddleton *et al.* reported that, for the polymerisation of methacrylates in the presence of halide salts, complete monomer conversion could be attained within a normal polymerisation time-frame (< 1 hour). However, this finding was noted as being contrary to previous studies.[103,104] Unfortunately, the same could not be said for the polymerisation of NIPAm in this work. Following sampling of the reaction after 1 hour, it was observed that only 77 % conversion had arisen (Figure 3.34) with no further monomer conversion being observed after 2 hours (79 % conversion;

Figure 3.34). The slow rate of polymerisation was further highlighted by near-complete conversion being attained after 18 hours (Figure 3.34).

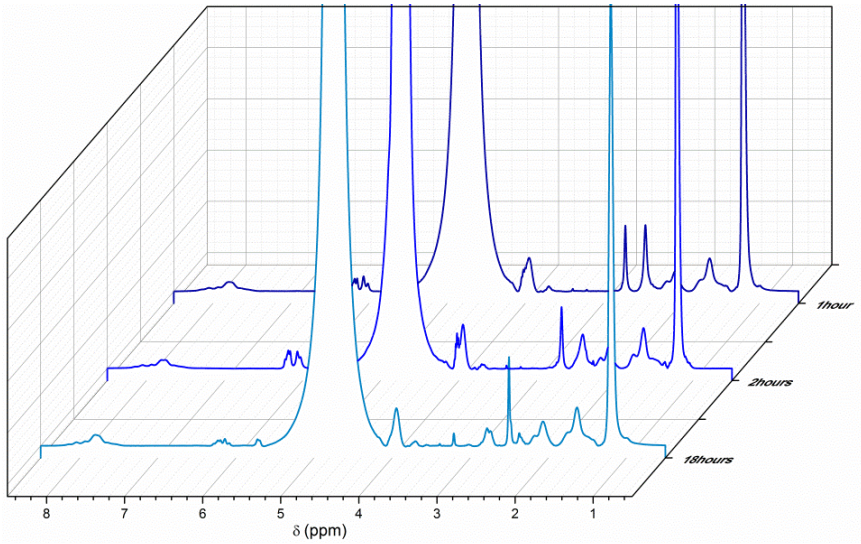

Figure 3.34 - The ^{1}H NMR spectra resulting from the aqueous $Cu^{(0)}$-mediated RDRP of NIPAm in the presence of PMDETA and external halide salts. Conditions: [M] : [I] : [L] : [$Cu^{(I)}$X] = [20] : [1.0] : [0.6] : [0.8] and 1.0 M NaBr. Where ── represents 1 hour, ── represents 2 hours, and ── represents 18 hours.

In spite of the slower rate of polymerisation, a greater degree of control was revealed upon characterisation by SEC ($Đ_m$ = 1.29; Figure 3.35). Given the mostly symmetrical nature of the trace it was concluded that under these conditions, the polymerisation of NIPAm had been adequately mediated.

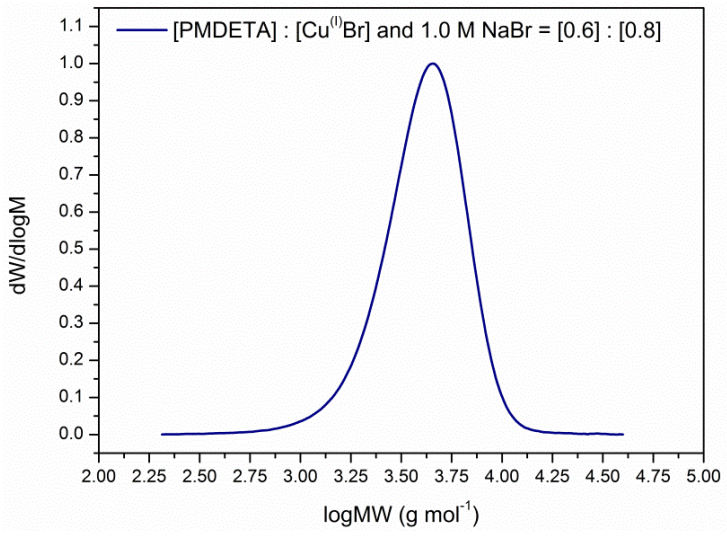

Figure 3.35 - The MWD resulting from the aqueous $Cu^{(0)}$-mediated RDRP of NIPAm in the presence of PMDETA and external halide salts. Conditions: [M] : [I] : [L] : [$Cu^{(I)}$X] = [20] : [1.0] : [0.6] : [0.8] and 1.0 M NaBr. $Đ_m$ = 1.29 and M_n = 2700 g mol^{-1}.

Although the polymerisation did not proceed with the same level of control as the current standard, dispersity values which are commonly associated with a controlled polymerisation were achieved. Depending upon the intended use, synthesising polymers with a lower dispersity may not be of the utmost importance. Given the absence of extensive organic synthesis and the inexpensive cost, it was reasoned that someone aiming to polymerise NIPAm (or perhaps other acrylamides) in an "off the shelf" manner should consider utilising the aqueous $Cu^{(0)}$-mediated RDRP methodology with PMDETA as the ligand.

3.2.8.2. Probing the polymerisation of NIPAm in the presence of TREN

To complete the study, the use of TREN as the ligand for the polymerisation of NIPAm was revisited. Although TREN produced similarly high dispersity values to that of Cyclam, it was postulated that this was due to sub-optimal reaction conditions. As part of the development of the aqueous $Cu^{(0)}$-mediated protocol, Haddleton *et al.* investigated the use of TREN as the ligand for the polymerisation of DP = 80 NIPAm.[22] Under conditions of [M] : [I] : [PMDETA] : [$Cu^{(I)}$Br] = [80] : [1] : [0.4] : [0.8], it was found that a near-quantitative conversion (99 %) and a mono-modal distribution ($Đ_m$ = 1.56) had been attained within 1 hour. Given that this was a significant improvement over the bimodal distribution described in Section 3.2.1, the polymerisation of DP = 20 NIPAm in the presence of TREN was conducted using the following ratios: [M] : [I] : [PMDETA] : [$Cu^{(I)}$Br] = [20] : [1] : [0.4] : [0.8].

The polymerisation of NIPAm proceeded to complete monomer conversion within 1 hour. However, instead of the broad bimodal distribution that was previously observed, or the broad mono-modal distribution reported by Haddleton *et al.*, a narrow MWD ($Đ_m$ = 1.15) was detected (Figure 3.36). Moreover, there was only a

small discrepancy between the molecular weight values ($M_{n,theoretical}$ = 2500 g mol^{-1}; $M_{n,experimental}$ = 3900 g mol^{-1}).

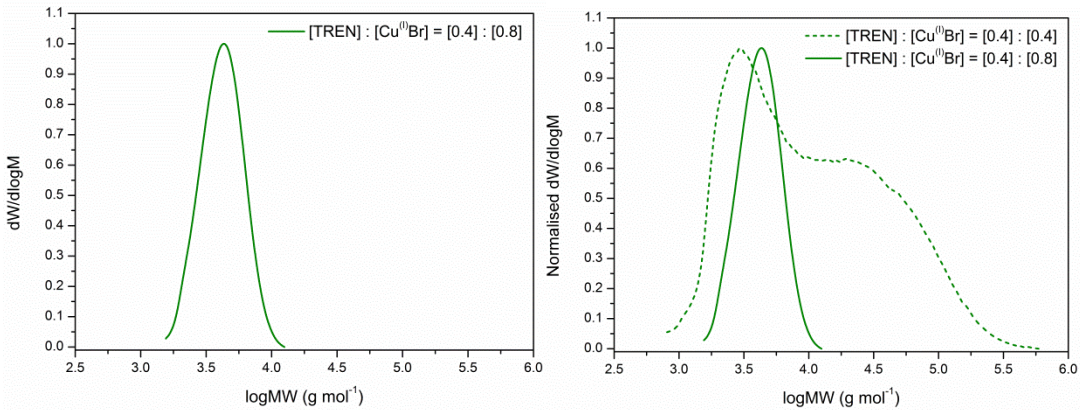

Figure 3.36 – The MWD resulting from the aqueous $Cu^{(0)}$-mediated RDRP of NIPAm in the presence of TREN. Conditions: [M] : [I] : [L] : [$Cu^{(I)}$X] = [20] : [1.0] : [0.4] : [0.8]. $Đ_m$ = 1.15 and M_n = 3900 g mol^{-1} (left); Comparison of the MWDs resulting from the polymerisation of NIPAm in the presence of TREN (right).

Unfortunately, when the polymerisation was repeated, it was found that these results could not be reproduced. Whilst high conversions were reached in all cases (> 90 % after 1 hour, Table 3.8), the dispersity values varied greatly (Table 3.8, Figure 3.37). Currently, the reason for the discrepancy in MWD is unknown; it is possible that the result from Attempt 1 was an outlier, however, given the range of findings that can be seen in Table 3.8 it seems unlikely that this was the case.

Attempt	Time (minutes)	Conversion (%)	$M_{n,th}$ (g mol^{-1})	$M_{n,SEC}$ (g mol^{-1})	$Đ_m$
1	60	100	2500	3900	1.15
2	30	86	2200	2700	1.31
2	60	93	2300	3300	1.21
3	30	100	2500	3500	1.49
3	60	100	2500	3700	1.52
4	30	82	2100	2200	1.44
4	60	92	2300	2800	1.29
5	30	89	2200	2700	1.34
5	60	92	2300	2800	1.41

Table 3.8 – A summary of the results that were obtained upon repeating the aqueous $Cu^{(0)}$-mediated RDRP of NIPAm in the presence of TREN. Conditions: [M] : [I] : [L] : [$Cu^{(I)}$X] = [20] : [1.0] : [0.4] : [0.8].

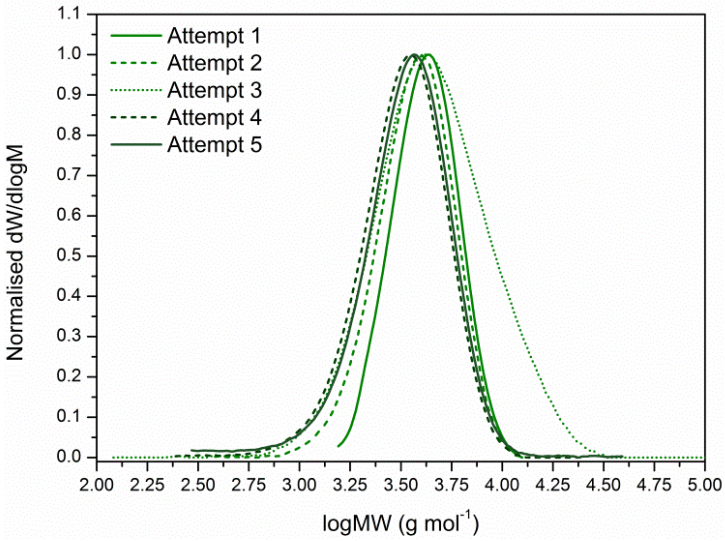

Figure 3.37 – A summary of the MWDs that were produced upon repeating the aqueous $Cu^{(0)}$-mediated RDRP of NIPAm in the presence of TREN. Conditions: [M] : [I] : [L] : [$Cu^{(I)}$X] = [20] : [1.0] : [0.4] : [0.8].

When the concentration of TREN was increased to 0.6 eq., the polymerisation of NIPAm reached completion within 30 minutes. However, upon analysing the resulting polymer by SEC, a broad MWD was observed ($Đ_m$ = 1.42; Figure 3.48). In addition to this, there was a slight loss of control over the number average molecular weight (M_n = 4000 g mol^{-1}).

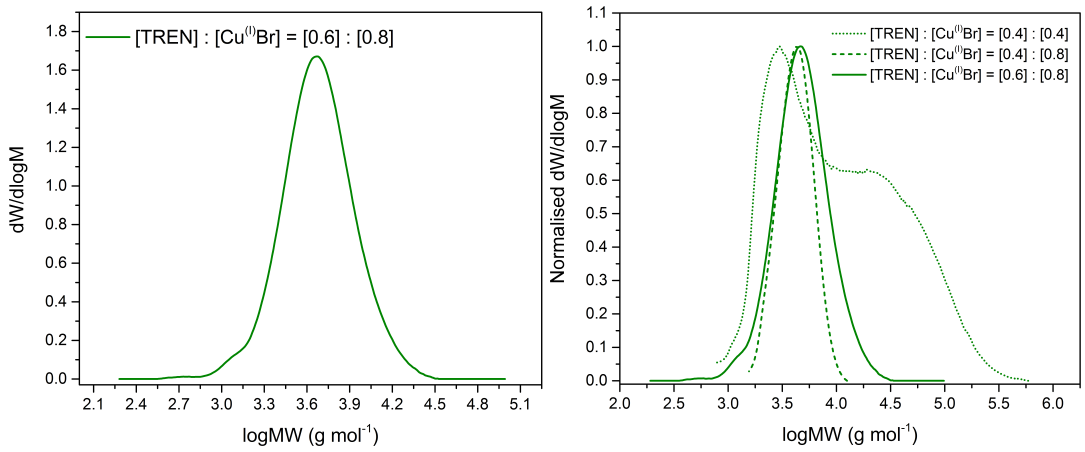

Figure 3.38 - The MWD resulting from the aqueous $Cu^{(0)}$-mediated RDRP of NIPAm in the presence of TREN. Conditions: [M] : [I] : [L] : [$Cu^{(I)}$X] = [20] : [1.0] : [0.6] : [0.8]. $Đ_m$ = 1.42 and M_n = 4000 g mol^{-1} (left); Comparison of the MWDs resulting from the polymerisation of NIPAm in the presence of TREN (right).

As it has been shown that the addition of external halide salts can improve both the MWD and molecular weight predictably, the effect of adding 1.0 M NaBr to the

polymerisation was investigated. Pleasingly, sampling of the crude reaction mixture after 30 minutes revealed that near-quantitative conversion (97 %), narrow MWDs ($Đ_m$ = 1.25) and controlled molecular weights (M_n = 3200 g mol^{-1}) had been achieved (Figure 3.39).

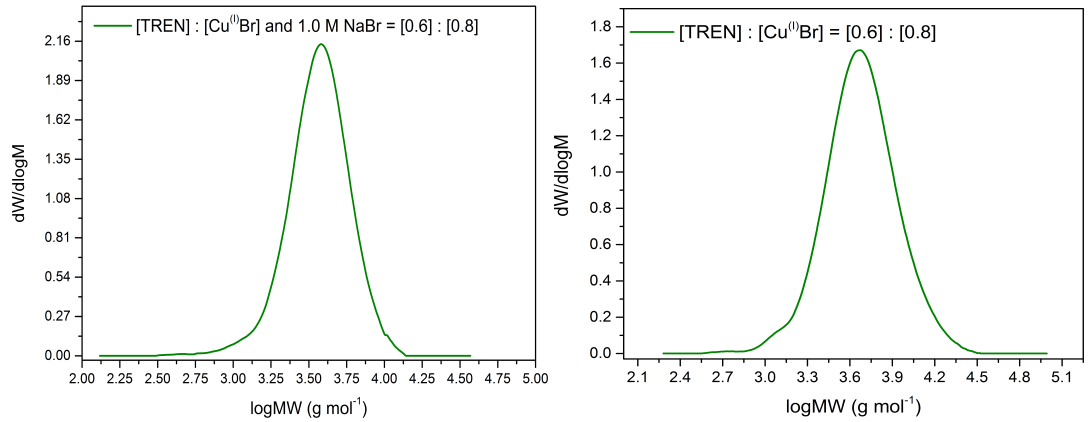

Figure 3.39 – The MWD resulting from the aqueous $Cu^{(0)}$-mediated RDRP of NIPAm in the presence of TREN and external halide salts (left) and without external halide salts (right). Conditions: [M] : [I] : [L] : $[Cu^{(I)}X]$ = [20] : [1.0] : [0.6] : [0.8].

It is evident that the TREN based complexes were less efficacious for the polymerisation of NIPAm in comparison to those with Me_6TREN. However, irrespective of this, it was possible for relatively controlled molecular weights and narrow MWDs to be obtained in both the presence and absence of external halide salts.

In a similar manner to PMDETA, TREN does not require synthesising and is relatively cheap to purchase. As such, it can feasibly be used as the ligand in "off the shelf", aqueous, $Cu^{(0)}$-mediated RDRPs of acrylamides. It is important to note, however, that the results from polymerisations involving TREN can vary significantly upon repetition.

3.3. Conclusion

The overall aim of this work was to take steps towards the development of an aqueous "off the shelf" $Cu^{(0)}$-mediated polymerisation system. To achieve this, an investigation was conducted into replacing Me_6TREN as the ligand for the polymerisation of acrylamides.

Six alternative commercially available ligands (TREN, PMDETA, HMTETA, EDA, TMEDA and Cyclam) were subsequently selected for screening as part of this study. The initial polymerisations of NIPAm in the presence of these materials highlighted PMDETA as the ligand with the most promise. This was due to the high conversion (96 %), predictable molecular weight (M_n = 2300 g mol^{-1}) and narrow dispersity value ($Đ_m$ = 1.54). The remainder of the ligands promoted polymerisations with broad ($Đ_m$ > 2.00) and occasionally bimodal (TREN and EDA) MWDs.

To gather more information about the various copper/ligand complexes, UV-Vis spectroscopy was used to determine their λ_{max} and their extinction coefficient. Unfortunately, upon analysing the results, there were no obvious correlations between the absorbed wavelengths of light and the extent to which the initial polymerisations were controlled. As such, it was concluded that λ_{max} could not be employed in a predictive manner.

Nevertheless, the UV-Vis spectroscopy investigation formed the basis for monitoring the extent to which each of the $Cu^{(I)}$Br/ligand complexes disproportionated. The findings from this study revealed that Me_6TREN, TREN, PMDETA, HMTETA and Cyclam were all capable of reaching 100 % disproportionation. Given the importance that is placed upon this phenomenon within the aqueous $Cu^{(0)}$-mediated RDRP methodology, EDA and TMEDA were subsequently deemed to be unsuitable alternatives to Me_6TREN.

Based on the findings that were obtained from both the initial polymerisations and the disproportionation studies, attempts were made to optimise the polymerisation of NIPAm in the presence of TREN and PMDETA. For PMDETA it was found that quantitative conversions and relatively narrow dispersity values ($Đ_m$ = 1.29) could be attained within 30 minutes. That is, providing that there is an external halide salt (1.0 M NaBr), and that the following reaction conditions: [M] : [I] : [L] : [$Cu^{(I)}$X] = [20] : [1.0] : [0.6] : [0.8] are employed. Since a dispersity of 1.29 is often taken to be indicative of a controlled polymerisation, it was reasoned that PMDETA is an acceptable choice of ligand.

Finally, in the case of TREN, it was shown that near-quantitative conversion and narrow MWDs ($Đ_m$ = ~ 1.25) could be achieved within 30 minutes; this was both in the presence and absence of external halide salts. As a result, it was proposed that TREN can be used as a replacement ligand for Me_6TREN. However, given the potential for this ligand to produce varying results, its use should be accompanied by some degree of caution.

3.4. Experimental

3.4.1. Materials

N-Isopropylacrylamide (NIPAm, Sigma-Aldrich, 97 %), copper$^{(II)}$bromide ($CuBr_2$, Sigma-Aldrich, 99 %), sodium bromide (NaBr, Fisher Scientific, > 99%), 1,1,4,7,10,10-hexamethyltriethylenetetramine (HMTETA, Sigma-Aldrich, 97 %), tris(2-aminoethyl)amine (TREN, Sigma-Aldrich, 96 %), *N,N,N′,N′*-tetramethylethylenediamine (TMEDA, Sigma-Aldrich, 99 %), ethylenediamine (EDA, Sigma-Aldrich, > 99 %), 1,4,8,11-tetraazacyclotetradecane (Cyclam, Sigma-Aldrich, 98 %), water (HPLC grade, VWR) and deionised water (RO grade), were used without further purification. Cuprisorb™ resin was purchased from Seachem.

N,N,N',N'',N''-Pentamethyldiethylenetriamine (PMDETA, Sigma-Aldrich, 99 %) was distilled under reduced pressure (55 °C, 10^{-1} mbar), deoxygenated, and stored in an ampule under nitrogen protection at 4 °C prior to use.

3-Dihydroxypropyl 2-bromo-2-methylpropanoate was synthesised according to the literature procedure.[55] *N,N,N',N',N'',N''*-Hexamethyl-[tris(aminoethyl)amine] (Me_6TREN) was synthesised according to the literature procedure, deoxygenated, and stored in an ampoule at 4 °C under N_2.[56] Copper$^{(I)}$bromide ($Cu^{(I)}Br$, Aldrich, > 98 %) was purified according to the method detailed by Keller and Wycoff.[105]

3.4.2. Characterisation and instrumentation

^{1}H NMR spectra were recorded on Brüker AV-250, HD-300 and DPX-400 spectrometers using deuterated solvents obtained from Sigma-Aldrich. The percentage conversion of NIPAm was determined *via* ^{1}H NMR through integration of the vinyl group (5.6 ppm, 1H, d) and integration of the C$\underline{H}$$(CH_3)_2$ proton (3.9 ppm, 1H, m). The following abbreviations were used to describe multiplicities; s = singlet, d = doublet, t = triplet, q = quartet and m = multiplet.

Size exclusion chromatography (SEC) measurements were performed on an Agilent PL50 equipped with 2 Agilent Polargel L Columns eluting with dimethylformamide containing 0.1 M LiBr as an additive at 50°C. The flow rate was 1 mL min^{-1} and detection was achieved using simultaneous refractive index (RI) and UV (λ = 280 nm) detectors. Molecular weights were calculated relative to narrow PMMA standards. All samples were stirred in the presence of Cuprisorb™ resin to remove residual copper species, dissolved in the appropriate eluent and filtered through disposable 0.45 μm PTFE filters before analysis. Molecular weight data was analysed using Agilent SEC software and plotted using OriginPro 8.5.

UV-Vis spectra were recorded on an Agilent Technologies Cary 60 UV-Vis in the range of 300 – 1100 nm. At the beginning of each experiment, the baseline was corrected for HPLC grade water and blanks were run prior to analysis. Before the sample was placed in a quartz cuvette, each sample was diluted to an appropriate concentration as determined by their calibrations. In instances where it was necessary to remove copper particles, samples were filtered through disposable 0.45 μm PTFE filters before analysis.

3.4.3. General experimental procedures

Typical procedure for the aqueous $Cu^{(0)}$-mediated RDRP of NIPAm in the presence of multidentate/macrocyclic ligands

To a Schlenk tube equipped with a magnetic stirring bar, HPLC grade water (3 mL) and a multidentate ligand (X μL, 0.09 mmol, 0.4 eq.) were added and purged of oxygen *via* nitrogen (N_2) bubbling for 2 minutes. The mixture was placed into an ice/water bath to regulate the temperature (0 °C) after which $Cu^{(I)}Br$ (12.7 mg, 0.09 mmol, 0.4 eq.) was added under an N_2 atmosphere. Upon addition of $Cu^{(I)}Br$ to the ligand-water mix, a coloured solution formed and red/brown $Cu^{(0)}$ particles were

visible. The resulting solution was stirred to achieve disproportionation whilst 3-dihydroxypropyl 2-bromo-2-methylpropanoate (53.3 mg, 0.22 mmol, 1.0 eq.) and NIPAm (500 mg, 4.42 mmol, 20 eq.) were dissolved in water (2 mL) and bubbled with nitrogen for 15 minutes. At the end of the deoxygenation period the initiator-monomer solution was transferred *via* a nitrogen purged syringe and needle into the Schlenk tube. Samples for NMR and SEC were taken using a nitrogen purged syringe, filtered through an alumina column, and diluted in the appropriate solvents.

The quantities of ligand for Me_6TREN, TREN, PMDETA, HMTETA and Cyclam were 23.6 µL, 13.2 µL, 18.5 µL, 24.0 µL and 17.7 mg, respectively.

Typical procedure for the aqueous $Cu^{(0)}$-mediated RDRP of NIPAm in the presence of bidentate ligands

To a Schlenk tube equipped with a magnetic stirring bar, HPLC grade water (3 mL) and a bidentate ligand (X µL, 0.18 mmol, 0.8 eq.) were added and purged of oxygen *via* nitrogen (N_2) bubbling for 2 minutes. The mixture was placed into an ice/water bath to regulate the temperature (0 °C) after which $Cu^{(I)}Br$ (12.7 mg, 0.09 mmol, 0.4 eq.) was added under an N_2 atmosphere. Upon addition of $Cu^{(I)}Br$ to the ligand-water mix, a coloured solution formed and red/brown $Cu^{(0)}$ particles were visible. The resulting solution was stirred to achieve disproportionation whilst 3-dihydroxypropyl 2-bromo-2-methylpropanoate (53.3 mg, 0.22 mmol, 1.0 eq.) and NIPAm (500 mg, 4.42 mmol, 20 eq.) were dissolved in water (2 mL) and bubbled with nitrogen for 15 minutes. At the end of the deoxygenation period the initiator-monomer solution was transferred *via* a nitrogen purged syringe and needle into the Schlenk tube. Samples for NMR and SEC were taken using a nitrogen purged syringe, filtered through an alumina column, and diluted in the appropriate solvents.

The quantities of EDA and TMEDA were 11.8 µL and 26.5 µL, respectively.

Procedure for the UV-Vis analysis of $Cu^{(II)}Br_2$ and each ligand in water

In order determine λ_{max} and the wavelengths of any additional charge-transfer events, a control spectra of each $Cu^{(II)}Br_2$/ligand was recorded by UV-Vis spectroscopy. To a vial equipped with a magnetic stirrer bar, the ligand and $Cu^{(II)}Br_2$ (10.91 mg, 0.05 mmol, 0.5 eq.) were added to 2 mL of HPLC grade water and placed in an ice/water bath. The resulting solution was stirred for 10 minutes at 600 rpm to ensure full dissolution. Before analysis, the sample was serially diluted with HPLC grade water to record an accurate UV-Vis spectrum. Following dilution, 2 mL of the solution was transferred to a quartz cuvette and UV-Vis measurements were taken.

The relevant quantities and conditions for each ligand have been provided in Table 3.9.

Ligand	Ligand (eq.)	Ligand (μL)	Ligand (mg)	Ligand (mmol)	Concentration of $Cu^{(II)}Br_2$ after dilution (mg/mL)
Me_6TREN	1.0	26.1	-	0.9	0.546
TREN	1.0	14.6	-	0.9	1.841
PMDETA	1.0	20.4	-	0.9	1.227
HMTETA	1.0	26.6	-	0.9	1.227
Cyclam	1.0	-	19.6	0.9	2.730
EDA	2.0	13.1	-	1.8	3.819
TMEDA	2.0	29.3	-	1.8	2.730

Table 3.9 – Relevant ligand quantities and conditions used for the UV-Vis analysis of each $Cu^{(II)}Br_2$/ligand complex in water.

UV-Vis calibration plot of $Cu^{(II)}Br_2$ and each ligand in water

To calculate the extinction coefficient, the concentration of $Cu^{(II)}Br_2$ following disproportionation, and the extent of disproportionation for each of the $Cu^{(I)}Br$/ligand complexes, a calibration plot of each $Cu^{(II)}Br_2$/ligand was generated.

To achieve this, several solutions were made up which contained the same concentration of ligand but differing amounts of $Cu^{(II)}Br_2$ (10.91 mg, 8.73 mg, 6.54

mg, 5.45 mg, 4.36 mg; 0.05 mmol, 0.04 mmol, 0.03 mmol, 0.02 mmol, 0.02 mmol; 0.5 eq.) in 2 mL of HPLC grade water. Each of the calibration solutions were then stirred for 10 minutes at 600 rpm in an ice/water bath to ensure that full dissolution had occurred. Before analysis, each of the samples were serially diluted with HPLC grade water to record an accurate UV-Vis spectrum. Following dilution, 2 mL of each of the solutions were transferred to a quartz cuvette and UV-Vis measurements were taken.

In the case of calculating the extent of disproportionation, 10.91 mg of $Cu^{(II)}Br_2$ with each ligand represented 100 % theoretical disproportionation, 8.73 mg 80 % theoretical disproportionation, 6.54 mg 60 % theoretical disproportionation, 5.45 mg 50 % theoretical disproportionation and 4.36 mg 40 % theoretical disproportionation.

The relevant quantities and conditions for each ligand have been provided in Table 3.9.

Concentration of $Cu^{(II)}Br_2$ after dilution (mg/mL) → Ligand ↓	10.91 mg $Cu^{(II)}Br_2$	8.73 mg $Cu^{(II)}Br_2$	6.54 mg $Cu^{(II)}Br_2$	5.45 mg $Cu^{(II)}Br_2$	4.36 mg $Cu^{(II)}Br_2$
Me_6TREN	0.546	0.436	0.327	0.270	0.218
TREN	1.841	1.473	1.104	0.920	0.736
PMDETA	1.227	0.982	0.736	0.613	0.491
HMTETA	1.227	0.982	0.736	0.613	0.491
Cyclam	2.730	2.183	1.635	1.365	1.090
EDA	3.819	3.056	2.289	1.908	1.526
TMEDA	2.730	2.183	1.635	1.365	1.090

Table 3.10 – The concentration of each $Cu^{(II)}Br_2$ calibration point following serial dilution.

Procedure for the visually observing the behaviour of $Cu^{(II)}Br_2$/Ligand complexes in water

To a large vial (capacity 28 mL) equipped with a magnetic stirring bar, HPLC grade water (3 mL) and a ligand were charged (0.09 mmol, 1.0 eq. for multidentate ligands and 0.18 mmol, 2.0 eq. for bidentate ligands). After 30 seconds, $Cu^{(II)}Br_2$ (14.0 mg,

0.06 mmol, 0.5 eq.) was added to the vial and the vial was sealed and placed in an ice/water bath. The resulting mixture was stirred at 600 rpm for 10 minutes. Upon addition of $Cu^{(II)}Br_2$ to the ligand-water mix, a coloured solution formed. The observations were subsequently recorded and a series of photographs were taken.

The multidentate ligands included in these experiments were Me_6TREN, TREN, PMDETA, HMTETA and Cyclam. The bidentate ligands included in these experiments were EDA and TMEDA. The relevant quantities of each ligand were as follows: Me_6TREN = 23.6 µL; TREN = 13.2 µL; PMDETA = 18.5 µL; HMTETA = 24.0 µL; EDA =11.8 µL; TMEDA = 26.5 µL; Cyclam = 17.7 mg.

Procedure for the visually observing the behaviour of $Cu^{(I)}Br$/ligand complexes in water

HPLC grade water (3 mL) and a ligand (0.09 mmol, 1.0 eq. for multidentate ligands and 0.18 mmol, 2.0 eq. for bidentate ligands) were charged to a Schlenk tube equipped with a magnetic stirring bar. The Schlenk tube was then sealed with a suba-seal, and the ligand/water mixture was purged of oxygen *via* nitrogen (N_2) bubbling for 30 seconds. The deoxygenated solution was then placed into an ice/water bath to regulate the temperature (0 °C). After this point, $Cu^{(I)}Br$ (12.7 mg, 0.09 mmol, 1.0 eq.) was added under an N_2 atmosphere and the Schlenk tube was re-sealed. The resulting mixture was then allowed to stir at 600 rpm whilst being bubbled with N_2 for 10 minutes. Upon addition of $Cu^{(I)}Br$ to the ligand-water mix, a coloured solution formed and in most cases, particles were visible. After 10 minutes, the solution was transferred to a vial for comparison with their respective [$Cu^{(II)}Br_2$/ligand] controls. Photographs were taken and observations were recorded immediately after the transfer to prevent any influence of oxygen upon the experiments.

The multidentate ligands included in these experiments were Me_6TREN, TREN, PMDETA, HMTETA and Cyclam. The bidentate ligands included in these experiments were EDA and TMEDA. The relevant quantities of each ligand were as follows: Me_6TREN = 23.6 μL; TREN = 13.2 μL; PMDETA = 18.5 μL; HMTETA = 24.0 μL; EDA =11.8 μL; TMEDA = 26.5 μL; Cyclam = 17.7 mg.

General procedure for monitoring the extent of disproportionation by UV-Vis for each $Cu^{(I)}$Br/ligand complex in water

HPLC grade water (6 mL) and a ligand (0.18 mmol, 1.0 eq. for multidentate ligands and 0.36 mmol, 2.0 eq. for bidentate ligands) were charged to a Schlenk tube equipped with a magnetic stirring bar. The Schlenk tube was then sealed with a suba-seal, and the ligand/water mixture was purged of oxygen *via* nitrogen (N_2) bubbling for 30 seconds. The deoxygenated solution was then placed into an ice/water bath to regulate the temperature (0 °C). After this point, $Cu^{(I)}$Br (25.4 mg, 0.18 mmol, 1.0 eq.) was added under an N_2 atmosphere and the Schlenk tube was re-sealed. The resulting mixture was then allowed to stir at 600 rpm whilst being bubbled with N_2 for 10 minutes. Upon addition of $Cu^{(I)}$Br to the ligand-water mix, a coloured solution formed and in most cases, particles were visible. After 10 minutes, 2 mL of the solution was transferred to a gas tight syringe and passed through disposable PTFE filters into a nitrogen purged vial. The resulting solution was then diluted in the same manner as with their respective calibrations to record an accurate UV-Vis spectrum. 2 mL of the diluted solution was then transferred to a quartz cuvette and UV-Vis measurements were taken. At the same time, the remainder of the solution in the Schlenk tube was stirred for a further 10 minutes. After a total time of 20 minutes, this process was repeated and spectra were recorded.

The multidentate ligands included in these experiments were Me_6TREN, TREN, PMDETA, HMTETA and Cyclam. The bidentate ligands included in these experiments were EDA and TMEDA. The relevant quantities of each ligand were as follows: Me_6TREN = 47.2 µL; TREN = 26.4 µL; PMDETA = 37.0 µL; HMTETA = 48.0 µL; EDA = 23.6 µL; TMEDA = 53.0 µL; Cyclam = 35.4 mg.

General procedure for kinetically monitoring the extent of disproportionation *in-situ* by UV-Vis for each $Cu^{(I)}$Br/ligand complex in water

HPLC grade water (3 mL) and a ligand (0.09 mmol, 1.0 eq. for multidentate ligands and 0.18 mmol, 2.0 eq. for bidentate ligands) were charged to a Schlenk tube equipped with a magnetic stirring bar. The Schlenk tube was then sealed with a suba-seal, and the ligand/water mixture was purged of oxygen *via* nitrogen (N_2) bubbling for 30 seconds. The deoxygenated solution was then placed into an ice/water bath to regulate the temperature (0 °C). After this point, $Cu^{(I)}$Br (0.09 mmol, 12.7 mg, 1.0 eq.) was added under an N_2 atmosphere and the Schlenk tube was re-sealed. The resulting mixture was then allowed to stir at 600 rpm whilst being bubbled with N_2 for 10 minutes. Upon addition of $Cu^{(I)}$Br to the ligand-water mix, a coloured solution formed and in most cases, particles were visible. After 10 minutes, 2 mL of the solution was transferred to a gas tight syringe and passed through disposable PTFE filters into a nitrogen purged vial. The resulting solution was then diluted in the same manner as with their respective calibrations to record an accurate UV-Vis spectrum. 2 mL of the diluted solution was then transferred to a quartz cuvette and UV-Vis measurements were taken every 10 minutes for 1 hour and then every 30 minutes for the remainder of the experiment.

The multidentate ligand included in these experiments was HMTETA. The bidentate ligands included in these experiments were EDA and TMEDA. The relevant

quantities of each ligand were as follows: HMTETA = 24.0 µL; EDA =11.8 µL; TMEDA = 26.5 µL.

For the experiments which did not involve the removal of copper particles, the sample was transferred directly to the quartz crystal cuvette without filtration and diluted to the appropriate concentration. UV-Vis spectra were then recorded in the same manner as with those that underwent filtration.

Procedure for probing the effect of oxygen on the extent of disproportionation by UV-Vis

HPLC grade water (3 mL) and Me_6TREN (23.6 µL, 0.09 mmol, 1.0 eq.) were charged to a Schlenk tube equipped with a magnetic stirring bar. The Schlenk tube was then sealed with a suba-seal, and the ligand/water mixture was stirred in the presence of oxygen for 30 seconds. The resulting solution was then placed into an ice/water bath to regulate the temperature (0 °C). After this point, $Cu^{(I)}Br$ (12.7 mg, 0.09 mmol, 1.0 eq.) was added under air and the Schlenk tube was re-sealed. The resulting mixture was then allowed to stir at 600 rpm in the absence of N_2 bubbling for 10 minutes. Upon addition of $Cu^{(I)}Br$ to the ligand-water mix, a coloured solution formed and copper particles were visible. After 10 minutes, 2 mL of the solution was transferred to a gas tight syringe and passed through disposable PTFE filters into an open vial. The resulting solution was then diluted in the same manner as with the Me_6TREN calibration to record an accurate UV-Vis spectrum. 2 mL of the diluted solution was then transferred to a quartz cuvette and UV-Vis measurements were taken.

Procedure for conducting the polymerisation of NIPAm in the presence of varying amounts of $Cu^{(I)}Br$ and PMDETA

To a Schlenk tube equipped with a magnetic stirring bar, HPLC grade water (3 mL) and PMDETA were added and purged of oxygen *via* nitrogen (N_2) bubbling for 2 minutes. The mixture was placed into an ice/water bath to regulate the temperature (0 °C) after which $Cu^{(I)}Br$ was added under an N_2 atmosphere. Upon addition of $Cu^{(I)}Br$ to the ligand-water mix, a coloured solution formed and red/brown $Cu^{(0)}$ particles were visible. The resulting solution was stirred and allowed to disproportionate whilst 3-dihydroxypropyl 2-bromo-2-methylpropanoate (53.3 mg, 0.22 mmol, 1.0 eq.) and NIPAm (500 mg, 4.42 mmol, 20 eq.) were dissolved in water (2 mL) and bubbled with nitrogen for 15 minutes. At the end of the deoxygenation period the initiator-monomer solution was transferred *via* a nitrogen purged syringe and needle into the Schlenk tube. Samples for NMR and SEC were taken using a nitrogen purged syringe, filtered through an alumina column, and diluted in the appropriate solvents.

The quantities/equivalents of $Cu^{(I)}Br$ and PMDETA have been given in Table 3.11.

Targeted DP	Ligand (eq.)	Ligand (μL)	Ligand (mmol)	$Cu^{(I)}Br$ (eq.)	$Cu^{(I)}Br$ (mg)	$Cu^{(I)}Br$ (mmol)
20	0.4	18.5	0.09	0.8	25.3	0.18
20	0.6	27.7	0.13	0.8	25.3	0.18

Table 3.11 - Conditions used to synthesise PNIPAm in water with differing amounts of $Cu^{(I)}Br$ and PMDETA.

Procedure for conducting the polymerisation of NIPAm in the presence of $Cu^{(I)}Br$, NaBr and PMDETA

To a Schlenk tube equipped with a magnetic stirring bar, HPLC grade water (3 mL), NaBr (551.5 mg, 1.0 M) and PMDETA (27.7 μL, 0.13 mmol, 0.6 eq.) were added and purged of oxygen *via* nitrogen (N_2) bubbling for 2 minutes. The mixture was

placed into an ice/water bath to regulate the temperature (0 °C) after which $Cu^{(I)}Br$ (25.3 mg, 0.18 mmol, 0.8 eq.) was added under an N_2 atmosphere. Upon addition of $Cu^{(I)}Br$ to the ligand-water mix, a coloured solution formed and red/brown $Cu^{(0)}$ particles were visible. The resulting solution was stirred and allowed to disproportionate whilst 3-dihydroxypropyl 2-bromo-2-methylpropanoate (53.3 mg, 0.22 mmol, 1.0 eq.) and NIPAm (500 mg, 4.42 mmol, 20 eq.) were dissolved in water (2 mL) and bubbled with nitrogen for 15 minutes. At the end of the deoxygenation period the initiator-monomer solution was transferred *via* a nitrogen purged syringe and needle into the Schlenk tube. Samples for NMR and SEC were taken using a nitrogen purged syringe, filtered through an alumina column, and diluted in the appropriate solvents.

Procedure for conducting the polymerisation of NIPAm in the presence of varying amounts of $Cu^{(I)}Br$ and TREN

To a Schlenk tube equipped with a magnetic stirring bar, HPLC grade water (3 mL) and TREN were added and purged of oxygen *via* nitrogen (N_2) bubbling for 2 minutes. The mixture was placed into an ice/water bath to regulate the temperature (0 °C) after which $Cu^{(I)}Br$ was added under an N_2 atmosphere. Upon addition of $Cu^{(I)}Br$ to the ligand-water mix, a coloured solution formed and red/brown $Cu^{(0)}$ particles were visible. The resulting solution was stirred and allowed to disproportionate whilst 3-dihydroxypropyl 2-bromo-2-methylpropanoate (53.3 mg, 0.22 mmol, 1.0 eq.) and NIPAm (500 mg, 4.42 mmol, 20 eq.) were dissolved in water (2 mL) and bubbled with nitrogen for 15 minutes. At the end of the deoxygenation period the initiator-monomer solution was transferred *via* a nitrogen purged syringe and needle into the Schlenk tube. Samples for NMR and SEC were taken using a nitrogen purged syringe, filtered through an alumina column, and diluted in the appropriate solvents.

The quantities/equivalents of $Cu^{(I)}Br$ and TREN have been provided in Table 3.12.

Targeted DP	Ligand (eq.)	Ligand (µL)	Ligand (mmol)	$Cu^{(I)}Br$ (eq.)	$Cu^{(I)}Br$ (mg)	$Cu^{(I)}Br$ (mmol)
20	0.4	13.2	0.09	0.8	25.3	0.18
20	0.6	19.8	0.13	0.8	25.3	0.18

Table 3.12 - Conditions used to synthesise PNIPAm in water with differing amounts of $Cu^{(I)}Br$ and TREN.

Procedure for conducting the polymerisation of NIPAm in the presence of $Cu^{(I)}Br$, NaBr and TREN

To a Schlenk tube equipped with a magnetic stirring bar, HPLC grade water (3 mL), NaBr (551.5 mg, 1.0 M) and TREN (19.8 µL, 0.13 mmol, 0.6 eq.) were added and purged of oxygen *via* nitrogen (N_2) bubbling for 2 minutes. The mixture was placed into an ice/water bath to regulate the temperature (0 °C) after which $Cu^{(I)}Br$ (25.3 mg, 0.18 mmol, 0.8 eq.) was added under an N_2 atmosphere. Upon addition of $Cu^{(I)}Br$ to the ligand-water mix, a coloured solution formed and red/brown $Cu^{(0)}$ particles were visible. The resulting solution was stirred and allowed to disproportionate whilst 3-dihydroxypropyl 2-bromo-2-methylpropanoate (53.3 mg, 0.22 mmol, 1.0 eq.) and NIPAm (500 mg, 4.42 mmol, 20 eq.) were dissolved in water (2 mL) and bubbled with nitrogen for 15 minutes. At the end of the deoxygenation period the initiator-monomer solution was transferred *via* a nitrogen purged syringe and needle into the Schlenk tube. Samples for NMR and SEC were taken using a nitrogen purged syringe, filtered through an alumina column, and diluted in the appropriate solvents.

3.5. References

1 T.-H. Yang, *Recent Patents Mater. Sci.*, 2008, 1, 29–40.

2 J. Zhu and R. E. Marchant, *Expert Rev. Med. Devices*, 2011, **8**, 607–626.

3 H. Che, M. Huo, L. Peng, Q. Ye, J. Guo, K. Wang, Y. Wei and J. Yuan, *Polym. Chem.*, 2015, **6**, 2319–2326.

4 E. Turos, R. Cormier and D. E. Kyle, 2009.

5 C. Y. Ang, S. Y. Tan, X. Wang, Q. Zhang, M. Khan, L. Bai, S. Tamil Selvan, X. Ma, L. Zhu, K. T. Nguyen, N. S. Tan and Y. Zhao, *J. Mater. Chem. B*, 2014, **2**, 1879–1890.

6 E. D. Goddard and J. V. Gruber, *Principles of Polymer Science and Technology in Cosmetics and Personal Care*, Marcel Dekker, 1999.

7 S. S. Wong, T. T. Teng, A. L. Ahmad, A. Zuhairi and G. Najafpour, *J. Hazard. Mater.*, 2006, **135**, 378–388.

8 A. Z. Abidin, T. Puspasari and W. A. Nugroho, *Procedia Chem.*, 2012, **4**, 11–16.

9 P. Raffa, A. A. Broekhuis and F. Picchioni, *J. Pet. Sci. Eng.*, 2016, **145**, 723–733.

10 D. J. King and R. R. Noss, *Rev. Environ. Health*, 1989, **8**, 3–16.

11 N. T. Program, *Int. J. Toxicol.*, 2016, **24**, 21–50.

12 M. J. Caulfield, G. G. Qiao and D. H. Solomon, *Chem. Rev.*, 2002, **102**, 3067–3084.

13 A. Shipp, G. Lawrence, R. Gentry, T. McDonald, H. Bartow, J. Bounds, N. Macdonald, H. Clewell, B. Allen and C. Van Landingham, *Crit. Rev. Toxicol.*, 2006, **36**, 481–608.

14 G. G. Odian, *Principles of Polymerization*, Wiley-Interscience, Hoboken, N.J., 4th edn., 2004.

15 D. Fu, S. Wu, X. He and J. Ni, *Colloids Surfaces A Physicochem. Eng. Asp.*, 2008, **326**, 122–128.

16 J. M. Lamarche, J. Persello and A. Foissy, *Ind. Eng. Chem. Prod. Res. Dev.*, 1983, **22**, 123–126.

17 G. Moad, E. Rizzardo and S. H. Thang, *Aust. J. Chem.*, 2006, 59, 669–692.

18 G. Moad, E. Rizzardo and S. H. Thang, *Aust. J. Chem.*, 2009, 62, 1402–1472.

19 G. Moad, E. Rizzardo and S. H. Thang, *Aust. J. Chem.*, 2012, 65, 985–1076.

20 R. B. Grubbs, *Polym. Rev.*, 2011, **51**, 104–137.

21 K. Matyjaszewski, *Macromolecules*, 2012, **45**, 4015–4039.

22 Q. Zhang, P. Wilson, Z. Li, R. McHale, J. Godfrey, A. Anastasaki, C. Waldron and D. M. Haddleton, *J. Am. Chem. Soc.*, 2013, **135**, 7355–7363.

23 C. M. R. Abreu, A. C. Serra, A. V Popov, K. Matyjaszewski, T. Guliashvili and J. F. J. Coelho, *Polym. Chem.*, 2013, **4**, 5629–5636.

24 C. Visnevskij and R. Makuska, *Macromolecules*, 2013, **46**, 4764–4771.

25 V. Percec, A. V Popov, E. Ramirez-Castillo, M. Monteiro, B. Barboiu, O. Weichold, A. D. Asandei and C. M. Mitchell, *J. Am. Chem. Soc.*, 2002, **124**, 4940–4941.

26 A. J. Convertine, B. S. Lokitz, A. B. Lowe, C. W. Scales, L. J. Myrick and C. L. McCormick, *Macromol. Rapid Commun.*, 2005, **26**, 791–795.

27 A. B. Lowe and C. L. McCormick, *Prog. Polym. Sci.*, 2007, **32**, 283–351.

28 W. Bai, L. Zhang, R. Bai and G. Zhang, *Macromol. Rapid Commun.*, 2008, **29**, 562–566.

29 D. A. Z. Wever, P. Raffa, F. Picchioni and A. A. Broekhuis, *Macromolecules*, 2012, **45**, 4040–4045.

30 J. T. Rademacher, M. Baum, M. E. Pallack, W. J. Brittain and W. J. Simonsick, *Macromolecules*, 2000, **33**, 284–288.

31 M. Teodorescu and K. Matyjaszewski, *Macromolecules*, 1999, **32**, 4826–4831.

32 M. Teodorescu and K. Matyjaszewski, *Macromol. Rapid Commun.*, 2000, **21**, 190–194.

33 Q. Duan, Y. Miura, A. Narumi, X. Shen, S.-I. Sato, T. Satoh and T. Kakuchi, *J. Polym. Sci. Part A Polym. Chem.*, 2006, **44**, 1117–1124.

34 G. Masci, L. Giacomelli and V. Crescenzi, *Macromol. Rapid Commun.*, 2004, **25**, 559–564.

35 X. Tang, X. Liang, Q. Yang, X. Fan, Z. Shen and Q. Zhou, *J. Polym. Sci. Part A Polym. Chem.*, 2009, **47**, 4420–4427.

36 S. Ding, M. Radosz and Y. Shen, *Macromol. Rapid Commun.*, 2004, **25**, 632–636.

37 A. Narumi, Y. Chen, M. Sone, K. Fuchise, R. Sakai, T. Satoh, Q. Duan, S. Kawaguchi and T. Kakuchi, *Macromol. Chem. Phys.*, 2009, **210**, 349–358.

38 F. Alsubaie, A. Anastasaki, P. Wilson and D. M. Haddleton, *Polym. Chem.*, 2015, **6**, 406–417.

39 S. R. Samanta, V. Nikolaou, S. Keller, M. J. Monteiro, D. A. Wilson, D. M. Haddleton and V. Percec, *Polym. Chem.*, 2015, **6**, 2084–2097.

40 G. R. Jones, Z. Li, A. Anastasaki, D. J. Lloyd, P. Wilson, Q. Zhang and D. M. Haddleton, *Macromolecules*, 2016, **49**, 483–489.

41 V. Nikolaou, A. Simula, M. Droesbeke, N. Risangud, A. Anastasaki, K. Kempe, P. Wilson and D. Haddleton, *Polym. Chem.*, 2016.

42 A. Anastasaki, A. J. Haddleton, Q. Zhang, A. Simula, M. Droesbeke, P. Wilson and D. M. Haddleton, *Macromol. Rapid Commun.*, 2014, **35**, 965–970.

43 A. Anastasaki, V. Nikolaou, G. Nurumbetov, P. Wilson, K. Kempe, J. F.

Quinn, T. P. Davis, M. R. Whittaker and D. M. Haddleton, *Chem. Rev.*, 2016, **116**, 835–877.

44 Y. Wang, T. Chen, M. Kitamura and T. Nakaya, *J. Polym. Sci. Part A Polym. Chem.*, 1996, **34**, 449–460.

45 P. Wilson, A. Anastasaki, M. R. Owen, K. Kempe, D. M. Haddleton, S. K. Mann, A. P. R. Johnston, J. F. Quinn, M. R. Whittaker, P. J. Hogg and T. P. Davis, *J. Am. Chem. Soc.*, 2015, **137**, 4215–4222.

46 Q. Zhang, M. Li, C. Zhu, G. Nurumbetov, Z. Li, P. Wilson, K. Kempe and D. M. Haddleton, *J. Am. Chem. Soc.*, 2015, **137**, 9344–9353.

47 J. Collins, S. J. Wallis, A. Simula, M. R. Whittaker, M. P. McIntosh, P. Wilson, T. P. Davis, D. M. Haddleton and K. Kempe, *Macromol. Rapid Commun.*, 2017, **38**, 1600534.

48 N. V Tsarevsky, T. Pintauer and K. Matyjaszewski, *Macromolecules*, 2004, **37**, 9768–9778.

49 W. G. M. and R. P. F. Perreault, A. Oukarroum, S. P. Melegari, *Chemosphere*, 2012, **87**, 1388–1394.

50 N. V Tsarevsky and K. Matyjaszewski, *Chem. Rev.*, 2007, **107**, 2270–2299.

51 Y. Wang, Y. Zhang, B. Parker and K. Matyjaszewski, *Macromolecules*, 2011, **44**, 4022–4025.

52 D. Konkolewicz, A. J. D. Magenau, S. E. Averick, A. Simakova, H. He and K. Matyjaszewski, *Macromolecules*, 2012, **45**, 4461–4468.

53 W. Jakubowski and K. Matyjaszewski, *Angew. Chemie Int. Ed.*, 2006, **45**, 4482–4486.

54 D. Yang, D. He, Y. Liao, Z. Xue, X. Zhou and X. Xie, *J. Polym. Sci. Part A Polym. Chem.*, 2014, **52**, 1020–1027.

55 S. Perrier, S. P. Armes, X. S. Wang, F. Malet and D. M. Haddleton, *J. Polym. Sci. Part A Polym. Chem.*, 2001, **39**, 1696–1707.

56 M. Ciampolini and N. Nardi, *Inorg. Chem.*, 1966, **5**, 41–44.

57 A. L. Aleksandrov, *B. Acad. Sci. USSR Ch.*, 1980, **29**, 1740–1744.

58 A. Simula, V. Nikolaou, F. Alsubaie, A. Anastasaki and D. M. Haddleton, *Polym. Chem.*, 2015, **6**, 5940–5950.

59 Q. Zhang, Z. Li, P. Wilson and D. M. Haddleton, *Chem. Commun.*, 2013, **49**, 6608–6610.

60 N. H. Nguyen, M. E. Levere and V. Percec, *J. Polym. Sci. Part A Polym. Chem.*, 2012, **50**, 35–46.

61 O. Bertrand, P. Wilson, J. A. Burns, G. A. Bell and D. M. Haddleton, *Polym. Chem.*, 2015, **6**, 8319–8324.

62 B. M. Rosen and V. Percec, *J. Polym. Sci. Part A Polym. Chem.*, 2007, **45**, 4950–4964.

63 A. Anastasaki, C. Waldron, P. Wilson, R. McHale and D. M. Haddleton,

Polym. Chem., 2013, **4**, 2672–2675.

64 W. Tang and K. Matyjaszewski, *Macromolecules*, 2006, **39**, 4953–4959.

65 A. J. Clark, G. M. Battle, A. M. Heming, D. M. Haddleton and A. Bridge, *Tetrahedron Lett.*, 2001, **42**, 2003–2005.

66 G. Kickelbick, T. Pintauer and K. Matyjaszewski, *New J. Chem.*, 2002, **26**, 462–468.

67 W. Tang, N. V Tsarevsky and K. Matyjaszewski, *J. Am. Chem. Soc.*, 2006, **128**, 1598–1604.

68 B. M. Rosen and V. Percec, *Chem. Rev.*, 2009, **109**, 5069–5119.

69 N. V Tsarevsky, W. Tang, S. J. Brooks and K. Matyjaszewski, in *Controlled/Living Radical Polymerization*, American Chemical Society, 2006, vol. 944, pp. 5–56.

70 J. Xia, X. Zhang and K. Matyjaszewski, in *Transition Metal Catalysis in Macromolecular Design*, American Chemical Society, 2000, vol. 760, pp. 13–207.

71 T. Hatano, B. M. Rosen and V. Percec, *J. Polym. Sci. Part A Polym. Chem.*, 2010, **48**, 164–172.

72 E. Nicol, T. Derouineau, F. Puaud and A. Zaitsev, *J. Polym. Sci. Part A Polym. Chem.*, 2012, **50**, 3885–3894.

73 W. Tang, Y. Kwak, W. Braunecker, N. V Tsarevsky, M. L. Coote and K. Matyjaszewski, *J. Am. Chem. Soc.*, 2008, **130**, 10702–10713.

74 J. N. Kizhakkedathu, R. Norris-Jones and D. E. Brooks, *Macromolecules*, 2004, **37**, 734–743.

75 P. Shivapooja, L. K. Ista, H. E. Canavan and G. P. Lopez, *Biointerphases*, 2012, **7**, 1–9.

76 R. P. Quirk and B. Lee, *Polym. Int.*, 1992, **27**, 359–367.

77 D. J. Lloyd, V. Nikolaou, J. Collins, C. Waldron, A. Anastasaki, S. P. Bassett, S. M. Howdle, A. Blanazs, P. Wilson, K. Kempe and D. M. Haddleton, *Chem. Commun.*, 2016, **52**, 6533–6536.

78 J. Ma, H. Chen, M. Zhang and L. Chen, *J. Polym. Sci. Part A Polym. Chem.*, 2011, **49**, 2588–2593.

79 L. Fan, H. Chen, Z. Hao and Z. Tan, *J. Polym. Sci. Part A Polym. Chem.*, 2012, **50**, 4871–4878.

80 L. Fan, H. Chen, G. Lv, J. Cao and Y. Fu, *J. Polym. Sci. Part A Polym. Chem.*, 2013, **51**, 3233–3239.

81 J. Xia and K. Matyjaszewski, *Macromolecules*, 1997, **30**, 7697–7700.

82 X. Lu, S. Gong, L. Meng, C. Li, S. Yang and L. Zhang, *Polymer (Guildf).*, 2007, **48**, 2835–2842.

83 K. Nakabayashi and H. Mori, *Eur. Polym. J.*, 2013, **49**, 2808–2838.

84 S. J. Shin, Y. C. Yu, J. D. Seo, S. J. Cho and J. H. Youk, *J. Polym. Sci. Part*

A Polym. Chem., 2014, **52**, 1607–1613.

85 J. Liu, A. Debuigne, C. Detrembleur and C. Jérôme, *Adv. Healthc. Mater.*, 2014, **3**, 1941–1968.

86 H. Yu, Y. Wu, J. Gao, W. Wang, Z. Zhang and X. Zhu, *J. Polym. Sci. Part A Polym. Chem.*, 2012, **50**, 4983–4989.

87 A. J. D. Magenau, Y. Kwak, K. Schröder and K. Matyjaszewski, *ACS Macro Lett.*, 2012, **1**, 508–512.

88 H. Datta, A. K. Bhowmick and N. K. Singha, *Macromol. Symp.*, 2006, **240**, 245–251.

89 K. Pan, L. Jiang, J. Zhang and Y. Dan, *J. Appl. Polym. Sci.*, 2007, **105**, 521–526.

90 Z. Hu, X. Shen, H. Qiu, G. Lai, J. Wu and W. Li, *Eur. Polym. J.*, 2009, **45**, 2313–2318.

91 J. Jiang, X. Lu and Y. Lu, *J. Polym. Sci. Part A Polym. Chem.*, 2007, **45**, 3956–3965.

92 P. Atkins, *Inorganic Chemistry*, OUP Oxford, 5th edn., 2010.

93 F. A. Cotton, G. Wilkinson and P. L. Gaus, *Basic Inorganic Chemistry*, John Wiley & Sons, Inc., 3rd edn., 1995.

94 V. Percec, T. Guliashvili, J. S. Ladislaw, A. Wistrand, A. Stjerndahl, M. J. Sienkowska, M. J. Monteiro and S. Sahoo, *J. Am. Chem. Soc.*, 2006, **128**, 14156–14165.

95 F. Alsubaie, A. Anastasaki, V. Nikolaou, A. Simula, G. Nurumbetov, P. Wilson, K. Kempe and D. M. Haddleton, *Macromolecules*, 2015, **48**, 6421–6432.

96 A. Anastasaki, V. Nikolaou and D. M. Haddleton, *Polym. Chem.*, 2016, **7**, 1002–1026.

97 M. E. Levere, N. H. Nguyen, H.-J. Sun and V. Percec, *Polym. Chem.*, 2013, **4**, 686–694.

98 H. G. Vogel, *Drug Discovery and Evaluation: Safety and Pharmacokinetic Assays*, Springer Science & Business Media, 2nd edn., 2006.

99 K. Krumova and G. Cosa, in *Singlet Oxygen: Applications in Biosciences and Nanosciences, Volume 1*, The Royal Society of Chemistry, 2016, vol. 1, pp. 1–21.

100 M. E. Levere, N. H. Nguyen, X. Leng and V. Percec, *Polym. Chem.*, 2013, **4**, 1635–1647.

101 A. Simula, A. Anastasaki and D. M. Haddleton, *Macromol. Rapid Commun.*, 2016, **37**, 356–361.

102 G. R. Jones, R. Whitfield, A. Anastasaki and D. M. Haddleton, *J. Am. Chem. Soc.*, 2016, **138**, 7346–7352.

103 A. Simakova, S. E. Averick, D. Konkolewicz and K. Matyjaszewski, *Macromolecules*, 2012, **45**, 6371–6379.

104 M. Zhang, M. F. Cunningham and R. A. Hutchinson, *Polym. Chem.*, 2015, **6**, 6509–6518.

105 H. D. Keller, R. N.; Wycoff, *Inorg. Synth.*, 1946, **2**, 1–4.

Chapter 4: Towards "off the shelf" polymerisation: screening of initiators for $Cu^{(0)}$-mediated RDRP in aqueous media

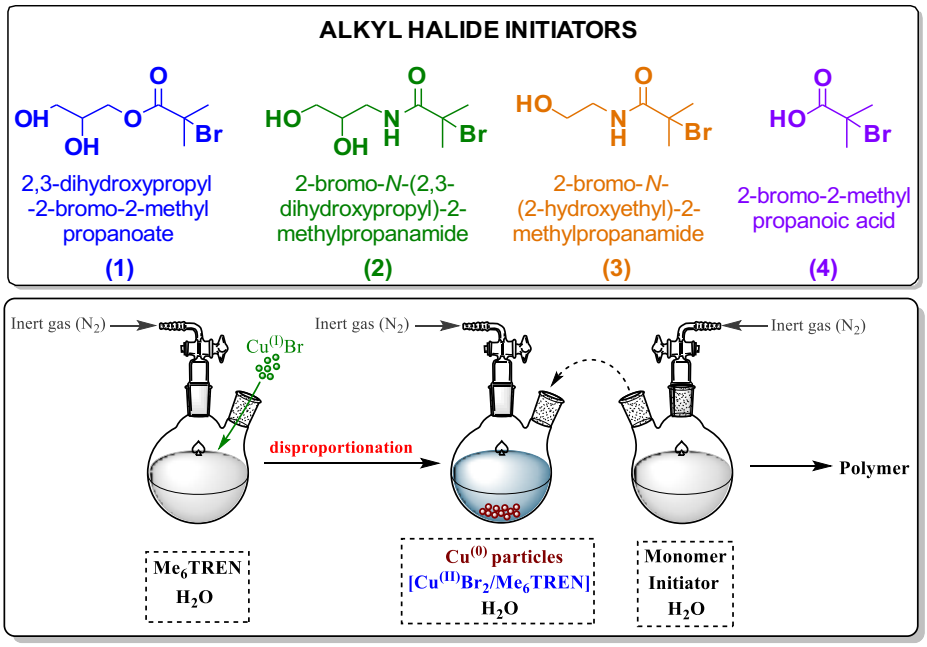

Four alkyl halides were screened as the initiator for the polymerisation of acrylamides via the aqueous $Cu^{(0)}$-mediated RDRP protocol. By comparing these results and factoring in the commercial availability of the chosen compounds, the eligibility of using each initiator in an "off the shelf" polymerisation was determined. The data suggested that in cases where organic synthesis or price was not a limitation of the user, then 2-bromo-N-(2-hydroxyethyl)-2-methylpropanamide was the most suitable initiator. The use of 2-bromo-2-methylpropanoic acid, an inexpensive and readily obtainable initiator, proved to be problematic. Whilst a controlled polymerisation was realised for DEAm, others resulted in a significant loss of molecular weight predictability and bimolecular termination. Thus, 2-bromo-2-methylpropanoic acid was considered to be incompatible with aqueous $Cu^{(0)}$-mediated RDRPs, and by proxy, an "off the shelf" $Cu^{(0)}$-mediated RDRP system.

4.1. Introduction

The aqueous $Cu^{(0)}$-mediated RDRP protocol has proven to be a versatile and robust synthetic tool.[1–7] This has mainly stemmed from its relative simplicity, its ability to afford well-defined polymers ($Đ_m$ < 1.2) within a short time-frame (between 30 minutes to 1 hour), and its tolerance to a range of chemical environments.[8–10] Unfortunately, the presence of copper within the system,[11,12] the toxicity of halide initiators,[13] and the requirement for reagent preparation has deterred this technique from being widely applied. Whilst the former of these issues is currently being addressed through the development of reduced catalyst concentration polymerisation methodologies,[14–19] the latter of these has received comparatively less focus within the academic community.[3,20]

As discussed in the previous chapter, an "off the shelf" polymerisation is one which exclusively employs commercially available reagents. In an ideal scenario, each of the required components would be both inexpensive and readily obtainable. Given the multi-component nature of $Cu^{(0)}$-mediated RDRPs, this means that it would be possible to purchase the initiator, the ligand, the solvent and the source of the metal centre(s) with relative ease.

With respect to aqueous polymerisation, there is not currently a set of conditions through which the controlled polymerisation of acrylamides can be realised in an "off the shelf" manner. Therefore, in a step towards the development of the ideal system, a variety of copper/ligand complexes were screened, as discussed in Chapter 3, as potential mediators for the aqueous $Cu^{(0)}$-mediated RDRP of NIPAm. Within this study, it was postulated that TREN and PMDETA showed the most promise as a less costly and *synthesis-free* alternative to Me_6TREN.

During the attempted optimisation of the reaction conditions for TREN, the concentration of $Cu^{(I)}Br$ was increased to 0.8 eq. with respect to the initiator; this

was with the aim of improving control over the polymerisation process.[5,21,22] However, upon using these conditions for the synthesis of PNIPAm, a range of dispersity values, average molecular weights, and conversions were attained. In addition to this, the use of external halide salts offered limited improvement in polymerisation control ($Đ_m$ = 1.25). Nevertheless, as TREN was able to promote the synthesis of relatively controlled polymers, it was recommended as a potential replacement for Me_6TREN. However, this conclusion was accompanied by a caution of TREN's potential to yield differing results.

In contrast, PMDETA and its copper complexes were deemed to be effective mediators for the aqueous $Cu^{(0)}$-mediated RDRP of NIPAm. Following the screening of a range of polymerisation conditions, it was found that the addition of 1.0 M NaBr allowed for quantitative conversions and relatively narrow MWDs ($Đ_m$ = 1.29) to be attained within 30 minutes. Given that a dispersity of <1.5 is generally taken to be indicative of a controlled polymerisation, it was suggested that PMDETA should be considered as an alternative ligand to Me_6TREN.

Although the use of both PMDETA and TREN allow for controlled polymerisations to be afforded, its respective copper complexes were not as effective at mediating the polymerisation of NIPAm as Me_6TREN.[7,10,23] Fortunately, in cases where a dispersity of <1.2 is required, an "off the shelf" polymerisation is still achievable; the proviso for this is that cost must not be an issue as, whilst Me_6TREN is available for purchase from several chemical suppliers, it is quite expensive to obtain (*e.g.* Sigma-Aldrich ~ £115 per mL).

4.1.1. The selection of appropriate initiators for further investigation

As discussed in Chapter 1, the choice of initiator for $Cu^{(0)}$-mediated RDRPs (and indeed all current TMM-LRPs) is vital to obtaining polymers with predictable

molecular weights and narrow MWDs.[24–27] For reactions which are conducted in organic media, there is a library of compounds from which the most suitable mono-functional initiator can be selected (Figure 4.1). Amongst these, methyl 2-bromopropionate (MBP)[28–30] and ethyl 2-bromoisobutyrate (EBiB)[25,28,31–33] are the most commonly reported. However, there are others such as methyl-2-bromo-2-phenylacetate (MBrPA),[20] 2-bromo-*N*-phenyl-propionamide (BrPPA),[34] ethyl 2-bromopropionate (EBP),[35] and phosphonic ester bearing initiators (PBI)[36,37] which have also been utilised. The availability of a range of initiators has not only enabled for polymerisations to be easily tailored, but has increased the attractiveness of this technique as a means of polymer synthesis.

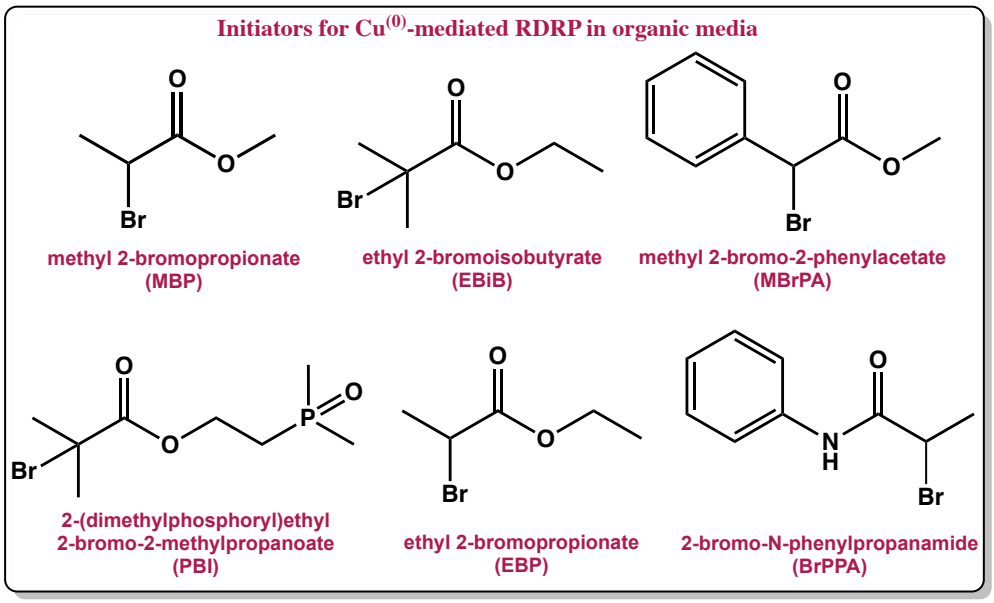

Figure 4.1 – Examples of mono-functional initiators that have been employed for Cu$^{(0)}$-mediated RDRPs conducted in organic media.

For Cu$^{(0)}$-mediated RDRPs which are performed in aqueous media, the pool of initiators is comparatively limited (Figure 4.2). Whilst there have been studies which employ 4-(*N*-(2-bromoisobutyryl)amino)phenylarsonic acid (AsI),[38] 2-hydroxyethyl 2-bromoisobutyrate (HEBiB),[39] and oligo(ethylene glycol) methyl ether 2-bromoisobutyrate (OEOMEBr),[40] the initiating species which has found the most use is 2,3-dihydroxypropyl-2-bromo-2-methylpropanoate (DHPBMP).[2,4,5,7–10,23,41–43]

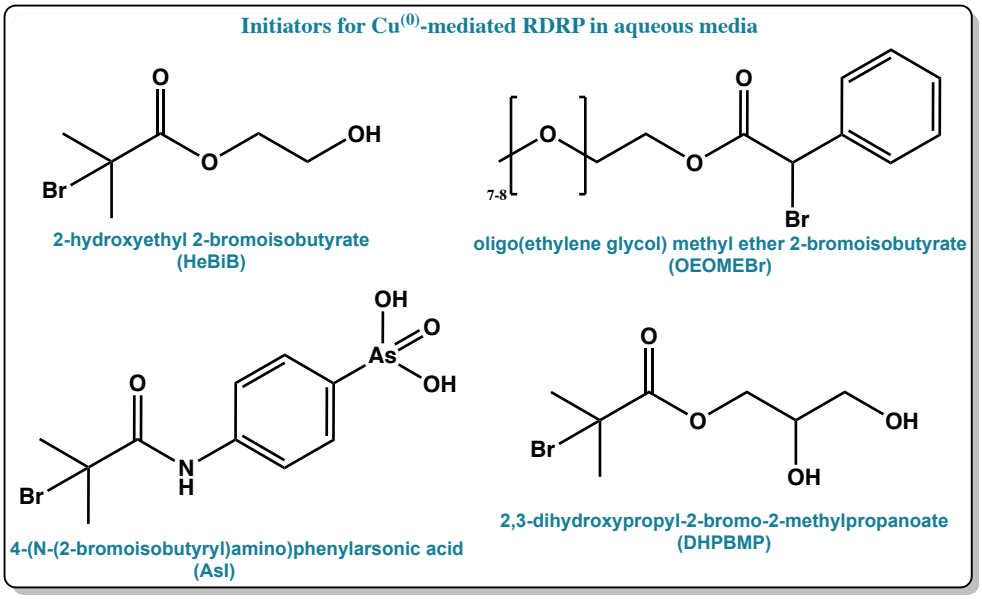

Figure 4.2 - Examples of mono-functional initiators that have been employed for $Cu^{(0)}$-mediated RDRPs conducted in aqueous media.

In part, the frequent use of DHPBMP has resulted from its use during the original development of the aqueous protocol.[7] Indeed, since the evolution of this methodology, DHPBMP has proven to be highly efficacious for the polymerisation of a wide range of monomers; this includes acrylamides,[4,5,23,42] acrylates,[7] and glyco-monomers.[43] When this is combined with the high level of documentation that surrounds this compound, it is relatively easy to find conditions which are appropriate for almost any situation.

Although DHPBMP is a viable choice for most researchers, it is not currently commercially available, and hence, requires the user to undertake a two-step synthesis and rigorous purification.[44] In a move towards finding a more feasible compound, three alkyl halides (Figure 4.3, structures **(2)** - **(4)**) were chosen for screening as initiators for the polymerisation of NIPAm in aqueous media. It is worth noting that Me_6TREN was employed as the ligand for this study as its complexes have found the most use as mediators within this technique.

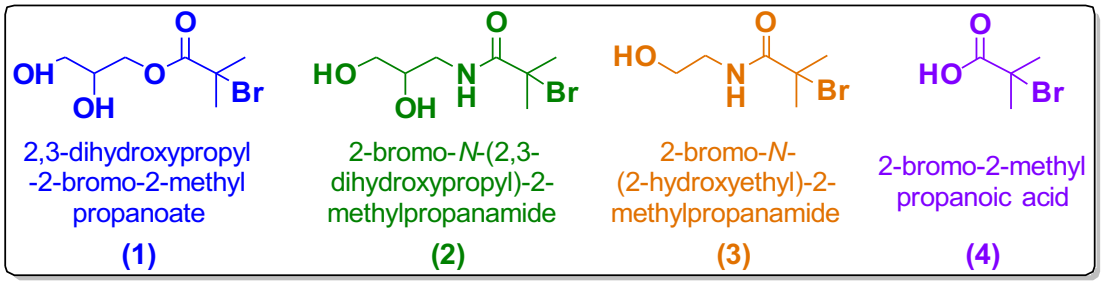

Figure 4.3 – The chemical structures of the initiators which were screened as part of this investigation.

4.2. Results and discussion

4.2.1. Using 2,3-dihydroxypropyl-2-bromo-2-methylpropanoate as the initiator for the aqueous Cu$^{(0)}$-mediated RDRP of NIPAm

4.2.1.1. Initial polymerisations with compound (1)

PNIPAm was synthesised using the aqueous Cu$^{(0)}$-mediated RDRP protocol under "standard conditions" (DP = 20: [NIPAm] : [compound **(1)**] : [Cu$^{(I)}$Br] : [Me_6TREN] = [20] : [1.0] : [0.4] : [0.4]).[8,10,23] Following ^{1}H NMR analysis of the resulting reaction after 30 minutes, it was found that quantitative monomer conversion had been attained (Figure 4.4). Subsequent evaluation of the polymer by SEC revealed a mono-modal and Poisson-like MWD ($Đ_m$ = 1.21; Figure 4.4). Whilst this would usually be indicative of a controlled polymerisation,[45] the disparity between the theoretical (M_n = 2500 g mol^{-1}) and experimental molecular weights (M_n = 7200 g mol^{-1}) implied that there was a loss of control during propagation. It is important to note that the average molecular weight could not be measured by ^{1}H NMR spectroscopy due to peak overlap. Therefore, the theoretical molecular values provided within this chapter were calculated according to Equation 4.1.

$$M_{n,th} = \left((\text{targeted DP x monomer MW}) + \text{initiator MW}\right) \text{x conversion} \quad \textbf{(Equation 4.1)}$$

Equation 4.1 – The equation which was used to calculate the theoretical molecular weight of a polymer ($M_{n,th}$).

When the same conditions were employed in Chapter 3, a MWD with a dispersity of 1.09 and polymers with greater molecular weight predictability (4300 g mol^{-1}) were obtained. It is worth highlighting that, despite the higher levels of control, there was still a disagreement between the molecular weight values.

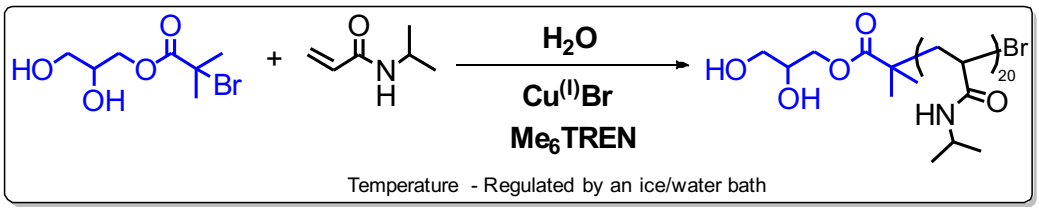

Scheme 4.1 - A schematic representation of the aqueous $Cu^{(0)}$-mediated RDRP of NIPAm initiated by compound (1).

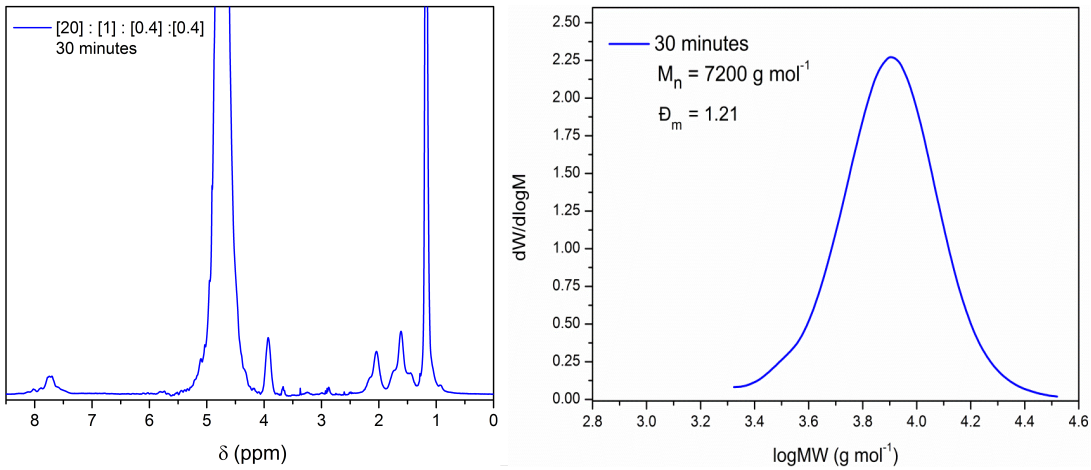

Figure 4.4 – The ^{1}H NMR spectrum (left) and SEC chromatogram (right) for the initial polymerisation of NIPAm utilising compound (1) as the initiator. Conditions: [NIPAm] : [I] : [$Cu^{(I)}Br$] : [Me_6TREN] = [20] : [1.0] : [0.4] : [0.4].

In TMM-RDRPs, poor agreement between experimental and theoretical molecular weights has been attributed to a broad range of factors including: the inefficient deactivation of propagating species,[16,46] the presence of "free ligand",[47] poor initiator efficiency (I_{eff}),[34,48–51] and differences in hydrodynamic volume (V_h) between the chosen SEC standard and the analysed sample.[52–55]

Data which is obtained *via* SEC is not absolute; experimental molecular weights are determined relative to those of a known standard, which is usually that of PMMA, polystyrene (PS), or polyethylene oxide (PEO). If the chosen standard possesses a

different V_h to that of the polymer being analysed, then it is possible for either an over- or under-estimation of the average molecular weight to be reported. In some instances, this can reasonably be used as an explanation for molecular weight disagreements. However, the results in Chapter 3 suggested that this was not applicable to this work.

Initiators which are said to be highly efficient are those which enable chain growth to occur in a uniform manner. They therefore promote the synthesis of polymers with the desired molecular weight and narrow MWDs. As the efficiency of the initiator decreases, chain growth becomes less uniform, and higher than targeted M_n values are often observed. Since a different batch of compound **(1)** was employed for the work in Chapter 3, it is plausible that poor initiator efficiency was responsible for the molecular weight disagreement. However, the overlap of the methyl protons in NIPAm and those of the initiator meant that it was not possible to determine if this was the case by ^{1}H NMR spectroscopy.

Alternatively, there have been studies conducted by Haddleton *et al.* which suggest that the presence of "free ligand" results in a loss of control over molecular weight predictability.[47,56,57] "Free ligand" is the term which is given to molecules of Me_6TREN (or the chelating agent of choice) that are not co-ordinated to the metal centre. As they remain unbound in solution, they are able to participate in side reactions (such as chain transfer to ligand,[47,56] and quarternisation/nucleophilic substitution of the ligand onto the ω-end of the polymer[47]) which are detrimental to the polymerisation process (Scheme 4.2). Depending upon the point at which these events occur, this can result in chain termination, a decrease in the I_{eff}, a loss of control over the MWD, or a combination of the above factors (Table 4.1).

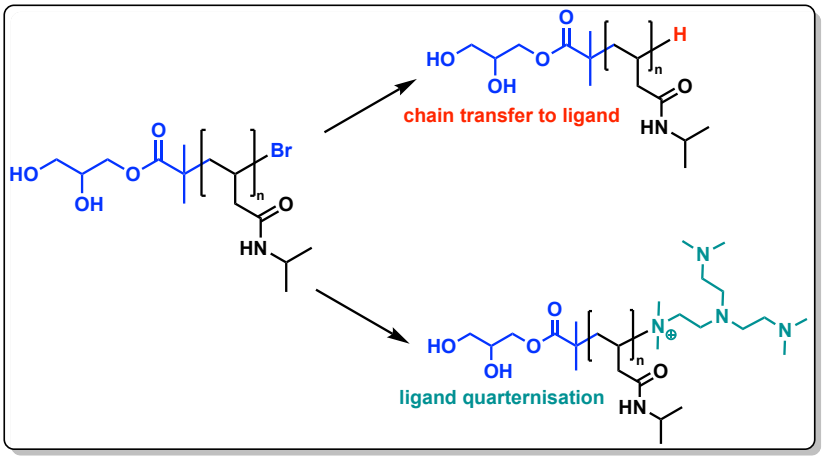

Scheme 4.2 – A schematic representation of the effects that chain transfer to ligand (red) and ligand quarternisation (cyan) have upon the $Cu^{(0)}$-mediated RDRP process.

Occurrence in the polymerisation	Effect upon the polymerisation
Early stages	• Lowers the I_{eff} • Results in polymers with a higher M_n than targeted • Comparatively broad MWD
Middle stages	• Some chain termination • Results in polymers with a slightly higher M_n than targeted • Comparatively broad MWD
Final stages	• Minimal chain termination • Negligible effect upon the resulting M_n • Comparatively narrow MWD

Table 4.1 – A summary of the effects that chain transfer to ligand and ligand quarternisation can have upon the $Cu^{(0)}$-mediated RDRP process.

Relating this back to the polymerisation of NIPAm under "standard conditions"; a disagreement between the theoretical and experimental molecular weights was recorded by SEC, with the overall dispersity of the polymer chains remaining comparatively broad. Based on the above information, the discrepancy in molecular weights was partially attributed to side reactions with Me_6TREN that were occurring within the early stages of the polymerisation.

Accordingly, to investigate whether decreasing the concentration of "free ligand" would result in a closer agreement between theoretical and experimental molecular weights, the concentration of $Cu^{(I)}Br$ within the system was increased to 0.8 eq. with respect to the initiator. Contrary to the initial conditions ([M] : [I] : [L] : [$Cu^{(I)}Br$] = [20]

: [1.0] : [0.4] : [0.4]), ^{1}H NMR analysis of the crude reaction mixture after 30 minutes revealed that the polymerisation of NIPAm was incomplete (Figure 4.5). Through integrating the vinyl protons (5.6 ppm) against the isopropyl methine proton present in both the monomer and the polymer (3.9 ppm), the conversion of NIPAm was determined to be 45 %. Pleasingly, following further sampling of the reaction, it was found that near-quantitative conversion (98 %) had been attained within 1 hour (Figure 4.5).

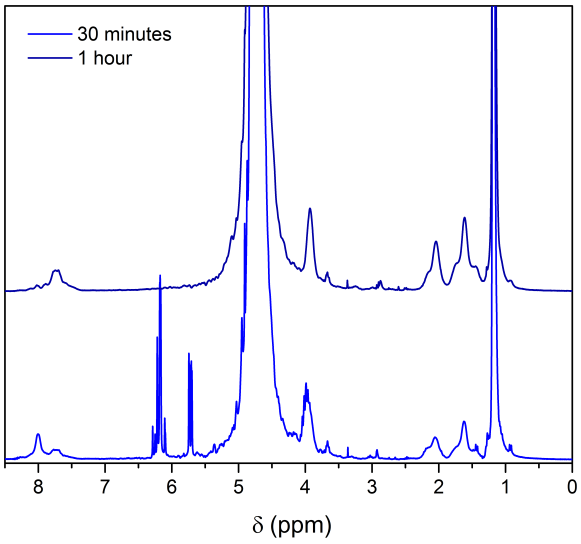

Figure 4.5 - The ^{1}H NMR spectra for the polymerisation of NIPAm utilising compound (1) as the initiator. Conditions: [NIPAm] : [I] : [$Cu^{(I)}Br$] : [Me_6TREN] = [20] : [1.0] : [0.8] : [0.4].

Since the aqueous $Cu^{(0)}$-mediated RDRP protocol is dependent upon the disproportionation of a $Cu^{(I)}$ species into $Cu^{(II)}$ and $Cu^{(0)}$,[7,58] it was reasonable to assume that an increase in $Cu^{(I)}Br$ led to a higher concentration of deactivating species. This in turn resulted in a shift of the polymerisation equilibrium to the left, such that the formation of dormant chains was favoured over the generation of active radicals. Given the nature of TMM-RDRPs, this explained why a lower k_p was observed for the polymerisation of NIPAm in the presence of 0.8 eq. $Cu^{(I)}Br$.

The SEC results that were obtained following the polymerisation highlighted a significantly closer agreement between the experimental (M_n = 2700 g mol^{-1}) and

theoretical (M_n = 2500 g mol^{-1}) molecular weights (Figure 4.6). In addition to this, the data revealed a narrowing of the MWD ($Đ_m$ = 1.11) (Figure 4.6), and minimal tailing in the low molecular weight region. Therefore, it was concluded that a controlled radical polymerisation of NIPAm had been realised under these conditions.

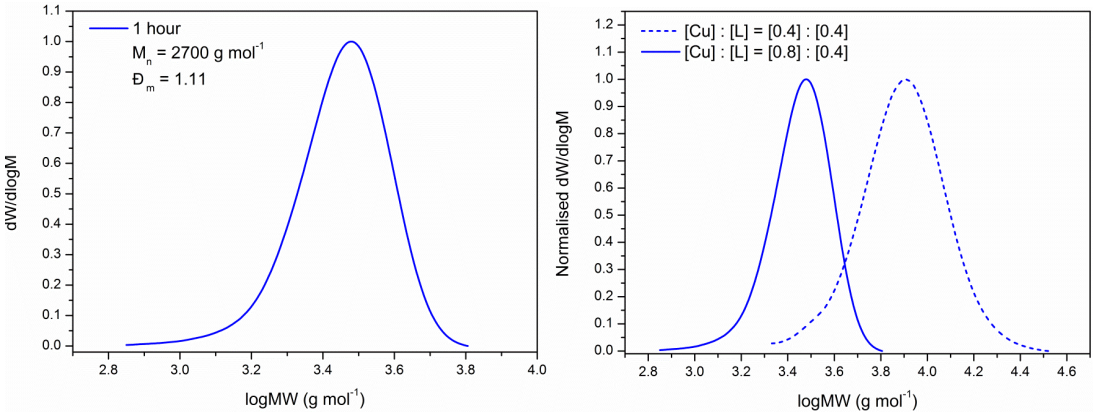

Figure 4.6 – The SEC chromatogram for the polymerisation of NIPAm using compound (1) as the initiator. Conditions: [NIPAm] : [I] : [$Cu^{(I)}$Br] : [Me_6TREN] = [20] : [1.0] : [0.8] : [0.4] (left). Comparison of the SEC chromatograms for the polymerisation of NIPAm using compound (1) as the initiator. The solid line (—) represents [$Cu^{(I)}$Br] : [L] = [0.4] : [0.4]; M_n = 2700 g mol^{-1} and $Đ_m$ = 1.11. The dashed line (- - -) represents [$Cu^{(I)}$Br] : [L] = [0.8] : [0.4]; M_n = 7200 g mol^{-1} and $Đ_m$ = 1.21 (right).

Perhaps more importantly, the data further discredited the theory that a difference in V_h was the cause of the earlier molecular weight discrepancy, and instead, supported that of the "free ligand" interacting with the initiator. When either quarternisation, or chain transfer to ligand transpires within the early stages of the polymerisation, the most likely outcome is the removal of the –Br end group from either a fraction of the initiating or oligomeric species.[56] As such species are unable to participate in the activation step, this results in a decrease in the I_{eff}, and consequently leads to the production of polymers with higher molecular weights.[59] By lowering the concentration of "free ligand", this effect was negated to such a degree that controlled molecular weights and lower dispersity values were achieved.

4.2.1.2. An investigation into the effect of varying the ligand concentration

For $Cu^{(0)}$-mediated RDRPs which are conducted in organic media, the ligand content can have a detrimental effect upon the polymerisation process.[60] Without careful optimisation of reaction conditions, an inappropriate concentration of ligand can result in slow polymerisations, low conversions, broad MWDs, and a variety of deleterious side events.[47,56,60]

The effects of excess ligand have already been discussed; that is, the interaction of "free ligand" with active species can result in termination events such as radical-radical coupling, chain transfer, and quarternisation.[47,56] However, when the concentration of ligand is too low, there is not enough of the activating species to allow for complete conversion to be attained. Subject to the mechanism, this either stems from a lack of solubilised $Cu^{(I)}$ complex (*i.e.* the activator), or is due to a reduction in both the rate and the extent of disproportionation.[24,61–63] With respect to the latter, this also results in a decrease in the deactivating species and hence, leads to high dispersity values.

The effect of the ligand upon aqueous $Cu^{(0)}$-mediated RDRPs has not been reported to the same extent. Nevertheless, current literature suggests that optimisation of ligand concentration is required for efficient polymerisations,[57,64] and that incomplete disproportionation has been observed in the presence of insufficient ligand.[58]

To further investigate the effect of the ligand concentration upon the polymerisation of acrylamides, a series of reactions were conducted whereby different molar equivalents of Me_6TREN (0.06 eq., 0.1 eq., 0.2 eq., 0.3 eq., 0.4 eq., 0.5 eq., 0.6 eq., 0.7 eq. and 0.8 eq.) were employed for the synthesis of low molecular weight (targeted 2500 g mol^{-1}) PNIPAm (Table 4.2).

Key									
Me_6TREN (eq.)	0.06	0.1	0.2	0.3	0.4	0.5	0.6	0.7	0.8
Conversion: 30 mins (%)	7	7	29	30	45	97	100	100	100
Conversion:24 hours (%)	66	66	68	77	100	97	100	100	100
$M_{n,th}$ ($g\ mol^{-1}$)	1700	1700	1700	1900	2500	2400	2500	2500	2500
$M_{n,SEC}$ ($g\ mol^{-1}$)	2100	2600	2500	2800	2700	4100	4900	4600	4500
$Đ_m$	1.21	1.21	1.21	1.28	1.11	1.09	1.06	1.14	1.12

Table 4.2 – A summary of the results from conducting the aqueous $Cu^{(0)}$-mediated RDRP of NIPAm in the presence of a variety (0.06 eq., 0.1 eq., 0.2 eq., 0.3 eq., 0.4 eq., 0.5 eq., 0.6 eq., 0.7 eq. and 0.8 eq.) of ligand concentrations. Other conditions: [M] : [I] : [$Cu^{(I)}Br$] = [20] : [1.0] : [0.8].

The results that were obtained from the experiments were in agreement with the existing literature (Table 4.2; Figure 4.7). At low ligand loading levels (<0.4 eq.) the rate of polymerisation was found to be slow, with incomplete monomer conversion being observed after 24 hours. Increasing the concentration of ligand to 0.4 eq. resulted in quantitative monomer conversion being attained overnight. However, the polymerisation failed to reach completion with the time-frame that is typical for the aqueous protocol (30 minutes). By employing >0.5 eq. of ligand, either near-quantitative, or quantitative conversion was attained within 30 minutes.

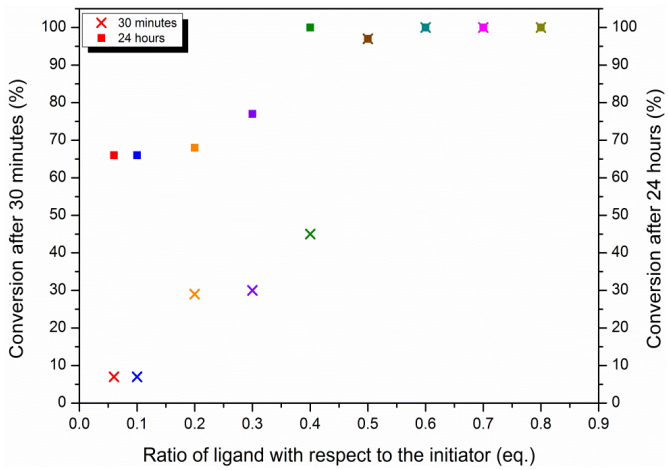

Figure 4.7 – A comparison of the % conversion attained when differing concentrations of Me_6TREN were employed for the polymerisation of NIPAm. Other conditions: [M] : [I] : [$Cu^{(I)}Br$] = [20] : [1.0] : [0.8].

Notably, the data suggested that in the absence of an alternative initiator to compound **(1)**, the polymerisation of NIPAm should be conducted in the presence of 0.8 eq. $Cu^{(I)}Br$. In addition to this, Me_6TREN should be employed in a ≥0.5 eq. with respect to the initiator, as the polymerisations were found to be comparatively faster than those which were conducted with ≤ 0.4 eq.

Analysis of the resulting polymers by SEC revealed that ligand loading levels of ≤0.3 eq. produced comparatively broad MWDs ($Đ_m$ = 1.21 to 1.28) with lower than predicted M_n values (Table 4.2; Figure 4.8). By taking into consideration the poor conversions and the small loss of polymerisation control, it was subsequently concluded that these ligand concentrations were indeed inappropriate for the $Cu^{(0)}$-mediated RDRP of NIPAm initiated by compound **(1)**.

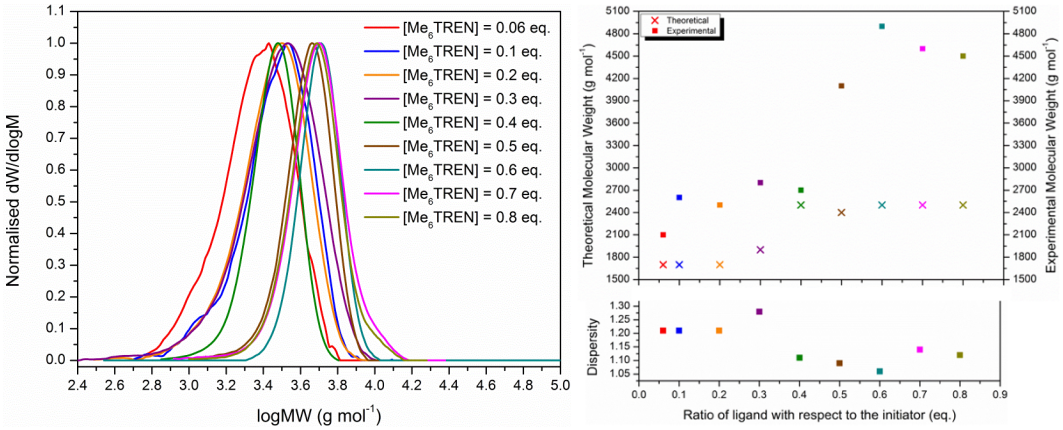

Figure 4.8 - A comparison of the SEC chromatograms (left) and a comparison of the dispersity, theoretical molecular weight ($M_{n,th}$) and experimental molecular weight ($M_{n,SEC}$) (right) resulting from the synthesis of PNIPAm in the presence of differing ligand concentrations (0.06 eq., 0.1 eq., 0.2 eq., 0.3 eq., 0.4 eq., 0.5 eq., 0.6 eq., 0.7 eq. and 0.8 eq.).

Upon using ≥0.5 eq. of Me_6TREN, a significant disagreement between the theoretical and experimental molecular weights was observed. It was deemed unlikely that this discrepancy resulted from radical-radical coupling as the accompanying dispersity values were low. Instead, due to the relatively high concentration of ligand, it was reasoned that side reactions with "free ligand" had arisen within the early stages of the polymerisation. The resultant lowering of the

initiator efficiency therefore led to the production of polymer chains with undesirable molecular weights.

Notably, the SEC results suggested that, contrary to the earlier suggestion, ≥0.5 eq. of Me_6TREN should not be employed for the $Cu^{(0)}$-mediated RDRP of NIPAm when compound **(1)** is the initiating species. Rather, if the slower polymerisation rate is deemed to be acceptable, a copper/ligand ratio of [Me_6TREN] : [$Cu^{(I)}$Br] = [0.4] : [0.8] should be used.

4.2.1.3. Summary of the investigation into the use of compound (1) as the initiator

Whilst the lack of commercially availability makes compound **(1)** unsuitable for use in an "off the shelf" polymerisation, its success and prolific documentation means that it may still find employment by some as the initiating species in aqueous $Cu^{(0)}$-mediated RDRPs. Therefore, to further the information relating to its use for the polymerisation of NIPAm, an investigation was carried out.

Under "standard conditions" ([NIPAm] : [I] : [$Cu^{(I)}$Br] : [Me_6TREN] = [20] : [1.0] : [0.4] : [0.4]), a significant disagreement was observed between the theoretical (2500 g mol^{-1}) and experimental (7200 g mol^{-1}) molecular weights. This was attributed to the presence of "free ligand" in the system, and its interaction with the initiating species. Upon increasing the concentration of $Cu^{(I)}$Br, the molecular weight discrepancy reduced.

Using these partially optimised conditions, the effect of ligand concentration upon the polymerisation of NIPAm was probed. The data suggested that a 0.4 eq. of Me_6TREN was the most optimal as it enabled for high conversion (>99 %), a narrow MWD ($Đ_m$ = 1.11), and a closer agreement between theoretical (2500 g mol^{-1}) and experimental (2700 g mol^{-1}) molecular weights to be attained.

4.2.2. Using 2-bromo-N-(2,3-dihydroxypropyl)-2-methylpropanamide as the initiator for aqueous $Cu^{(0)}$-mediated RDRPs

In addition to the lack of commercial availability and the resultant need for organic synthesis, a pitfall of using compound **(1)** is the potential loss of the dihydroxy-functional group upon hydrolysis.[65] Given the slight acidity of the polymerisation media,[8] the most likely mechanistic route was that of acid-catalysed hydrolysis (Scheme 4.3).

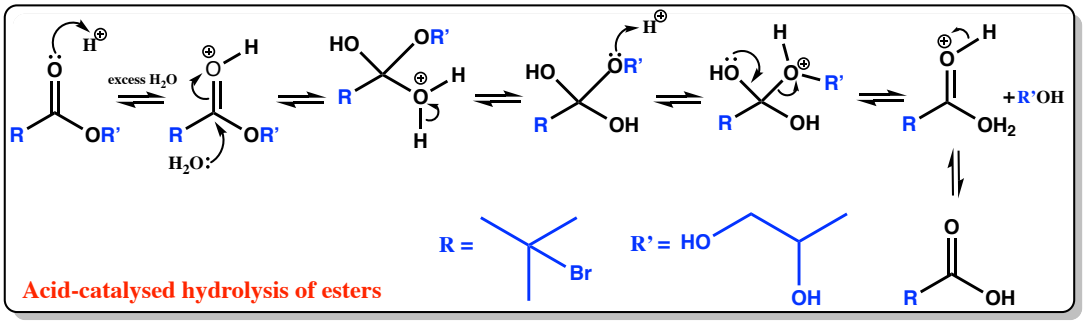

Scheme 4.3 – The mechanism for the acid-catalysed hydrolysis of ester-based compounds. The R groups for compound (1) have been highlighted in blue.

As amines are poor leaving groups, amide-based compounds are more stable towards hydrolysis than their ester analogues (Chapter 1, Section 1.5.5.2.).[66] Regardless of this, their use in copper-mediated RDRPs has proven to be problematic, with polymerisations often resulting in low conversions, radical-radical coupling, broad MWDs, and a loss of molecular weight predictability.[51,67–69] The observed lack of polymerisation control has been attributed to a number of factors, including complexation of the –NH bond with copper species[70,71] and difficulty in generating the primary radical as a result of a high bond dissociation energy (BDE) (Chapter 1, Section 1.5.5.2.).[72]

Work conducted by Holder *et al.* suggested that the high BDE stemmed from a strengthening of the C-Br bond and was as a consequence of intramolecular hydrogen bonding.[72] Single point energy calculations highlighted that the use of

ethanol reduced the BDE and enabled for easier cleavage of the carbon-halide bond. As ethanol is a polar, protic solvent, the lowering of the BDE was attributed to hydrogen bonding with the solvent interrupting the intramolecular hydrogen bonds.[73]

Given that water is also a polar, protic solvent, it was reasoned that the aqueous Cu$^{(0)}$-mediated RDRP protocol might allow for controlled polymerisations to be achieved with amide initiators. Thus, in an effort to minimise the loss of functionality and to provide a direct comparison between initiating species, the amide analogue of compound **(1)** (2-bromo-*N*-(2,3-dihydroxypropyl)-2-methylpropanamide (Figure 4.3, compound **(2)**)) was employed for the polymerisation of NIPAm (Scheme 4.4). As compound **(2)** has not previously been used as the initiator in any TMM-RDRP technique, optimisation of the reaction conditions, or more specifically that of the copper/ligand ratio, was required.

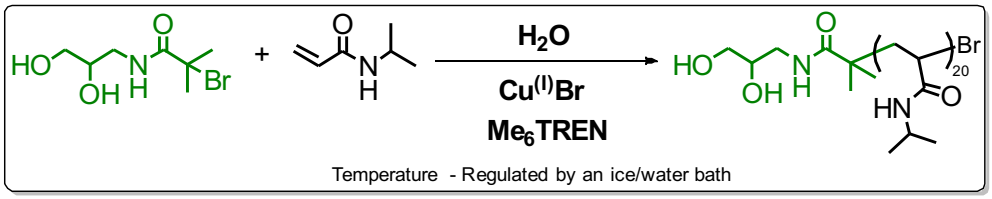

Scheme 4.4 – A schematic representation of the aqueous Cu$^{(0)}$-mediated RDRP of NIPAm initiated by compound (2).

4.2.2.1. Initial polymerisations with compound (2)

Under "standard conditions", it was found that the polymerisation of NIPAm had proceeded to complete conversion within 30 minutes, as determined by ^{1}H NMR spectroscopy (Figure 4.9). Further analysis of the resulting polymer by SEC revealed a mono-modal MWD, with only a slight amount of tailing in the high molecular weight region. Whilst the dispersity value was relatively low ($Đ_m$ = 1.21), a disagreement between the experimental (3600 g mol^{-1}) and the theoretical molecular weight values (2500 g mol^{-1}) was observed (Figure 4.9).

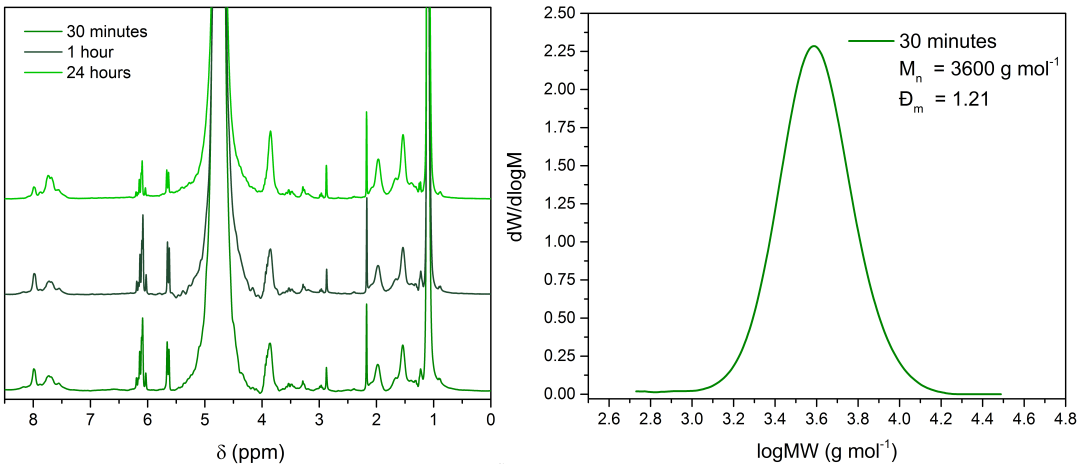

Figure 4.9 - The ^{1}H NMR spectra for the initial polymerisation of NIPAm using compound (2) as the initiator (left). The SEC chromatogram for the initial polymerisation of NIPAm using compound (2) as the initiator (right). Conditions: [NIPAm] : [I] : [$Cu^{(I)}Br$] : [Me_6TREN] = [20] : [1.0] : [0.4] : [0.4].

Considering the copper/ligand ratio and hence the presence of "free ligand", it was reasoned that there had been a loss of end group functionality from a proportion of the initiating units. This consequently led to a reduction of the initiator efficiency and resulted in the production of polymers with higher than the targeted molecular weights. Irrespective of this, the low dispersity value implied that there was a notable level of efficiency to the propagation process.

The molecular weight discrepancy was less pronounced than it was for compound **(1)**, suggesting that compound **(2)** was more efficient at initiating the polymerisation of NIPAm. Unfortunately, due to peak overlap in the ^{1}H NMR spectrum, a more definitive evaluation of the initiator efficiency was not obtained.

With the aim of improving the agreement between molecular weight values, the concentration of $Cu^{(I)}Br$ was increased to 0.8 eq. with respect to the initiator. Unsurprisingly, considering the increase in deactivating species, sampling of the crude reaction mixture after 30 minutes indicated that the polymerisation had not reached completion. Contrary to compound **(1)**, allowing the reaction to continue overnight did not result in quantitative monomer conversion (70 % conversion, t = 24 hours) (Figure 4.10). Evaluation of the reaction by SEC highlighted a deviation

from the targeted molecular weight, with the experimental M_n being recorded as 3000 g mol^{-1} rather than the predicted 1800 g mol^{-1} (Figure 4.10). Nevertheless, the resulting MWD was found to be narrow ($Đ_m$ = 1.10), and was in line with literature relating to the aqueous protocol.[1,4,7]

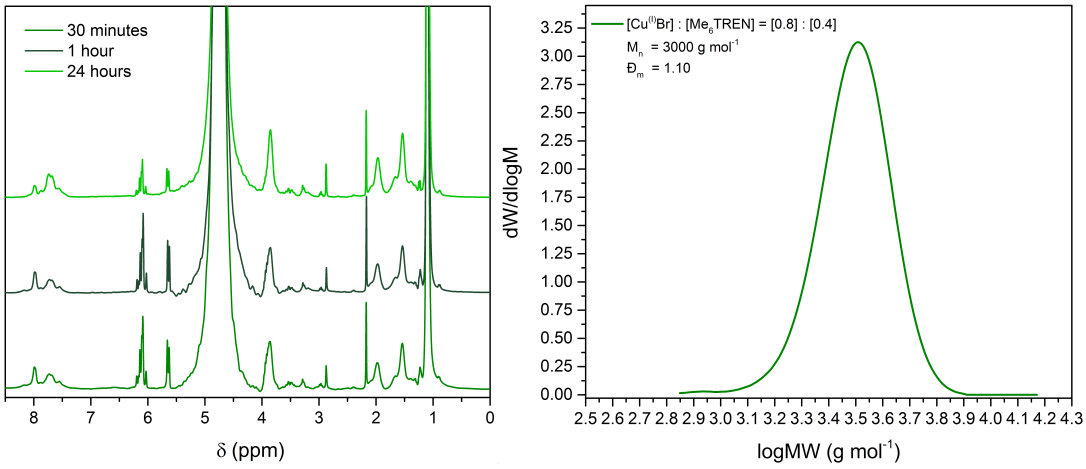

Figure 4.10 - The ^{1}H NMR spectra for the initial polymerisation of NIPAm using compound (2) as the initiator (left). The SEC chromatogram for the initial polymerisation of NIPAm using compound (2) as the initiator (right). Conditions: [NIPAm] : [I] : [Cu$^{(I)}$Br] : [Me$_6$TREN] = [20] : [1.0] : [0.8] : [0.4].

The incomplete conversion and slow rate of polymerisation implied that the issues with molecular weight discrepancy rested with the activation step rather than the presence of "free ligand". Indeed, considering the increase in Cu$^{(I)}$Br and the findings in Section 1.4.2.2, it was deemed unlikely that the concentration of "free ligand" was high enough to have had any noticeable impact upon the initiator efficiency or the polymerisation process in general.

In Section 1.4.2.1. it was theorised that an increase in Cu$^{(I)}$Br led to an increase in the concentration of deactivating species. When combined with the Cu$^{(II)}$Br$_2$ that was produced from unavoidable chain termination, this would have shifted the dynamic equilibrium such that the deactivation step was favoured over the activation of dormant species. This in turn would have caused a decrease in the rate of both activation and propagation, and resulted in low conversion after 24 hours. Given the

comparative difficulty in generating primary radicals from amide species, the effect of this was more pronounced for compound **(2)** than it was for compound **(1)**.

To increase the rate of polymerisation, the concentration of ligand was increased to 0.6 eq. with respect to the initiator (polymerisation conditions [M] : [I] : [$Cu^{(I)}Br$] : [Me_6TREN] = [20] : [1.0] : [0.8] : [0.6]). Characterisation by ^1H NMR spectroscopy revealed that quantitative conversion had been achieved within 30 minutes (Figure 4.11). Ensuing analysis by SEC found the resulting polymers to be narrowly disperse ($Đ_m$ = 1.10), with close agreement between the theoretical (2500 g mol^{-1}) and experimental (3000 g mol^{-1}) molecular weights (Figure 4.11). This therefore highlighted the controlled nature of the polymerisation and further strengthened the suggestion that compound **(2)** was a more efficient initiator than compound **(1)**.

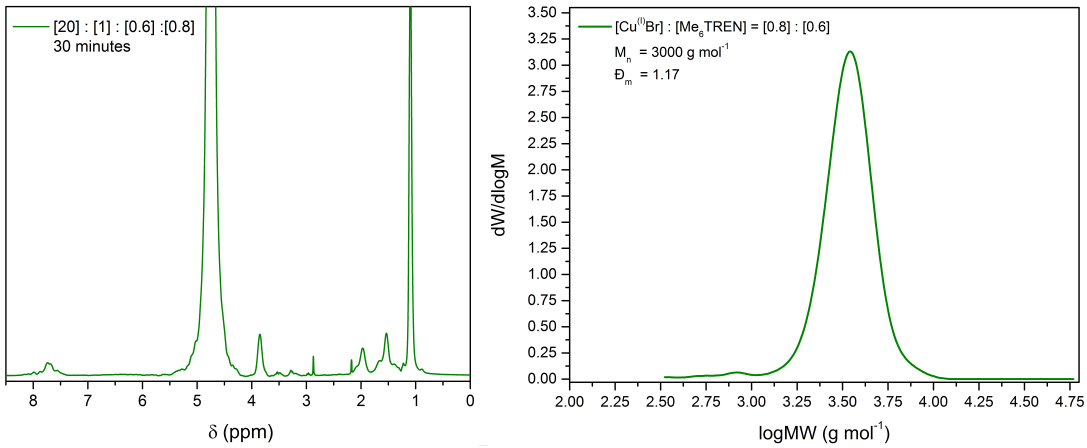

Figure 4.11 - The ^1H NMR spectrum for the initial polymerisation of NIPAm using compound (2) as the initiator (left). The SEC chromatogram for the initial polymerisation of NIPAm using compound (2) as the initiator (right). Conditions: [NIPAm] : [I] : [$Cu^{(I)}Br$] : [Me_6TREN] = [20] : [1.0] : [0.8] : [0.6].

Attempts at conducting kinetic studies revealed that complete monomer conversion had been attained within 30 seconds rather than the previously assumed 30 minutes, according to ^1H NMR spectroscopy. Interestingly, this arose without any appreciable loss of dispersity control ($Đ_m$ = 1.13; Figure 4.12).

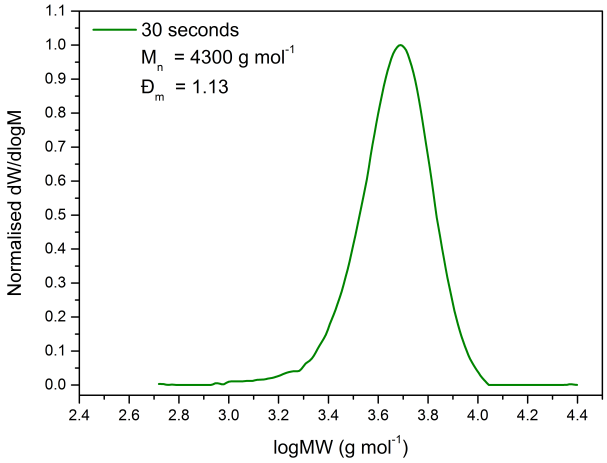

Figure 4.12 - The SEC chromatogram produced after sampling the polymerisation of NIPAm using compound (2) after 30 seconds. Conditions: [NIPAm] : [I] : [$Cu^{(I)}$Br] : [Me_6TREN] = [20] : [1.0] : [0.8] : [0.6].

Initially, a high disparity between the molecular weight values was observed (Table 4.3). This was found to decrease upon allowing the polymerisation to continue for a further 2.5 minutes, as evidenced by the noticeable shift in the SEC distribution (Figure 4.13).

Initiator	Time (minutes)	Conversion (%)	$M_{n,th}$	$M_{n,SEC}$	$Đ_m$
compound (2)	0.5	100	2500	4300	1.13
compound (2)	1	100	2500	4100	1.16
compound (2)	3	100	2500	3400	1.14

Table 4.3 – The data from the attempted kinetic study of the polymerisation of NIPAm using compound (2). Conditions: [NIPAm] : [I] : [$Cu^{(I)}$Br] : [Me_6TREN] = [20] : [1.0] : [0.8] : [0.6].

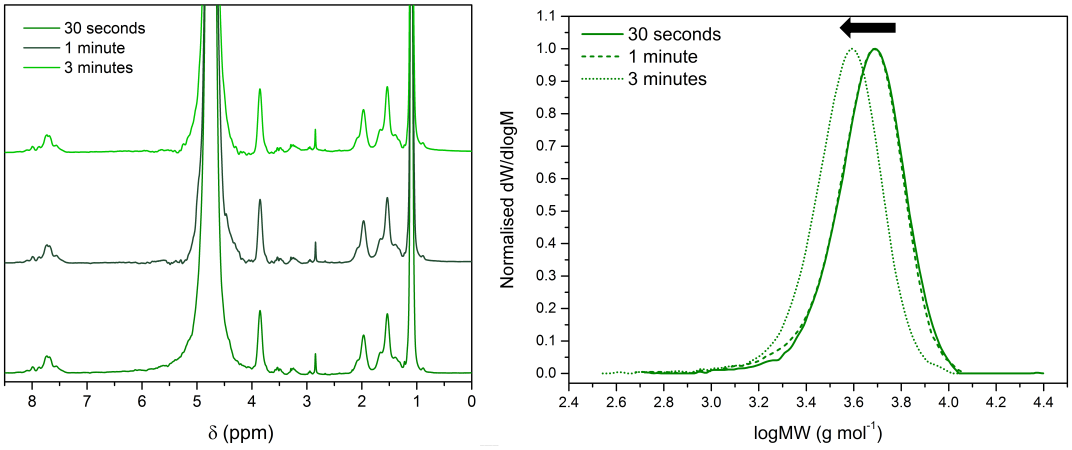

Figure 4.13 – The ^{1}H NMR spectra (left) and SEC chromatograms (right) for the attempted kinetic study of the polymerisation of NIPAm using compound (2). Conditions: [NIPAm] : [I] : [$Cu^{(I)}$Br] : [Me_6TREN] = [20] : [1.0] : [0.8] : [0.6].

To further explore the degree of control obtained under these conditions, the polymers were analysed utilising MALDI-ToF MS (Figure 4.14). Notably, only one major distribution was detected, which corresponded to the sodium adduct of ω-hydroxy-terminated PNIPAm initiated by compound **(2)**. Moreover, whilst peaks attributable to side products were observed, these were of low concentration in comparison to the main peaks. Unfortunately, the data suggested that there had been a complete loss of –Br end-group functionality, as the majority of chains were found to be terminated by hydroxyl groups. Given the nature of the reaction medium, this may have occurred during the "work-up" stage.

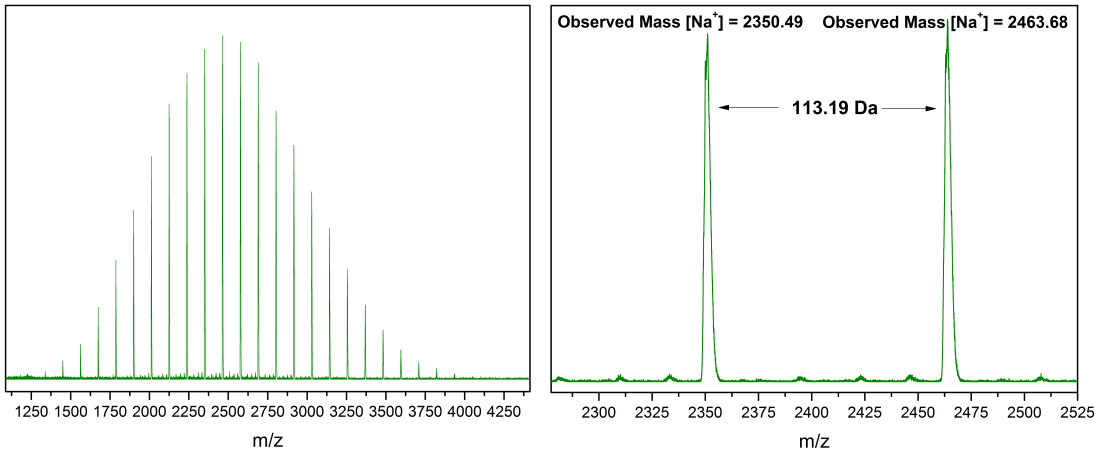

Figure 4.14 – MALDI-ToF MS analysis of the polymer resulting from the attempted kinetic study of the polymerisation of NIPAm using compound (2). Conditions: [NIPAm] : [I] : [$Cu^{(I)}$Br] : [Me_6TREN] = [20] : [1.0] : [0.8] : [0.6].

In Section 4.2.1.2, the same conditions were employed for the polymerisation of DP = 20 NIPAm with compound **(1)** as the initiating species ([$Cu^{(I)}$Br] : [Me_6TREN] = [0.8] : [0.6]) (Table 4.2). However, there was less control over the molecular weight; this was illustrated by the disparity between SEC traces (Figure 4.15).

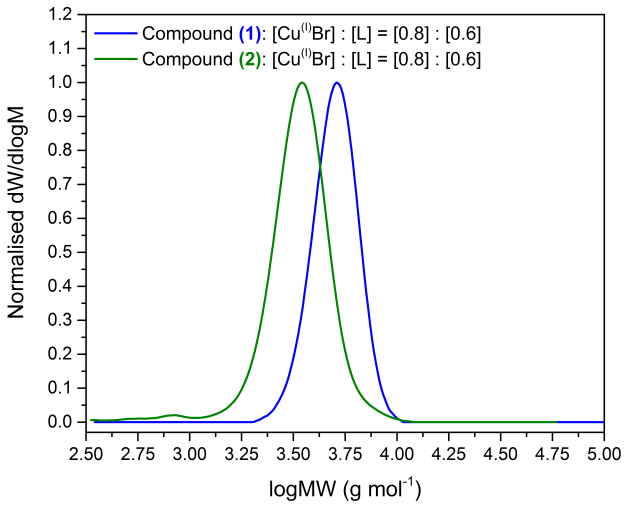

Figure 4.15 – A comparison of the SEC chromatograms resulting from the polymerisation of NIPAm using compound (2) and compound (1). Conditions: [NIPAm] : [I] : [$Cu^{(I)}Br$] : [Me_6TREN] = [20] : [1.0] : [0.8] : [0.6].

In order to provide a direct comparison between the two initiators, MADLI-ToF MS was conducted on PNIPAm synthesised under the following conditions: [NIPAm] : [compound **(1)**] : [$Cu^{(I)}Br$] : [Me_6TREN] = [20] : [1.0] : [0.8] : [0.6] (Figure 4.16). Upon analysis of the data, multiple and complex mass distributions were revealed. As only a single distribution was observed for compound **(2)**, it was theorised that a greater level of control had been achieved with the amide initiator.

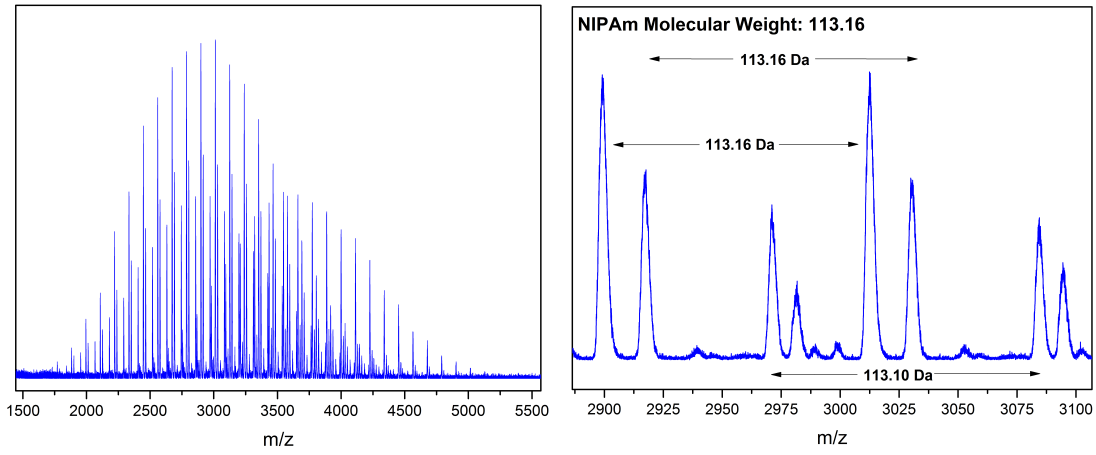

Figure 4.16 - MALDI-ToF MS analysis of the polymer resulting from the attempted kinetic study of the polymerisation of NIPAm using compound (1). Conditions: [NIPAm] : [I] : [$Cu^{(I)}Br$] : [Me_6TREN] = [20] : [1.0] : [0.8] : [0.6].

The major distributions that were observed were found to correspond to the sodium adduct of ω-eliminated PNIPAm initiated by compound **(1)**; the sodium adduct of ω-

hydroxy-terminated PNIPAm initiated by compound **(1)**; and the potassium adduct of ω-hydroxy-terminated PNIPAm with the α-chain end possessing the hydrolysis product of compound **(1)**.

As with the data that was obtained from compound **(2)**, the MALDI-ToF MS spectrum indicated that there was an absence of bromine functionality on the ω-chain ends. Since the ability to perform "*in-situ*" chain extensions with polymers synthesised by this route has been well-documented,[1,4,5,23,42] the presence of hydroxy-terminated chain ends was attributed to the occurrence of hydrolysis during the "work-up" and/or sample preparation stages.

It is worth noting that one of the distributions was assigned to "the potassium adduct of ω-hydroxy-terminated PNIPAm with the α-chain end possessing the hydrolysis product of compound **(1)**". This assignment represented the proportion of compound **(1)** which had undergone hydrolysis to form acid terminated α-chain ends (Scheme 4.2). Given that this was not detected for compound **(2)** (Figure 4.17), these results also illustrated the greater susceptibility of ester-based compounds towards hydrolysis and the retention of α-chain end functionality for amide-based compounds.

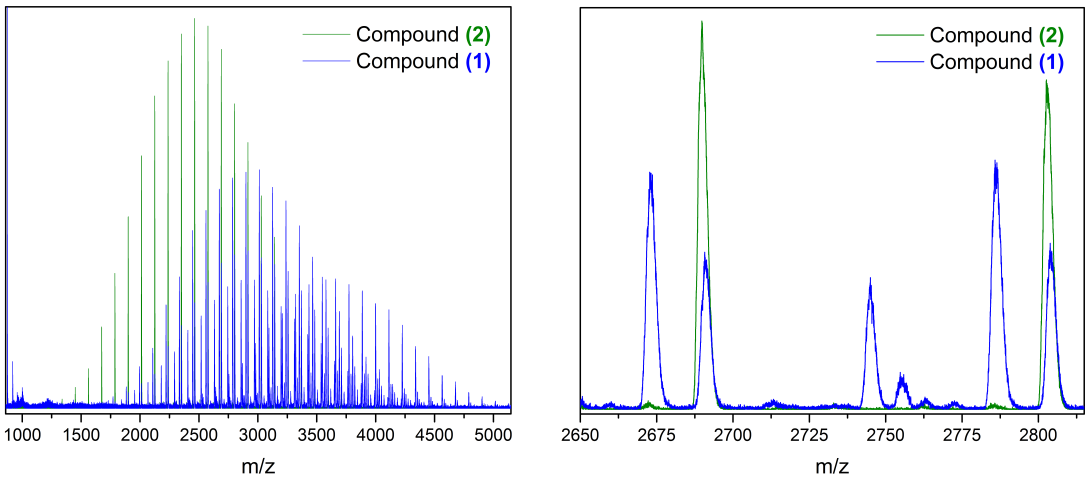

Figure 4.17 – A comparison of the MALDI-ToF MS spectra obtained for PNIPAm initiated by compound (1) and compound (2). Conditions: [NIPAm] : [I] : [$Cu^{(I)}Br$] : [Me_6TREN] = [20] : [1.0] : [0.8] : [0.6].

4.2.2.2. Summary of the investigation into the use of compound (2) as the initiator

2-Bromo-*N*-(2,3-dihydroxypropyl)-2-methylpropanamide (Figure 4.3, compound **(2)**) was screened as the initiator for the aqueous $Cu^{(0)}$-mediated RDRP of NIPAm. During these polymerisations, the copper/ligand ratio was varied to optimise the polymerisation conditions. Employing a copper/ligand ratio of 0.8 eq. to 0.6 eq. enabled for rapid and quantitative conversions (t = 3 minutes; 100 % conversion) and relatively controlled polymerisations (M_n = 3400 g mol^{-1}; $Đ_m$ = 1.14) to be obtained.

However, upon further characterisation by MADLI-ToF MS, a complete loss of end group fidelity was detected. Interestingly, the presence of hydroxy-terminated chain ends was also observed when polymers were synthesised under the same conditions ([$Cu^{(I)}Br$] : [Me_6TREN] = [0.6] : [0.8]) with compound **(1)**. Given that the aqueous protocol has been utilised for the "*in-situ*" synthesis of co-polymers,[1,4,5,23,42] the absence of bromine-terminated chain ends was not considered to be indicative of poor polymerisation control.

Unfortunately, since compound **(2)** is a novel initiator, it is not commercially available. As with compound **(1)**, its production requires the user to perform organic synthesis and a lengthy purification procedure. For this reason, it was decided that further investigation into the use of compound **(2)** would not be undertaken as, regardless of the results, it is unsuitable for use in an "off the shelf" polymerisation.

4.2.3. Using 2-bromo-N-(2-hydroxyethyl)-2-methylpropanamide as the initiator for aqueous $Cu^{(0)}$-mediated RDRPs

Using compound **(2)** as the initiating species rapidly resulted in high conversions, polymers with predictable molecular weights, low dispersity values, and single mass distributions. The use of amide-based compounds as initiators for copper-mediated RDRPs was therefore deemed to be feasible with the aqueous $Cu^{(0)}$-mediated RDRP methodology.

In a step towards the development of an "off the shelf" polymerisation, 2-bromo-*N*-(2-hydroxyethyl)-2-methylpropanamide (Figure 4.3, compound **(3)**) was chosen as a prospective replacement for compound **(1)** and screened for the polymerisation of NIPAm *via* the aqueous $Cu^{(0)}$-mediated RDRP protocol (Scheme 4.5).

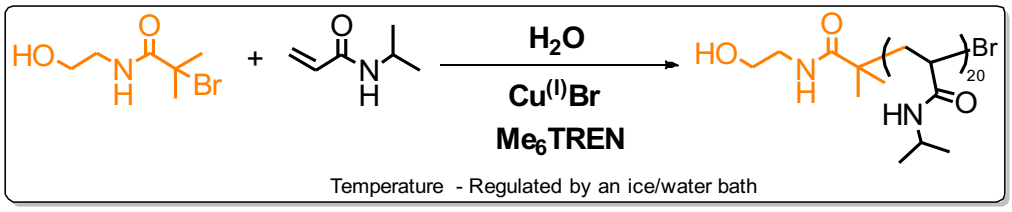

Scheme 4.5 - A schematic representation of the aqueous $Cu^{(0)}$-mediated RDRP of NIPAm initiated by compound (3).

4.2.3.1. Initial polymerisations with compound (3)

Initially, the "standard conditions" for a targeted DP = 20 were used for the polymerisation of NIPAm initiated by compound **(3)**. According to ^{1}H NMR spectroscopy, the polymerisation was rapid and reached completion within 30 minutes (Figure 4.18). Contrary to the previous findings, analysis by SEC revealed that the polymerisation lacked both dispersity and molecular weight control ($M_{n,theoretical}$ = 2500 g mol^{-1}; $M_{n,experimental}$ = 4100 g mol^{-1}; $Đ_m$ = 1.38; Figure 4.18).

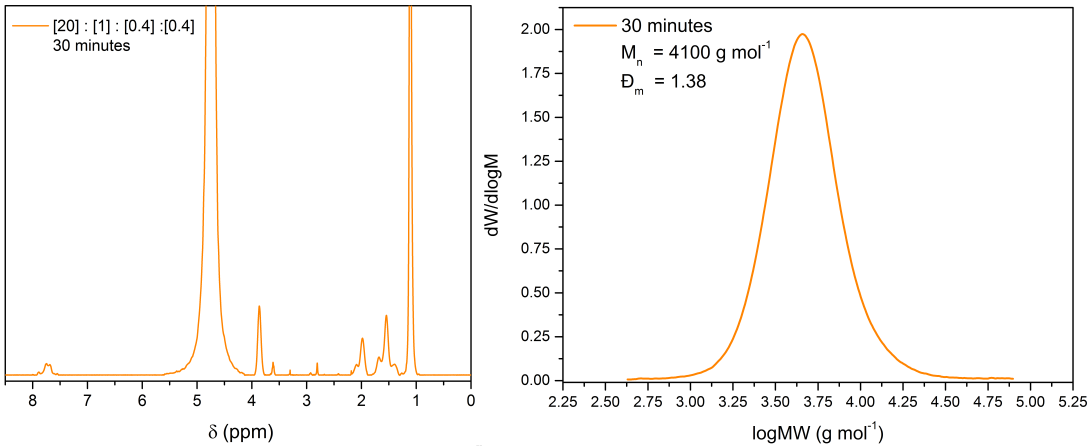

Figure 4.18 - The ^{1}H NMR spectrum for the initial polymerisation of NIPAm using compound (3) as the initiator (left). The SEC chromatogram for the initial polymerisation of NIPAm using compound (3) as the initiator (right). Conditions: [NIPAm] : [I] : [$Cu^{(I)}$Br] : [Me_6TREN] = [20] : [1.0] : [0.4] : [0.4].

Assuming that a higher concentration of copper species would improve control over the polymerisation process, the copper/ligand ratio was altered to [$Cu^{(I)}$Br] : [Me_6TREN] = [0.8] : [0.4]. In line with the previous findings, a decrease in the rate of polymerisation was detected, with a maximum conversion of 87 % being achieved after the polymerisation was left overnight (Figure 4.19). Subsequent characterisation by SEC showed a narrowing of the MWD ($Đ_m$ = 1.20) and a significant improvement in molecular weight predictability ($M_{n,theoretical}$ = 2200 g mol^{-1}; $M_{n,experimental}$ = 3400 g mol^{-1}).

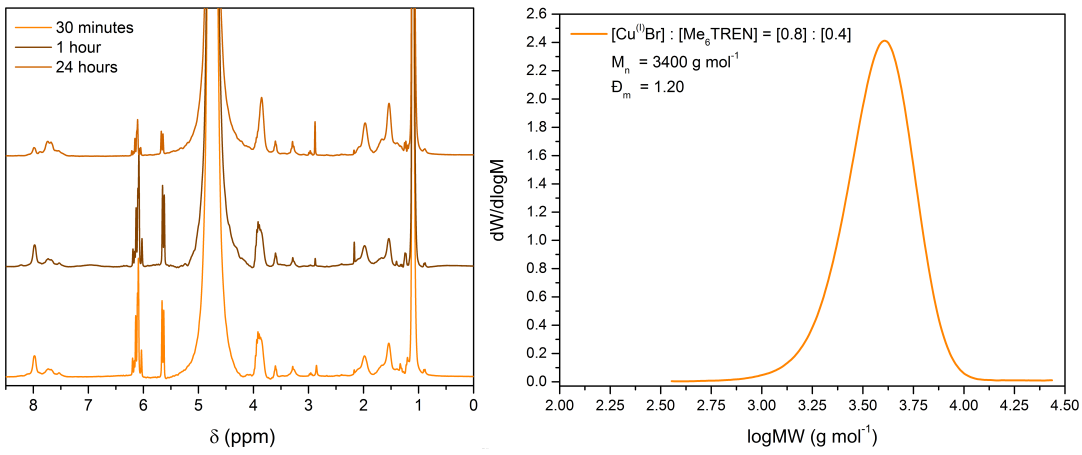

Figure 4.19 - The ^{1}H NMR spectra for the initial polymerisation of NIPAm using compound (3) as the initiator (left). The SEC chromatogram for the initial polymerisation of NIPAm using compound (3) as the initiator (right). Conditions: [NIPAm] : [I] : [$Cu^{(I)}$Br] : [Me_6TREN] = [20] : [1.0] : [0.8] : [0.4].

To increase the rate of polymerisation without compromising control over the resulting polymer, a higher concentration of ligand was employed relative to $Cu^{(I)}Br$ ($[Cu^{(I)}Br] : [Me_6TREN] = [0.8] : [0.6]$). This resulted in full monomer conversion within 30 minutes, and a decrease in the dispersity value ($Đ_m$ = 1.13; Figure 4.20). However, this was not accompanied by a further reduction in the average molecular weight ($M_{n,theoretical}$ = 2500 g mol^{-1}; $M_{n,experimental}$ = 3800 g mol^{-1}). Irrespective of this, it was concluded that a controlled polymerisation was achieved, and that compound **(3)** was a relatively efficient initiator.

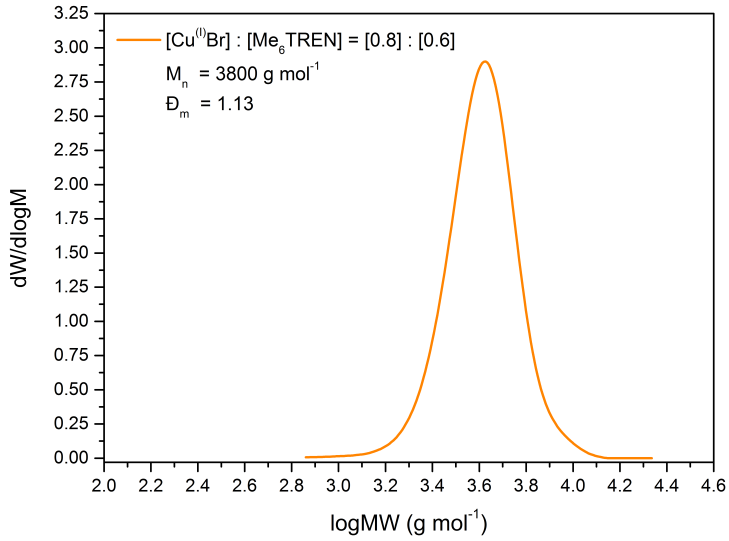

Figure 4.20 - The SEC chromatogram for the initial polymerisation of NIPAm using compound (3) as the initiator. Conditions: [NIPAm] : [I] : $[Cu^{(I)}Br]$: $[Me_6TREN]$ = [20] : [1.0] : [0.8] : [0.6].

In a similar manner to compound **(2)**, the attempted kinetic analysis of the $Cu^{(0)}$-mediated RDRP of NIPAm initiated by compound **(3)** revealed that the polymerisation had reached completion within 30 seconds (Table 4.4; Figure 4.21); this was accomplished without losing control over the size or shape of the MWD ($Đ_m$ = 1.13; Figure 4.21). However, there was a disagreement between the theoretical and experimental molecular weight values according to SEC (Table 4.4). Fortunately, as with compound **(2)**, this discrepancy was found to decrease upon allowing the polymerisation to continue for a total of 3 minutes (Figure 4.21).

Initiator	Time (minutes)	Conversion (%)	$M_{n,th}$	$M_{n,SEC}$	$Đ_m$
compound (3)	0.5	100	2500	5200	1.13
compound (3)	1	100	2500	4200	1.21
compound (3)	3	100	2500	4200	1.13

Table 4.4 – The data from the attempted kinetic study of the polymerisation of NIPAm using compound (3). Conditions: [NIPAm] : [I] : [$Cu^{(I)}Br$] : [Me_6TREN] = [20] : [1.0] : [0.8] : [0.6].

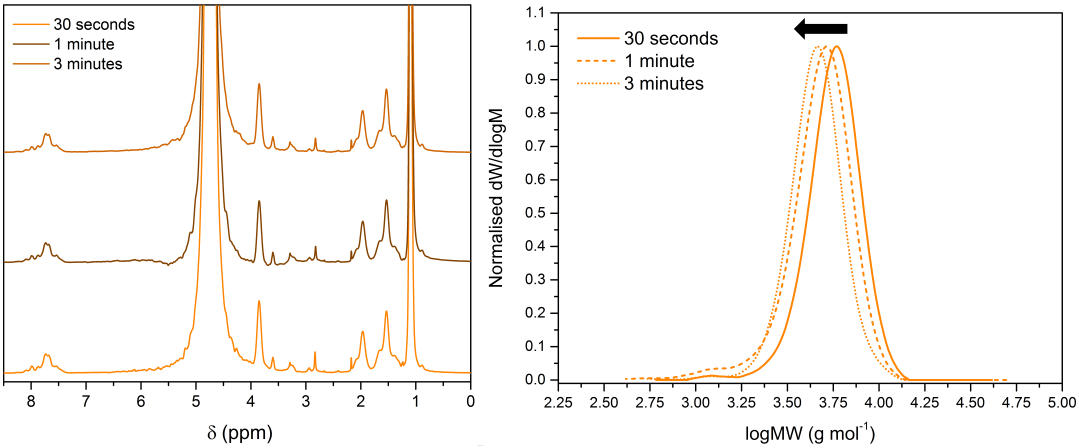

Figure 4.21 - The ^1H NMR spectra (left) and the SEC chromatograms (right) for the attempted kinetic study of the polymerisation of NIPAm using compound (3). Conditions: [NIPAm] : [I] : [$Cu^{(I)}Br$] : [Me_6TREN] = [20] : [1.0] : [0.8] : [0.6].

Upon further analysis of the polymerisation by MALDI-ToF MS, one major and two minor mass distributions were observed (Figure 4.22). The major mass distribution was found to correspond to the sodium adduct of ω-eliminated PNIPAm initiated by compound (3), and one of the minor distributions was assigned to the sodium adduct of ω-hydroxy-terminated PNIPAm initiated by compound (3).

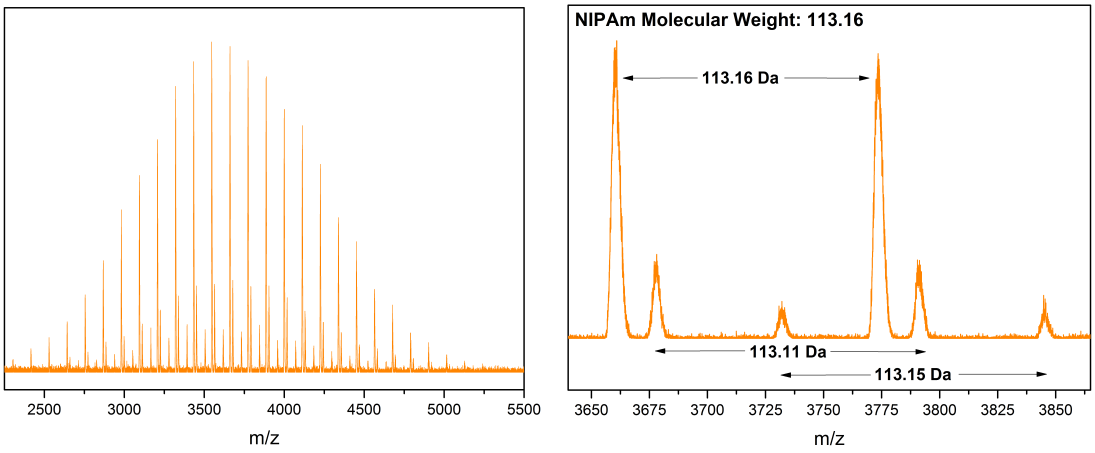

Figure 4.22 - MALDI-ToF MS analysis of the polymer resulting from the attempted kinetic study of the polymerisation of NIPAm using compound (3). Conditions: [NIPAm] : [I] : [$Cu^{(I)}Br$] : [Me_6TREN] = [20] : [1.0] : [0.8] : [0.6].

The presence of multiple mass distributions suggested that compound **(3)** was less suited to the polymerisation of NIPAm than compound **(2)**. Pleasingly, upon comparison of the MADLI-ToF data, the mass spectrum for compound **(3)** was deemed to be less complex than that which was obtained for compound **(1)** (Figure 4.23). This implied that whilst compound **(3)** was less suited to the polymerisation of NIPAm than compound **(2)**, it was still an improvement over compound **(1)**.

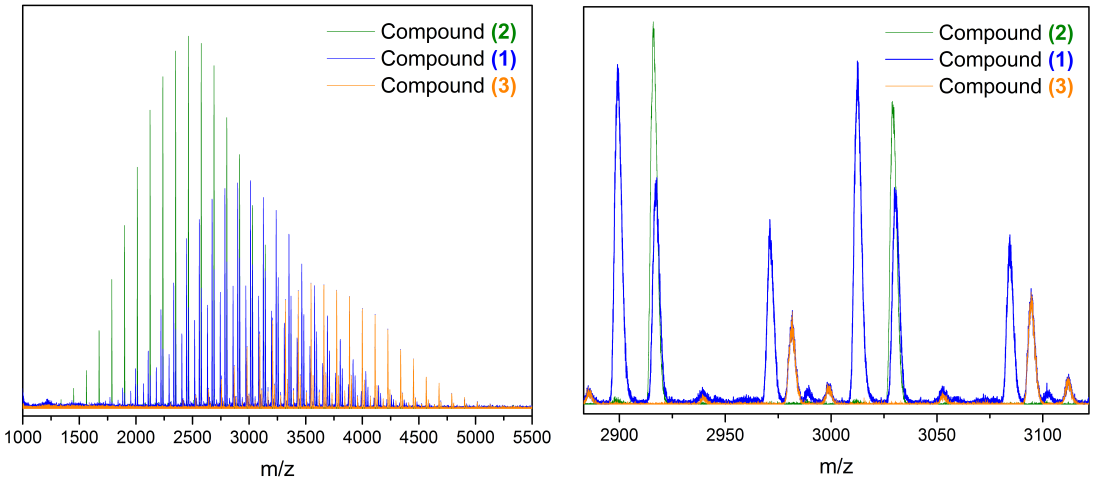

Figure 4.23 – A comparison of the MALDI-ToF MS spectra obtained for PNIPAm initiated by compound (1), compound (2) and compound (3). Conditions: [NIPAm] : [I] : [$Cu^{(I)}Br$] : [Me_6TREN] = [20] : [1.0] : [0.8] : [0.6].

More importantly, the use of compound **(3)** for the synthesis of low molecular weight PNIPAm enabled for low dispersity values, relatively good agreement between molecular weights, and quantitative conversions to be achieved. Given its commercial availability and its simpler synthesis route, it was subsequently concluded that compound **(3)** was a viable alternative to compound **(1)**. As such, further study into its use as the initiator for aqueous $Cu^{(0)}$-mediated RDRPs was undertaken.

4.2.3.2. Polymerising high molecular weight polymers with compound (3)

Targeting higher degrees of polymerisation (DP = 60, 120 and 360), the synthesis of PNIPAm initiated by compound **(3)** was conducted under the previously optimised

conditions ([I] : [L] : [$Cu^{(I)}Br$] = [1.0] : [0.6] : [0.8]). In all cases, very high conversions (≥98 %) were reached within 30 minutes (Table 4.5). For DP = 60 and 120, narrow MWDs ($Đ_m$ = ≤1.23) were obtained (Figure 4.24). Unfortunately, this was accompanied by a discrepancy between the theoretical and experimental molecular weights (Table 4.5). In the case of DP = 360, a broad MWD was observed in addition to a poor correlation between the average M_n values (Figure 4.24; Table 4.5).

Initiator	Targeted DP	Time (minutes)	Conversion (%)	$M_{n,th}$	$M_{n,SEC}$	$Đ_m$
compound (3)	60	30	100	7000	8900	1.23
compound (3)	120	30	100	13,800	17,000	1.22
compound (3)	360	30	98	40,100	52,400	1.32

Table 4.5 – The data obtained from polymerising NIPAm to higher DPs using compound (3). Conditions: [NIPAm] : [I] : [$Cu^{(I)}Br$] : [Me_6TREN] = [Targeted DP] : [1.0] : [0.8] : [0.6].

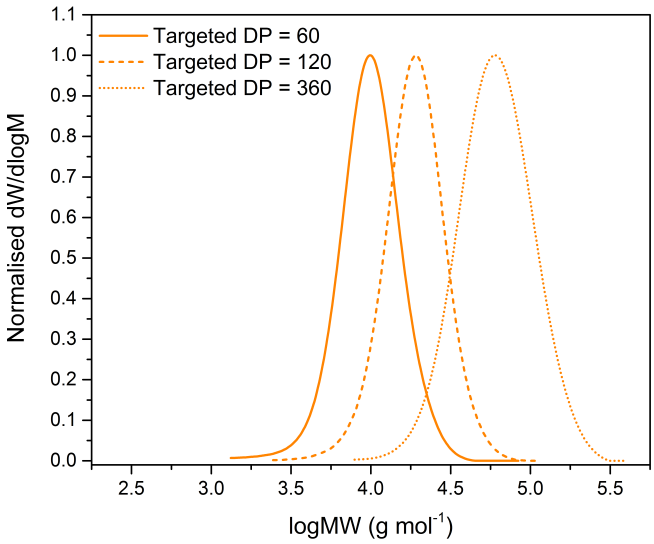

Figure 4.24 – The SEC chromatograms resulting from the polymerisation of NIPAm to differing DPs, initiated by compound (3). Conditions: [NIPAm] : [I] : [$Cu^{(I)}Br$] : [Me_6TREN] = [Targeted DP] : [1.0] : [0.8] : [0.6].

Kinetically monitoring the synthesis of DP = 120 PNIPAm revealed that the polymerisation had occurred at a rapid rate. High conversions were achieved after 1.5 minutes (90%; Table 4.6), with quantitative conversion being reached within a total of 10 minutes (Table 4.6).

Initiator	Time (minutes)	Conversion (%)	$M_{n,th}$	$M_{n,SEC}$	$Đ_m$
compound (3)	0	0	0	0	0
compound (3)	0.5	27	3700	13,600	1.41
compound (3)	1	77	10,600	14,800	1.22
compound (3)	1.5	90	12,400	15,300	1.19
compound (3)	2	94	13,000	15,200	1.26
compound (3)	2.5	96	13,200	14,000	1.20
compound (3)	3	97	13,400	13,400	1.21
compound (3)	3.5	97	13,400	14,500	1.18
compound (3)	4	97	13,400	13,900	1.26
compound (3)	4.5	98	13,500	13,700	1.19
compound (3)	5	99	13,700	15,200	1.17
compound (3)	10	100	-	-	-

Table 4.6 – The data obtained from kinetically monitoring the polymerisation of DP = 120 PNIPAm initiated by compound (3). Conditions: [I] : [$Cu^{(I)}Br$] : [Me_6TREN] = [1.0] : [0.8] : [0.6].

Initially, a significant discrepancy was observed between the theoretical and experimental molecular weights. This was accompanied by a broad MWD and the presence of a low molecular weight tail (Figure 4.25). Given the speed of the reaction and the sub-optimal polymerisation conditions, the initial tailing in the low molecular weight region was taken to be indicative of radical-radical coupling. Pleasingly, despite this, the dispersity value was found to decrease with time, and the average M_n remained relatively stable after 1.5 minutes (Table 4.6; Figure 4.25).

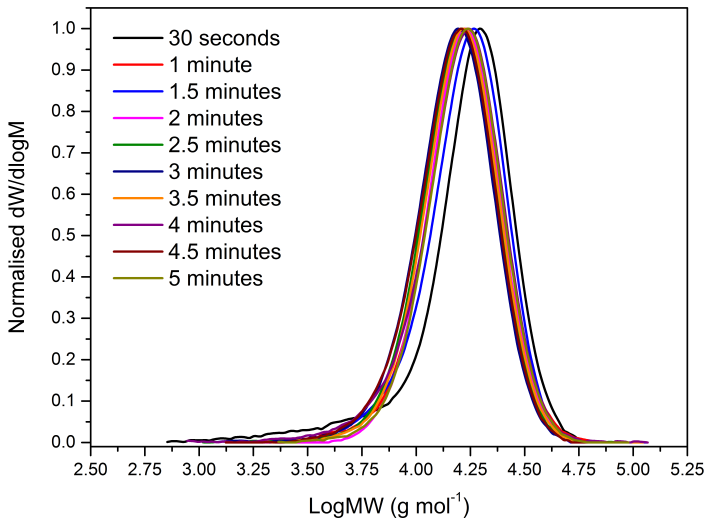

Figure 4.25 - The SEC chromatograms for the attempted kinetic study of the synthesis of DP = 20 PNIPAm using compound (3). Conditions: [I] : [$Cu^{(I)}Br$] : [Me_6TREN] = [1.0] : [0.8] : [0.6].

The plot of time vs. $\ln([M_0]/[M_t])$ indicated that for the first 2.5 minutes, the reaction progressed with a comparatively fast apparent rate of polymerisation (K_p = 1.339 min^{-1}), as expected (Figure 4.26). However, peculiarities were observed over the last 20 % of monomer conversion.

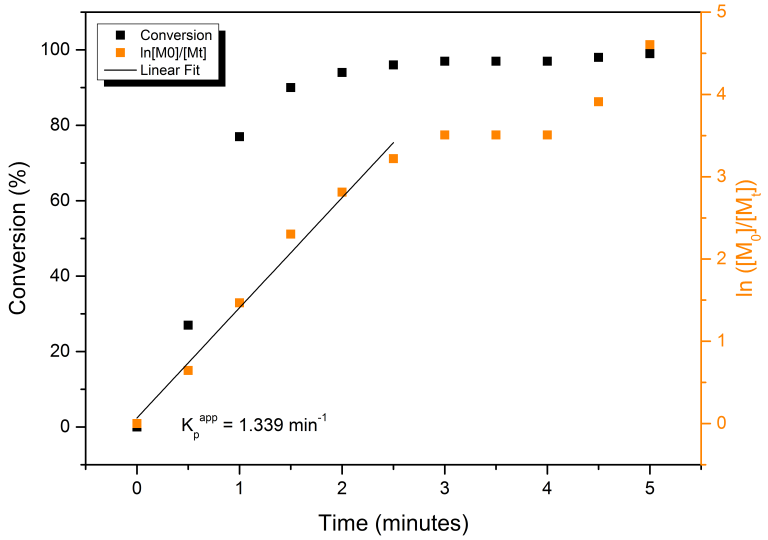

Figure 4.26 – The kinetic data for the polymerisation of DP = 120 PNIPAm initiated by compound (3). Conditions: [NIPAm] : [I] : [$Cu^{(I)}Br$] : [Me_6TREN] = [120] : [1.0] : [0.8] : [0.6].

Importantly, the aim of this work was not to find the ideal polymerisation conditions for a broad range of molecular weights. Rather, it was to investigate whether it was feasible to replace compound **(1)** as the initiating species. This was with the aim of generating a polymerisation system that was less reliant upon reagent preparation. Therefore, it was decided that attempts to improve the molecular weight predictability for DP = 60, 120 and 360 would not be undertaken. Nevertheless, as high conversions and relatively narrow MWDs were achieved, it was believed that the synthesis of high molecular weight polymers with compound **(3)** was a realistic future goal.

4.2.3.3. Expanding the system to other acrylamide monomers

Thus far, compound **(3)** has only been investigated as the initiating species for the aqueous $Cu^{(0)}$-mediated RDRP of NIPAm. Therefore, in an effort to expand this system to other acrylamide-based monomers, the polymerisation of HEAm with a targeted of DP = 20 was attempted (Scheme 4.6). In keeping with the earlier work, three copper/ligand ratios were selected for screening; these were: [$Cu^{(I)}$Br] : [Me_6TREN] = [0.4] : [0.4], [0.8] : [0.4] and [0.8] : [0.6].

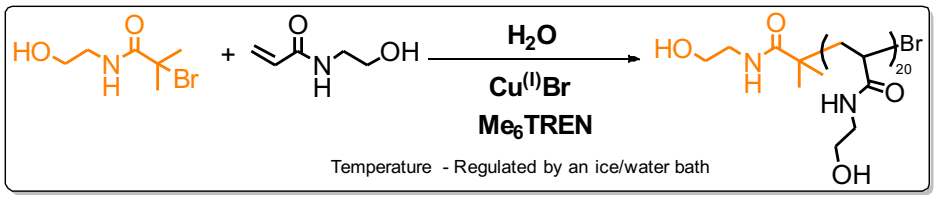

Scheme 4.6 – A schematic representation of the aqueous $Cu^{(0)}$-mediated RDRP OF HEAm initiated by compound (3).

Employing an equimolar and 0.4 eq. of $Cu^{(I)}$Br and ligand resulted in near-quantitative conversion (98 %) and narrow MWDs ($Đ_m$ = 1.23) being attained within 30 seconds (Figure 4.27). As with the previous reactions, control over the average molecular weight of the polymer chains was poor; where the experimental M_n value was found to be double that of the theoretical M_n (Table 4.7). Increasing the concentration of $Cu^{(I)}$Br led to minimal conversion after 24 hours (24 %), broad and non-symmetrical MWDs ($Đ_m$ = 1.30), and similarly poor molecular weight control (Figure 4.27; Table 4.7). As with the polymerisations involving compound **(2)**, this was attributed to inefficient activation.

The addition of more ligand to the polymerisation subsequently resulted in complete conversion, an improvement in molecular weight predictability (Table 4.7), and low dispersity values ($Đ_m$ = 1.20) being reached within 30 seconds (Figure 4.27). As such, it was concluded that the controlled polymerisation of HEAm had been realised with compound **(3)** as the initiating species.

Initiator	[$Cu^{(I)}Br$] : [Me_6TREN]	Time	Conversion (%)	$M_{n,th}$	$M_{n,SEC}$	$Đ_m$
compound (3)	0.4 : 0.4	30 seconds	98	2500	5000	1.23
compound (3)	0.8 : 0.4	24 hours	23	600	1300	1.30
compound (3)	0.8 : 0.6	30 seconds	100	2500	4000	1.20

Table 4.7 – The data obtained from polymerising HEAm using three different copper/ligand ratios and compound (3) as the initiating species.

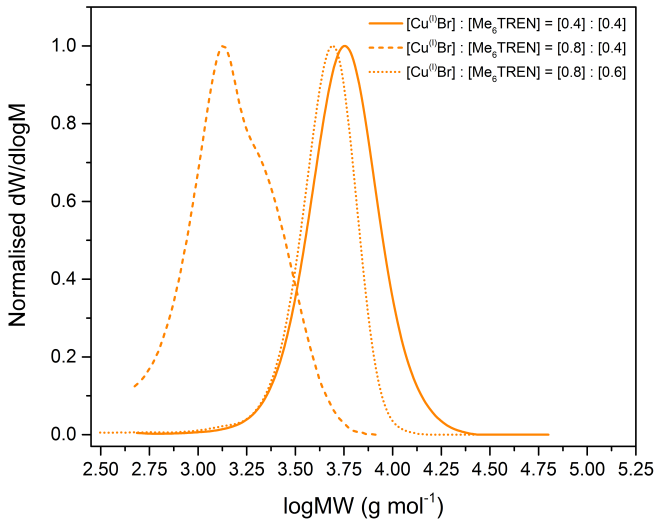

Figure 4.27 – The SEC chromatograms produced from the aqueous $Cu^{(0)}$-mediated RDRP of HEAm utilising compound (3) as the initiating species.

The polymerisation of DEAm was also attempted using compound **(3)** as the initiator (Scheme 4.7). Given the success of [I] : [$Cu^{(I)}Br$] : [Me_6TREN] = [1.0] : [0.8] : [0.6] for the polymerisation of both NIPAm and HEAm, it was decided that the testing of alternative copper/ligand ratios was unnecessary. Indeed, the polymerisation proceeded to completion within 30 minutes, with excellent agreement between the molecular weight values (Table 4.8) and a narrow MWD ($Đ_m$ = 1.13; Figure 4.28). Therefore, the polymerisation of DEAm under these conditions was also reasoned to have occurred in a controlled manner.

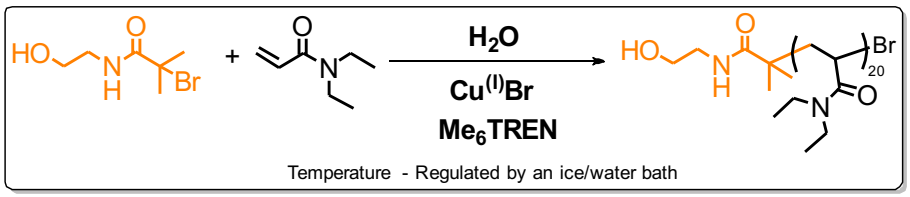

Scheme 4.7 – A schematic representation of the aqueous $Cu^{(0)}$-mediated RDRP OF DEAm initiated by compound (3).

Initiator	[$Cu^{(I)}Br$] : [Me_6TREN]	Time (hours)	Conversion (%)	$M_{n,th}$	$M_{n,SEC}$	$Đ_m$
compound (3)	0.8 : 0.6	0.5	100	2800	3200	1.13

Table 4.8 – The data obtained from polymerising DEAm using 0.8 eq. $Cu^{(I)}Br$ and 0.6 eq. Me_6TREN and compound (3) as the initiator.

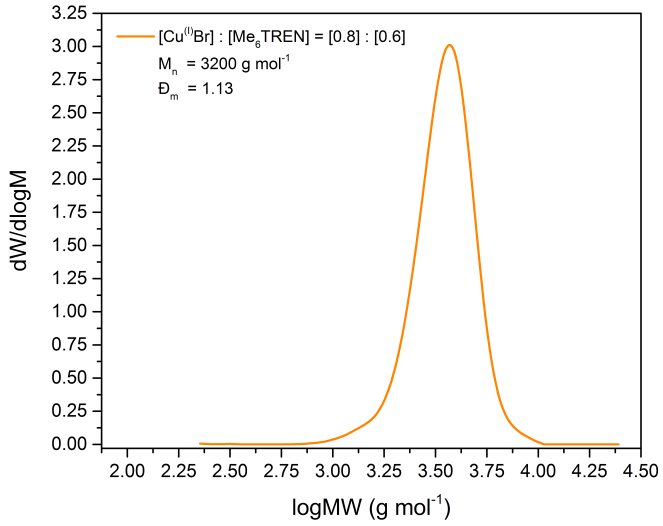

Figure 4.28 - The SEC chromatogram produced from the aqueous $Cu^{(0)}$-mediated RDRP of DEAm using compound (3) as the initiating species. Conditions: [DEAm] : [I] : [$Cu^{(I)}Br$] : [Me_6TREN] = [20] : [1.0] : [0.8] : [0.6].

4.2.3.4. Summary of the investigation into the use of compound (3) as the initiator

Initially, 2-bromo-*N*-(2-hydroxyethyl)-2-methylpropanamide (Figure 4.3, compound (3)) was screened as the initiator for the synthesis of PNIPAm with a targeted DP = 20. Following the use of different copper/ligand concentrations, a [$Cu^{(I)}Br$] : [Me_6TREN] ratio of [0.8] : [0.6] was identified as being the most optimal. Not only did its use enable for rapid and quantitative conversions (t = 3 minutes; 100 %

conversion), compound **(3)** promoted the synthesis of polymers with relatively controlled molecular weights ($M_{n,experimental}$ = 4200 g mol^{-1}; $M_{n,theoretical}$ = 2500 g mol^{-1}), and narrow MWDs ($Đ_m$ = 1.13).

To determine whether it was possible to use compound **(3)** for the synthesis of high molecular weight polymers, attempts were made to polymerise NIPAm to a targeted DP = 60, 120 and 360. Unfortunately, discrepancies between the molecular weight values were recorded upon characterisation by SEC. Nevertheless, the symmetrical nature of the MWDs and the high conversions (≥98 %), led to the hypothesis that controlled polymers would be furnished with further optimisation and future work.

Expanding the system to other acrylamide-based monomers (HEAm and DEAm) proved to be successful. In both cases, employing a [$Cu^{(I)}Br$] : [Me_6TREN] ratio of [0.8] : [0.6] resulted in quantitative conversion, low dispersity values ($Đ_m$ ≤1.2), and polymers with predictable molecular weights. Therefore, not only was compound **(3)** able to promote the controlled polymerisation of NIPAm, but it was also found to be effective for the synthesis of other acrylamide-based polymers.

Moreover, as compound **(3)** can be purchased from a select few chemical suppliers (Otava Chemicals: £65.50 per 100 mg; MCULE: £79 per 10 mg; Aurora Fine Chemicals: £1056 per 25 g), it was considered to be appropriate for use in an "off the shelf" polymerisation system.

4.2.4. Using 2-bromo-2-methylpropionic acid as the initiator for aqueous $Cu^{(0)}$-mediated RDRPs

With the aim of creating an inexpensive "off the shelf" polymerisation system in mind, the use of 2-bromo-2-methylpropionic acid (Figure 4.3, compound **(4)**) as the initiator for the polymerisation of NIPAm was investigated (Scheme 4.8).

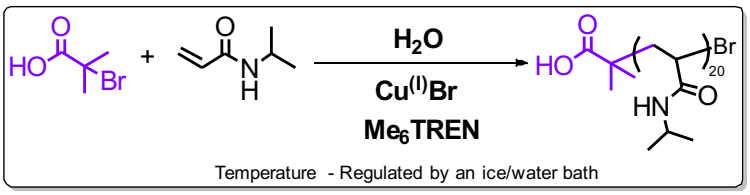

Scheme 4.8 - A schematic representation of the aqueous $Cu^{(0)}$-mediated RDRP of NIPAm initiated by compound (4).

Compound **(4)** is a commercially available alkyl halide which can be inexpensively purchased from a wide range of chemical vendors (*e.g.* Sigma-Aldrich: £17.30 per 25 g, Alfa Aesar: £12.20 per 25 g and Manchester Organics: £32 per 100 g). However, it is not a compound which would usually be considered for use in copper-mediated RDRP techniques as the presence of a pendant acid group on the α-terminus (and hence the potential for complexation and ligand protonation) increases the potential for a loss of polymerisation control.[74,75]

4.2.4.1. Initial polymerisations with compound (4)

Given the success of [M] : [I] : [$Cu^{(I)}Br$] : [Me_6TREN] = [20] : [1.0] : [0.6] : [0.8] for the previous polymerisations, it was decided that the investigation would begin with these conditions. Contrary to compounds **(1)** - **(3)**, analysis of the resulting reaction by ^1H NMR spectroscopy highlighted a slow and incomplete polymerisation. Although the final conversion was found to be 92 %, this occurred over a 24 hour period rather than 30 minutes (Figure 4.29). Moreover, while subsequent characterisation by SEC revealed a narrow MWD ($Đ_m$ = 1.23; Figure 4.29), the average M_n (7700 g mol^{-1}) was recorded as being greater than three times that which was targeted (2400 g mol^{-1}) and was ascribed to poor initiator efficiency. In addition to this, a large amount of tailing was visible in the low molecular weight region, indicative of radical-radical coupling. Given the magnitude of the molecular weight discrepancy and the occurrence of bimolecular termination, it was concluded that the polymerisation had not occurred in a controlled manner.

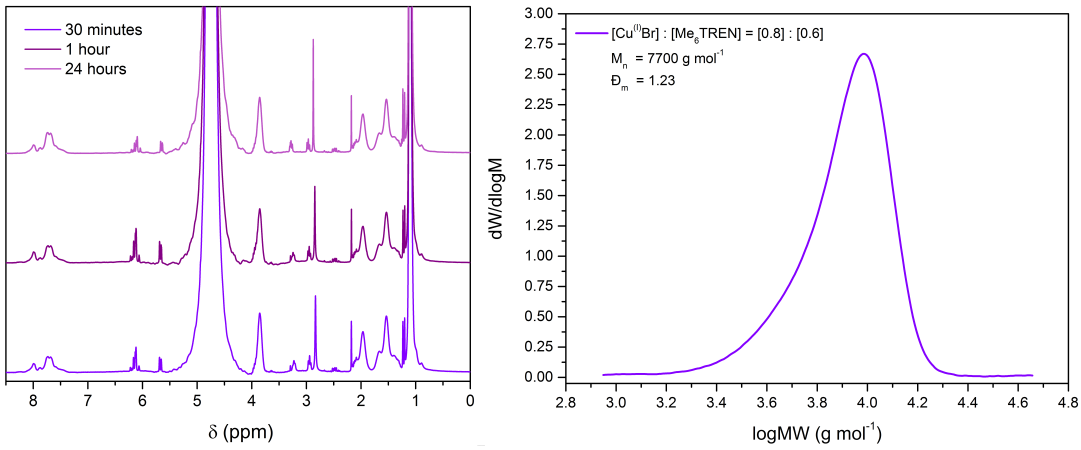

Figure 4.29 – The ^{1}H NMR spectra (left) and the SEC chromatogram (right) produced from the aqueous $Cu^{(0)}$-mediated RDRP of NIPAm using compound (4) as the initiating species. Conditions: [NIPAm] : [I] : [$Cu^{(I)}$Br] : [Me_6TREN] = [20] : [1.0] : [0.8] : [0.6].

The effect of acidic conditions upon the aqueous $Cu^{(0)}$-mediated RDRP of NIPAm was investigated in Chapter 2. Within this work it was found that low pH resulted in a loss of polymerisation control and the occurrence of termination events. Therefore, in an effort to improve the molecular weight predictability, the concentration of copper/ligand was increased to [M] : [I] : [$Cu^{(I)}$Br] : [Me_6TREN] = [20] : [1.0] : [1.0] : [1.0]. Pleasingly, this enabled for quantitative conversion to be reached within 30 minutes and a symmetrical MWD ($Đ_m$ = 1.07; Figure 4.30). Unfortunately, this was not accompanied improved agreement of the average molecular weights ($M_{n,experimental}$ = 7600 g mol^{-1}; $M_{n,theoretical}$ = 2400 g mol^{-1}).

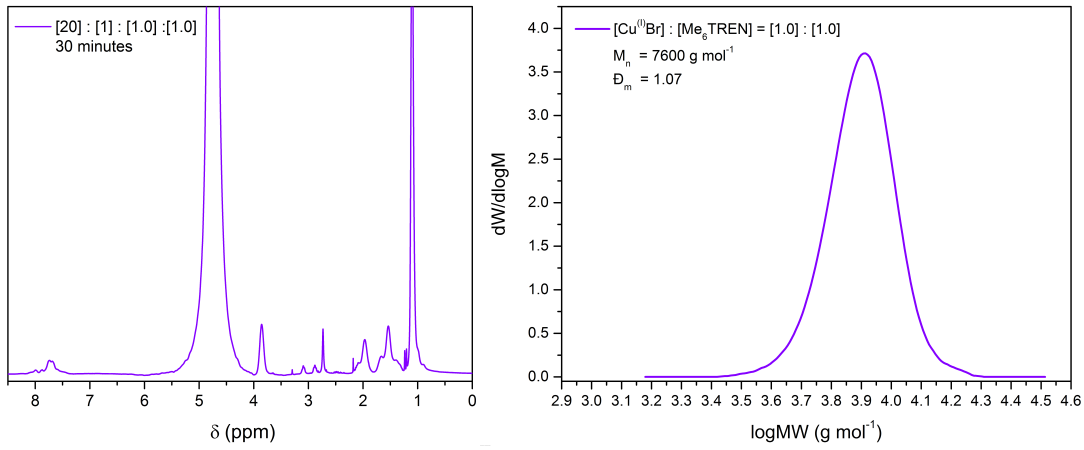

Figure 4.30 - The ^{1}H NMR spectrum (left) and the SEC chromatogram (right) produced from the aqueous $Cu^{(0)}$-mediated RDRP of NIPAm using compound (4) as the initiating species.

Attempts at conducting a kinetic study of the reaction yielded similar findings to compounds **(1)** - **(3)**, with full monomer conversion being achieved within 30 seconds. A slight improvement in polymerisation control was observed after halting the polymerisation at t = 3 minutes (Table 4.9; Figure 4.31). However, the disagreement between molecular weights was not considered to be acceptable and the polymerisation was classed as uncontrolled.

Initiator	Time (minutes)	Conversion (%)	$M_{n,th}$	$M_{n,SEC}$ (g mol^{-1})	$Đ_m$
compound **(4)**	0.5	100	2400	6600	1.31
compound **(4)**	1	100	2400	6100	1.28
compound **(4)**	3	100	2400	5900	1.19

Table 4.9 – The data obtained from the attempted kinetic study of the polymerisation of NIPAm using compound (4). Conditions: [I] : [$Cu^{(I)}Br$] : [Me_6TREN] = [1.0] : [1.0] : [1.0].

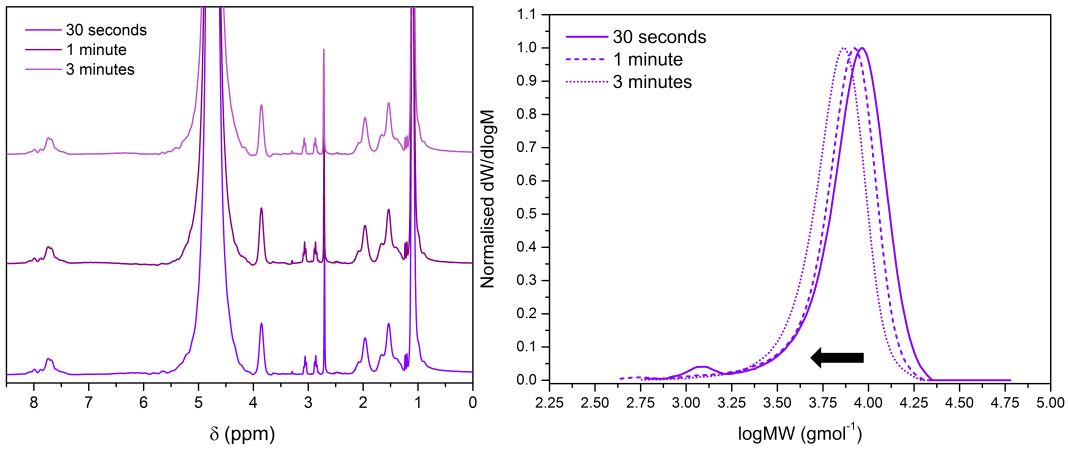

Figure 4.31 - The ^1H NMR spectra (left) and SEC chromatograms (right) for the attempted kinetic study of the polymerisation of NIPAm using compound (4). [$Cu^{(I)}Br$] : [Me_6TREN] = [1.0] : [1.0].

Given the acidic nature of the end-group, it was theorised that interaction of the polymer with the SEC column was affecting the average M_n value such that poor initiator efficiency was implied. To determine whether this was the case, the polymer was characterised using MALDI-ToF MS (Figure 4.32). The data obtained from this analysis suggested that the average molecular weight was ~ 7500 g mol^{-1}. As this result was similar to that from SEC (7600 g mol^{-1}), it was concluded that the molecular weight discrepancy was not due to column interactions.

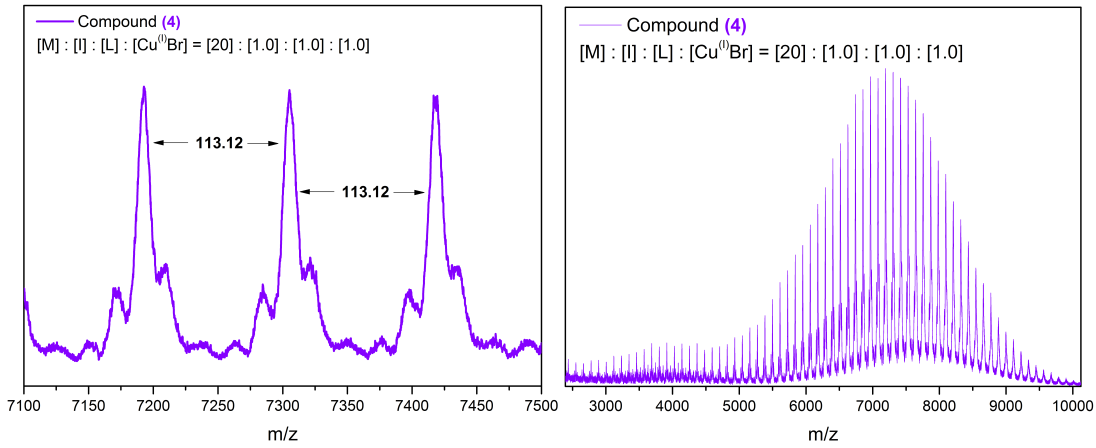

Figure 4.32 – MALDI-ToF MS analysis of the polymer resulting from the attempted kinetic study of the polymerisation of NIPAm using compound (4). Conditions: [NIPAm] : [I] : [$Cu^{(I)}Br$] : [Me_6TREN] = [20] : [1.0] : [1.0] : [1.0].

4.2.4.2. Polymerising high molecular weight polymers with compound (4)

Targeting polymers with higher molecular weights, the synthesis of DP = 60, DP = 120, and DP = 360 PNIPAm initiated by compound **(4)** was conducted using a [I] : [$Cu^{(I)}Br$] : [Me_6TREN] ratio of [1.0] : [1.0] : [1.0]. For all polymerisations, analysis by ^1H NMR spectroscopy revealed that near-quantitative conversion had been achieved within 30 minutes (Table 4.10). Moreover, SEC highlighted the presence of MWDs with dispersity values of <1.3. In the case of DP = 60, a bimodal distribution was detected (Figure 4.33) with a large discrepancy between the theoretical and experimental molecular weights (Table 4.10).

Initiator	Targeted DP	Time (minutes)	Conversion (%)	$M_{n,th}$	$M_{n,SEC}$	$Đ_m$
compound (4)	60	30	100	7000	12,200	1.23
compound (4)	120	30	100	13,700	20,600	1.14
compound (4)	360	30	98	40,100	40,600	1.26

Table 4.10 – The data obtained from polymerising NIPAm to higher DPs using compound (4). Conditions: [NIPAm] : [I] : [$Cu^{(I)}Br$] : [Me_6TREN] = [Targeted DP] : [1.0] : [1.0] : [1.0].

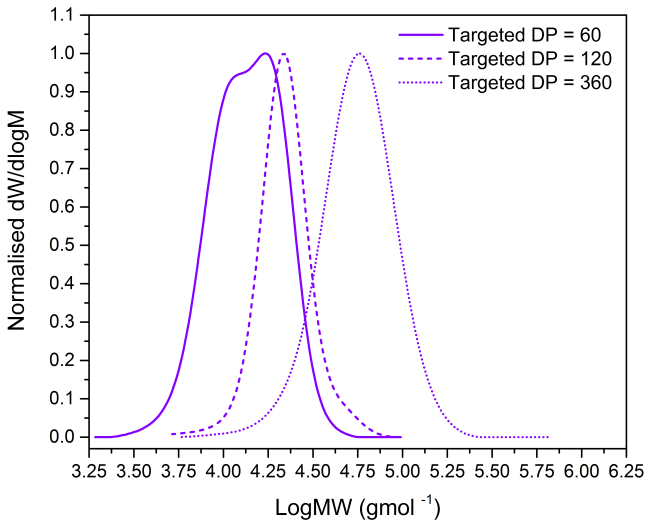

Figure 4.33 – The SEC chromatograms resulting from the polymerisation of NIPAm to differing DPs, initiated by compound (4). Conditions: [I] : [$Cu^{(I)}Br$] : [Me_6TREN] = [1.0] : [1.0] : [1.0].

Pleasingly, the experimental M_n value for DP = 120 (20,600 g mol^{-1}) was almost double that of DP = 60 (12,200 g mol^{-1}), suggesting that there had been some degree of control over the polymerisation process. This was further exhibited by the close agreement between the molecular weight values recorded for DP = 360 ($M_{n,theoretical}$ = 40,100 g mol^{-1}; $M_{n,experimental}$ = 40,600 g mol^{-1} ;Table 4.10). Although the discrepancy between molecular weights was not ideal, it was theorised that the polymerisation of NIPAm in the presence of compound **(4)** could be improved with a more in-depth study.

Regardless of the need for further optimisation, the synthesis of DP = 120 PNIPAm was kinetically monitored. Following analysis by ^1H NMR spectroscopy, it was found that the polymerisation had occurred at a rapid rate; with 89 % conversion being reached within the first 30 seconds, and quantitative monomer conversion being achieved after 10 minutes (Table 4.11).

Initiator	Time (minutes)	Conversion (%)	$M_{n,th}$	$M_{n,SEC}$	$Đ_m$
compound (4)	0	0	0	0	0
compound (4)	0.5	89	12,200	6200	1.17
compound (4)	1	98	13,500	17,100	1.13
compound (4)	1.5	98	13,500	14,800	1.14
compound (4)	2	98	13,500	14,300	1.23
compound (4)	2.5	99	13,600	13,000	1.23
compound (4)	3	99	13,600	14,500	1.21
compound (4)	3.5	99	13,600	14,400	1.18
compound (4)	4	99	13,600	13,700	1.19
compound (4)	4.5	99	13,600	14,300	1.16
compound (4)	5	99	13,600	15,100	1.15
compound (4)	10	100	-	-	-

Table 4.11 – The data obtained from kinetically monitoring the polymerisation of DP = 120 PNIPAm initiated by compound (4). Conditions: [I] : [$Cu^{(I)}Br$] : [Me_6TREN] = [1.0] : [1.0] : [1.0].

Initially, a very large discrepancy was observed between the theoretical and experimental molecular weights. This was found to decrease with time and remained relatively stable after 1.5 minutes (Table 4.11). Remarkably however, each kinetic sample displayed a narrow MWD that retained its low dispersity value as the polymerisation progressed (Figure 4.34).

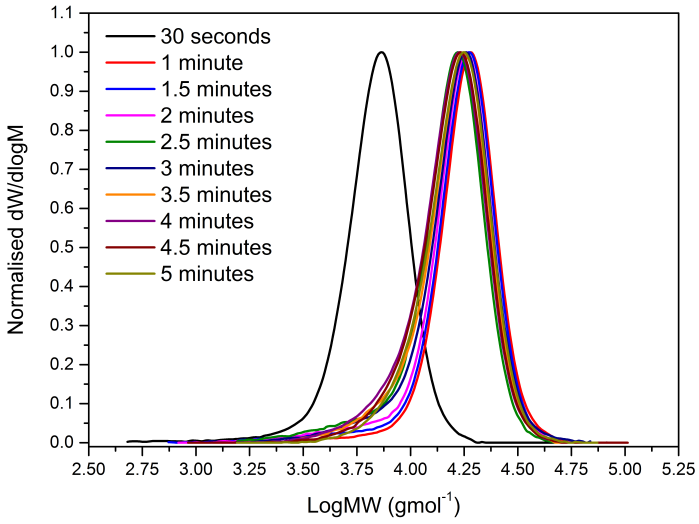

Figure 4.34 - The SEC chromatograms for the attempted kinetic study of the polymerisation of NIPAm using compound (4). Conditions: [NIPAm] : [I] : [$Cu^{(I)}Br$] : [Me_6TREN] = [120] : [1.0] : [1.0] : [1.0].

A plot of time vs. $\ln([M_0]/[M_t])$ revealed that until t = 1 minute, the reaction proceeded with a very fast apparent rate of polymerisation (K_p = 3.912 min^{-1}); this was expected given the conversion that was achieved after 30 seconds. After this time-point, a cessation of propagation was recorded and lasted for approximately 1.5 minutes. At t = 2.5 minutes, the polymerisation resumed until the monomer had been completely consumed.

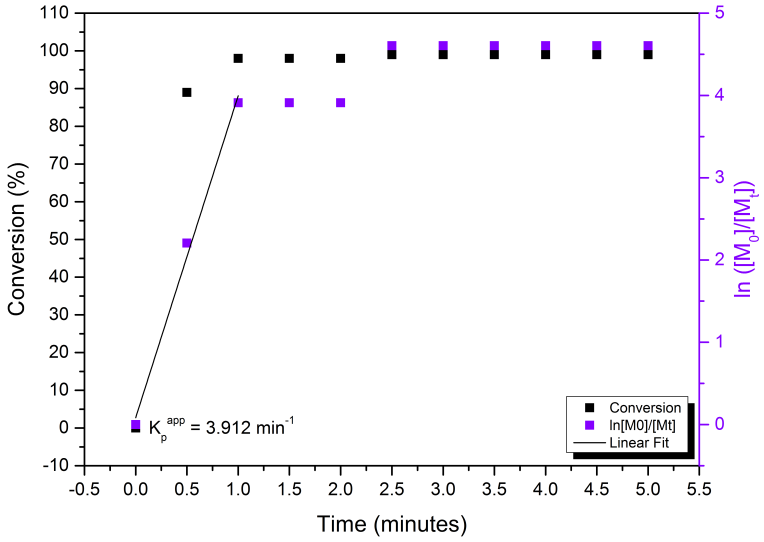

Figure 4.35 - The kinetic data for the polymerisation of DP = 120 PNIPAm initiated by compound (4). Conditions: [NIPAm] : [I] : $[Cu^{(I)}Br]$: $[Me_6TREN]$ = [120] : [1.0] : [0.8] : [0.6].

4.2.4.3. Expanding the system to other acrylamide monomers

With the aim of expanding the use of compound (4) as the initiator for the aqueous $Cu^{(0)}$-mediated RDRP of acrylamides, the synthesis of DP = 20 PHEAm was attempted (Scheme 4.9).

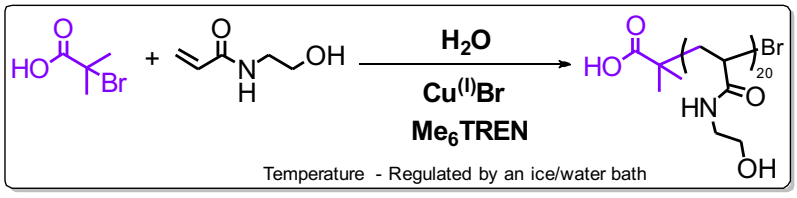

Scheme 4.9 - A schematic representation of the aqueous $Cu^{(0)}$-mediated RDRP of HEAm initiated by compound (4).

In a similar manner to the polymerisation of NIPAm, the use of [0.6] : [0.8] = [Me_6TREN] : [$Cu^{(I)}$Br] resulted in a slow and incomplete polymerisation after 24 hours (Table 4.12). Upon further characterisation by SEC, broad MWDs were observed with a high amount of tailing in the low molecular weight region, indicative of radical-radical coupling (Figure 4.36). Increasing the concentration of copper and ligand to 1.0 eq. with respect to the initiator yielded a rapid polymerisation (t = 30 seconds) and quantitative monomer conversion. However, although the MWD was Poisson-like in nature, the dispersity value was still relatively high and thus suggested that radical-radical coupling and a loss of polymerisation control had arisen (Table 4.12; Figure 4.36).

Initiator	[$Cu^{(I)}$Br] : [Me_6TREN]	Time	Conversion (%)	$M_{n,th}$	$M_{n,SEC}$	$Đ_m$
compound (4)	0.8 : 0.6	24 hours	54	1300	10,200	1.40
compound (4)	1.0 : 1.0	30 seconds	100	2400	4500	1.29

Table 4.12 – The data obtained from polymerising HEAm using four different copper/ligand ratios and compound (4) as the initiating species.

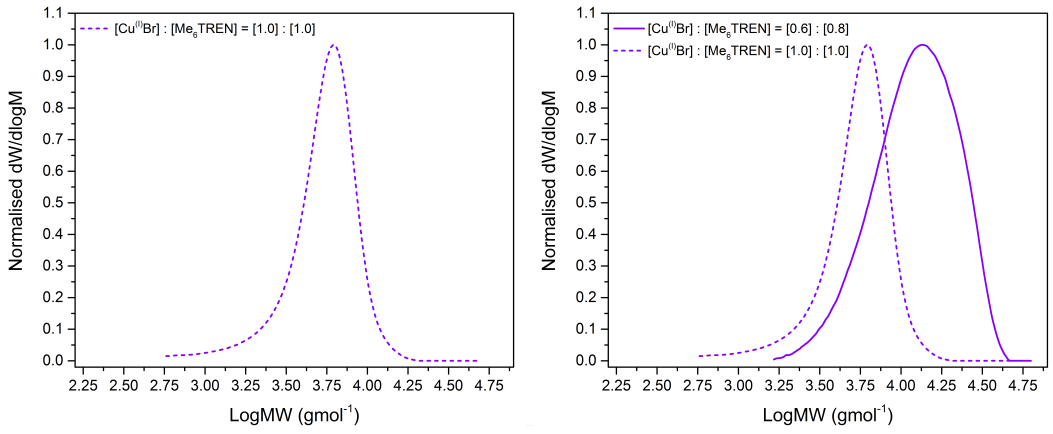

Figure 4.36 – The SEC chromatogram resulting from the aqueous $Cu^{(0)}$-mediated RDRP of HEAm utilising 1 eq. of both copper and ligand with compound (4) as the initiating species (left). A comparison of the SEC chromatograms produced from the aqueous $Cu^{(0)}$-mediated RDRP of HEAm with compound (4) as the initiating species (right).

In addition to the polymerisation of HEAm, compound (4) was employed as the initiator for the aqueous $Cu^{(0)}$-mediated RDRP of DEAm (Scheme 4.10). Given the comparative success of [I] : [$Cu^{(I)}$Br] : [Me_6TREN] = [1.0] : [1.0] : [1.0] for the

polymerisation of both NIPAm and HEAm, it was decided that the testing of alternative copper/ligand ratios was unnecessary.

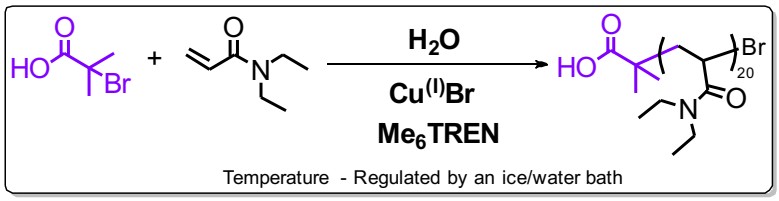

Scheme 4.10 - A schematic representation of the aqueous $Cu^{(0)}$-mediated RDRP of DEAm initiated by compound (4).

Indeed, under these conditions, the synthesis of PDEAm with a targeted DP = 20 reached completion within 30 minutes, according to ^{1}H NMR spectroscopy (Table 4.13). Although SEC analysis of the resulting polymer highlighted a disagreement between the theoretical (2400 g mol^{-1}) and experimental (5500 g mol^{-1}) molecular weights, the resulting MWD was narrow and mono-modal ($Đ_m$ = 1.11) (Table 4.13; Figure 4.37).

Initiator	$[Cu^{(I)}Br]$: $[Me_6TREN]$	Time (minutes)	Conversion (%)	$M_{n,th}$	$M_{n,SEC}$	$Đ_m$
compound (4)	1.0 : 1.0	30	100	2400	5500	1.11

Table 4.13 - The data obtained from polymerising DEAm using 1.0 eq. $Cu^{(I)}Br$ and 1.0 eq. Me_6TREN and compound (4) as the initiating species.

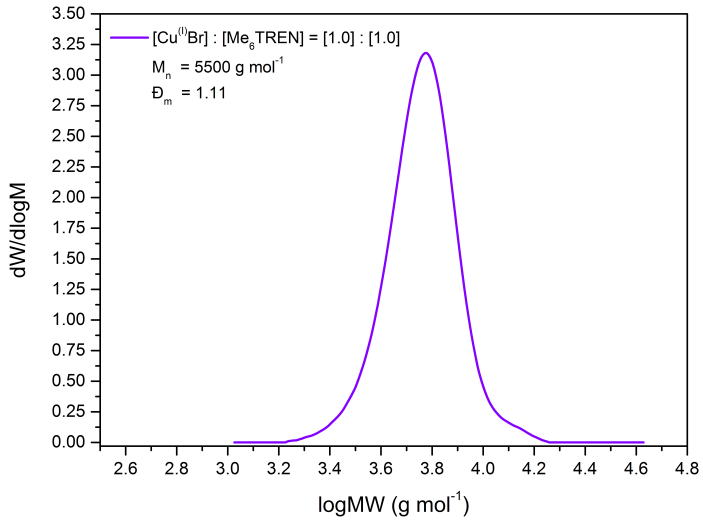

Figure 4.37 - The SEC chromatogram produced from the aqueous $Cu^{(0)}$-mediated RDRP of DEAm using compound (4) as the initiating species. Conditions: [DEAm] : [I] : $[Cu^{(I)}Br]$: $[Me_6TREN]$ = [20] : [1.0] : [1.0] : [1.0].

4.3. Conclusion

The overall aim of this work was to find an initiator which was suitable for conducting aqueous $Cu^{(0)}$-mediated RDRPs in an "off the shelf" manner. To achieve this, four alkyl halide compounds (Figure 4.3) were selected for screening as the initiating species for the polymerisation of acrylamide-based monomers.

As part of this study, the concentration of copper and ligand within the system was varied such that optimal control over low molecular weight (targeted DP = 20) polymerisations was achieved. For compounds **(1)** – **(3)**, three copper/ligand ratios were selected for testing; these were [$Cu^{(I)}Br$] : [Me_6TREN] = [0.4] : [0.4]; [0.8] : [0.4] and [0.8] : [0.6]. In all instances, the polymerisations were best mediated when the latter $Cu^{(I)}Br/Me_6TREN$ ratio was used. However, for compound **(4)**, a further increase in the concentration of copper and ligand was required ([$Cu^{(I)}Br$] : [Me_6TREN] = [1.0] : [1.0]).

Despite the high levels of polymerisation control, compounds **(1)** and **(2)** were deemed to be unsuitable for use in an "off the shelf" polymerisation. This stemmed from their commercial unavailability, and the subsequent need for a lengthy organic synthesis. For cases where organic synthesis was not a hindrance, and an initiator with dihydroxy-functionality was required, it was suggested that compound **(2)** should be selected over compound **(1)** to avoid unwanted hydrolysis.

The use of compound **(3)** as the initiating species for the synthesis of PNIPAm with a targeted DP = 20 enabled for rapid and quantitative conversions (t = 3 minutes; 100 % conversion) to be obtained. This was accompanied by polymers with relatively controlled molecular weights ($M_{n,experimental}$ = 4200 g mol^{-1}; $M_{n,theoretical}$ = 2500 g mol^{-1}), and narrow MWDs ($Đ_m$ = 1.13).

Attempts were made to expand the system to the polymerisation of higher molecular weight polymers (DP = 60, 120 and 360). Unfortunately, characterisation by SEC

revealed a poor correlation between the molecular weight values. Irrespective of this, the Poisson-like nature of the MWDs and high conversions (≥98 %) suggested that controlled polymers would be furnished with future work and optimisation.

Pleasingly, the polymerisation of other acrylamide-based monomers (HEAm and DEAm) proved to be successful. Using a [$Cu^{(I)}Br$] : [Me_6TREN] ratio of [0.8] : [0.6], complete conversions, low dispersity values (≤ 1.2), and polymers with predictable molecular weights were obtained. For that reason, compound **(3)** was concluded as being a viable initiator for the polymerisation of multiple acrylamide-based polymers.

Unlike the preceding two compounds, compound **(3)** was formed using a one-step synthesis procedure and facile purification. Given the easier synthesis, it was proposed that compound **(3)** should be used as the initiating species for the aqueous $Cu^{(0)}$-mediated RDRP of acrylamides, rather than compounds **(1)** or **(2)**. More importantly, as compound **(3)** was found to be commercially available, it was deemed eligible for use in an "off the shelf" system.

The use of compound **(4)** as the initiating species for the polymerisation of NIPAm resulted in polymers with average M_n values which were three times higher than those which were targeted. Attempts to synthesise higher molecular weight polymers proved to be more successful; with a closer molecular weight agreement being observed upon increasing the DP.

Unfortunately, however, the polymerisation of HEAm proved to be problematic. Although increasing the copper/ligand ratio resulted in a closer agreement between molecular weight values, this was at the expense of dispersity control. The wide variety of results, the need for comparatively large amounts of copper and ligand, and the difficulty in expanding the system to other monomers meant that compound **(4)** was determined to be unsuitable for $Cu^{(0)}$-mediated RDRPs and hence, an "off the shelf" polymerisation.

4.4. Experimental

4.4.1. Materials

N-Isopropylacrylamide (NIPAm, Sigma-Aldrich, 97 %), 2-bromo-2-methylpropionic acid (compound **(4)**, Sigma-Aldrich, 98 %), 2,2-dimethyl-1,3-dioxolan-4-yl)methanamine (Sigma-Aldrich, 97 %), anhydrous tetrahydrofuran (THF, HPLC grade, Sigma-Aldrich), triethylamine (TEA, Sigma-Aldrich, ≥ 99 %), 2-bromoisobutyryl bromide (Sigma-Aldrich, 98 %), diethyl ether (Fisher-Scientific, ≥ 99 %), anhydrous sodium carbonate (Na_2CO_3, Fisher-Scientific, ≥ 99.5 %), anhydrous sodium sulphate (Na_2SO_4, Fisher-Scientific, ≥ 99 %), glacial acetic acid (Sigma-Aldrich, ≥ 99.8 %), methoxybenzene (≥ 99.9 %, Sigma-Aldrich), anhydrous magnesium sulphate ($MgSO_4$, Fisher-Scientific, ≥ 99 %), ethanolamine (Sigma-Aldrich, ≥ 99.5 %), hexane (HPLC grade, Sigma-Aldrich), ethyl acetate (EtOAc, HPLC grade, Sigma-Aldrich), and water (HPLC grade, VWR) were used without further purification. Cuprisorb™ resin was purchased from Seachem.

3-Dihydroxypropyl 2-bromo-2-methylpropanoate was synthesised according to the literature procedure (compound **(1)**).[44] *N,N,N',N',N'',N''*-Hexamethyl-[tris(aminoethyl)amine] (Me_6TREN) was synthesised according to the literature procedure, deoxygenated, and stored in an ampoule at 4 °C under N_2.[76] *N*-Hydroxyethyl acrylamide (HEAm, Sigma-Aldrich, 97 %) and *N,N*-diethylacrylamide (DEAm, Sigma-Aldrich, 99 %) were uninhibited using basic alumina prior to use in the polymerisations. Copper$^{(I)}$bromide ($Cu^{(I)}Br$, Aldrich, > 98 %) was purified according to the method detailed by Keller and Wycoff.[77]

Synthesis of 2-bromo-*N*-((2,2-dimethyl-1,3-dioxolan-4-yl)methyl)-2-methylpropanamide (precursor to compound (2))

2,2-Dimethyl-1,3-dioxolan-4-yl)methanamine (15.0 g, 0.11 mol, 1.0 eq.), dry THF (150 mL) and triethylamine (52.7 mL, 0.52 mol, 4.7 eq.) were stirred in a 3-neck RBF at 0°C, under N_2. 2-Bromoisobutyryl bromide (19.7 mL, 0.17 mol, 1.55 eq.) was added dropwise to the solution, which was stirred overnight, and then allowed to warm to room temperature. The reaction mixture was washed with water (200 mL) and extracted with diethyl ether (300 mL). The organic layers were washed thrice with saturated Na_2CO_3 (600 mL) and then dried with Na_2SO_4. The solvent was removed *in vacuo* following gravity filtration, and the product was obtained as a yellow oil, which was used without further purification (yield = 5.03 g, 16 %).

^{1}H NMR ($CDCl_3$, 400 MHz), δ (ppm): 1.36 (s, 3H, R-(C*H*$_3$)$_2$-O-R'), 1.47 (s, 3H, R-(C*H*$_3$)$_2$-O-R), 1.96 (s, 6H, R-(C*H*$_3$)$_2$-C-Br), 3.47 (m, 2H, R-NH-C*H*$_2$-CH-R'), 3.64 (m, 1H, R-(CH$_3$)$_2$-C-O-C*H*$_2$-R), 4.04 (R-(CH$_3$)$_2$-C-O-C*H*$_2$-R), 4.28 (m, 1H, R-(CH$_3$)$_2$-C-O-C*H*-R), 7.06 R-NH-C*H*$_2$-CH-R') **^{13}C NMR ($CDCl_3$, 400 MHz), δ (ppm):** 26.72 ((*C*H$_3$)$_2$-C-Br-R), 25.10 (R-(*C*H$_3$)$_2$-C-O-CH$_2$-R), 41.71 (R-NH-*C*H$_2$-CH-R'), 62.63 (R-(CH$_3$)$_2$-*C*-Br), 66.36 (R-(CH$_3$)$_2$-C-O-*C*H$_2$-R), 74.12 (R-(CH$_3$)$_2$-C-O-*C*H-R), 109.37 (R-(CH$_3$)$_2$-*C*-O-CH-R), 172.32 ((CH$_3$)$_2$-C-Br-*C*O-R) **ESI-MS (*m/z*):** [M+] 281.00 (*280.16 Th*eo.)

Synthesis of 2-bromo-*N*-(2,3-dihydroxypropyl)-2-methylpropanamide (compound (2))

Compound **(2)** was prepared by adding glacial acetic acid (15 mL), water (40 mL) and a catalytic amount of methoxybenzene to 2-bromo-*N*-((2,2-dimethyl-1,3-dioxolan-4-yl)methyl)-2-methylpropanamide (5.03 g, 0.018 mol, 1 eq.). The resulting reaction mixture was then refluxed for 2 hours at 80°C to de-protect the 1,2-diol.

This solution was then cooled to ambient temperature and diethyl ether (300 mL) was added. The aqueous layer was saturated with Na_2CO_3 until the evolution of CO_2 ceased, and the product was subsequently extracted into diethyl ether (300 mL). The organic layers were then combined, dried using anhydrous $MgSO_4$, and the solvent removed *in vacuo* to yield a yellow oil. The crude product was purified using silica gel column chromatography (1:2 hexane:EtOAc) to obtain the pure product as a white solid (yield = 0.43 g, 10 %).

^{1}H NMR (D_2O, 400 MHz), δ (ppm): 1.95 (s, 6H, R-(C*H*$_3$)$_2$-C-Br), 3.49 (m, 2H, R-NH-C*H*$_2$-CH-R'), 3.83 (m, 2H, OH-C*H*$_2$-R), 4.13 (m, 1H, OH-CH$_2$-C*H*-R), 4.37 (s, 1H, R'-CH-O*H*-R), 7.42 (t, J = 5.87 Hz, R-N*H*-CH$_2$-CH-R') **^{13}C NMR ($CDCl_3$, 400 MHz), δ (ppm):** 32.16 ((*C*H$_3$)$_2$-C-Br-R), 42.77 (R-NH-C*H*$_2$-CH-R'), 61.47 ((CH$_3$)$_2$-*C*-Br), 63.84 (OH-*C*H$_2$-CH-R),), 70.54 (OH-CH$_2$-*C*H-R), 173.81 ((CH$_3$)$_2$-C-Br-*C*O-R) **ESI-MS (*m/z*):** [M+] 239.00 (*240.10 Th*eo.)

Synthesis of 2-bromo-*N*-(2-hydroxyethyl)-2-methylpropanamide (compound (3))

A solution of ethanolamine (2.5 mL, 0.044 mol, 1 eq.) and triethylamine (6.1 mL, 0.043 mol, 1 eq.) in dry THF (200 mL) under a nitrogen atmosphere was cooled to 0 ºC in an ice bath and 2-bromoisobutyryl bromide (5.38 mL, 0.043 mol, 1 eq.) was added dropwise. The mixture was then left to react overnight at room temperature with vigorous stirring. A white precipitate formed (TEA bromide salt) and was removed from the solution by gravity filtration. The product was then extracted into diethyl ether, dried using anhydrous $MgSO_4$, and the solvent removed from the reaction mixture *in vacuo* to yield a yellow oil. The crude product was purified by precipitation into hexane to produce a white solid (yield = 1.58 g, 17 %)

^{1}H NMR (D_2O, 400 MHz), δ (ppm): 1.89 (s, 6H, R-C-(C$\underline{H_3}$)$_2$-Br), 3.32 (t, J = 5.50 Hz 2H, R-C$\underline{H_2}$-CH_2-OH), 3.61 (t, J = 5.75 Hz 3H, R-CH_2-C$\underline{H_2}$-OH), 8.08 (s, 1 H, HO-CH_2-CH_2-N$\underline{H}$-R **^{13}C NMR (D_2O, 400 MHz), δ (ppm):** 30.8 (($\underline{C}H_3$)$_2$-C-Br-R), 42.0 (R-$\underline{C}H_2$-CH_2-OH), 59.9 (R-CH_2-$\underline{C}H_2$-OH), 175.1 ((CH_3)$_2$-C-Br-$\underline{C}$O-R) **ESI-MS (*m/z*):** [M+] 209.00 (*210.07 Th*eo.)

4.4.2. Characterisation and instrumentation

^{1}H NMR spectra were recorded on Brüker HD-300 and DPX-400 and spectrometers using deuterated solvents obtained from Sigma-Aldrich. The percentage conversion of NIPAm was determined *via* ^{1}H NMR through integration of the vinyl group (5.6 ppm, 1H, d) and integration of the C$\underline{H}$(CH_3)$_2$ proton (3.9 ppm, 1H, m). The percentage conversion of HEAm was calculated by ^{1}H NMR through integration of the vinyl group (5.65 ppm, 1H, d) and integration of the C$\underline{H_2}$NH peak (3.93 ppm, 2H, q). The percentage conversion of DEAm was determined *via* ^{1}H NMR through integration of the vinyl group (5.95 ppm, 1H, d) and integration of the C$\underline{H_2}CH_3$ peak (3.65 ppm, 2H, qn). The following abbreviations were used to describe multiplicities; s = singlet, d = doublet, t = triplet, q = quartet, qn = quintet and m = multiplet.

Size exclusion chromatography (SEC) measurements were performed on an Agilent PL50 equipped with 2 Agilent Polargel M Columns eluting with dimethylformamide containing 0.1 wt % LiBr as an additive at 50°C. The flow rate was 1 mL min^{-1} and detection was achieved using simultaneous refractive index (RI) and UV (λ = 280 nm) detectors. Molecular weights were calculated relative to narrow PMMA standards. All samples were stirred in the presence of Cuprisorb™ resin to remove residual copper species, dissolved in the appropriate eluent and filtered through disposable 0.45 μm PTFE filters before analysis. Molecular weight data was analysed using Agilent SEC software and plotted using OriginPro 8.5.

MALDI-ToF mass spectrometry was carried out using a Bruker Daltonics Ultraflex II MALDI-ToF mass spectrometer, equipped with a nitrogen laser delivering 2 ns laser pulses at 337 nm. Positive ion ToF detection was conducted using an accelerating voltage of 25 kV. A saturated solution of α-Cyano-4-hydroxycinnamic acid (CHCA, 200 mg/mL) in 50 µL of THF was used as the matrix. The cationisation agent was sodium iodide (4.0 mg/mL) and was dissolved in methanol (MeOH). 4.0 mg/mL of sample was mixed with the matrix and the cationisation agent, and 0.7 µL of this solution was applied to the target plate. Spectra were recorded in reflector mode with polyethylene glycol (PEG) 2500 Da used as a calibration standard.

4.4.3. General experimental procedures

Typical procedure for the aqueous $Cu^{(0)}$-mediated RDRP of DP = 20 PNIPAm

To a Schlenk tube equipped with a magnetic stirring bar, HPLC grade water (3 mL) and Me_6TREN were added and purged of oxygen *via* nitrogen (N_2) bubbling for 2 minutes. The mixture was placed into an ice/water bath to regulate the temperature (0 °C) after which $Cu^{(I)}Br$ was added under an N_2 atmosphere. Upon addition of $Cu^{(I)}Br$ to the ligand-water mix, a coloured solution formed and red/brown $Cu^{(0)}$ particles were visible. The resulting solution was stirred to achieve disproportionation whilst the initiator and NIPAm were dissolved in water (2 mL) and bubbled with nitrogen for 15 minutes. At the end of the deoxygenation period the initiator-monomer solution was transferred *via* a nitrogen purged syringe and needle into the Schlenk tube. Samples for ^{1}H NMR spectroscopy and SEC were taken using a nitrogen purged syringe, filtered through an alumina column, and diluted in the appropriate solvents.

The relevant quantities of Me_6TREN, $Cu^{(I)}Br$, Initiator and NIPAm have been provided in Tables 4.14 – 4.17.

[M] : [I] : [$Cu^{(I)}Br$] : [Me_6TREN]	NIPAm (mg)	$Cu^{(I)}Br$ (mg)	Me_6TREN (µL)	Compound (1) (mg)
[20] : [1.0] : [0.4] : [0.4]	500	12.7	23.6	53.3
[20] : [1.0] : [0.8] : [0.06]	500	25.3	3.5	53.3
[20] : [1.0] : [0.8] : [0.1]	500	25.3	5.9	53.3
[20] : [1.0] : [0.8] : [0.2]	500	25.3	11.8	53.3
[20] : [1.0] : [0.8] : [0.3]	500	25.3	17.7	53.3
[20] : [1.0] : [0.8] : [0.4]	500	25.3	23.6	53.3
[20] : [1.0] : [0.8] : [0.5]	500	25.3	29.5	53.3
[20] : [1.0] : [0.8] : [0.6]	500	25.3	35.4	53.3
[20] : [1.0] : [0.8] : [0.7]	500	25.3	41.3	53.3
[20] : [1.0] : [0.8] : [0.8]	500	25.3	47.2	53.3

Table 4.14 – Relevant quantities used for the aqueous $Cu^{(0)}$-mediated RDRP of NIPAm in the presence of compound (1).

[M] : [I] : [$Cu^{(I)}Br$] : [Me_6TREN]	NIPAm (mg)	$Cu^{(I)}Br$ (mg)	Me_6TREN (µL)	Compound (2) (mg)
[20] : [1.0] : [0.4] : [0.4]	500	12.7	23.6	53.0
[20] : [1.0] : [0.8] : [0.4]	500	25.3	23.6	53.0
[20] : [1.0] : [0.8] : [0.6]	500	25.3	35.4	53.0

Table 4.15 – Relevant quantities used for the aqueous $Cu^{(0)}$-mediated RDRP of NIPAm in the presence of compound (2).

[M] : [I] : [$Cu^{(I)}Br$] : [Me_6TREN]	NIPAm (mg)	$Cu^{(I)}Br$ (mg)	Me_6TREN (µL)	Compound (3) (mg)
[20] : [1.0] : [0.4] : [0.4]	500	12.7	23.6	46.4
[20] : [1.0] : [0.8] : [0.4]	500	25.3	23.6	46.4
[20] : [1.0] : [0.8] : [0.6]	500	25.3	35.4	46.4
[60] : [1.0] : [0.8] : [0.6]	500	4.2	11.8	15.5
[120] : [1.0] : [0.8] : [0.6]	500	2.1	5.9	7.7
[360] : [1.0] : [0.8] : [0.6]	500	0.7	2.0	2.6

Table 4.16 – Relevant quantities used for the aqueous $Cu^{(0)}$-mediated RDRP of NIPAm in the presence of compound (3).

[M] : [I] : [$Cu^{(I)}Br$] : [Me_6TREN]	NIPAm (mg)	$Cu^{(I)}Br$ (mg)	Me_6TREN (µL)	Compound (4) (mg)
[20] : [1.0] : [0.8] : [0.6]	500	25.3	35.4	36.9
[20] : [1.0] : [1.0] : [1.0]	500	31.7	59.0	36.9
[60] : [1.0] : [1.0] : [1.0]	500	10.6	19.7	12.3
[120] : [1.0] : [1.0] : [1.0]	500	5.3	9.8	6.2
[360] : [1.0] : [1.0] : [1.0]	500	1.7	3.3	2.1

Table 4.17 – Relevant quantities used for the aqueous $Cu^{(0)}$-mediated RDRP of NIPAm in the presence of compound (4).

Typical procedure for the aqueous $Cu^{(0)}$-mediated RDRP of HEAm

To a Schlenk tube equipped with a magnetic stirring bar, HPLC grade water (3 mL) and Me_6TREN were added and purged of oxygen *via* nitrogen (N_2) bubbling for 2 minutes. The mixture was placed into an ice/water bath to regulate the temperature (0 °C) after which $Cu^{(I)}Br$ was added under an N_2 atmosphere. Upon addition of $Cu^{(I)}Br$ to the ligand-water mix, a coloured solution formed and red/brown $Cu^{(0)}$ particles were visible. The resulting solution was stirred to achieve disproportionation whilst the initiator and HEAm were dissolved in water (2 mL) and bubbled with nitrogen for 15 minutes. At the end of the deoxygenation period the initiator-monomer solution was transferred *via* a nitrogen purged syringe and needle into the Schlenk tube. Samples for NMR and SEC were taken using a nitrogen purged syringe, filtered through an alumina column, and diluted in the appropriate solvents. The relevant quantities of Me_6TREN, $Cu^{(I)}Br$, Initiator and HEAm have been provided in Tables 4.18 – 4.19.

[M] : [I] : [$Cu^{(I)}Br$] : [Me_6TREN]	NIPAm (mg)	$Cu^{(I)}Br$ (mg)	Me_6TREN (µL)	Compound (3) (mg)
[20] : [1.0] : [0.4] : [0.4]	500	12.5	23.2	45.6
[20] : [1.0] : [0.8] : [0.4]	500	24.9	23.2	45.6
[20] : [1.0] : [0.8] : [0.6]	500	24.9	34.8	45.6

Table 4.18 – Relevant quantities used for the aqueous $Cu^{(0)}$-mediated RDRP of HEAm in the presence of compound (3).

[M] : [I] : [$Cu^{(I)}Br$] : [Me_6TREN]	NIPAm (mg)	$Cu^{(I)}Br$ (mg)	Me_6TREN (µL)	Compound (4) (mg)
[20] : [1.0] : [0.8] : [0.6]	500	24.9	34.8	36.3
[20] : [1.0] : [1.0] : [1.0]	500	31.1	58.0	36.3

Table 4.19 – Relevant quantities used for the aqueous $Cu^{(0)}$-mediated RDRP of HEAm in the presence of compound (4).

Typical procedure for the aqueous $Cu^{(0)}$-mediated RDRP of DEAm

To a Schlenk tube equipped with a magnetic stirring bar, HPLC grade water (3 mL) and Me_6TREN (X µL, 0.11 mmol, 0.6 eq.) were added and purged of oxygen *via* nitrogen (N_2) bubbling for 2 minutes. The mixture was placed into an ice/water bath to regulate the temperature (0 °C) after which $Cu^{(I)}Br$ (X mg, 0.16 mmol, 0.8 eq.) was added under an N_2 atmosphere. Upon addition of $Cu^{(I)}Br$ to the ligand-water mix, a coloured solution formed and red/brown $Cu^{(0)}$ particles were visible. The resulting solution was stirred to achieve disproportionation whilst the initiator (X mg, 0.29 mmol, 1.0 eq.) and DEAm (X mg, 3.93 mmol, 20 eq.) were dissolved in water (2 mL) and bubbled with nitrogen for 15 minutes. At the end of the deoxygenation period the initiator-monomer solution was transferred *via* a nitrogen purged syringe and needle into the Schlenk tube. Samples for NMR and SEC were taken using a nitrogen purged syringe, filtered through an alumina column, and diluted in the appropriate solvents.

The relevant quantities of Me_6TREN, $Cu^{(I)}Br$, Initiator and DEAm have been provided in Tables 4.20 – 4.21.

[M] : [I] : [$Cu^{(I)}Br$] : [Me_6TREN]	NIPAm (mg)	$Cu^{(I)}Br$ (mg)	Me_6TREN (µL)	Compound (3) (mg)
[20] : [1.0] : [0.8] : [0.6]	0.5	22.5	31.5	41.3

Table 4.20 – Relevant quantities used for the aqueous $Cu^{(0)}$-mediated RDRP of DEAm in the presence of compound (3).

[M] : [I] : [$Cu^{(I)}Br$] : [Me_6TREN]	NIPAm (mg)	$Cu^{(I)}Br$ (mg)	Me_6TREN (µL)	Compound (4) (mg)
[20] : [1.0] : [1.0] : [1.0]	0.5	28.2	52.5	32.8

Table 4.21 – Relevant quantities used for the aqueous $Cu^{(0)}$-mediated RDRP of DEAm in the presence of compound (3).

4.5. References

1 R. Aksakal, M. Resmini and C. R. Becer, *Polym. Chem.*, 2016, **7**, 171–175.

2 J. Collins, S. J. Wallis, A. Simula, M. R. Whittaker, M. P. McIntosh, P. Wilson, T. P. Davis, D. M. Haddleton and K. Kempe, *Macromol. Rapid Commun.*, 2017, **38**, 1600534.

3 A. Simula, V. Nikolaou, F. Alsubaie, A. Anastasaki and D. M. Haddleton, *Polym. Chem.*, 2015, **6**, 5940–5950.

4 A. Anastasaki, A. J. Haddleton, Q. Zhang, A. Simula, M. Droesbeke, P. Wilson and D. M. Haddleton, *Macromol. Rapid Commun.*, 2014, **35**, 965–970.

5 G. R. Jones, Z. Li, A. Anastasaki, D. J. Lloyd, P. Wilson, Q. Zhang and D. M. Haddleton, *Macromolecules*, 2016, **49**, 483–489.

6 Q. Zhang, M. Li, C. Zhu, G. Nurumbetov, Z. Li, P. Wilson, K. Kempe and D. M. Haddleton, *J. Am. Chem. Soc.*, 2015, **137**, 9344–9353.

7 Q. Zhang, P. Wilson, Z. Li, R. McHale, J. Godfrey, A. Anastasaki, C. Waldron and D. M. Haddleton, *J. Am. Chem. Soc.*, 2013, **135**, 7355–7363.

8 D. J. Lloyd, V. Nikolaou, J. Collins, C. Waldron, A. Anastasaki, S. P. Bassett, S. M. Howdle, A. Blanazs, P. Wilson, K. Kempe and D. M. Haddleton, *Chem. Commun.*, 2016, **52**, 6533–6536.

9 Q. Zhang, Z. Li, P. Wilson and D. M. Haddleton, *Chem. Commun.*, 2013, **49**, 6608–6610.

10 C. Waldron, Q. Zhang, Z. Li, V. Nikolaou, G. Nurumbetov, J. Godfrey, R. McHale, G. Yilmaz, R. K. Randev, M. Girault, K. McEwan, D. M. Haddleton, M. Droesbeke, A. J. Haddleton, P. Wilson, A. Simula, J. Collins, D. J. Lloyd, J. A. Burns, C. Summers, C. Houben, A. Anastasaki, M. Li, C. R. Becer, J. K. Kiviaho and N. Risangud, *Polym. Chem.*, 2014, **5**, 57–61.

11 W. G. M. and R. P. F. Perreault, A. Oukarroum, S. P. Melegari, *Chemosphere*, 2012, **87**, 1388–1394.

12 N. V Tsarevsky and K. Matyjaszewski, *Chem. Rev.*, 2007, **107**, 2270–2299.

13 H. Ma, X. Wan, X. Chen and Q.-F. Zhou, *J. Polym. Sci. Part A Polym. Chem.*, 2003, **41**, 143–151.

14 A. Simakova, S. E. Averick, D. Konkolewicz and K. Matyjaszewski, *Macromolecules*, 2012, **45**, 6371–6379.

15 Y. Kwak, A. J. D. Magenau and K. Matyjaszewski, *Macromolecules*, 2011, **44**, 811–819.

16 K. Matyjaszewski, W. Jakubowski, K. Min, W. Tang, J. Huang, W. A. Braunecker and N. V Tsarevsky, *Proc. Natl. Acad. Sci.* , 2006, **103**, 15309–15314.

17 T. Pintauer and K. Matyjaszewski, *Chem. Soc. Rev.*, 2008, **37**, 1087–1097.

18 D. Konkolewicz, A. J. D. Magenau, S. E. Averick, A. Simakova, H. He and K. Matyjaszewski, *Macromolecules*, 2012, **45**, 4461–4468.

19 H.-C. Lee, M. Antonietti and B. V. K. J. Schmidt, *Polym. Chem.*, 2016, **7**,

7199–7203.

20 R. Whitfield, A. Anastasaki, V. Nikolaou, G. R. Jones, N. G. Engelis, E. H. Discekici, C. Fleischmann, J. Willenbacher, C. J. Hawker and D. M. Haddleton, *J. Am. Chem. Soc.*, 2017, **139**, 1003–1010.

21 V. Percec, T. Guliashvili, J. S. Ladislaw, A. Wistrand, A. Stjerndahl, M. J. Sienkowska, M. J. Monteiro and S. Sahoo, *J. Am. Chem. Soc.*, 2006, **128**, 14156–14165.

22 A. Anastasaki, C. Waldron, P. Wilson, C. Boyer, P. B. Zetterlund, M. R. Whittaker and D. Haddleton, *ACS Macro Lett.*, 2013, **2**, 896–900.

23 F. Alsubaie, A. Anastasaki, P. Wilson and D. M. Haddleton, *Polym. Chem.*, 2015, **6**, 406–417.

24 B. M. Rosen and V. Percec, *Chem. Rev.*, 2009, **109**, 5069–5119.

25 L. Voorhaar, S. Wallyn, F. E. Du Prez and R. Hoogenboom, *Polym. Chem.*, 2014, **5**, 4268–4276.

26 N. H. Nguyen, J. Kulis, H.-J. Sun, Z. Jia, B. van Beusekom, M. E. Levere, D. A. Wilson, M. J. Monteiro and V. Percec, *Polym. Chem.*, 2013, **4**, 144–155.

27 W. Tang, Y. Kwak, W. Braunecker, N. V Tsarevsky, M. L. Coote and K. Matyjaszewski, *J. Am. Chem. Soc.*, 2008, **130**, 10702–10713.

28 S. R. Samanta, A. Anastasaki, C. Waldron, D. M. Haddleton and V. Percec, *Polym. Chem.*, 2013, **4**, 5555–5562.

29 S. R. Samanta, M. E. Levere and V. Percec, *Polym. Chem.*, 2013, **4**, 3212–3224.

30 X. Jiang, S. Fleischmann, N. H. Nguyen, B. M. Rosen and V. Percec, *J. Polym. Sci. Part A Polym. Chem.*, 2009, **47**, 5591–5605.

31 X. Leng, N. H. Nguyen, B. van Beusekom, D. A. Wilson and V. Percec, *Polym. Chem.*, 2013, **4**, 2995–3004.

32 Q. Zhang, A. Anastasaki, G.-Z. Li, A. J. Haddleton, P. Wilson and D. M. Haddleton, *Polym. Chem.*, 2014, **5**, 3876–3883.

33 R. Aksakal, M. Resmini and C. R. Becer, *Polym. Chem.*, 2016, **7**, 6564–6569.

34 P. M. Wright, G. Mantovani and D. M. Haddleton, *J. Polym. Sci. Part A Polym. Chem.*, 2008, **46**, 7376–7385.

35 J. Tom, B. Hornby, A. West, S. Harrisson and S. Perrier, *Polym. Chem.*, 2010, **1**, 420–422.

36 J. S. Basuki, L. Esser, H. T. T. Duong, Q. Zhang, P. Wilson, M. R. Whittaker, D. M. Haddleton, C. Boyer and T. P. Davis, *Chem. Sci.*, 2014, **5**, 715–726.

37 J. S. Basuki, L. Esser, P. B. Zetterlund, M. R. Whittaker, C. Boyer and T. P. Davis, *Macromolecules*, 2013, **46**, 6038–6047.

38 P. Wilson, A. Anastasaki, M. R. Owen, K. Kempe, D. M. Haddleton, S. K. Mann, A. P. R. Johnston, J. F. Quinn, M. R. Whittaker, P. J. Hogg and T. P. Davis, *J. Am. Chem. Soc.*, 2015, **137**, 4215–4222.

39 M. Zhang, M. F. Cunningham and R. A. Hutchinson, *Polym. Chem.*, 2015, **6**, 6509–6518.

40 S. R. Samanta, V. Nikolaou, S. Keller, M. J. Monteiro, D. A. Wilson, D. M. Haddleton and V. Percec, *Polym. Chem.*, 2015, **6**, 2084–2097.

41 Q. Zhang, G. Nurumbetov, A. Simula, C. Zhu, M. Li, P. Wilson, K. Kempe, B. Yang, L. Tao and D. M. Haddleton, *Polym. Chem.*, 2016, **7**, 7002–7010.

42 V. Nikolaou, A. Simula, M. Droesbeke, N. Risangud, A. Anastasaki, K. Kempe, P. Wilson and D. Haddleton, *Polym. Chem.*, 2016.

43 Q. Zhang, P. Wilson, A. Anastasaki, R. McHale and D. M. Haddleton, *ACS Macro Lett.*, 2014, **3**, 491–495.

44 S. Perrier, S. P. Armes, X. S. Wang, F. Malet and D. M. Haddleton, *J. Polym. Sci. Part A Polym. Chem.*, 2001, **39**, 1696–1707.

45 R. P. Quirk and B. Lee, *Polym. Int.*, 1992, **27**, 359–367.

46 K. Mukumoto, M. Zhong and K. Matyjaszewski, *Eur. Polym. J.*, 2014, **56**, 11–16.

47 A. Anastasaki, C. Waldron, P. Wilson, R. McHale and D. M. Haddleton, *Polym. Chem.*, 2013, **4**, 2672–2675.

48 H. S. Sundaram and D. Raghavachari, *J. Polym. Sci. Part A Polym. Chem.*, 2012, **50**, 996–1007.

49 M. J. Sienkowska, B. M. Rosen and V. Percec, *J. Polym. Sci. Part A Polym. Chem.*, 2009, **47**, 4130–4140.

50 N. H. Nguyen, C. Rodriguez-Emmenegger, E. Brynda, Z. Sedlakova and V. Percec, *Polym. Chem.*, 2013, **4**, 2424–2427.

51 Y. Li, Y. Tang, R. Narain, A. L. Lewis and S. P. Armes, *Langmuir*, 2005, **21**, 9946–9954.

52 J.-J. Wang, Y.-N. Zhou, P. Wang and Z.-H. Luo, *RSC Adv.*, 2013, **3**, 5045–5055.

53 J. R. Gois, N. Rocha, A. V Popov, T. Guliashvili, K. Matyjaszewski, A. C. Serra and J. F. J. Coelho, *Polym. Chem.*, 2014, **5**, 3919–3928.

54 K. A. Davis and K. Matyjaszewski, *Macromolecules*, 2000, **33**, 4039–4047.

55 N. H. Nguyen, X. Leng and V. Percec, *Polym. Chem.*, 2013, **4**, 2760–2766.

56 C. Boyer, A. Atme, C. Waldron, A. Anastasaki, P. Wilson, P. B. Zetterlund, D. Haddleton and M. R. Whittaker, *Polym. Chem.*, 2013, **4**, 106–112.

57 A. Simula, V. Nikolaou, A. Anastasaki, F. Alsubaie, G. Nurumbetov, P. Wilson, K. Kempe and D. M. Haddleton, *Polym. Chem.*, 2015, **6**, 2226–2233.

58 F. Alsubaie, A. Anastasaki, V. Nikolaou, A. Simula, G. Nurumbetov, P. Wilson, K. Kempe and D. M. Haddleton, *Macromolecules*, 2015, **48**, 6421–6432.

59 M. Buback, H. Frauendorf, F. Günzler, F. Huff and P. Vana, *Macromol. Chem. Phys.*, 2009, **210**, 1591–1599.

60 N. H. Nguyen, X. Jiang, S. Fleischmann, B. M. Rosen and V. Percec, *J. Polym. Sci. Part A Polym. Chem.*, 2009, **47**, 5629–5638.

61 D. Konkolewicz, Y. Wang, P. Krys, M. Zhong, A. A. Isse, A. Gennaro and K. Matyjaszewski, *Polym. Chem.*, 2014, **5**, 4396–4417.

62 F. Alsubaie, A. Anastasaki, V. Nikolaou, A. Simula, G. Nurumbetov, P. Wilson, K. Kempe and D. M. Haddleton, *Macromolecules*, 2015, **48**, 5517–5525.

63 D. Konkolewicz, Y. Wang, M. Zhong, P. Krys, A. A. Isse, A. Gennaro and K. Matyjaszewski, *Macromolecules*, 2013, **46**, 8749–8772.

64 V. Nikolaou, PhD. Thesis, The University of Warwick, 2016.

65 J. Clayden, N. Greeves and S. Warren, *Organic Chemistry*, OUP Oxford, 2nd edn., 2012.

66 F. A. Carey and R. J. Sundberg, *Advanced Organic Chemistry: Part A: Structure and Mechanisms*, Springer Science & Business Media, 5th edn., 2007.

67 J. Couet and M. Biesalski, *Macromolecules*, 2006, **39**, 7258–7268.

68 A. Limer and D. M. Haddleton, *Macromolecules*, 2006, **39**, 1353–1358.

69 D. J. Adams and I. Young, *J. Polym. Sci. Part A Polym. Chem.*, 2008, **46**, 6082–6090.

70 A. A. Kavitha and N. K. Singha, *Macromol. Chem. Phys.*, 2009, **210**, 1536–1543.

71 J. T. Rademacher, M. Baum, M. E. Pallack, W. J. Brittain and W. J. Simonsick, *Macromolecules*, 2000, **33**, 284–288.

72 A. Kleine, C. L. Altan, U. E. Yarar, N. A. J. M. Sommerdijk, S. Bucak and S. J. Holder, *Polym. Chem.*, 2014, **5**, 524–534.

73 A. Kleine, PhD. Thesis, University of Kent, 2015.

74 N. V Tsarevsky, T. Pintauer and K. Matyjaszewski, *Macromolecules*, 2004, **37**, 9768–9778.

75 K. Matyjaszewski and J. Xia, *Chem. Rev.*, 2001, **101**, 2921–2990.

76 M. Ciampolini and N. Nardi, *Inorg. Chem.*, 1966, **5**, 41–44.

77 H. D. Keller, R. N.; Wycoff, *Inorg. Synth.*, 1946, **2**, 1–4.

Chapter 5: Conclusions and future work

The purpose of this thesis was to explore the effect of solvent, initiator and ligand upon the $Cu^{(0)}$-mediated reversible deactivation radical polymerisation ($Cu^{(0)}$-mediated RDRP) of water-soluble monomers in aqueous media. Overall, this aim was achieved, with; adaptations to the solvent being made in Chapter 2; a range of ligands being screened in Chapter 3, and the testing of different alkyl halide initiators in Chapter 4.

Given the simplicity and versatility of the aqueous $Cu^{(0)}$-mediated RDRP protocol, a secondary objective was introduced; the expansion of the methodologies' scope, and the determination of reaction conditions for "off the shelf" polymerisation. This goal was realised through the development of a system for the polymerisation, depolymerisation, and repolymerisation of acrylamides and acrylates, and the identification of compounds which were suitable for synthesising narrowly disperse ($Đ_m$ = < 1.25) polyacrylamides in an "off the shelf" manner.

The first chapter of this thesis provided an overview of the polymerisation techniques which have commonly been employed for the synthesis of macromolecules. Considering the focus of this work, particular emphasis was placed upon discussing transition metal mediated polymerisations such as atom transfer radical polymerisation (ATRP) and $Cu^{(0)}$-mediated RDRPs. Any relevant information that was not discussed within this section was provided at the beginning of each chapter.

Building on a publication from the Haddleton Group entitled, "*Absolut* "copper catalyzation perfected"; robust living polymerisation of NIPAM: *Guinness* is good for SET-LRP", the polymerisation of NIPAm was attempted using commercial carbonated water as the solvent. The presence of carbon dioxide within the reaction

medium led to the hypothesis that a successful polymerisation could be achieved in the absence of typical deoxygenation procedures. Indeed within 30 minutes, NIPAm was quantitatively polymerised, and low dispersity polymers were obtained. Interestingly, further sampling of the crude reaction mixture after 1 hour indicated that the resulting polymers had depolymerised into their constituent monomers and lower molecular weight species.

Contrary to previously reported systems, depolymerisation occurred in a controlled manner, with narrow MWDs and low molecular weight polymers being detected. In addition to this, N_2 deoxygenation of the reaction mixture post-depolymerisation led to the repolymerisation of the reformed monomer. Remarkably, this was achieved without sacrificing control over the molecular weight, the mass distribution, or the conversion. The controlled nature of this system was further highlighted by the ability to conduct "*in-situ*" chain extensions without the need for purification, and the presence of single mass distributions within the MALDI-ToF mass spectra.

Whilst a mechanism for depolymerisation was not established, the study provided key insight into the potential causes and pre-requisites for this phenomenon. Considering that depolymerisation did not occur when reactions were performed at ambient temperature; when a bromine ω-terminated polymer was subjected to the standard CO_2 reaction conditions; or when polymerisations were conducted under high pressure; further investigation into the dependence of depolymerisation upon these factors is warranted. Moreover, the potential modification of the $Cu^{(II)}Br_2$/Me_6TREN co-ordination complex in the presence of dissolved CO_2 should be probed as a potential explanation for this phenomenon. Finally, and perhaps most importantly, the commercial and environmental potential for the controlled reversal of acrylic/vinyl polymerisations means that the expansion of this system to other polymerisation techniques should be attempted.

Resulting from the relatively simple polymerisation procedure and the industrial interest in $Cu^{(0)}$-mediated RDRPs, Chapters 3 and 4 focused on generating reaction conditions and finding materials which would enable for well-defined polymers to be synthesised in an "off the shelf" manner. To provide direction, three criteria of differing importance were established; the absolute minimum of these was that each of the components could be made using a simple synthesis route, suitable for both synthetic and non-synthetic scientists. Alternatively, and for instances where the absence of organic synthesis was a pre-requisite, each of the materials would be available for purchase at any cost. Finally, as an ideal scenario, each of the materials would not only be commercially available, but would be inexpensive and readily obtainable.

Based on the materials most commonly employed for aqueous $Cu^{(0)}$-mediated RDRPs, the ligand and the initiator were identified as the reaction components which needed replacing. Although the ligand (Me_6 TREN) was available for purchase, the price was determined to be undesirable (£125 per mL, Sigma-Aldrich). Thus, with the earlier criteria in mind, the initial part of this investigation related to finding effective and low-cost ligands for the $Cu^{(0)}$-mediated RDRP of acrylamides in aqueous media. To that end, six ligands were selected for screening for the polymerisation of NIPAm. These were: TREN, PMDETA, HMTETA, EDA, TMEDA and Cyclam.

Initially, polymerisations were conducted in the presence of each ligand under "standard conditions". The SEC and ^{1}H NMR data that was obtained from these experiments highlighted PMDETA as the ligand with the most promise. This was due to the near-quantitative conversion (96 %), and the apparent control over the molecular weight ($M_{n,experimental}$ = 2300 g mol^{-1}; $M_{n,theoretical}$ = 2500 g mol^{-1}) and dispersity values ($Đ_m$ = 1.54).

To gather more information about the various copper/ligand complexes, and to probe the potential link between λ_{max} and polymerisation control, UV-Vis spectroscopy was employed. Upon comparing the findings, no obvious correlations were observed between the absorbed wavelengths of light and the results from the initial polymerisations. This led to the conclusion that λ_{max} could not be employed in a predictive manner. Irrespective of this, the UV-Vis spectroscopy investigation formed the basis for monitoring the extent of disproportionation. The data from this study revealed that only Me_6TREN, TREN, PMDETA, HMTETA and Cyclam were capable of reaching 100 % disproportionation.

Based on the findings that were obtained from both the initial polymerisations and the disproportionation studies, the polymerisation of NIPAm in the presence of both TREN and PMDETA was optimised. For PMDETA, quantitative conversions and narrow dispersity values ($Đ_m$ = 1.29) were attained within 30 minutes with the addition of an external halide salt (1.0 M NaBr) and the following reaction conditions: [M] : [I] : [L] : [$Cu^{(I)}$X] = [20] : [1.0] : [0.6] : [0.8]. In the case of TREN, high conversions and narrow MWDs ($Đ_m$ = ~ 1.25) were achieved in both the presence and absence of external halide salts. It was therefore reasoned that the aim of finding acceptable ligands for "off the shelf" polymerisations had been achieved.

In Chapter 4, four alkyl halides were tested as initiators for the aqueous $Cu^{(0)}$-mediated RDRP protocol. These were: 2,3-dihydroxypropyl-2-bromo-2-methylpropanoate **(1)**, 2-bromo-*N*-(2,3-dihydroxypropyl)-2-methylpropanamide **(2)**, 2-bromo-*N*-(2-hydroxyethyl)-2-methylpropanamide **(3)** and 2-bromo-2-methylpropionic acid **(4)**.

Using compounds **(1)** and **(2)** as the initiator resulted in complete monomer conversion, predictable molecular weights, and narrow MWDs according to characterisation by ^{1}H NMR spectroscopy and SEC. In the case of compound **(2)**,

further analysis of the polymers by MALDI-ToF MS highlighted a single mass distribution which corresponded the sodium adduct of ω-hydroxy-terminated PNIPAm. Contrary to previous literature, it was therefore concluded that the $Cu^{(0)}$-mediated RDRP of acrylamides could be conducted with amide-based initiators. Nevertheless, since compounds **(1)** and **(2)** were commercially unavailable, and thus required the user to perform organic synthesis and a follow a lengthy purification procedure, it was reasoned that both compounds were unsuitable for use in "off the shelf" polymerisations.

Employing compound **(3)** as the initiating species for the synthesis of PNIPAm, PDEAm, and PHEAm enabled for rapid and quantitative conversions, controlled molecular weights, and narrow MWDs to be obtained. As compound **(3)** was formed using a one-step synthesis procedure and facile purification process, and was also commercially available (albeit expensively so: Aurora Fine Chemicals: £1056 per 25 g), it was deemed eligible for "off the shelf" polymerisations.

Whilst the use of an inexpensive and readily obtainable initiator (compound **(4)**, Manchester Organics: £32 per 100 g) resulted in quantitative conversions and low dispersity values, the molecular weight predictability was deemed to be undesirable. As such, it was concluded that future work into the optimisation of polymerisations was required with compound **(4)** before the criteria for an ideal and "off the shelf" polymerisation had been fulfilled and attempts were made to polymerise acrylates under these conditions.

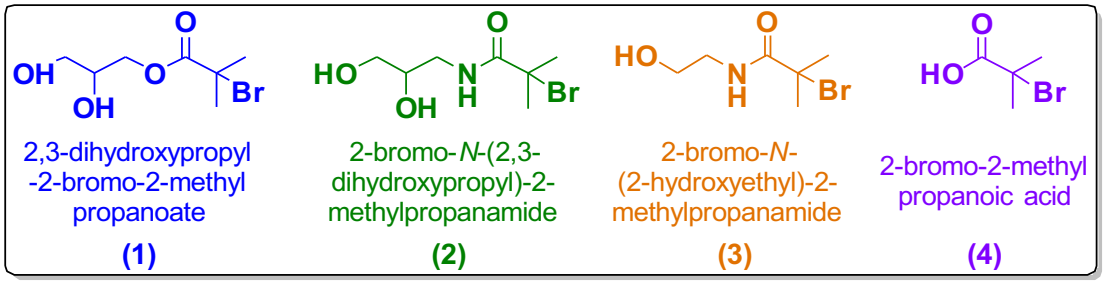

Figure 5.1 – The chemical structures of the initiators screened within Chapter 4.